Curves and Surfaces 2022

Arcachon, France
June 20 – June 24, 2022

Book of Abstracts

cs2022.sciencesconf.org

	Monday 20		Tuesday 21		Wednesday 22		Thursday 23		Friday 24
08:45-09:00	Welcoming remarks								
09:00-10:00	Plenary lecture *Johannes Wallner*		Plenary lecture *Gabriele Steidl*		Plenary lecture *Jean Bernard Lasserre*		Plenary lecture *Rachel Ward*	09:00 11:05	MS15 Deep learning in geometry processing MS16 Graphs embedded on surfaces CS15 Sampling CS16 Splines
10:00-10:30	Coffee break		Coffee break		Coffee break		Coffee break	11:05 11:30	Coffee break
10:30-12:35	MS1 Nonlocal and Geometric Data Analysis MS2 Random matrices and approximation CS1 Optimization CS2 Splines		MS5 Greedy and sparse approximation MS6 Advances in phase retrieval CS5 PDEs CS6 Isogeometric Analysis		MS9 Interactive Simulation MS10 Point configurations on curves and surfaces CS9 Learning CS10 CAGD		MS11 Approximation and deep network MS12 Optimization on manifolds CS11 Multiresolution CS12 Approximation	11:30 12:30	Plenary lecture *Rida Farouki*
Lunch									Closing remarks
14:30-15:30	Plenary lecture *Michael Griebel*	14:30 15:30	Plenary lecture Yaron Lipman			14:30 15:30	Plenary lecture *Keenan Crane,*		
15:30-16:00	Coffee break	15:30 16:30	Posters			15:30 16:30	Posters		
16:00-18:30	MS3 Sparsity, optimization and learning MS4 Advances in IGA and its applications CS3 Imaging CS4 CAGD	16:30 19:30	MS7 Advances in subdivision MS8 Advances in PH curves and PN surfaces CS7 Approximation CS8 Sampling			16:30 19:30	MS13 High dimensional approximation and PDEs MS14 Optimal transport, shapes CS13 Geometry CS14 Sampling		
18:30-20:30	Welcome cocktail			19:00 22:00	Optional boat excursion and dinner cocktail				

Plenary lectures

Moments, positive polynomials and the Christoffel function

Jean B. Lasserre
LAAS-CNRS & Institute of Mathematics, Université de Toulouse
lasserre@laas.fr

In the first part of the talk we briefly describe the Moment-SOS hierarchy [1, 2], a methodology to solve the Generalized Moment Problem(GMP) with algebraic data, whose list of potential applications is almost endless, and global optimization being its simplest instance. In a second part we briefly consider the inverse problem of recovering the algebraic boundary of a basic semi-algebraic set from the sole knowledge of moments of the Lebesgue measure on the set [4]. Finally, the third part of the talk is devoted to the Christoffel function [3], a well-known tool in theory of approximation and orthogonal polynomials. We will describe how it nicely connects with the first two parts of the talk, in particular for recovering the graph of a function from moments of the measure supported on the graph, but also for its role in a key aspect of algorithmic polynomial optimization.

References

[1] J. B. Lasserre. *Moments, Positive Polynomials and Their Applications*, Imperial College Press, London, UK, 2009.

[2] J. B. Lasserre. *An Introduction to Polynomial and Semi-Algebraic Optimization,* Cambridge University Press, Cambridge, UK, 2015.

[3] J. B. Lasserre, E. Pauwels, M. Putinar. *The Christoffel-Darboux Kernel for Data Analysis*, Cambridge University Press, Cambridge, UK, 2022.

[4] J. B. Lasserre, M. Putinar. Algebraic-exponential Data Recovery from Moments, *Discrete & Comput. Geom.*, 54: 993–1012, 2015.

Generalized sparse grid methods and applications

Michael Griebel
Institut für Numerische Simulation, Universität Bonn, Germany
griebel@ins.uni-bonn.de

High-dimensional problems appear in various mathematical models. Their numerical approximation involves the well-known curse of dimension, which renders any direct discretization obsolete. One approach to circumvent this issue, at least to some extent, is the use of generalized sparse grid methods, which can exploit additional smoothness properties if present in the underlying problem.

In this talk, we will discuss the main principles and basic features of generalized sparse grids and show their application in such diverse areas as econometrics, fluid dynamics, quantum chemistry, uncertainty quantification and machine learning.

Computing with isometries and developable surfaces

Johannes Wallner
TU Graz
j.wallner@tugraz.at

Developable surfaces constitute a prominent class of surfaces, besides being important for applications – they represent the shapes of thin sheet material as it bends from a flat state into space without stretching or tearing. Unfortunately, geometric modeling with developables is a notoriously difficult subject, and consequently there has been a great number of individual contributions to it. Nearly all of the well-known geometric properties of developables have been pressed into service for characterizing developability for different kinds of surface representations. These include global ones like the existence of an orthgonal network of geodesic curves, local ones like vanishing Gauss curvature, or the special geometry of tangent planes and rulings which developables are known to possess. Quite a few of these properties have led to effective computational treatments of developables, often by means of global optimization.

This presentation reports on some progress made in recent years. For example, both splines and meshes have been successfully used to model developables with curved creases [4, 1]. Very promising approaches to developability arise in connection with so-called checkerboard patterns which are associated to general quad meshes with regular combinatorics. One way to use them is to model developables not directly, but via isometric mappings from a planar domain. As it turns out, the possibility of modeling isometric mappings is highly useful in its own right [2, 3]. We do not believe that the checkerboard pattern method is exhausted yet, and in fact work on this topic is ongoing.

References

[1] C. Jiang, K. Mundilova, F. Rist, J. Wallner, and H. Pottmann. Curve-pleated structures. *ACM Trans. Graphics* 38(6), article no. 169 (13pp.), 2019.

[2] C. Jiang, C. Wang, F. Rist, J. Wallner, and H. Pottmann. Quad-mesh based isometric mappings and developable surfaces. *ACM Trans. Graphics* 39(4), article no. 128 (13pp.), 2020.

[3] C. Jiang, H. Wang, V. Ceballos Inza, F. Dellinger, F. Rist, J. Wallner, and H. Pottmann. Using isometries for computational design and fabrication. *ACM Trans. Graphics* 40(4), article no. 42 (12 pp.), 2021.

[4] C. Tang, P. Bo, J. Wallner, and H. Pottmann. Interactive design of developable surfaces. *ACM Trans. Graphics* 35(2) article no. 12 (12 pp.), 2016.

Global constraints in Hermite interpolation problems

Rida T. Farouki
University of California Davis
farouki@ucdavis.edu

Hermite interpolation of discrete data — points, tangents, curvatures, etc. — is a common approach to the construction of planar and spatial curves. The imposition of global (integral) constraints is more difficult, and therefore less commonly considered. We consider two types of global constraints that can be exactly achieved by using Pythagorean–hodograph curves. The first is the imposition of an exact arc length for the interpolant, and it is shown that this can be achieved for both for planar and spatial G^1 end–point data by use of quintic Pythagorean–hodograph curves [1, 2]. The second constraint involves the construction of a rational adapted orthonormal frame (comprising the curve tangent and two unit vectors spanning the curve normal plane) that satisfies prescribed initial/final orientations. Since the well–known rotation–minimizing frames are solutions of an initial–value problem, they are incompatible with this constraint. Consequently, the *minimal–twist frame* is introduced — an orthonormal frame with prescribed initial and final instances, with the least possible value for the integral of the tangent component of its angular velocity. The construction of rational minimal twist frames on both open and smooth closed–loop Pythagorean–hodograph curves is demonstrated [3, 4].

Joint work with: Soo Hyun Kim, Hwan Pyo Moon.

References

[1] R. T. Farouki. Construction of G^1 planar Hermite interpolants with prescribed arc lengths. *Computer Aided Geometric Design*, 46:64–75, 2016.

[2] R. T. Farouki. Existence of Pythagorean–hoodgraph quintic Hermite interpolants to spatial G^1 Hermite data with prescribed arc lengths. *Journal of Symbolic Computation*, 95:202–216, 2019.

[3] R. T. Farouki and H. P. Moon. Rational frames of minimal twist along space curves under specified boundary conditions. *Advances in Computational Mathematics*, 44:1627–1650, 2018.

[4] R. T. Farouki, S. H. Kim, and H. P. Moon. Construction of periodic adapted orthonormal frames on closed space curves. *Computer Aided Geometric Design*, 76: article 101802, 2020.

Geometry Processing with Intrinsic Triangulations

Keenan Crane
Carnegie Mellon University
keenanc@andrew.cmu.edu

The intrinsic viewpoint was a hallmark of 19th century geometry, enabling one to reason about shapes without needing to consider an embedding in space—and leading to major developments in the 20th century such as Einstein's theory of general relativity. Yet 21st century digital geometry processing still largely adopts an extrinsic mindset, where the geometry of a polyhedral surface is expressed via vertex positions in n-dimensional space. This talk explores how the intrinsic view of polyhedral surfaces helps relax some standard assumptions in geometric computing, leading to algorithms that are often more flexible and numerically more robust. In particular we will examine fundamental data structures for intrinsic triangulations, extensions of important triangulation algorithms to curved surfaces,

Designing Invariant and Equivariant Neural Networks

Yaron Lipman
Weizmann Institute, Meta AI
yaron.lipman@weizmann.ac.il,ylipman@fb.com

Many tasks in machine learning (ML) require learning functions that are invariant or equivariant with respect to symmetric transformations of the data. For example, graph classification is invariant to permutations of its nodes, while recognizing the shape of a point cloud is invariant to both permutation and Euclidean motion of its points. Designing parameteric models (i.e., neural networks) that are *by construction* invariant or equivariant to symmetries of the data has been proven successful in many ML tasks involving data such as images, sets and point-clouds, and graphs. In designing invariant/equivariant neural network model there are few factors that should be taken into account: (i) The expressive/approximation power of the model; (ii) the computational and memory complexity of the model; (iii) the model's practical performance (inductive bias).

In this talk I will review two methodologies for designing invariant/equivariant networks: The *intrinsic method*, and the *extrinsic method*. The intrinsic method first characterizes invariant/equivariant primitive functions, such as linear transformations, and then composes these with non-linear activations to build the final parametric model. Extrinsic methods, on the other hand, apply symmetrization to general parametric functions. In the talk I will review some earlier works in this space, and provide an in-depth description of *Frame Averaging*, a recent symmetrization approach, that in some cases allows designing efficient and maximally expressive invariant/equivariant models.

Joint work with: Omri Puny, Matan Atzmon, Heli Ben-Hamu, Ishan Misra, Aditya Grover, Edward J. Smith

Approximation of Measures by Measures supported on Curves

Gabriele Steidl
TU Berlin
steidl@math.tu-berlin.de

The approximation of probability measures on manifolds by measures supported in lower dimensions is a classical task in approximation and complexity theory with a wide range of applications. In this talk, we focus on measures supported on curves, where we highlight two approaches:

i) *Principal curves* are natural generalizations of principal lines arising as first principal components in the Principal Component Analysis. They can be characterized from a stochastic point of view as so-called self-consistent curves based on the conditional expectation and from the variational-calculus point of view as saddle points of the expected difference of a random variable and its projection onto some curve, where the current curve acts as argument of the energy functional. We show that principal curves in $\mathbb{R}^d$ can be computed as solutions of a system of ordinary differential equations and we provide several examples for principal curves related to the uniform distribution on certain domains, see [1].

ii) *Discrepancy minimizing curves* aim to minimize so-called discrepancies between measures. Besides proving optimal approximation rates in terms of the curve's length and Lipschitz constant, we are interested in the numerical minimization of the discrepancy between a given probability measure and the set of push-forward measures of Lebesgue measures on the unit interval by Lipschitz curves. We present numerical examples for measures on the 3-dimensional torus, the 2-sphere, the rotation group on $\mathbb{R}^3$ and the Grassmannian of all 2-dimensional linear subspaces of $\mathbb{R}^3$. Our algorithm of choice is a conjugate gradient method on these manifolds, which incorporates second-order information. For efficient gradient and Hessian evaluations within the algorithm, we approximate the given measures by truncated Fourier series and use fast Fourier transform techniques on these manifolds, see [2]. Finally, we are interested in the relation of our approach to Wasserstein gradient flows of discrepancies.

Joint work with: R. Beinert, A, Bërdëllima, M. Ehler, M. Gräf, S. Neumayer

References

[1] R. Beinert, A, Bërdëllima, M. Gräf, and G. Steidl. On the dynamical system of principal curves in $\mathbb{R}^d$. *Preprint arXiv*:2108.00227, 2021.

[2] M. Ehler, M. Gräf, S. Neumayer, and G. Steidl. Curve based approximation of measures on manifolds by discrepancy minimization. *Foundations of Computational Mathematics*, 21(6), 1595–1642, 2021.

Concentration for random matrix products, with applications

Rachel Ward
University of Texas at Austin
rward@math.utexas.edu

We will survey recent concentration inequalities for products of independent random matrices. Such random matrices naturally appear in the analysis of stochastic and online optimization such as stochastic gradient descent. We illustrate the power of these results with two applications: improved rates of convergence for streaming Principal Component Analysis beyond rank-1 updates, and a proof that minibatch stochastic gradient descent with Polyak momentum achieves the optimal fast linear rate of convergence as in the deterministic setting, provided the minibatch size is above a critical threshold. We conclude by discussing several open problems inspired by applications.

Contributed lectures and posters

Fast and accurate optimization on the orthogonal manifold without retractions

Pierre Ablin
CNRS-PSL University-Université Paris-Dauphine
pierre.ablin@dauphine.psl.eu

We let $f : \mathbb{R}^{p\times p} \to \mathbb{R}$ a smooth function, and consider the problem of minimizing f over the orthogonal manifold $\mathcal{O}_p = \{X \in \mathbb{R}^{p\times} |\ X^\top X = I_p\}$. We study iterative algorithms that produce a sequence of iterates X_k that should converge to the solution of the problem. In order to find X_{k+1}, Riemannian gradient descent [1] first computes the Riemannian gradient G_k, i.e. the projection of $\nabla f(X_k)$ in the tangent space at X_k, which is the linear space $T_{X_k} = \{AX_k |\ A^\top = -A\}$. Simple computations give $G_k = \mathrm{Skew}(\nabla f(X_k)X_k^\top)X_k$. This algorithm then uses a retraction to move in the opposite direction while staying on the manifold. For instance, the classical exponential retraction gives $X_{k+1} = \exp(-\eta \mathrm{Skew}(\nabla f(X_k)X_k^\top))X_k$, with $\eta > 0$ a step size: it is straightforward to check that if X_k is orthogonal, then X_{k+1} is still orthogonal, and that as η gets small, we have $X_{k+1} \simeq X_k - \eta G_k$. Unfortunately, the numerical computation of retractions on the orthogonal manifold always involves some expensive linear algebra operation, such as matrix inversion, exponential or square-root. These operations quickly become expensive as the dimension p grows.

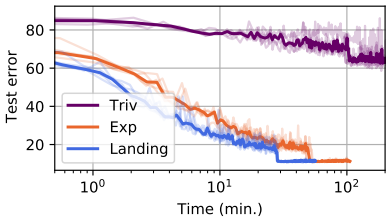

Figure 1: Learning curves for a deep residual network with orthogonal weights on CIFAR10

To bypass this limitation, we propose the landing algorithm which does not use retractions. Letting $\mathcal{N}(X) = \frac{1}{4}\|X^\top X - I_p\|_F^2$ the "distance" to the manifold, we define the landing field as

$$\Lambda(X) = \mathrm{Skew}(\nabla f(X)X^\top)X + \lambda \nabla \mathcal{N}(X),$$

and the landing algorithm simply iterates $X_{k+1} = X_k - \eta\Lambda(X_k)$. The algorithm is not constrained to stay on the manifold but the term $\nabla\mathcal{N}(X)$ progressively attracts it towards the manifold.

One iteration of the landing algorithm only involves matrix multiplications, which makes it cheap compared to its retraction counterparts, especially on modern hardware like GPU's. Fig 2 illustrates the computational cost of the landing field compared to most classical retractions. Theoretically, we show that the algorithm converges with the usual rate for a non-convex problem: with small enough step-size η, we get $\sup_{k\geq K} \mathcal{N}(X_k) = O(\frac{1}{K})$ and $\sup_{k\geq K} \|G_k\|^2 = O(\frac{1}{K})$, showing that the algorithm reaches stationary points of the optimization problem at a $1/\sqrt{K}$ rate, just like Riemannian gradient descent [2]. Numerical experiments demonstrate the promises of our approach in settings where computing retractions is very costly, such as training of deep neural networks with orthogonal weights. Fig. 1 displays the test error of a deep residual network with orthogonal weights trained on the CIFAR 10 dataset: the landing method is the fastest.

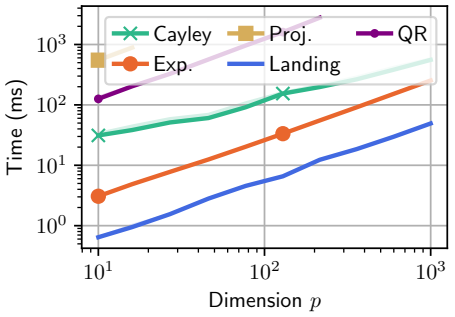

Figure 2: Time required to compute 500 retractions when A and X are of size $p \times p$, on a GPU.

Joint work with: Gabriel Peyré (CNRS - PSL University - ENS)

References

[1] Pierre-Antoine Absil, Robert Mahony and Rodolphe Sepulchre. Optimization algorithms on matrix manifolds. *Princeton University Press*, 2009.

[2] Nicolas Boumal, Pierre-Antoine Absil, and Coralia Cartis. Global rates of convergence for nonconvex optimization on manifolds. *IMA Journal of Numerical Analysis* 39.1 (2019): 1-33.

Non-Parametric Estimation of Manifolds from Noisy Data

Barak Sober
Department of Statistics and Data Science, Digital Humanities
The Hebrew University of Jerusalem
Barak.Sober@mail.huji.ac.il

A common observation in data-driven applications is that high dimensional data has a low intrinsic dimension, at least locally. In this work, we consider the problem of estimating a d dimensional sub-manifold of $\mathbb{R}^D$ from a finite set of noisy samples. Assuming that the data was sampled uniformly from a tubular neighborhood of $\mathcal{M} \in \mathcal{C}^k$, a compact manifold without boundary, we present an algorithm that takes a point r from the tubular neighborhood and outputs $\hat{p}_n \in \mathbb{R}^D$, and $\widehat{T_{\hat{p}_n}\mathcal{M}}$ an element in the Grassmanian $Gr(d, D)$. We prove that as the number of samples $n \to \infty$ the point $\hat{p}_n$ converges to $p \in \mathcal{M}$ and $\widehat{T_{\hat{p}_n}\mathcal{M}}$ converges to $T_p\mathcal{M}$ (the tangent space at that point) with high probability. Furthermore, we show that the estimation yields asymptotic rates of convergence of $n^{-\frac{k}{2k+d}}$ for the point estimation and $n^{-\frac{k-1}{2k+d}}$ for the estimation of the tangent space. These rates are known to be optimal for the case of function estimation.

Joint work with: Yariv Aizenbud.

Design by planar and spatial PH B-Spline curves

Gudrun Albrecht
Escuela de Matemáticas, Universidad Nacional de Colombia, Sede Medellín
galbrecht@unal.edu.co

This talk deals with the recently introduced classes of planar and spatial Pythagorean Hodograph (PH) B-Spline curves. PH B-Spline curves are odd-degree, non-uniform, parametric B-Spline curves whose arc length is a B-Spline function of the curve parameter and can thus be computed explicitly without numerical quadrature. Thus, although Pythagorean-Hodograph B-Spline curves have fewer degrees of freedom than general B-Spline curves of the same degree, they offer unique advantages for computer-aided design and manufacturing, robotics, motion control, path planning, computer graphics, animation, and related fields. Further details about these curves can be found in [1, 2, 3].

After shortly reviewing their construction and main properties we address solutions to several curve design applications, including the design of a PH B-Spline curve closest to a given reference curve, the interpolation of point and second order Hermite data as well as the construction of almost rotation minimizing spatial PH B-Spline curves as spine curves of rational tensor product B-Spline pipe surfaces.

Joint work with: Carolina Beccari, Lucia Romani.

References

[1] G. Albrecht, C. V. Beccari, J. Ch. Canonne, L. Romani. Planar Pythagorean-Hodograph B-Spline curves. *Computer-Aided Geom. Design*, 57, 57–77, 2017.

[2] G. Albrecht, C.V. Beccari, L. Romani. Spatial Pythagorean-Hodograph B-Spline curves and 3D point data interpolation. *Computer-Aided Geom. Design*, 80, 101868, 2020.

[3] G. Albrecht, C.V. Beccari, L. Romani. G^2/C^1 Hermite interpolation by planar PH B-spline curves with shape parameter. *Applied Mathematics Letters*, 121, 107452, 2021.

Projective equivalences and μ-bases of rational curves in any dimension.

Juan G. Alcázar
Universidad de Alcalá(UAH), Madrid, Spain
juange.alcazar@uah.es

The notion of a μ-basis was developed several years ago in the context of curves implicitization [2]. From a geometric point of view, a μ-basis of a rational curve in $\mathbb{R}^n$ is a set of n rational curves of smaller degree, that can replace the original curve for several operations like implicitizing, detecting properness, inverting, etc [2, 4, 5]. On the other hand, projective equivalences between rational curves in $\mathbb{R}^n$ have been studied in recent years [1, 3]. The algorithms for checking projective equivalence depend heavily on the degrees of the curves to be analyzed. In this talk, we will show how projective equivalences between rational curves in $\mathbb{R}^n$ are transferred to the elements of smallest degree of the μ-bases of the curves. These elements of smallest degree can be found without computing the whole μ-basis. As a result, we have a way to reduce the cost of computing the projective equivalences between rational curves in $\mathbb{R}^n$ by replacing the given curves for the curves represented by the elements of smallest degree of the μ-bases of the curves, which have a much smaller degree compared to the original degree of the curves.

Joint work with: Carlos Hermoso (UAH), Sonia Pérez-Díaz (UAH), Li-Yong Shen (UCAS).

References

[1] Bizzarri M., Lávička M., Vršek J. (2020) Computing projective equivalences of special algebraic varieties. *Journal of Computational and Applied Mathematics*, Vol. 367, 112438.

[2] Cox D.A., Sederberg T.W., Chen F. (1998) The Moving Line Ideal Basis of Planar Rational Curves. *Computer Aided Geometric Design*, Vol. 15, pp. 803–827.

[3] Hauer M., Jüttler B. (2018) Projective and affine symmetries and equivalences of rational curves in arbitrary dimension. *Journal of Symbolic Computation*, Vol. 87, pp. 68–86. *Doklady Akademii Nauk*, 37(2):227–229, 1942.

[4] Pérez-Díaz S., Shen L-Y. (2021) Inversion, Degree, Reparametrization and Implicitization of Rational Planar Curves Using μ-Basis. *Computer Aided Geometric Design*, Vol. 84, 101957.

[5] Song N., Goldman R. (2009) *mu*-bases for polynomial systems in one variable. *Computer Aided Geometric Design*, Vol. 26, ppp. 217–230.

From Delaunay to Curved Optimal Delaunay Triangulations

Pierre Alliez
Inria
pierre.alliez@inria.fr

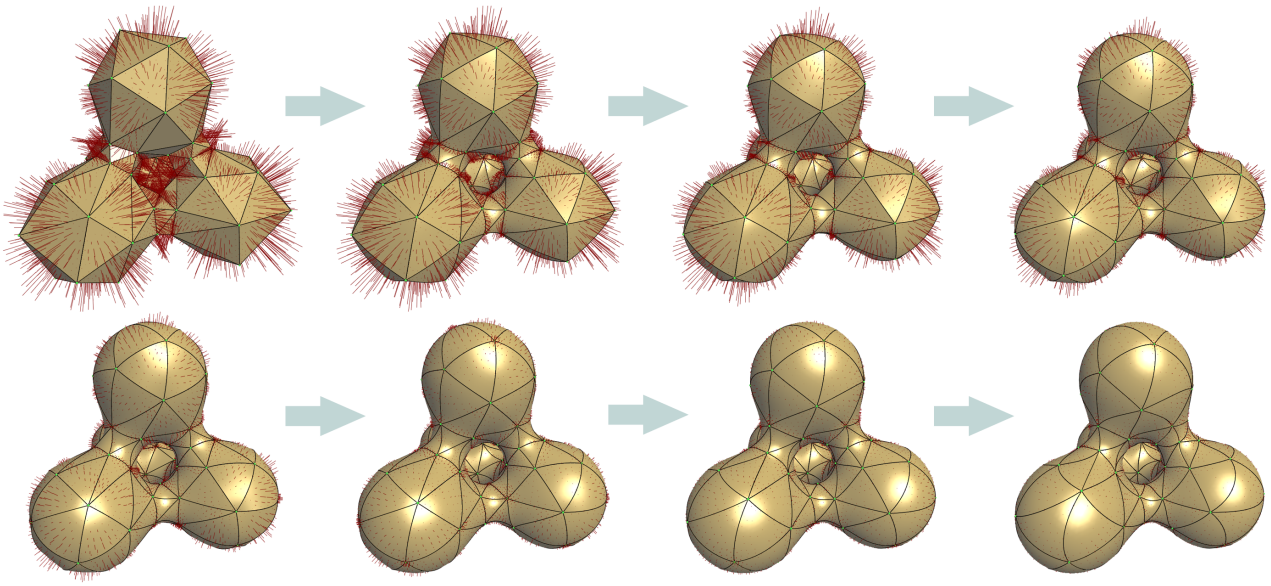

Figure 1: A Bézier mesh (here with 200 cubic patches) can capture a curved domain with orders of magnitude less elements than a linear counterpart, for a given Hausdorff distance.

Meshes with curvilinear elements hold the appealing promise of higher-order numerical accuracy compared to their commonly-used straight-edge counterparts. However, the generation of curved meshes remains a computationally expensive endeavor: high-order parametric elements are notoriously difficult to conform to a given boundary geometry, and enforcing a smooth and non-degenerate Jacobian everywhere brings additional numerical difficulties to the meshing of complex domains. We extend Optimal Delaunay Triangulations (ODT) [1] to curved and graded isotropic meshes. We show that the measure of element distortion underlying the ODT approach can be re-expressed as a potential energy whose minimization amounts to an equidistribution of the gradient of the deformation field, thus regularizing simultaneously the size and shape of the simplicial elements. After formulating a non-shrinking traction to favor uniform and isotropic elements at the boundary, we show that this interpretation of ODT also applies for curved meshes made of Bézier simplices. The resulting curved meshes provide coarse geometric descriptions of arbitrary 2D or 3D domains with a much improved fit to the domain boundary due to their piecewise polynomial nature, see Figure 1. Moreover, our construction naturally promotes smoothness of the gradient of the induced geometric map inside and across elements [2].

Joint work with: Leman Feng, Laurent Busé, Hervé Delingette and Mathieu Desbrun.

References

[1] Long Chen, Jin-chao Xu. Optimal Delaunay Triangulations. *J. Computational Mathematics*, 299–308, 2004.

[2] Leman Feng, Pierre Alliez, Laurent Busé, Hervé Delingette and Mathieu Desbrun. Curved Optimal Delaunay Triangulation. *ACM Transactions on Graphics - Proceedings of SIGGRAPH*, 2018.

Lebesgue-type inequalities in greedy approximation with respect to bases

José L. Ansorena
University of La Rioja
joseluis.ansorena@unirioja.es

Let $(\mathcal{G}_m)_{m=1}^{\infty}$ denote the thresholding greedy algorithm (TGA for short) of a basis of a Banach space $\mathbb{X}$. To measure the efficiency of the TGA is customary to use the Lebesgue parameters $(\boldsymbol{L}_m)_{m=1}^{\infty}$, defined for each $m \in \mathbb{N}$ as the optimal constant $C = C(m)$ such that

$$\|f - \mathcal{G}_m(f)\| \leq C \, \|f - g\|$$

for all $f \in \mathbb{X}$ and all linear combinations, g, of m vectors of the basis.

Calculating the exact value of the Lebesgue constants can be in general a difficult task, so in order to study the efficiency of non-greedy bases we must settle for obtaining easy-to-handle parameters that control the asymptotic growth of $(\boldsymbol{L}_m)_{m=1}^{\infty}$. Most of of such parameters and estimates have sprung from the celebrated characterization of greedy bases by Konyagin and Telmyakov [1]. In fact, several authors have obtained estimates for the Lebesgue constants, either of general bases or of bases with some special features, in terms of the unconditionality constants $(\boldsymbol{k}_m)_{m=1}^{\infty}$ and a sequence of democracy-like parameters that fits their purposes.

In this talk, we introduce a new sequence of democracy-like parameters, which we call $(\boldsymbol{\lambda}_m)_{m=1}^{\infty}$, which combined linearly with the unconditionality parameters determines the growth of the Lebesgue parameters. That is,

$$\boldsymbol{L}_m \approx \max\{\boldsymbol{k}_m, \boldsymbol{\lambda}_m\}, \quad m \in \mathbb{N}.$$

This result provides an answer to a problem raised by Temlyakov during the *Concentration week on greedy algorithms in Banach spaces and compressed sensing* held on 18–22 July, 2011, at Texas A&M University.

Joint work with: Fernando Albiac, Pablo Berná.

References

[1] S. L. Konyagin and V. N. Temlyakov. A remark on greedy approximation in Banach spaces. *East J. Approx.*, 5(3):365–379, 1999.

Diffeomorphic Deformations and Topological Changes for Trees of 3D Curves

Pierre Louis Antonsanti
Université de Paris - GE Healthcare
pierrelouis.antonsanti@ge.com

The study of tree structures has many applications in for instance the evolution of species (phylogenetic trees), biological structures (plants) or anatomical ones (vascular or pulmonary trees). When labeling the extremities of these trees, the leaves, we face a type of topological change related to the order of appearance of the different branches in the trees. In the presented work we propose a framework for the alignment of 3D curve trees allowing both geometrical and topological deformations of an object, the source, onto a target. For this end we combine the tree space representation proposed by [1] by immersing the trees in a space composed of juxtaposed Euclidean spaces called orthant with a LDDMM deformation guided by Optimal Transport such as [2]. Each orthant is associated with a given topology found in a database or built from a priori knowledge. The trees are considered *rooted* and binary, and one topology corresponds to a unique bifurcation ordering. The source tree of our registration problem is moving inside the tree space.

The LDDMM then provide a realistic diffeomorphic deformation of the shape along with its ambient space. The Optimal Transport is used in the data attachment term to enforce a pairing of the branches from the deformed source and the target. The overall registration is formulated as the minimization of a cost function, sum of the classic LDDMM cost function and a regularization term in the tree space.

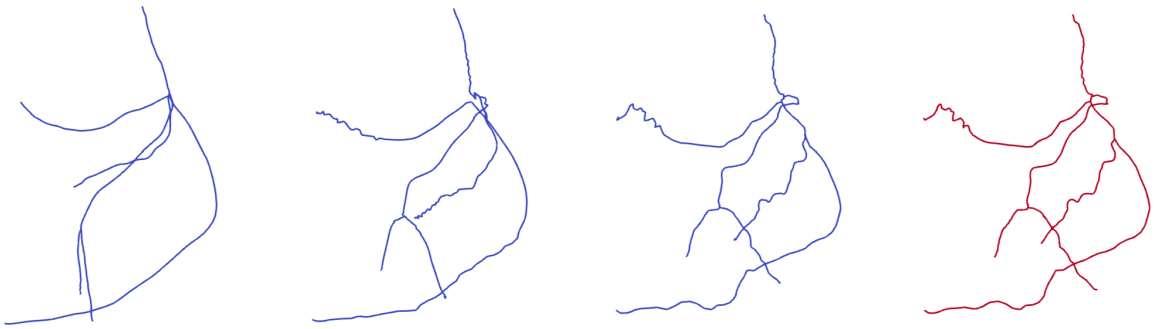

(a) (b) (c) (d)

Figure 1: Registration of a template tree (a) obtained with the Sturm Mean in the space of tree-like shapes obtained with 20 trees and 11 possible topologies. The intermediate registration at coarse scale of the data attachment term in the optimization (b) seeks for the correct topology. The registration at the end of the minimization procedure (c) is aligned to the target's geometry and topology (d).

Joint work with: Joan Glaunès.

References

[1] A. Feragen. Toward a theory of statistical tree-shape analysis. *IEEE transactions on pattern analysis and machine intelligence*, 35(8):2008–2021, 2012.

[2] J. Feydy. Optimal Transport for Diffeomorphic Registration. *Lecture Notes in Computer Science*, 291–299, 2017.

Lower bounds in rational approximation to delays

Laurent Baratchart
INRIA Sophia-Antipolis
Laurent.Baratchart@inria.fr

It is well-known that transfer functions of delay systems are hard to approximate by rational functions. This phenomenon, which is interesting from the point of view of approximation theory, is also a concern in problems where the frequency response of a device must be approximated by a model involving rational elements; *e.g.* in identification and matching. For instance, the transfer function $s \mapsto \exp\{-\tau s\}$ of a pure delay τ, where the complex variable s ranges over the right half-plane, has best rational approximant 0 on the imaginary axis: no nonzero rational function r exists such that $\|\exp^{-\tau \cdot} - r\|_{L^\infty(i\mathbf{R})} < 1$; here, $L^\infty(i\mathbf{R})$ refers to the *sup* norm on the imaginary axis, which represents the frequency axis in a system-theoretic context. We shall discuss a band-limited and norm-constrained version of the issue just mentioned, namely:

given an interval $I_0 = [-\omega_0, \omega_0]$ and $M > 0$, how small can the maximum of $|e^{-i\tau\omega} - r_n(i\omega))|$ be for r_n a rational function of type (n, n) (the ratio of two polynomials of degree at most n) wand $\omega \in I_0$, under the constraint that $\|e^{-i\tau\omega} - r_n(i\omega)\|_{L^\infty(\mathbf{R}\setminus I_0)} \leq M$?

Specifically, we will offer a lowerbound for this quantity.

The path we go is by perturbation of $s \mapsto \exp\{-\tau s\}$ into a Blaschke product and then comparison with L^2-approximation, using results from [1] which depend on a topological argument.

References

[1] L. Baratchart, S. Chevillard, T. Qian. Minimax principle and lower bounds in H2 rational approximation. *Journal of Approximation Theory*, 206:17–47, 2016.

Global convergence of ResNets: From finite to infinite width using linear parameterization

Raphaël Barboni
École Normale Supérieure - PSL
raphael.barboni@ens.fr

Overparameterization is a key factor in the absence of convexity to explain global convergence of gradient descent (GD) for neural networks. Beside the well studied lazy regime, infinite width (mean field) analysis has been developed for shallow networks, using on convex optimization technics. To bridge the gap between the lazy and mean field regimes, we study Residual Networks (ResNets) in which the residual block has linear parameterization while still being nonlinear. Such ResNets admit both infinite depth and width limits, encoding residual blocks in a Reproducing Kernel Hilbert Space (RKHS). In this limit, we prove a local Polyak-Lojasiewicz inequality. Thus, every critical point is a global minimizer and a local convergence result of GD holds, retrieving the lazy regime. In contrast with other mean-field studies, it applies to both parametric and non-parametric cases under an expressivity condition on the residuals. Our analysis leads to a practical and quantified recipe: starting from a universal RKHS, Random Fourier Features are applied to obtain a finite dimensional parameterization satisfying with high-probability our expressivity condition.

Joint work with: Gabriel Peyré, François-Xavier Vialard.

Gaussian Processes in the Flat Limit

Simon Barthelmé
Gipsa-lab, CNRS
name.surname@gipsa-lab.fr

Gaussian processes (GPs) are a cornerstone of modern Bayesian methods, used almost wherever one may require nonparametric priors. The most typical use of GPs is in Gaussian process regression, also known as kriging. Quite naturally, the theory of Gaussian Process methods is well-developed. Aside from limited special cases in which Fourier analysis is applicable, GP-based methods have mostly been studied under large-n asymptotics , which involve treating measurement locations as random and letting their number go to infinity. In this paper we report intriguing theoretical results obtained under a different asymptotic, one that treats the data as fixed, rather than random, with fixed sample size. The limit we look at is the so-called "flat limit", pioneered by Driscoll & Fornberg in 2002. The flat limit consists in letting the spatial width of the kernel function go to infinity, which results in the covariance function becoming flat over the range of the data.

Studying Gaussian processes under the flat limit may seem at first sight to be entirely pointless - does that not correspond to a prior that contains only flat functions? Surprisingly, we show that the answer is no. This occurs because covariance functions have a second hyperparameter that sets the vertical scale (pointwise variance). When one lets pointwise variance grow as the covariance becomes wider, the actual function space spanned by Gaussian processes remains interesting and useful. In the cases studied here, they are (multivariate) polynomials and (polyharmonic) splines.

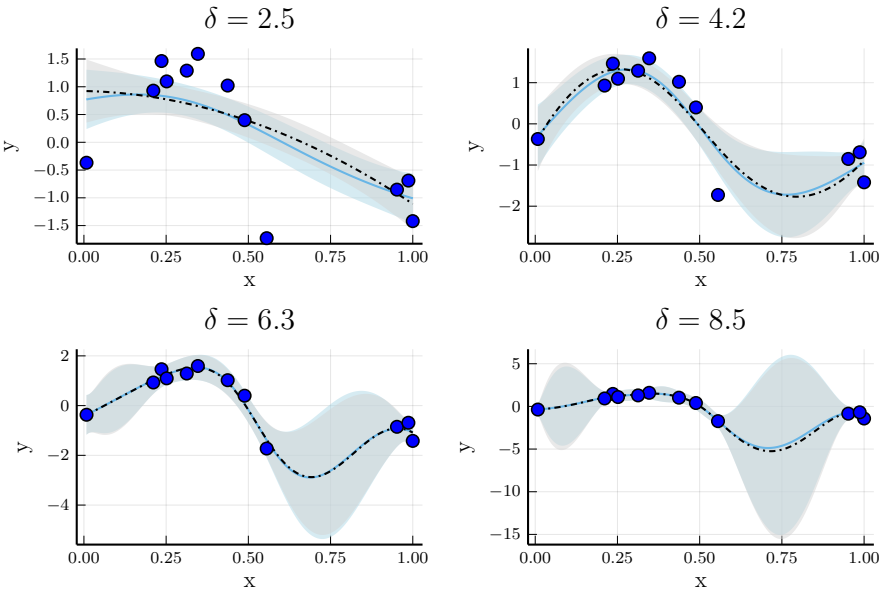

The figure shows GP regression compared to its flat limit approximation. In each panel, the solid black line represents the fit of a GP to the datapoints shown in blue kernel. We use a stationary Matèrn kernel with a fixed spatial scale, but vary its vertical scale parameter across the four panels, so that the resulting fit has different degrees of freedom δ. With more degrees of freedom, the fit becomes closer to the measurements. In light blue, the confidence bands of the fit. Superimposed, we show a "flat limit" approximation to the GP, which corresponds to fitting a smoothing spline model that would be equivalent with the spatial scale parameter going to infinity. The good quality of the approximation in such cases shows that our results could have interesting practical applications.

A technical report is available at https://arxiv.org/abs/2201.01074.

Joint work with: Pierre-Olivier Amblard, Konstantin Usevich, Nicolas Tremblay.

Tobin A Driscoll and Bengt Fornberg. Interpolation in the limit of increasingly flat radial basis. *Computers & Mathematics with Applications*, 43(3-5):413–422,2002.

Super-resolution on compact manifolds

Dmitry Batenkov
Department of Applied Mathematics, Tel-Aviv University, Israel
dbatenkov@tauex.tau.ac.il

Consider the problem of recovering a Dirac spike train $F(x) = \sum_{k=1}^{K} a_k \delta_{x_k}$, where each $x_k \in (\mathbb{R}/2\pi\mathbb{Z})$ is an unknown point on a 1D circle, from its low-frequency trigonometric moments $\widehat{F}(n) = \sum_{k=1}^{K} a_k e^{jx_k n}$, for $|n| \leq N$. This is the well-known question of sparse super-resolution, providing a popular model for several problems in computational mathematics and engineering, including spectral estimation, direction of arrival, imaging of point sources, sampling of signals with finite rate of innovation below the Nyquist limit, among others. Over the years, several extensions and generalizations of the above problem have been developed, including additional parametric models, and additional domains such as the torus or the sphere. On the other hand, allowing for high-order derivatives of Diracs enables to tackle problems such as recovery of polygons from moments, and high-accuracy recovery of piecewise-smooth functions [1].

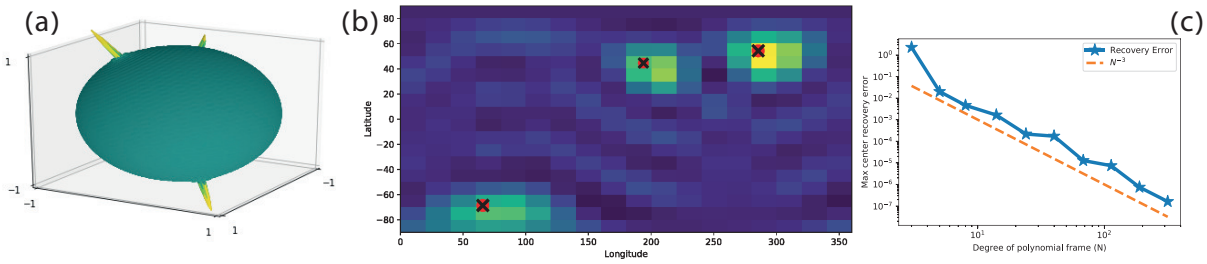

Figure 1: Generalized super-resolution on the sphere. (a) The original signal with $R = 2$ and $K = 3$. (b) An example reconstruction with $N = 8$ and additive error of magnitude $O(N^{-2})$. The red circles represent the true $\{x_k\}$ while the black crosses represent the reconstructed locations. The background is the original low-resolution data used in the algorithm. (c) Decay of the error is super-linear: $|\tilde{x_k} - x_k| \sim N^{-R-1}$.

Let $\mathcal{M}$ be a homogeneous compact Riemannian manifold (without boundary), and denote by $\{\lambda_n, \varphi_n\}_{n=0}^{\infty}$ the spectral decomposition of the manifold Laplacian, where $0 = \lambda_0^2 < \lambda_1^2 \leq \cdots \uparrow +\infty$ are repeated according to multiplicity, while the real-valued orthonormal eigenfunctions $\{\varphi_n\}_{n=0}^{\infty}$ constitute a basis for the Hilbert space $L^2(\mathcal{M})$. In this work we consider the problem of super-resolution recovery of signals F which are modelled as sparse linear combinations $F \sim \sum_{k=1}^{K} \sum_{r=0}^{R} a_{k,r} G_r(x; x_k)$, where the "Bernoulli spline" G_r is the Green's function of the fractional Laplacian operator $(I + \Delta)^{r/2}$, from their low-frequency measurements $\widehat{F}_n := \langle F, \varphi_n \rangle_{\mathcal{M}}, \quad \lambda_n \leqslant N$. We build a constructive method to recover the model parameters by a hybrid two-stage approach. Assuming that the centers $\{x_k\}$ are separated by $\gtrsim \frac{1}{N}$, we first apply a "sharpening" filter in the spectral domain, constructed using a localized Paley-Wiener type theory developed in [2] – obtaining an approximate locations of the centers $\{x_k\}$ and the amplitudes $\{a_{k,0}\}$. Subsequently, we fine-tune the initial estimates by a nonlinear least squares fit, and analyze the stability of this optimization problem. Our numerical experiments in Figure 1 for the 2D sphere with noisy data show super-linear convergence for recovering $\{x_k\}$ as $N \to \infty$. Our reconstruction procedure can in principle be used to localize supports of measures supported on curves, or submanifolds, of $\mathcal{M}$, and even on arbitrary metric measure spaces.

Joint work with: H.Mhaskar.

References

[1] Dmitry Batenkov. Stability and super-resolution of generalized spike recovery. *Applied and Computational Harmonic Analysis*, 45(2):299–323, 2018.

[2] H. N. Mhaskar. A generalized diffusion frame for parsimonious representation of functions on data defined manifolds. *Neural Networks*, 24(4):345–359, 2011.

High-probability Convergence Bounds for Non-convex Stochastic Gradient Descent, with applications to learning

Stephen Becker
Department of Applied Mathematics, University of Colorado Boulder
stephen.becker@colorado.edu

Stochastic gradient descent is one of the most common iterative algorithms used in machine learning. While being computationally cheap to implement, recent literature suggests it may have implicit regularization properties that prevent over-fitting. This paper analyzes the properties of stochastic gradient descent from a theoretical standpoint to help bridge the gap between theoretical and empirical results. We specifically tackle the case of heavy-tailed noise, since recent results have shown empirically that noise due to mini-batch sampling can be non-Gaussian.

Most theoretical results either assume convexity or only provide convergence results in mean, while this paper proves convergence bounds in high probability without assuming convexity. By high-probability, we mean that our bounds are of the form "with probability at least $1 - \delta$, $\text{error}_k \leq g(k, \delta)$", for some function g (decreasing in the number of iterations k) that depends at most polynomially on $\log(\delta^{-1})$, rather than on δ^{-1}.

Assuming strong smoothness, we prove high probability convergence bounds in two settings:

1. assuming the Polyak-Łojasiewicz inequality and norm sub-Gaussian gradient noise, and
2. assuming norm sub-Weibull gradient noise.

In the first setting, in the setting of statistical learning, we combine our convergence bounds with existing generalization bounds based on algorithmic stability in order to bound the true risk and show that for a certain number of epochs, convergence and generalization balance in such a way that the true risk goes to the empirical minimum as the number of samples goes to infinity.

In the second setting, as an intermediate step to proving convergence, we prove a probability result of independent interest. The probability result extends Freedman-type concentration beyond the sub-exponential threshold to heavier-tailed martingale difference sequences.

Joint work with: Liam Madden, Emiliano Dall'Anese.

References

[1] L. Madden, E. Dall'Anese, S. Becker. High-probability Convergence Bounds for Non-convex Stochastic Gradient Descent. *arXiv* https://arxiv.org/abs/2006.05610, 2021.

Using photogrammetry for the objective study of ancient bowed instruments: a machine learning approach

Philémon Beghin, Anne-Emmanuelle Ceulemans, François Glineur
UCLouvain
philemon.beghin@uclouvain.be, anne-emmanuelle.ceulemans@uclouvain.be,
francois.glineur@uclouvain.be

The morphology of today's violin differs greatly from that of the first instruments of the late 16th century. Between 1750 and 1850, in order to meet the standards suggested by famous orchestras and conservatories, many ancient violins have been reduced. For example, the following figure shows a reduced pre-1750 violin as it looks today (left) and an estimate of its original dimensions (right) [1].

Figure 1: Reduced violin and estimation of its original dimensions.
Height of the sound box: now 35.4 cm - original c. 38 cm.

Given the paucity of written sources, the only way to improve our understanding of the violin family in this period is to study the instruments themselves. Hence, we aim at developing a set of tools able to analyse three-dimensional geometrical shapes acquired by photogrammetry. Our purpose is to differentiate ancient reduced violins from ancient unreduced violins. Using their geometrical representation, we want to quantify their specific characteristics, detect possible anomalies and, if applicable, reconstruct their original morphology. Ultimately, we will classify a corpus of ancient violins according to these aspects, thanks to unsupervised and supervised machine learning techniques.

Photogrammetry outputs point clouds and polygonal meshes, which are relatively large-scale and unstructured, hence are not the most suitable to apply standard classification techniques or models. Our first objective is thus to identify mathematical models that are precise enough to describe the three-dimensional shape of our digitised violins, but which are at the same time convenient for a classification purpose.

More precisely, we will focus mainly on the surface of the violin soundboard which we wish to represent as a piecewise function. This function will correspond to the height of the soundboard with respect to a symmetry plane of the violin (identified using Principal Component Analysis). The domain of this function will be carefully computed from the photogrammetric point cloud and mesh, so that the graph corresponds only to the upper part of the soundboard, eliminating the ribs (lateral parts). We will then apply different regression techniques on the point cloud to compute the piecewise representations of the surface (such as linear regression, B-splines, etc.), on a predefined partition of the domain, and use the coefficients of those fitted representations to classify instruments with standard machine learning techniques. We will present preliminary results obtained after performing photogrammetry on a collection of 40 ancient instruments taken from the Museum of Musical Instruments, Brussels.

References

[1] K. Moens *Les voix médianes dans l'orchestre français sous le règne de Louis XIV, L'orchestre à cordes sous Louis XIV.*, dir. J. Duron – F. Gétreau, Paris, 2015, 119–138.

On a linear Gromov–Wasserstein distance

Florian Beier
Technische Universität Berlin
f.beier@tu-berlin.de

Gromov–Wasserstein (GW) distances [2] are a generalization of Wasserstein distances and allow for a comparison and coupling of metric measure (mm-) spaces. Moreover, GW is invariant under certain distance preserving transformations making them very appealing for applications such as shape matching and comparison. However, calculating GW distances can be computationally challenging and things become even worse when all pairwise distances of a set of mm-spaces are required such as e.g. for classification tasks. To alleviate computing all pairwise distances in the Wasserstein context, the authors in [3] proposed a framework referred to as linear optimal transport. This poster shows how to extend this approach to the Gromov–Wasserstein setting. The main idea is to fix a reference space from which the GW is computed to all input spaces. The obtained couplings can be used to define approximate couplings between the inputs. The resulting framework reduces the number of GW computations from $\binom{N}{2}$ to N when requiring the pairwise distances of N mm-spaces. We provide numerical experiments highlighting that linear GW can be successfully used in classification tasks of 2d and 3d shapes.

Joint work with: Robert Beinert, Gabriele Steidl

References

[1] F. Beier, R. Beinert and G. Steidl On a linear Gromov–Wasserstein distance. *arXiv:2112.11964* 2021

[2] F. Mémoli Gromov–Wasserstein distances and the metric approach to object matching. *Found. Comput. Math.*, 11(4):417–487 2011.

[3] W. Wang, D. Slepčev, S. Basu, J. A. Ozolek, and G. K. Rohde A linear optimal transportation framework for quantifying and visualizing variations in sets of images *Int. J. Comput. Vis.*, 101(2):254–269 2011.

Cardinal and semi-cardinal interpolation with Matérn kernels

Aurelian Bejancu
Kuwait University
aurelianbejancu@gmail.com

Let $\phi : \mathbb{R}^d \to \mathbb{R}$ be a continuous and symmetric function (i.e. $\phi(-x) = \phi(x)$, $x \in \mathbb{R}^d$), satisfying a suitable decay condition for large $\|x\|$, and define the shift-invariant space

$$S(\phi) = \{ \sum_{k \in \mathbb{Z}^d} c_k \phi(\cdot - k) : (c_k) \in \ell^\infty(\mathbb{Z}^d) \}.$$

The problem of *cardinal interpolation* with the kernel ϕ is to find, for some data $(y_j)_{j \in \mathbb{Z}^d}$, a function $s \in S(\phi)$, such that $s(j) = y_j$, for all $j \in \mathbb{Z}^d$. If this problem admits a unique solution for any bounded data, it is known that specific algebraic or exponential decay of the kernel ϕ is transferred to the corresponding *Lagrange function* for cardinal interpolation on $\mathbb{Z}^d$, leading to a well-localized Lagrange representation of the solution s.

The first part of the talk presents a similar result obtained for the related problem of *semi-cardinal interpolation*, in which the multi-integer grid $\mathbb{Z}^d$ is replaced by a half-space lattice $H \subset \mathbb{Z}^d$. Despite the loss of shift-invariance in this case, we prove that the algebraic or exponential decay still carries over from ϕ to the corresponding H-indexed family of semi-cardinal Lagrange functions, with constants that are independent of the index $j \in H$ (see [1]).

In the second part, we discuss two recent applications and refinements of the above results for the Matérn kernel $\phi := \phi_{m,d}$, defined, for a positive integer $m > d/2$, as the exponentially decaying fundamental solution of the elliptic operator $(1 - \Delta)^m$ in $\mathbb{R}^d$, where Δ is the Laplace operator. Namely, for a scaling parameter $h > 0$, we consider non-stationary interpolation to data prescribed on $h\mathbb{Z}^d$ from the *flat ladder* collection $\{S_h(\phi)\}_h$ generated by ϕ via

$$S_h(\phi) = \{ \sum_{k \in \mathbb{Z}^d} c_k \phi(\cdot - hk) : (c_k) \in \ell^\infty(\mathbb{Z}^d) \}.$$

For this problem, we prove that the Lebesgue constant of the associated interpolation operator is uniformly bounded as $h \to 0$, which allows us to deduce the maximal L^∞-convergence rate $O(h^{2m})$ for the Matérn flat ladder interpolation scheme (see [2]). On the other hand, if $d = 1$, then the translates of the Matérn kernel $\phi_{m,1}$ span a linear space of exponential splines, for which we show that non-stationary semi-cardinal interpolation on the scaled grid $h\mathbb{Z}_+$ achieves the convergence rate $O(h^m)$ in $L^\infty(\mathbb{R}_+)$, amounting to half of the approximation order of the corresponding cardinal scaled scheme.

Acknowledgements: This work was supported by Kuwait University, Research Grant No. SM01/18.

References

[1] A. Bejancu. Wiener-Hopf difference equations and semi-cardinal interpolation with integrable convolution kernels. *Preprint*, arXiv:2006.05282, 2020.

[2] A. Bejancu. Uniformly bounded Lebesgue constants for scaled cardinal interpolation with Matérn kernels. *Preprint*, arXiv:2009.00711, 2020.

Approximations with discrete neural networks

Aleksandr Beknazaryan
University of Tyumen
a.beknazaryan@utmn.ru

We consider approximating capabilities of classes of neural networks whose weights belong to given finite sets and present their statistical applications. In particular, the empirical risk minimizers over those classes, which are always identifiable in a finite number of steps, can achieve good rates of estimation of unknown regression functions.

Implicit differentiation for fast hyperparameter selection in non-smooth convex learning

Quentin Bertrand
Mila, Université de Montral
quentin.bertrand@mila.quebec

Finding the optimal hyperparameters of a model can be cast as a bilevel optimization problem, typically solved using zero-order techniques such as grid search or random search. In this work we study first-order methods when the inner optimization problem is convex but non-smooth. We show that the forward-mode differentiation of proximal gradient descent and proximal coordinate descent yield sequences of Jacobians converging toward the exact Jacobian. Using implicit differentiation, we show it is possible to leverage the non-smoothness of the inner problem to speed up the computation. Finally, we provide a bound on the error made on the hypergradient when the inner optimization problem is solved approximately. Results on regression and classification problems reveal computational benefits for hyperparameter optimization, especially when multiple hyperparameters are required. This work is illustrated in Figure 1 and is based on the following publications [1, 2].

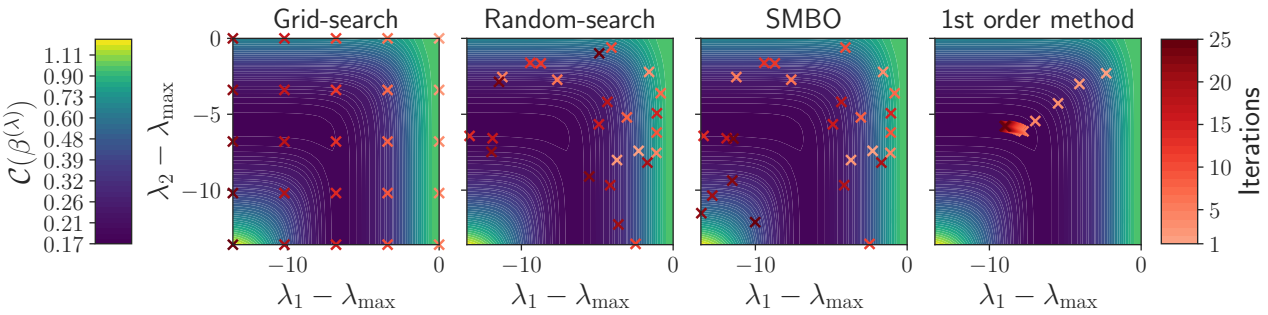

Figure 1: **5-fold cross-validation error** $\mathcal{C}(\beta^{(\lambda)})$: elastic net CV error with respect to λ_1 and λ_2 for multiple hyperparameter optimization methods on the *rcv1* dataset. Crosses represent the 25 first error evaluations for each method.

References

[1] Q. Bertrand, Q. Klopfenstein, S. Vaiter, A. Gramfort, and J. Salmon. Implicit differentiation for Lasso-type problems *ICML 2020*.

[2] Q. Bertrand, Q. Klopfenstein, M. Massias, S. Vaiter, A. Gramfort, and J. Salmon. Implicit differentiation for fast hyperparameter selection in non-smooth convex learning *JMLR 2022*.

Provably convergent deep learning-based methods for imaging inverse problems

Carola-Bibiane Schönlieb
Department of Applied Mathematics and Theoretical Physics, University of Cambridge
cbs31@cam.ac.uk

Deep learning had remarkable empirical success in recent years in solving a variety of inverse problems in imaging, including image denoising, deblurring, tomographic image reconstruction, and image inpainting, just to name a few. This has catalyzed an ongoing quest for precise characterization of correctness and reliability of such data-driven methods in critical use-cases, e.g., those arising in medical imaging.

Notwithstanding the excellent empirical performance of data-driven methods for image reconstruction, concerns have been raised regarding their stability, or lack thereof, with serious practical implications. In applications where imaging is used for discovering new scientific phenomena, it is important to have mathematical guarantees to ensure the correctness and reliability of the reconstructed images.

In this talk, we will introduce different notions of convergence pertaining to image reconstruction problems and provide a broad overview of recent data-driven techniques that satisfy some of those convergence properties. In particular, the talk will focus on data-driven regularization methods through explicit functionals parametrized by neural networks [1–5] and via plug-and-play deeply-learned denoisers [6, 7]. We will highlight the requisite properties that such a regularization functional or a denoiser must satisfy to establish convergence guarantees of different types.

Joint work with: Martin Burger, Marcello Carioni, Sören Dittmer, Sebastian Lunz, Subhadip Mukherjee, Ozan Öktem and Zakhar Shumaylov

References

[1] S. Lunz, O. Öktem, and C.-B. Schönlieb, "Adversarial regularizers in inverse problems," in *Advances in Neural Information Processing Systems*, 2018, pp. 8507–8516.

[2] H. Li, J. Schwab, S. Antholzer, and M. Haltmeier, "NETT: solving inverse problems with deep neural networks," *Inverse Problems*, vol. 36, no. 6, 2020.

[3] S. Mukherjee, S. Dittmer, Z. Shumaylov, S. Lunz, O. Öktem, and C.-B. Schönlieb, "Learned convex regularizers for inverse problems," *arXiv:2008.02839*, 2020.

[4] S. Mukherjee, C.-B. Schönlieb, and M. Burger, "Learning convex regularizers satisfying the variational source condition for inverse problems," in *NeurIPS 2021 Workshop on Deep Learning and Inverse Problems*, 2021.

[5] S. Mukherjee, M. Carioni, O. Öktem, and C.-B. Schönlieb, "End-to-end reconstruction meets data-driven regularization for inverse problems," in *Advances in Neural Information Processing Systems*, 2021.

[6] S. H. Chan, X. Wang, and O. A. Elgendy, "Plug-and-play ADMM for image restoration: Fixed-point convergence and applications," *IEEE Transactions on Computational Imaging*, vol. 3, no. 1, pp. 84–98, 2017.

[7] P. Nair, R. G. Gavaskar, and K. N. Chaudhury, "Fixed-point and objective convergence of plug-and-play algorithms," *IEEE Transactions on Computational Imaging*, vol. 7, pp. 337–348, 2021.

Optimal Learning

Peter Binev
University of South Carolina
binev@math.sc.edu

Learning an unknown function f from given data observations is a dominant theme in data science. The central problem is to use data observations of f to construct a function $\hat{f}$ which approximates f away from the data. There are numerous settings for this learning problem depending on (i) what additional information we have about f, (ii) how we measure the accuracy of how well $\hat{f}$ predicts f, (iii) what is known about the data and data sites. The main theme of this talk is twofold:

- to determine the optimal performance possible (the smallest possible error of recovery) in a given learning setting;
- to understand which discrete optimization formulations, when successfully numerically implemented, give a (near) optimal solution to the learning problem.

The remaining step is then to give a viable numerical method with convergence guarantees and bounds on computation which solves the discrete optimization formulation. It often remains an open question as to whether a proposed numerical optimization strategy, such as gradient descent methods, actually converges in the given learning setting to a near optimal solution.

This talk is concerned with evaluating how well an approximation $\hat{f}$ performs and determining the best possible performance among all choices of an $\hat{f}$. Given answers to these fundamental questions, one can then turn to the construction of numerical procedures and evaluate their performance against the known best possible performance.

Joint work with: Andrea Bonito, Ronald DeVore, and Guergana Petrova.

A Stable Method for Discretizing Differential Operators on Curves and Surfaces Using the RBF-FD Method

Jacob Blazejewski
Michigan Technological University
jblazeje@mtu.edu

Partial Differential Equations (PDEs) on arbitrary surfaces arise in many applied and natural science models. A notable example of solving PDEs on static surfaces is image processing. Applications of PDEs on evolving surfaces occur in material science and fluid dynamics. Additionally the fields of biology and computer graphics have applications for PDEs on both static and evolving surfaces.
There are three main categories of methods for solving PDEs on arbitrary surfaces: the methods that rely (i) on parametrization, (ii) on an embedding, and (iii) on triangulation. Embedding-type methods are quite simple in that they are based on the discretization of standard $\mathbf{R^3}$ operators rather than curve or surface-specific operators. One of the most common embedding methods is the closest point method (CPM), [1]. The surface is enclosed inside a thick layer of nodes that belong to a dense three-dimensional grid. Each one of these nodes takes the function value of the one associated with their closest point to the surface, implicitly imposing that the normal derivatives at each node is null. Under that constraint, the surface Laplacian is equivalent to its $\mathbf{R^3}$ analog.
The Radial Basis Functions Orthogonal Gradients method (RBF-OGr) is another embedding method, and was introduced in [2]. It benefits from the meshfree character of RBFs, which gives the flexibility to represent complex geometries in any spatial dimension while providing a high order of accuracy. This method is different from the CPM in that its computational domain is the point cloud that defines the manifold, instead of being being a thick layer of nodes around the surface. Every computation is performed on the surface, including the constraints of having null normal derivatives.
The fast RBF-OGr method [3] uses the finite-difference based RBF method, instead of the global standard RBFs which gave rise to dense differentiation matrices, a limiting factor on the size of the point cloud representing the surface. However, going from the global to the local RBF method have introduced a few sources of instabilities in the process. In this presentation, we will address the different stability issues and provide solutions. We will illustrate the procedure with a number of interesting examples.

Joint work with: C. Piret, C. Jacobs.

References

[1] S. J. Ruuth, B. Merriman. A simple embedding method for solving partial differential equations on surfaces. *J. Comput. Phys.*, 227, 2008, pp. 1943–1961.

[2] C. Piret. The Orthogonal Gradients Method: a radial basis functions method for solving partial differential equations on arbitrary surfaces. *J. Comput. Phys.*, 231, 2012, pp. 4662–4675.

[3] C. Piret, J. Dunn. Fast RBF OGr for solving PDEs on arbitrary surfaces. *AIP Conference Proceedings*, 1776(1), 070005.

Phase retrieval for finitely supported complex measures

Bernhard Bodmann
University of Houston
bgb@math.uh.edu

This work investigates the recovery of a distribution of finite support, a complex measure $\mu = \sum_{j=1}^{s} c_j \delta_{t_j}$, where $\{t_1, t_2, \ldots, t_s\} \subset [0, \Lambda]$ for some $\Lambda > 0$ and $c \in \mathbb{C}^s$, from the (squared) magnitudes of a set of linear functionals applied to μ. The linear functionals we use are obtained by evaluating $\hat{\mu}$, the Fourier transform of μ, or by taking differences between point evaluations. We show that a choice of $N \geq \frac{6(d+1)(1+6/\ln(s/\Lambda\Omega))s}{1-2\sqrt{d-1}/d}$ intensity samples is sufficient for injectivity of the measurement, where d is independent of the measure, and $0 < \Omega\Lambda < 1/2$. To establish this, we build on a construction method by Alexeev et al. [1] to obtain a sufficient set of quantities that are linear in μ. A concrete recovery algorithm results in combination with an operator-based Prony method [3] to recover the unknown support and the coefficient vector c, up to some residual ambiguity. The noisy case is addressed as well, with methods based on prior results with Hammen [2].

This is joint work with: Ahmed Abouserie.

References

[1] Boris Alexeev, Afonso S. Bandeira, Matthew Fickus, and Dustin G. Mixon, Phase Retrieval with Polarization, *SIAM Journal on Imaging Sciences* 7(1) (2014), 35–66.

[2] Bernhard G. Bodmann and Nathaniel Hammen, Algorithms and error bounds for noisy phase retrieval with low-redundancy frames, *Applied and Computational Harmonic Analysis* volume=43(3) (2017), 482–503.

[3] Ingeborg Keller and Gerlind Plonka, Modifications of Prony's Method for the Recovery and Sparse Approximation of Generalized Exponential Sums, Eprint, arxiv.org/abs/2001.03651, (2020).

Discontinuity indicators based on null rules for non-regular surface reconstruction

Cesare Bracco
Department of Mathematics and Computer Science - Università degli Studi di Firenze
cesare.bracco@unifi.it

The detection of discontinuity curves of bivariate functions (and of their gradients) is an important problem that arises in many contexts, ranging from surface and scattered data reconstruction to edge detection in image and geometric processing, see for example [1, 3] and references therein. We present a fault detection method based on the so-called null rules, computed as a vector in the null space of certain collocation matrices [4]. These rules are used as weights in a linear combination of function evaluations to indicate the local behavior of the function itself. By analyzing the asymptotic properties of the rules, we introduce two indicators (one for faults and one for gradient faults) by locally computing just one rule with degree of precision 2. This leads to a cheap and reliable scheme, which allows us to effectively detect and classify points close to discontinuities. We then show how this information can be suitably combined with adaptive approximation methods based on hierarchical spline spaces [5, 2] in the reconstruction process of surfaces with discontinuities. The considered adaptive methods exploit the ability of the hierarchical spaces to be locally refined, and the fault detection is a natural way to guide the refinement with low computational cost. Several numerical tests will be presented in order to show the behavior of the proposed methods.

Joint work with: Francesco Calabrò, Carlotta Giannelli.

References

[1] M. Bozzini, L. Lenarduzzi, M. Rossini. Non-regular Surface Approximation. in M. Floater et al., *Mathematical Methods for Curves and Surfaces: 8th International Conference, MMCS 2012, Oslo, Norway*, pages 68-87, 2014.

[2] C. Bracco, C. Giannelli, D. Großmann A. Sestini. Adaptive fitting with THB-splines: Error analysis and industrial applications. *Computer Aided Geom. D.*, 62:239-252, 2018.

[3] C. Bracco, O. Davydov, C. Giannelli, A. Sestini. Fault and gradient fault detection and reconstruction form scattered data. *Computer Aided Geom. D.*, 75, 2019.

[4] F. Calabrò, D. Bravo, C. Carissimo, E. Di Fazio, A. Di Pasquale, A. Eldray, C. Fabrizi, J. Gerges, S. Palazzo, J. Wassef. Null rules for the detection of lower regularity of functions. *J. Comp. Appl. Math.*, 361: 547-553, 2019.

[5] G. Kiss, C. Giannelli, U. Zore, B. Jüttler, D. Großmann, J. Barner. Adaptive CAD model (re-)construction with THB-splines. *Graph. Models*, 76: 273-288, 2014.

Spherical Fibonacci Points: Hyperuniformity, and more

Johann S. Brauchart
Graz University of Technology
j.brauchart@tugraz.at

One way of explicitly constructing point sets on the unit sphere in $\mathbb{R}^3$ is to map a suitable set in the unit square to the sphere by means of an area-preserving Lambert transformation.

Using the example of the Fibonacci lattice in the unit square, we study properties of its spherical analogue. In particular, we consider hyperuniformity aspects (cf. [1, 2]).

Joint work with: Josef Dick (UNSW, Yuan Xu (University of Oregon).

References

[1] J. S. Brauchart, P. J. Grabner, and W. Kusner. Hyperuniform point sets on the sphere: deterministic aspects. *Constr. Approx.*, 50(1):45–61, 2019.

[2] J. S. Brauchart, P. J. Grabner, W. Kusner, and J. Ziefle. Hyperuniform point sets on the sphere: probabilistic aspects. *Monatsh. Math.*, 192(4):763–781, 2020.

Learning mean curvature flows with neural networks

Simon Masnou
Université Claude Bernard Lyon 1
masnou@math.univ-lyon1.fr

The mean curvature flow is an emblematic geometric flow which is very naturally related to various numerical and physical applications, e.g. in image / data processing or in material sciences. The talk will be devoted to new, efficient, and accurate numerical methods based on neural networks for the approximation of the mean curvature flow of either oriented or non-orientable surfaces [1]. To learn the correct interface evolution law, the neural networks are trained on phase field representations of exact evolving interfaces. The structure of the networks draws inspiration from splitting schemes used for the discretization of the Allen-Cahn equation. But when the latter approximates the mean curvature motion of oriented interfaces only, the proposed approach extends very naturally to the non-orientable case. In addition, although trained on smooth flows only, the proposed networks can handle singularities as well. Furthermore, they can be coupled easily with additional constraints. Various applications will be shown to illustrate the flexibility and efficiency of our approach: mean curvature flows with volume constraint, multiphase mean curvature flows, numerical approximation of Steiner trees, numerical approximation of minimal surfaces.

Joint work with: Elie Bretin, Roland Denis, Garry Terii.

References

[1] E. Bretin R. Denis S. Masnou G. Terii, Learning phase field mean curvature flows with neural networks, arXiv:2112.07343, 2021.

Life beyond orthogonality: Sparse recovery in randomly sampled bounded Riesz systems – theory and applications

Simone Brugiapaglia
Department of Mathematics and Statistics
Concordia University
Montréal, QC, Canada
simone.brugiapaglia@concordia.ca

In compressive sensing and sparse recovery, a wide class of popular measurement schemes can be analyzed within the framework of randomly sampled bounded orthonormal systems. This setting includes random measurement matrices such as subsampled isometries, partial Fourier matrices, and sampling matrices associated with orthogonal polynomials. All these random measurement matrices are formed by independent, identically distributed, and uniformly bounded rows with trivial covariance.

Despite the generality of this framework, the orthogonality assumption is too restrictive in applications where the sampling matrix does not have trivial covariance. In this talk, we will discuss how to address this issue by working in the framework of randomly sampled bounded Riesz systems proposed and studied in [1]. Relaxing the orthogonality assumption, this leads to a wider class of structured random measurement matrices having independent, identically distributed, and uniformly bounded rows with nontrivial covariance.

The main theoretical tool of our analysis is a new upper bound for the expectation of the supremum of a Bernoulli process associated with the restricted isometry constant of the random matrix of interest. Using this bound, we will illustrate a restricted isometry analysis that (i) extends previous results from bounded orthonormal to bounded Riesz systems and (ii) improves the dependence of the sample complexity estimate on the restricted isometry constant while keeping the number of logarithmic factors equal to the best currently known one. In addition, we will show a robust null space property analysis in bounded Riesz systems, an application to local coherence-based sampling schemes, and discuss the extension to the weighted sparsity setting.

Going beyond orthogonality, the additional flexibility of bounded Riesz systems allows for applications to a wider class of problems. Here, we will illustrate applications in scientific computing such as function approximation in high dimensions and numerical methods for partial differential equations, including compressive Petrov-Galerkin and spectral collocation methods.

Joint work with: Sjoerd Dirksen (Utrecht University), Hans C. Jung (DeepL), Holger Rauhut (RWTH Aachen University), Weiqi Wang (Concordia University)

References

[1] S. Brugiapaglia, S. Dirksen, H.C. Jung, and H. Rauhut. Sparse recovery in bounded Riesz systems with applications to numerical methods for PDEs. *Applied and Computational Harmonic Analysis*, 53, pages 231-269, 2021.

The Geometry of Adversarial Training

Leon Bungert
Hausdorff Center for Mathematics, University of Bonn
leon.bungert@hcm.uni-bonn.de

In this talk I will show that "Adversarial Training" [1]—a methodology designed for the training of adversarially robust classifiers—is equivalent to a variational regularization problem involving a nonlocal perimeter term. Using this structure one can show that adversarial training admits a convex relaxation which is reminiscent of the Chan-Esedoglu model from image denoising [2]. Furthermore, this allows to prove existence of solutions and study finer properties and regularity. Finally, I hint at how to modify adversarial training to an Almgren-Taylor-Wang [3] like scheme for mean curvature flow.

Joint work with: Nicolás García Trillos, Ryan Murray.

References

[1] A. Madry, et al. Towards deep learning models resistant to adversarial attacks. *ICLR'18*.

[2] Tony F. Chan, S. Esedoglu. Aspects of total variation regularized L^1 function approximation. *SIAM Journal on Applied Mathematics*, 65(5): 1817–1837, 2005.

[3] F. Almgren, J. E. Taylor, L. Wang. Curvature-driven flows: a variational approach. *SIAM Journal on Control and Optimization*, 31(2), 387–438, 1993.

A General Framework for Smoothing Arbitrary Signals in Computer Graphics and Biomedicine

Simone Cammarasana
CNR-IMATI, Via de Marini 6, Genova (Italy)
simone.cammarasana@ge.imati.cnr.it

Signal smoothing is a relevant topic in many applications, such as image processing in biomedicine [1], and geology [2]. Previous work has proposed denoising methods tailored to the input signal, such as external learning applied to 2D images [3], diffusive methods applied to volumetric images [4], wavelets applied to vector fields [5], and low-rank methods applied to 2D videos [6].

We propose a novel framework [7] for the smoothing of arbitrary signals, which combines regularisation with learning-based models and is general with respect to the input signal, the noise type (e.g., speckle, Gaussian noise), the selected regulariser/denoising (e.g., SVD - Singular Values Decomposition, block matching), and the learning architecture (e.g., network's weights optimisation). Given a data set of ground-truth signals, we apply an artificial noise and extract data groups with high similarity. For an arbitrary signal, we apply a regularisation and compute the parameters that allow us the best reconstruction of the ground-truth signal from the regularised signal. Then, the data groups (e.g., the 3D blocks of the block-matching algorithm) are aggregated to reconstruct the smoothed signal. We iterate this approach, where the input signal of each iteration is the smoothed signal at the previous step. The input and optimal parameters compose the training data set, which is used to train a learning model to predict the optimal coefficients of the regularisation.

As example, we apply the SVD to images, where the optimal coefficients to be predicted are the threshold values of the shrinkage of the singular values. After the optimisation of the weights of the learning-based network, the trained models are used to smooth images with a different noise, such as 2D/3D ultrasound images affected by speckle noise, or synthetic images and videos with Gaussian noise.

Joint work with: Paolo Nicolardi, Giuseppe Patané.

Keywords: Image and signal Processing, Smoothing, Computer Graphics, Life Sciences.

References

[1] Zhang, Ju, and Yun Cheng: Despeckling Methods for Medical Ultrasound Images. In: Springer, 2020.

[2] Zhan, Yunjun and Dai, Tengda and Huang, Jiejun and Dong, Yusen and Ye, Fawang and Tang, Cong Double iterative optimal dictionary learning-based SAR image filtering method. In: Signal, Image and Video Processing.

[3] Dong, W., Zhang, L., Shi, G., Li, X.: Nonlocally centralized sparse representation for image restoration. In: Trans. on Image Processing 22(4),1620–1630 (2012), IEEE.

[4] Patanè G.: Diffusive Smoothing of 3D Segmented Medical Data. In: Journal of Advanced Research, Elsevier, Volume 6, Issue 3, May 2015, Pages 425-431

[5] M. A. Westenberg, and T. Ertl: Denoising 2-D vector fields by vector wavelet thresholding. In: J. WSCG, vol. 13, no. 1, pp. 33–40, 2005.

[6] H. Ji, C. Liu, Z. Shen, and Y. Xu: Robust video denoising using low rank matrix completion. Proc. IEEE Int. Conf. Computer Vision and Pattern Recognition, 2010.

[7] Simone Cammarasana, Paolo Nicolardi, Giuseppe Patanè: A Universal Deep Learning Framework for Real-Time Denoising of Ultrasound Images In: arXiv preprint arXiv:2101.09122 (2021)

Hyperbolic-polynomial penalized splines: existence, uniqueness, and reproduction properties

Rosanna Campagna
University of Campania "Luigi Vanvitelli", Italy
rosanna.campagna@unicampania.it

The advent of P-splines, first introduced by Eilers and Marx in 2010 (see [4]), has led to important developments in data regression through splines. With the aim of generalizing polynomial P-splines, in [1] we have recently defined a model of penalized regression spline, called HP-spline, in which polynomial B-splines are replaced by hyperbolic-polynomial bell-shaped basis functions, and a suitably tailored penalization term replaces the classical second-order forward difference operator.

HP-splines inherit from P-splines all model advantages and extend some of them. Indeed, they separate the data from the spline knots -so avoiding overfitting and boundary effects-, exactly fit exponential data, and conserve two type of 'exponential' moments.

HP-splines are particularly interesting in applications that require analysis and forecasting of data with exponential trends: the starting idea of this work is the definition of a polynomial-exponential smoothing spline model to be used in the framework of the Laplace transform inversion as done in [2, 3].

The talk discusses the existence, uniqueness, and reproduction properties of HP-splines, and provides several examples supporting their effective usage in data analysis.

Joint work with: Costanza Conti.

References

[1] C. Conti, R. Campagna. Penalized exponential-polynomial splines. *Appl. Math. Letters*, 118, (2021) 107–159

[2] R. Campagna, C. Conti, S. Cuomo. Computational Error Bounds for Laplace Transform Inversion Based on Smoothing Splines. *Appl. Math. Comput.*, 383, (2020) 125–376

[3] R. Campagna, C. Conti, S. Cuomo. Smoothing exponential-polynomial splines for multiexponential decay data. *Dolomites Research note on Approximation*, (2019) 86–10.

[4] P.H.C. Eilers and B.D. Marx. Splines, knots, and penalties. *WIREs Comp. Stat.*, 2, (2010) 637-653.

Aesthetic planar curves

Alicia Cantón
Universidad Politécnica de Madrid
alicia.canton@upm.es

In Geometric Design, it is of interest the representation of curves and surfaces that are aesthetically pleasing. In order to have a notion amenable to implementation in CAGD, *aesthetic curves* have been defined as those with monotonic curvature and, for spatial curves, monotonic torsion. There are several approaches to obtain aesthetic Bézier curves, but we will follow the lead of [4] and [3].

In [4], Mineur, Lichah, Castelain and Giaume obtain the edges of the control polygon of a planar Bézier spiral by a rotation and a dilation of the previous edge in the control polygon of the curve, what the authors name *typical curve*. Certain relations between the scaling factor and the rotation angle give rise to aesthetic Bézier spirals starting with any initial edge of the control polygon and for any degree of the Bézier curve.

Inspired by this work, in [3] Farin extends the method by considering Bézier curves whose control polygon is obtained by the action of a given matrix on the previous edge of the control polygon. His insight is to exploit the invariance of the curvature and torsion under subdivision to give some conditions on the matrix and its singular values that give rise to aesthetic Bézier curves for any initial edge, what he calls *Class A matrices* and *Class A Bézier curves*.

However, counterexamples to Farin's conditions have been produced (see [2] and [5]), that is, matrices for which these conditions hold but they do not generate curves with monotonic curvature. Moreover in [2], Cao and Wang give conditions on the eigenvalues of a (2×2 or 3×3) symmetric matrix that generates an aesthetic (planar or spatial) Bézier curve.

In this talk, we present a simple explicit formula for the curvature of planar Bézier curves generated by Farin's method. This formula is easily obtained by the invariance under subdivision property and from it there can be derived conditions on the eigenvalues of a general matrix and the initial edge of the control polygon that give rise to aesthetic Bézier curves. This approach gives a common framework to the previous works and recovers the results in [4] and [2] as particular cases. For more details we refer to [1].

Joint work with: Leonardo Fernández-Jambrina, María Jesús Vázquez-Gallo.

References

[1] A. Cantón, L. Fernández-Jambrina, M.J. Vázquez-Gallo. Curvature of planar aesthetic curves. *Journal of Computational and Applied Mathematics*, 381:113042, 2021.

[2] J. Cao, G. Wang. A note on Class A Bézier curves. *Computer Aided Geometric Design*, 25:523–528, 2008.

[3] G. Farin. Class A Bézier curves. *Computer Aided Geometric Design*, 23:573–581, 2006.

[4] Y. Mineur, T. Lichah, H. Castelain, J.M. Giaume. A shape controlled fitting method for Bézier curves. *Computer Aided Geometric Design*, 15:879–891, 1998.

[5] A. Wang, G. Zhao. Counter examples of "Class A Bézier curves". *Computer Aided Geometric Design*, 61:6–8, 2018.

Approximating Singular Measures on the Torus with Moment Polynomials

Paul Catala
Institute of Mathematics, University of Osnabrück
paul.catala@uos.de

We discuss polynomial approximations of nonnegative Radon measures supported on *arbitrary* domains of the d-dimensional torus, given moments up to some degree n. We introduce new estimates, that can be computed from the truncated moment matrices of the measures and provide complementary recovery guarantees.

Our first estimate for a measure μ is given by the convolution of μ with the Fejér kernel. A similar construction was also considered in [1]. The resulting trigonometric polynomial can be evaluated efficiently on a grid using only Fast Fourier Transforms. We establish sharp bounds on the rate of convergence of this proxy towards μ with respect to the Wasserstein-1 distance. Second, we introduce a certifying polynomial, that can identify exactly the Zariski closure of the support at finite degrees. This polynomial can be computed from the singular value decomposition of the moment matrix, and we show that it converges pointwisely towards the characteristic function of the support.

Joint work with: Mathias Hockmann, Stefan Kunis, Markus Wageringel.

References

[1] Mhaskar, H. Super-Resolution Meets Machine Learning: Approximation of Measures. *J. Fourier Anal. Appl., 25(2)*, pages 3104–3122, 2019.

An adaptive residual sub-sampling algorithm for kernel interpolation based on maximum likelihood estimations

Roberto Cavoretto
University of Turin
roberto.cavoretto@unito.it

In this contribution we propose an enhanced version of the residual sub-sampling method (RSM) in [1] for adaptive interpolation by radial basis functions (RBFs). More precisely, we introduce in the context of sub-sampling methods a maximum profile likelihood estimation (MPLE) criterion for the optimal selection of the RBF shape parameter. This choice is completely automatic, provides highly reliable and accurate results for any RBFs, and, unlike the original RSM, guarantees that the RBF interpolant exists uniquely. The efficacy of this new method, called MPLE-RSM, is tested by numerical experiments on some 1D and 2D benchmark target functions.

Joint work with: Alessandra De Rossi.

References

[1] T.A. Driscoll, A.R.H. Heryudono. Adaptive residual subsampling methods for radial basis function interpolation and collocation problems. *Comput. Math. Appl.*, 53:927–939, 2007.

Discrete Developable Meshes

Victor Ceballos Inza
King Abdullah University of Science and Technology
victor.ceballosinza@kaust.edu.sa

Geometric modeling of developable surfaces is an actively researched topic, with important practical applications ranging from manufacturing and architecture, to art and paper-craft or *origami*. In particular, there still exists a demand for an intuitive design paradigm for composite piecewise C^2-smooth developable surfaces, which decompose into ruled pieces and planar patches. Such a type of surface can be equivalently characterized in several forms, such as:

- defined as torsal ruled surfaces; that is, surfaces containing at least one parametric family of lines, with constant tangent planes along such lines;
- through the theory of isometric mappings, by being mapped to local planar domains;
- surfaces with a singular shape operator; or, equivalently, exhibiting zero Gaussian curvature.

Each of these definitions has been the motivation for new classes of discrete developable meshes in recent work [1, 2]. We review some of these, propose a novel one, and explore related tools for interactive manipulation, such as handle deformation, curve folding, cutting and gluing, and others.

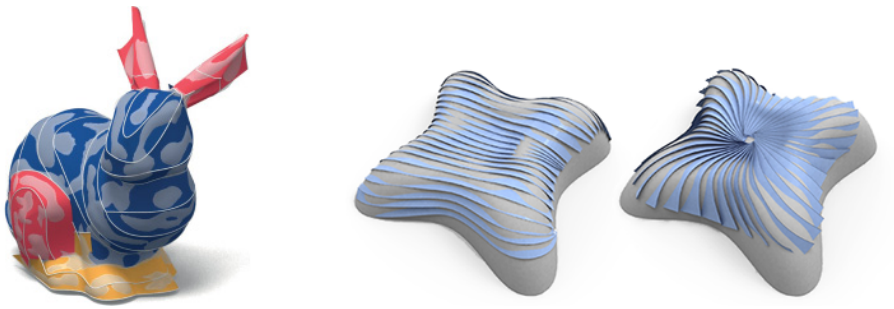

Figure 1: Recent advances in geometric modelling of developable surfaces have produced methods to approximate reference surfaces with piecewise developables (left) and with curve-pleated surfaces (right) [2, 3].

Joint work with: Florian Rist, Johannes Wallner, Helmut Pottmann

References

[1] Caigui Jiang, Cheng Wang, Florian Rist, Johannes Wallner, and Helmut Pottmann. Quad-mesh based isometric mappings and developable surfaces. *ACM Trans. Graph.*, 39(4), jul 2020.

[2] Chengcheng Tang, Pengbo Bo, Johannes Wallner, and Helmut Pottmann. Interactive design of developable surfaces. *ACM Trans. Graph.*, 35(2), jan 2016.

[3] Caigui Jiang, Klara Mundilova, Florian Rist, Johannes Wallner, and Helmut Pottmann. Curve-pleated structures. *ACM Trans. Graph.*, 38(6), nov 2019.

Locally refined quad meshing based on convolutional neural networks

Felix Scholz
Johannes Kepler University Linz
felix.scholz@tafsm.org

We discuss a new method for the generation of locally refined finite element meshes using convolutional neural networks. As a model problem we consider a linear elasticity problem on a two-dimensional domain with holes that has a polygonal boundary.

When applying a Galerkin discretization using quadrilateral finite elements, one usually has to perform adaptive refinement to properly resolve maxima of the stress distribution. Such an adaptive scheme requires a local error estimator and a corresponding local refinement strategy, which leads to a high computational cost. We propose to reduce the complexity of obtaining a suitable discretization by training a neural network whose evaluation replaces the adaptive refinement procedure.

The resulting displacement and distribution of stresses depend on the geometry of the domain and on the boundary conditions. We train a neural network on a large class of possible domains and boundary conditions from different classes of geometric complexity and we analyze its behavior on unseen data.

In order to process the geometry data independently of the underlying discretization scheme, we interpret computational domain and boundary conditions as pixelated images. Likewise, the output of the networks is an grayscale image that predicts the optimal local mesh density distribution. Besides the increased flexibility, this representation makes it possible to employ powerful network architectures based on convolutional networks.

Joint work with: Chiu Ling Chan, Thomas Takacs.

References

[1] C. Chan, F. Scholz, T.Takacs. Locally refined quad meshing for linear elasticity problems based on convolutional neural networks. *submitted.*

Linear-size ε-Emulators for Planar Graphs

Hsien-Chih Chang
Dartmouth College, USA
hsien-chih.chang@dartmouth.edu

We study vertex sparsification for distances, in the setting of planar graphs with distortion: Given a planar graph G (with edge weights) and a subset of k terminal vertices, the goal is to construct an *ε-emulator*, which is a small planar graph G' that contains the terminals and preserves the distances between the terminals up to factor $1+\varepsilon$.

We design the first ε-emulators for planar graphs of linear size $k/\varepsilon^{O(1)}$. In terms of k, this is a dramatic improvement over the previous quadratic upper bound of Cheung, Goranci and Henzinger [ICALP 2016], and breaks below known quadratic lower bounds for exact emulators (the case when $\varepsilon = 0$). Moreover, our emulators can be computed in near-linear time, with applications to fast $(1+\varepsilon)$-approximation algorithms for basic optimization problems on planar graphs such as minimum (s,t)-cut and diameter.

A central technical contribution is to carry out a *spread reduction* for the all-terminal-pairs shortest path problem when the input graph is planar and the terminals all lie on the outerface (called a *one-hole instance*); the *spread* is defined to be the ratio between the largest and the smallest distances between terminals. To construct an emulator for a one-hole instance G we adapt a recursive *split-and-combine* strategy. We will attempt to split the input instance into multiple one-hole instances along some shortest paths that distribute the terminals evenly. Every time we slice the graph G open along a shortest path P, we compute a small collection of vertices on P called the *portals*, that approximately preserve the distances from terminals in G to the vertices on P. We need the portals to be dense enough so that only a small error term will be added to the distortion of the emulator after the gluing; at the same time, the number of portals cannot be too large, as they are added to the terminal set, causing the number of terminals per piece to go down slowly and creating too many pieces. Even when the original input has a polynomial spread to start with, in general we cannot control the spread of all the pieces occurring during the split-and-combine process. Thus new ideas are needed. To this end we prove a combinatorial lemma counting the sum of degrees of big faces in the arrangement of non-crossing shortest paths within a disk.

Joint work with: Zihan Tan and Robert Krauthgamer.

Iterative coordinates

Qingjun Chang
Università della Svizzera italiana
qingjun.chang@usi.ch

Barycentric coordinates provide a simple way of expressing the linear interpolant to data given at the vertices of a triangle and have numerous applications in computer graphics and other fields. The generalization of barycentric coordinates to polygons with more than three vertices is not unique and many constructions have been proposed [3]. Among them, mean value coordinates in [2] stand out by having a simple closed form and being well-defined for arbitrary polygons, but they may take on large negative values in the case of concave polygons, leading to artefacts in applications like shape deformation (see Fig. 1).

We present a modification of mean value coordinates [1] that is based on the observation that the mean value coordinates of some point v inside a polygon can be negative if the central projection of the polygon onto the unit circle around v folds over. By iteratively smoothing the projected polygon and carrying over this smoothing procedure to the barycentric coordinates of v, these fold-overs as well as the negative coordinate values and shape deformation artefacts gradually disappear, and they are guaranteed to completely vanish after a finite number of iterations.

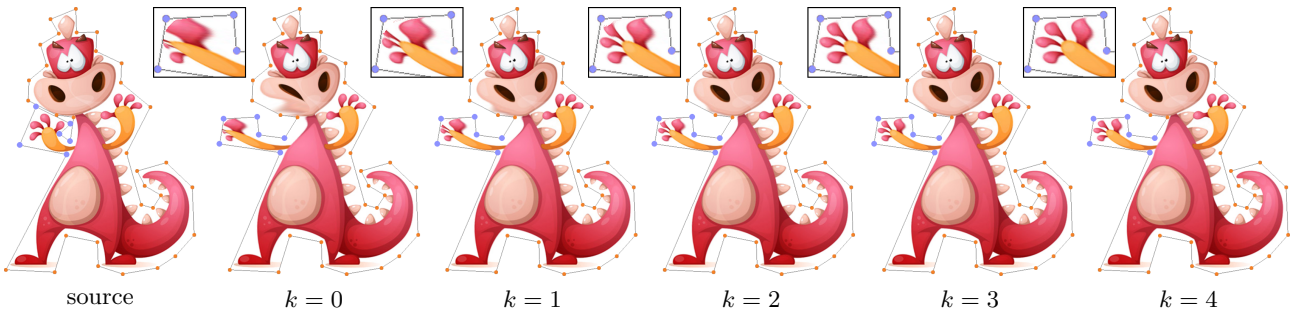

Figure 1: Deformation of a source image (left), obtained by moving six vertices (blue) of the control polygon. The deformation based on mean value coordinates ($k = 0$) exhibits severe artefacts, caused by negative coordinate values. Using iterative coordinates, these deformation artefacts gradually disappear as the number of iterations increases ($k = 1, 2, 3, 4$).

Joint work with: Chongyang Deng, Kai Hormann.

References

[1] C. Deng, K. Hormann and Q. Chang. Iterative coordinates. *Computer Aided Geometric Design*, 79:Article 101861, 2020.

[2] M. S. Floater. Mean value coordinates. *Computer Aided Geometric Design*, 20(1):19–27, 2003.

[3] K. Hormann and N. Sukumar, editors. *Generalized Barycentric Coordinates in Computer Graphics and Computational Mechanics*. Taylor & Francis, CRC Press, Boca Raton, 2017.

Stable Phase Retrieval from Locally Connected Measurements

Cheng Cheng
Sun Yat-sen University
cheng_cheng87@126.com

In finite-dimensional spaces, frames that allow phase retrieval are stable, with a finite stability constant; yet when one considers nested hierarchies of finite-dimensional approximation spaces these constants tend to infinity as the dimension grows, possibly suffering a "curse of dimensionality", i.e. growth may be exponential in the dimension. In this talk, we will consider the locally stable phase retrieval for frames in infinite-dimensional or finite-but large-dimensional Banach spaces. To study the local stability of phase retrievable signals, we introduce the notion of "locally stable and conditionally connected" (LSCC) measurement scheme associated with frames. We then characterize the phase retrieval stability of the signal by two measures that are commonly used to quantify the connectivity of the graph: the Cheeger constant and the algebraic connectivity.

Joint work with: Ingrid Daubechies, Nadav Dym, Jianfeng Lu.

Lattices enumeration via linear programming.

Moulay Abdellah CHKIFA
Université Mohammed 6 Polytechnique, Maroc
abdellah.chkifa@um6p.ma

Given a positive integer d and $\boldsymbol{a}^{(1)}, \dots, \boldsymbol{a}^{(m)}$ m vectors in $\mathbb{R}^d$, $\{k_1\boldsymbol{a}^{(1)} + \cdots + k_m\boldsymbol{a}^{(m)} : k_1, \dots, k_m \in \mathbb{Z}\} \subset \mathbb{R}^d$ is the so-called lattice generated by the family of vectors, or by the matrix $\boldsymbol{A} = (\boldsymbol{a}^{(1)}|\dots|\boldsymbol{a}^{(m)}) \in \mathbb{R}^{d\times m}$. In high dimensional integration, prescribed lattices are used for constructing reliable quadrature schemes. The quadrature points are the lattice points lying on the integration domain, typically the unit hypercube $[0,1)^d$ or a shifted hypercube. It is crucial to be able to enumerate the lattice points in such domains inexpensively. Undeniably, the lack of fast enumeration procedures hinders the applicability of lattice rules. Existing enumeration procedures exploit intrinsic properties of the lattice at hand, such as $\mathbb{Z}$-periodicity, orthogonality, recurrences, etc, e.g. [1, 2, 3, 4]. We present a general-purpose lattice enumeration strategies based on linear programming, [5]. We demonstrate how to combine duality and parametric linear programming in order to accelerate these strategies, producing performances comparable to the enumeration strategies that are fine-tuned to special lattices. In addition, we discuss a variety of relaxation and reduction techniques that allow further acceleration of the introduced algorithms. Numerical experiments in high dimension are also presented.

References

[1] I.H. Sloan and S. Joe. *Lattice Methods for Multiple Integration*. Oxford University Press, New York, 1994.

[2] C. Kacwin, J. Oettershagen, and T. Ullrich. On the orthogonality of the Chebyshev-Frolov lattice and applications. *Monatsh Math*, 184:425–441, 2017.

[3] C. Kacwin, J. Oettershagen, M. Ullrich, and T. Ullrich. Numerical performance of optimized Frolov lattices in tensor product reproducing kernel Sobolev spaces. *Found Comput Math* 21, 849–889 (2021).

[4] K. Suzuki and T. Yoshiki. Enumeration of the Chebyshev-Frolov lattice points in axis-parallel boxes. *Hiroshima Math. J.*, 49(1):139–159, 2019.

[5] M.A. CHKIFA. Lattices enumeration via linear programming. Submitted to *Numerische Mathematik*.

Efficient evaluation of Bézier-type objects and their derivatives

Filip Chudy
Institute of Computer Science, University of Wrocław, Poland
filip.chudy@cs.uni.wroc.pl

A linear-time algorithm for computing a point on a polynomial or rational curve in Bézier form with good geometric and numerical properties has been recently given in [2]. This approach has also found applications in accelerating the evaluation of Bézier surfaces and even B-spline curves (for details, see [1]). We show that the method proposed in [2] can be generalized to efficiently compute the quantities $R'_n(t), R''_n(t), \ldots, R^{(k)}_n(t)$, where R_n is a d-dimensional rational Bézier curve of degree n and $t \in [0, 1]$. Moreover, the algorithm may be adapted for a more general family of rational parametric objects. Some remarks are given about applying it to Bézier surfaces.

Joint work with: Paweł Woźny (Institute of Computer Science, University of Wrocław, Poland)

References

[1] F. Chudy, *New algorithms for Bernstein polynomials, their dual bases and B-spline functions*, Ph.D. Thesis, University of Wrocław, 2022 (available on request).

[2] P. Woźny and F. Chudy, Linear-time geometric algorithm for evaluating Bézier curves, *Computer Aided-Design* 118 (2020), 102760.

To be announced

Tikhonov Regularization of Circle-Valued Signals

Laurent Condat
King Abdullah University of Science and Technology (KAUST), Thuwal, Saudi Arabia
contact: see webpage `https://lcondat.github.io/`

It is common to have to process signals or images whose values are cyclic and can be represented as points on the complex circle, like wrapped phases, angles, orientations, or color hues. We consider a Tikhonov-type regularization model to smoothen or interpolate circle-valued signals defined on arbitrary graphs. We propose a convex relaxation of this nonconvex problem as a semidefinite program, and an efficient algorithm to solve it.

Let $\mathbb{S} = \{z \in \mathbb{C} \ : \ |z| = 1\}$ denote the complex unit circle. We want to estimate a signal $x = (x_n)_{n\in V}$, with values $x_n \in \mathbb{S}$, defined on an undirected graph (V, E), where V is the set of nodes and E is the set of edges, which are sets of two distinct nodes. Typically, we are given a noisy signal $y = (y_n)_{n\in V}$ defined on the same graph and the sought signal x is a smoothed, or denoised, version of y, which achieves a tradeoff between closeness to y and smoothness, in some sense.

For real-valued signals, Tikhonov-regularized smoothing consists in solving the following convex problem: given $y = (y_n)_{n\in V}$ and nonnegative weights $(w_n)_{n\in V}$ and $(\lambda_{n,n'})_{\{n,n'\}\in E}$, $x = (x_n)_{n\in V}$ is the solution to

$$\underset{x_n\in\mathbb{R}\,:\,n\in V}{\text{minimize}} \sum_{n\in V} \frac{w_n}{2}(x_n - y_n)^2 + \sum_{\{n,n'\}\in E} \frac{\lambda_{n,n'}}{2}(x_n - x_{n'})^2. \tag{1}$$

We formulate a similar problem for signals x and y with values in $\mathbb{S}$. For this, we adopt a Bayesian view and replace the Gaussian distribution, whose anti-log-likelihood gives the squared differences in (1), by the von Mises distribution. This yields the nonconvex problem

$$\underset{x_n\in\mathbb{S}\,:\,n\in V}{\text{minimize}} \sum_{n\in V} w_n\big(1 - \Re(x_n y_n^*)\big) + \sum_{\{n,n'\}\in E} \lambda_{n,n'}\big(1 - \Re(x_n x_{n'}^*)\big), \tag{2}$$

where $\Re$ denotes the real part and $\cdot^*$ denotes the complex conjugation. The main contribution of this work is a new convex relaxation of this nonconvex problem, which takes the form of linear minimization over the product of complex elliptopes. It originates from a fomulation using optimal transport of measures on the circle, parameterized by a finite number of their Fourier coefficients [2]. The benefits of the proposed approach will be illustrated with numerical experiments, like the one in Figure 1. This work is described in [1].

[1] L. Condat, "Tikhonov Regularization of Circle-Valued Signals," preprint arXiv:2108.02602, 2021.
[2] L. Condat, "Atomic norm minimization for decomposition into complex exponentials and optimal transport in Fourier domain,' Journal of Approximation Theory, vol. 258, Oct. 2020.

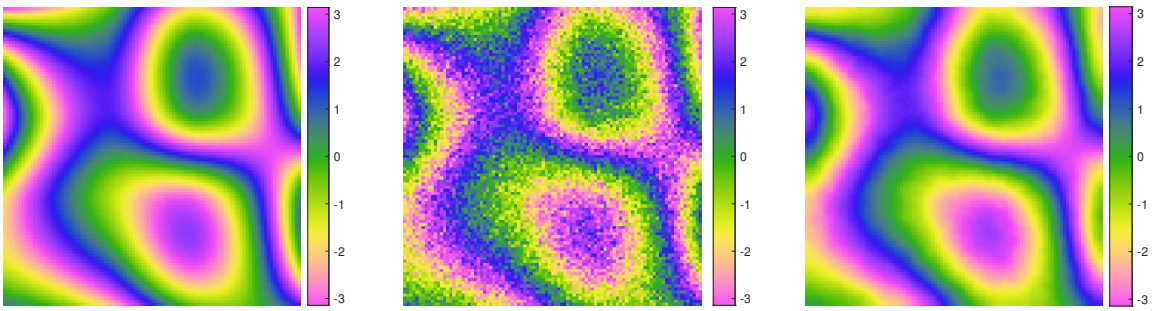

(a) (b) (c)

Figure 1: Denoising of a circle-valued image: (a) the ground-truth image, (b) the noisy image, (c) the image denoised with the proposed method, for which the convex relaxation is exact: the image is the exact solution of the nonconvex problem. All images have their values in $\mathbb{S}$, whose argument in $(-\pi, \pi]$ is displayed using a cyclic colormap.

Multiple Multiresolution Analysis for Image Compression

Mariantonia Cotronei
Università Mediterranea di Reggio Calabria, Italy
mariantonia.cotronei@unirc.it

We present a technique for compressing images based on their multiple multiresolution decomposition. As an extension of standard wavelet and wavelet-like approaches, in a multiple multiresolution analysis data are processed with a tree of filterbanks consisting of filters and decimation matrices that can vary depending on the level. Our algorithm takes advantage of the redundancy in the transformed image by employing an efficient selection strategy of the portion of coefficients to be kept while still retaining most of the energy of the data. Furthermore, our method is able to capture the peculiar anisotropic information of the image while maintaining a low implementation complexity thanks to an efficient filterbank implementation and to the possibility of expressing the employed 2-D filters in an almost separable aspect [1, 2].

Joint work with: Dörte Rüweler and Tomas Sauer (Univertität Passau, Germany).

References

[1] M. Cotronei, M. Rossini, T. Sauer, and E. Volontè. Filters for anisotropic wavelet decompositions. *J. Comput. Appl. Math.*, 349:316–330, 2019.

[2] M. Cotronei, D. Rüweler, and T. Sauer. Multiple filterbanks for image processing: Implementation issues. *Math. Comput. Simul.*, 176:147 – 159, 2020.

Negative curvature obstructs acceleration for geodesically convex optimization, even with exact first-order oracles

Christopher Criscitiello
EPFL, Switzerland
christopher.criscitiello@epfl.ch

Optimization on nonlinear manifolds has applications in many areas, including machine learning, statistics, robotics, imaging and even computational complexity theory. We show that when the underlying manifold is negatively curved, optimization can be more difficult than in (flat) Euclidean spaces. The talk will provide a brief introduction to manifolds, curvature, optimization on manifolds and its applications, and Nesterov's accelerated gradient method in Euclidean spaces. We will then present our main results, which show that acceleration (in the sense of Nesterov's accelerated gradient method) is unachievable in a large class of negatively curved Riemannian manifolds when the algorithm receives *exact* gradient and function value information. Our work builds on the recent work of Hamilton and Moitra [1] who show that acceleration on the class of strongly geodesically convex functions is unachievable in the hyperbolic plane when the algorithm receives gradients and function values corrupted by a small amount of *noise*.

Joint work with: Nicolas Boumal.

References

[1] L. Hamilton and A. Moitra, No-go Theorem for Acceleration in the Hyperbolic Plane. arXiv: 2101.05657. 2021. https://arxiv.org/abs/2101.05657

Blending lower-dimensional sparse interpolants

Annie Cuyt
University of Antwerp
Antwerpen, Belgium
annie.cuyt@uantwerpen.be

Multi-dimensional sparse interpolation, as presented in [2], works very well when the underlying physical phenomenon $f(X), X = (x_1, \ldots, x_d)$ truly behaves according to the model

$$f(X) = \sum_{j=1}^{n} \alpha_j \exp(\langle \phi_j, X \rangle), \qquad \phi_j = (\phi_{j1}, \ldots, \phi_{jd}) \in \mathbb{C}^d, \qquad \langle \phi_j, X \rangle = \sum_{k=1}^{d} \phi_{jk} x_k$$

on the whole d-dimensional space. However, in some particular cases, such as in [1], this model only holds for lower-dimensional subspaces and thus the method discussed in [2] cannot be applied.

Since the exponential model does hold on lower-dimensional subspaces, one can take advantage of this to develop a new strategy. We propose to blend the lower-dimensional models into one large model for the whole space.

Joint work with: Ferre Knaepkens (University of Antwerp, Belgium).

References

[1] Abdelmajid Ben Yahya, Nick Van Oosterwyck, Ferre Knaepkens, Simon Houwen, Stijn Herregodts, Jan Herregodts, Bart Vanwalleghem, Annie Cuyt, and Stijn Derammelaere. CAD based design optimization of four-bar mechanisms: a coronaventilator case study. *Mechanics Based Design of Structures and Machines*, 2022.

[2] Annie Cuyt and Wen-shin Lee. Multivariate exponential analysis from the minimal number of samples. *Adv. Comput. Math.*, 44:987–1002, 2018. (Published online November 16, 2017).

Image Segmentation Using Hidden Markov Models and convolutional neural network

DALIMI Hanane
Departement of physics, University Hassan II Casablanca
hanane.dalimi@gmail.com

- Artificial neural networks (ANNs) reflect the behavior of the human brain, allowing computer programs to recognize patterns and solve common problems in the fields of Artificial Intelligence. Bayesian methods have been applied in recent years to neural networks by various authors MacKay1992, MacKay92, Neal1992, Mangi2018, Zhaoying2020, Gao2021.In this work, We propose to use hidden Markov model (HMM) to weight the fields and finally use convolutional neural network (CNN) segment images. Promising experiment results are achieved on the RGB-D images.

Joint work with: AFIFI Mohames, AMAR Said.

References

[1] D. J. C. MacKay. Bayesian interpolation. *Neural Computation* ,4(3), 415–447, 1992.

[2] D. J. C. MacKay. A Practical Bayesian Framework for Backpropagation Networks. *Neural Computation* ,4(3), 448-472, 1992.

[3] R. M. Neal. Bayesian Training of Backpropagation Networks by the Hybrid Monte Carlo Method. *Technical Report CRG-TR-92-1, Department of Computer Science, University of Toronto* ,1992.

[4] K. Mangi, A. Jaelim, L. Kichun . Opinion mining using ensemble text hidden Markov models for text classification. *Expert Systems with Applications*, Volume 94, Pages 218—227, 15 March 2018.

[5] L. Zhaoying, K. Haipeng, Z. Ting , L. Yujian. DUKMSVM: A Framework of Deep Uniform Kernel Mapping Support Vector Machine for Short Text Classification. *Appl. Sci.* , 10(7), 2348, 2020.

[6] B. Gao , Z. Wenqiang. A Method of Combining Hidden Markov Model and Convolutional Neural Network for the 5G RCS Message Filtering. *Appl. Sci.* ,11, 6350, 2021.

Quadrilateral mesh create from a given cross field

Kokou Dotse, Vincent Mouysset, Sébastien Pernet
ONERA
kokou.dotse@onera.fr
vincent.mouysset@onera.fr
sebastien.pernet@onera.fr

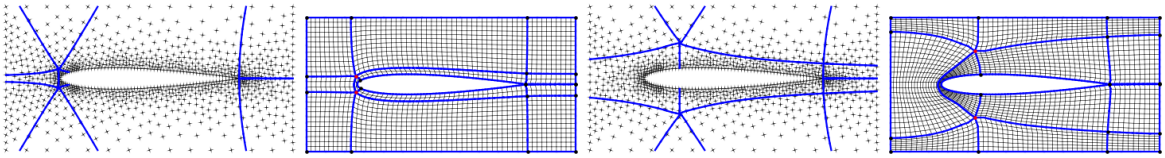

Figure 1: Representation of quadrilateral meshes from two different cross fields

Several high precision schemes with excellent quality and efficiency properties are built on quadrilateral meshes. However, the automatic generation of quadrilateral meshes with good quality elements is still a challenge. The method proposed in the article is of great interest with a final mesh structured by block, respecting the geometry and with good quality elements. However, it has some limitations, such as its unable to produce on very stretched geometries or on some domains without corners (for example, a 2D ring), a valid cross field which is the main notion on which the method is based. On the other hand, the variant of the Ginzburg-landau theory presented in [2] does not allow to deal with non-simply connected domains. In our work, we propose a new point of view allowing to solve the above mentioned limitations while keeping the structured aspect of the mesh and opening other possibilities on the generation of the cross field. To do this, our idea is to abstract, within the method, the generation of the cross-fields from the rest of partitioning process. We give ourselves a representation field which we then process in order to obtain a partitioning in blocks of 4 sides. We thus obtain different meshes according to the initial representation field.

More concretely, let Ω be a bounded domain and $\partial\Omega$ its boundary. We have $\Omega = \cup_i \Gamma_i$ when Ω is a non-simply connected domain and Γ_i, $\forall i$ denotes the connected components of $\partial\Omega$. We give ourselves a cross field u_c such that $deg(u_c, \partial\Omega) = deg(N_c, \partial\Omega)$ where N_c is the cross field associated with the normal of $\partial\Omega$, [2] and $deg(u_c, \partial\Omega)$, $deg(N_c, \partial\Omega)$ denote the Brouwer degrees of u_c and N_c on $\partial\Omega$ respectively. We then look for a field of angle ϕ on $\partial\Omega$ in order to align u_c on N_c by the rotation of angle ϕ of u_c. Our calculation of ϕ is inspired by the work presented in [2]. It consists in continuously propagating through the domain the angular difference between N_c and u_c which will allow to rectify the initial field and to align it on N_c. We strengthen this correction by introducing a new field w characterized by the formula $deg(w, \Gamma_i) = deg(N_c, \Gamma_i) - deg(u_c, \Gamma_i)$, $\forall i$. The introduction of this new field w is necessary when the initial cross field u_c does not respect the degree hypotesis presented above. This is especially the case when Ω is a non-simply connected domain where the Brouwer degree hypothesis is not necessarily respected on each connected component of $\partial\Omega$.

Our reformulation keeps the interesting property of producing structured block meshes while allowing to benefit from cross fields coming from the user. In our presentation, we will detail our reinterpretation and explain our argument with some algorithms, and then show the contribution of our point of view through several examples.

References

[1] N. Kowalski, F. Ledoux, and P. Frey, A PDE based approach to multi-domain partitionning and quadrilateral meshing, 2012, https://hal.sorbonne-universite.fr/hal-01076754

[2] R. Viertel and B. Osting, An Approach to Quad Meshing Based on Harmonic Cross-Valued Maps and the Ginzburg–Landau Theory, 2019, SIAM Journal on Scientific Computing

A framework for bilevel optimization that enables stochastic and global variance reduction algorithms

Mathieu Dagréou
Université Paris-Saclay, Inria, CEA, Palaiseau, 91120, France
mathieu.dagreou@inria.fr

Bilevel optimization, the problem of minimizing a *value function* which involves the arg-minimum of another function, appears in many areas of machine learning such as hyperparameter selection [4], neural architecture search [3] or Deep Equilibrium Networks [1]. In a large scale setting where the number of samples is huge, it is crucial to develop stochastic methods, which only use a few samples at a time to progress.

However, computing the gradient of the value function involves solving a linear system, which makes it difficult to derive unbiased stochastic estimates. To overcome this problem we introduce a novel framework, in which the solution of the inner problem, the solution of the linear system, and the main variable evolve at the same time. These directions are written as a sum, making it straightforward to derive unbiased estimates. The simplicity of our approach allows us to develop global variance reduction algorithms, where the dynamics of all variables is subject to variance reduction.

In this framework, we propose SOBA, a natural extension of stochastic gradient descent, and SABA, a natural adaptation of the variance reduction algorithm SAGA [2]. We demonstrate that SABA has $O(\frac{1}{T})$ convergence rate, and that it achieves linear convergence under Polyak-Łojasciewicz assumption. This is the first stochastic algorithm for bilevel optimization that verifies either of these properties. Numerical experiments on hyperparameter selection for ℓ^2-regularized logistic regression (Figure 1) validate the usefulness of our method.

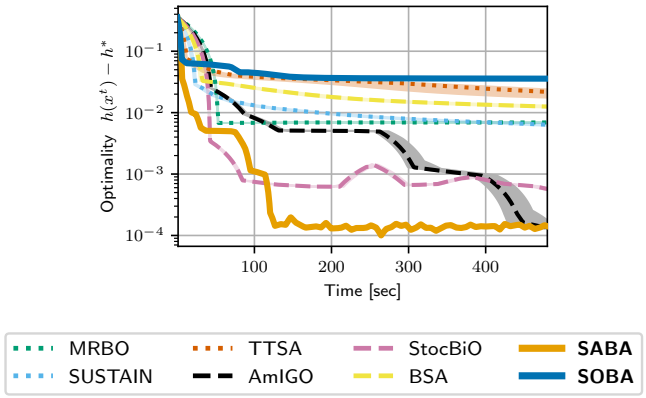

Figure 1: Suboptimality gap for hyperparameter selection for ℓ^2 penalized logistic regression on IJCNN1 dataset

Joint work with: Pierre Ablin, Samuel Vaiter, Thomas Moreau.

References

[1] S. Bai, J. Z. Kolter, V. Koltun. Deep Equilibrium Models. In *Advances in Neural Information Processing Systems (NeurIPS)*, 2019.

[2] A. Defazio, F. Bach, S. Lacoste-Julien. SAGA: A Fast Incremental Gradient Method With Support for Non-Strongly Convex Composite Objectives. In *Advances in Neural Information Processing Systems (NeurIPS)*, 2014.

[3] H. Liu, K. Simonyan, Y. Yang. Darts: Differentiable architecture search. In *International Conference on Learn-ing Representations (ICLR)*, 2018.

[4] F. Pedregosa. Hyperparameter optimization with approximate gradient. In *International Conference on MachineLearning (ICML)*, 2016.

Spherical cap discrepancy of perturbed lattices under the Lambert projection

Damir Ferizović
KU Leuven
damir.ferizovic@kuleuven.be

Given any full rank lattice $\Lambda \subset \mathbb{R}^2$ and a natural number N, we regard the point set $\Lambda/N \cap (0,1)^2$ under the Lambert map to the unit sphere $\mathbb{S}^2$, and show that its spherical cap discrepancy is at most of order N, with leading coefficient given explicitly and depending on Λ only. The proof is established using a lemma that bounds the amount of intersections of certain curves with fundamental domains that tile $\mathbb{R}^2$, and even allows for local perturbations of Λ without affecting the bound, proving to be stable for numerical applications. A special case yields the smallest constant for the leading term of the cap discrepancy for deterministic algorithms up to date.

References

[1] D. Ferizović. Spherical cap discrepancy of perturbed lattices under the Lambert projection. *In Preparation*, 2022.

From (β, γ)-Chebyshev functions of the interval to (β, γ)-Lissajous curves of the square

Francesco Marchetti
Dipartimento di Matematica "Tullio Levi-Civita" - Università degli Studi di Padova
francesco.marchetti@math.unipd.it

Chebyshev polynomials are a classical topic in scientific literature, and they have been considered in many fields of research. For example, the related zeros are particularly suitable for polynomial interpolation on the interval $[-1, 1]$ due to their well conditioning. Moreover, the extrema of Chebyshev polynomials, along with the set $\{-1, 1\}$, form the set of *Chebyshev-Lobatto* (CL) points, which are *quasi-optimal* interpolation nodes as well [1, 2]. In [3], we introduced and analysed a new class of (β, γ)-Chebyshev functions and points, which can be seen as a generalisation of classical Chebyshev polynomials and points (see Figure 1). The achieved theoretical findings have been employed in [4] for reducing the effects of both Runge's and Gibbs phenomena, in the framework of the *fake nodes approach* [5].

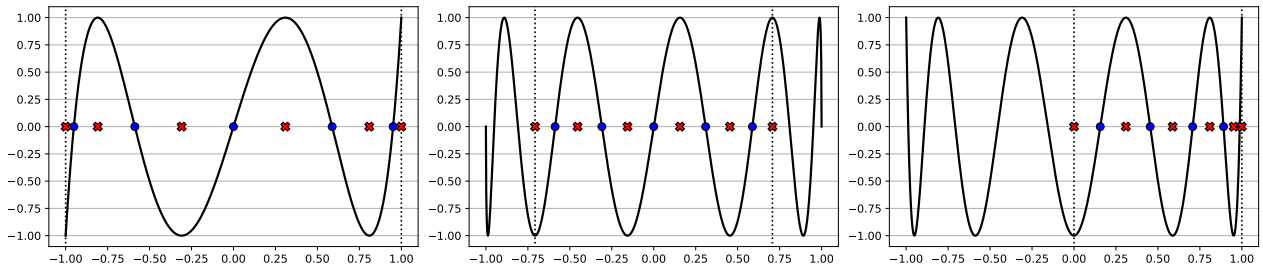

Figure 1: Left: an example of Chebyshev polynomial (solid line), Chebyshev points of the first kind (blue circles) and CL points (red crosses). Centre and right: two examples of (β, γ)-Chebyshev functions (solid line), (β, γ)-Chebyshev points (blue circles) and (β, γ)-CL points (red crosses). Depending on the choice of the parameters, they can be symmetric or not with respect to the origin.

In the square $[-1, 1]^2$, unions of tensor-product Chebyshev grids provide sets of nodes that guarantee a stable polynomial interpolation process and that can be characterised as self-intersection or square-tangency points of Lissajous curves [6]. This paves the way for the study of (β, γ)-Chebyshev grids and for the analysis of polynomial approximation schemes along (β, γ)-Lissajous curves in $[-1, 1]^2$, in view of designing a unified generalised framework.

Joint work with: Stefano De Marchi, Giacomo Elefante.

References

[1] T.J. Rivlin An Introduction to the Approximation of Functions. *Dover Publications*, New York, 1969.

[2] J.C. Mason, D.C. Handscomb Chebyshev Polynomials (1st ed.). *Chapman and Hall/CRC*, 2002.

[3] S. De Marchi, G. Elefante, F. Marchetti. On (β, γ)-Chebyshev functions and points of the interval. *J. Approx. Theory*, 105634, 2021.

[4] S. De Marchi, G. Elefante, F. Marchetti. Stable discontinuous mapped bases: the Gibbs-Runge-Avoiding Stable Polynomial Approximation (GRASPA) method. *Comp. Appl. Math.*, 40:299, 2021.

[5] S. De Marchi, F. Marchetti, E. Perracchione, D. Poggiali. Polynomial interpolation via mapped bases without resampling. *J. Comput. Appl. Math.*, 364:112347, 2020.

[6] W. Erb, C. Kaethner, P. Dencker, M. Ahlborg. A survey on bivariate Lagrange interpolation on Lissajous nodes. *Dolom. Res. Notes on Approx.*, 8:23–36, 2015.

Manifold rewiring for unlabeled imaging in large noise

Valentin Debarnot
Univerty of Basel
valentin.debarnot@unibas.ch

In X-ray tomography the task is to reconstruct an unknown density from its projections in a number of directions. Stable recovery requires a sufficient number of projections and the knowledge of the relative projection angles. In some applications, however, projection angles are unknown; an important example is single-particle Cryo-EM. With small or moderate noise it is relatively straightforward to infer the viewing directions in Cryo-EM [1]. As the noise increases, direction recovery becomes hard. We propose a general graph-learning framework to recover unknown parameters in Cryo-EM-like problems where the unknown quantity (such as viewing direction) has a manifold structure.

Concretely, let $\mathcal{M}$ denote a smooth manifold and $\mu \in \mathcal{P}_1(\mathcal{M})$ a probability measure on $\mathcal{M}$. We observe (very) noisy measurements through a function $f : \mathcal{M} \to \mathbb{R}^N$,

$$y_i = f(\theta_i) + \eta_i, \tag{1}$$

where $\theta_i \overset{i.i.d.}{\sim} \mu$, and $\eta_i \overset{i.i.d.}{\sim} \mathcal{N}(0, \sigma^2 \mathrm{I}_N)$ is a Gaussian random vector. Put differently, we observe $y_i \overset{i.i.d.}{\sim} \nu$ where $\nu \overset{\text{def.}}{=} f_{\#}\mu \star \mathcal{N}(0, \sigma^2 \mathrm{I}_N)$, $f_{\#}\mu$ denotes the pushforward of μ by f, and $\star$ is the convolution of measures.

Fig. 1 shows an embedding of 3D Cryo-EM projections. The underlying metric quotients out the so-called in-plane rotations so the embedding lives on $\mathbb{SO}(3)/\mathbb{S}^1 \simeq \mathbb{S}^2$ rather than $\mathbb{SO}(3)$ [2]. The function f corresponds to the 3D X-ray transform and the underlying manifold is $\mathcal{M} = \mathbb{S}^2$, see Fig. 1a. In the absence of noise, the parameters $(\theta_i)_i$ on the sphere can be deduced from the graph Laplacian embedding of the measurements $(y_i)_i$; Fig. 1b. For large noise, the graph Laplacian embedding collapses and the relative position of the observation cannot be deduced; Fig. 1c.

This is because the noisy neighborhood graph contains false and misses true links. We propose to use the recent WalkPooling neural network architecture [3] to denoise the K-NN graph. The WalkPooling architecture captures the topological properties of $\mathcal{M}$ by learning to construct graphs from points sampled from the distribution μ. This leads to significant improvements in embedding quality and enables reconstruction at extreme noise levels; Fig. 1d.

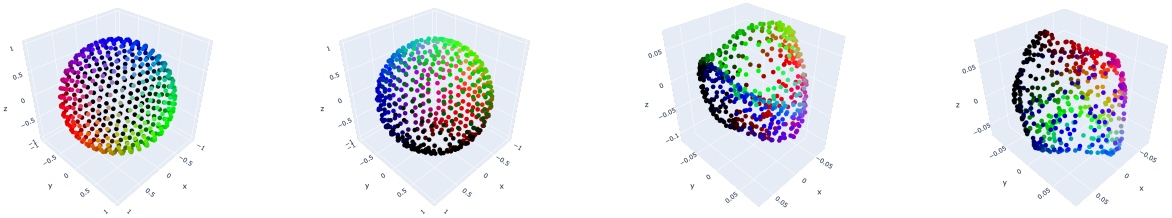

(a) Underlying manifold: S^2. (b) Noiseless embedding. (c) Noisy embedding(0dB). (d) WalkPooling (0dB).

Figure 1: Single particle 3D cryo-EM motivation example: the measurments are function of parameters in S^2. The Graph-Laplacian embedding allows to retrieve the relative position of each projection only using WalkPooling to denoise the graph.

Joint work with: Ivan Dokmanić, Vinith Kishore, Cheng Shi.

References

[1] Ronald R Coifman, Yoel Shkolnisky, Fred J Sigworth, and Amit Singer. Graph laplacian tomography from unknown random projections. *IEEE Transactions on Image Processing*, 17(10):1891–1899, 2008.

[2] Yoel Shkolnisky and Amit Singer. Viewing direction estimation in cryo-em using synchronization. *SIAM journal on imaging sciences*, 5(3):1088–1110, 2012.

[3] Liming Pan, Cheng Shi, and Ivan Dokmanić. Neural link prediction with walk pooling. In *International Conference on Learning Representations*, 2022.

Blind inverse problems with isolated spikes

Valentin Debarnot
Univerty of Basel
valentin.debarnot@unibas.ch

Assume that an unknown integral operator living in some known subspace is observed indirectly, by evaluating its action on a discrete measure containing a few isolated Dirac masses at an unknown location. Is this information enough to recover the impulse response location and the operator with a sub-pixel accuracy? We study this question and bring to light key geometrical quantities for exact and stable recovery. We also propose an in depth study of the presence of additive white Gaussian noise. We illustrate the well-foundedness of this theory on the challenging optical imaging problem of blind deconvolution and blind deblurring with unstationary operators.

This work is based on the preprint [1].

Joint work with: Pierre Weiss.

References

[1] Valentin Debarnot and Pierre Weiss. Blind inverse problems with isolated spikes. *arXiv preprint arXiv:2111.02093*, 2021.

A checkerboard pattern approach to isothermic surfaces

Felix Dellinger
TU Vienna; TU Graz
felix.dellinger@tuwien.ac.at

A checkerboard pattern is a quadrilateral net with $\mathbb{Z}^2$ combinatorics where every second face is a parallelogram. Such a mesh can be easily obtained through midpoint subdivision from a general quadrilateral net. The structure of a checkerboard pattern is very suitable to describe discrete differential geometric properties of the net. In particular, we can use it to consistently define conjugate nets, principal curvature nets, a shape operator and Koenigs nets.

We find that the class of discrete principal curvature nets is invariant under Möbius transformations and can be studied in the projective model of Möbius geometry. Koenigs nets are exactly those nets that allow a discrete dualization. Analogously to the smooth case, they can be characterized by the existence of certain osculating conics (compare [1]) or by the equality of their Laplace invariants.

Isothermic nets can then be characterized as Koenigs nets that are also principal curvature nets. Again we can transform them using the Möbius transformation or dualization. The combination of both allows us to easily create examples of discrete minimal surfaces and their Goursat transformations.

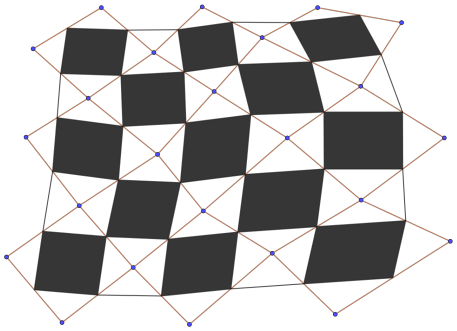

Figure 1: A checkerboard pattern created by midpoint subdivision. Every black face is a parallelogram.

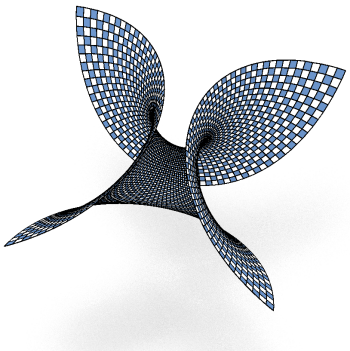

Figure 2: An isothermic checkerboard pattern on a discrete version of the Enepper surface.

References

[1] A. Doliwa. Geometric discretization of the Koenigs nets. *Journal of Mathematical Physics*, 44:2234-2249, 2003.

Weighted least-squares approximation in expected L^2 norm

Matthieu Dolbeault
Sorbonne Université
matthieu.dolbeault@sorbonne-universite.fr

We investigate the problem of approximating a function u in L^2 with a linear space of functions of dimension n, using only evaluations of u at m chosen points, with m of the order of n. A first approach [2], based on weighted least-squares at i.i.d random points, provides a near-best approximation of u, but requires m of order $n\log(n)$. To reduce the sample size while preserving the quality of approximation, we need a result on sums of rank-one matrices from [3], which answers to the Kadison-Singer conjecture. The results presented here, expressed in expected L^2 norm of the approximation error, can be found in [1] and will be compared to alternative approaches [4, 5].

Joint work with: Albert Cohen.

References

[1] A. Cohen and M. Dolbeault. Optimal pointwise sampling for L2 approximation. *Journal of Complexity*, 68, 101602, 2022.

[2] A. Cohen and G. Migliorati. Optimal weighted least squares methods. *SMAI Journal of Computational Mathematics*, 3, pages 181–203, 2017.

[3] A. Marcus, D. Spielman and N. Srivastava. Interlacing families II: Mixed characteristic polynomials and the Kadison-Singer problem. *Annals of Mathematics* pages 327–350, 2015.

[4] N. Nagel, M. Schäfer, and T. Ullrich. A new upper bound for sampling numbers. *Foundations of Computational Mathematics*, pages 1–24, 2021.

[5] V. N. Temlyakov. On optimal recovery in L^2. *Journal of Complexity*, 65, 101545, 2020.

Multivariate Up-like Functions

Nira Dyn

School of Mathematical Sciences, Tel Aviv University, Israel

l

This talk presents the generation of multivariate C^∞ functions with coompact small supports by non-stationary subdivision schemes. Following the construction of such a univariate function, called "Up function", by a non-stationary scheme based on masks of stationary schemes generating B-splines of growing degrees, we term the multivariate functions we generate Up-like functions, and generate them by non-stationary schemes based on masks of stationary schemes generating box-splines of growing supports .

To analyze the convergence and smoothness of these non-stationary schemes, we develped new tools for analyizing convergence and smoothness of certain classes of non-stationary schemes which are wider than the class of schemes generating Up-like functions. These new tools are also presented in the talk, as well as a method for achieving small compact supports, by which we obtain in the univariate case Up-like functions with supports $[0, 1+\epsilon]$, with ϵ arbitrarily small, in comparison to the support $[0, 2]$ of the Up function.

Joint work with: Maria Charina, Costanza Conti

niradyn@tauex.tau.ac.il

C^2 quartic splines on mixed macro-structures

Salah Eddargani
MISI Laboratory, Hassan First University of Settat, Settat 26000, Morocco
s.eddargani@gmail.com

The polynomial spline functions defined on triangulations are tools widely used in many different fields, both theoretical and applied [1]. It is well known that C^r-regularity of a spline on a given triangulation is obtained if all derivatives up to order $2r$ at the vertices of the triangles, in which case the degree must be greater than or equal to $4r + 1$ [2]. As in practice it is essential to use splines of the lowest degree for a given class, different finite elements obtained by subdividing every triangle have been introduced and analysed in the literature, among them the Clough-Tocher (3-CT), Powell-Sabin (6-PS) and Morgan-Scott (MS-) splits [3, 4, 5], so that C^2 smoothness results, for minimum degrees 6, 5 and 5, respectively. The construction of C^2-continuous quartic splines on a triangulation endowed with a mixed split consisting of macro-triangles with PS-6 or Modified Morgan-Scott (MMS-10) refinements is addressed. Indeed, in [5, 6] it is proved that under a certain geometrical conditions between macro-triangles and edge split points, the space of almost C^2-continuous splines introduced in [7] becomes a subspace of the space of C^2-continuous functions. Joining the opposite vertices of every two triangles sharing an edge gives, in general, a mixed-type triangulation in the above sense. This procedure may result in a PS-6 refinement or an MS-split, from which an MMS-10 split is easily obtained.

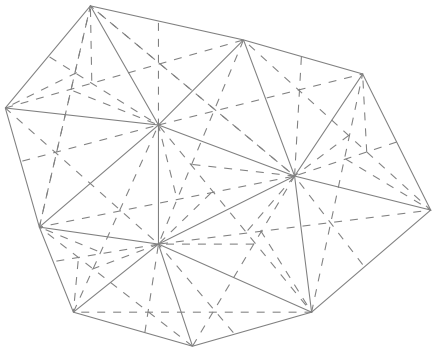

For the mixed-type sub-triangulation, the construction of a basis of B-spline-like functions will be provided to establish a suitable representation of the C^2-continuous functions of the space.

Joint work with: Domingo Barrera Rosillo.

References

[1] M. J. Lai, L.L. Schumaker. Spline Functions on Triangulations, *CUP, Cambridge*, 2007.

[2] A. Ženíšek. A general theorem on triangular finite $C^{(m)}$-elements, *Rev Fr Automat Infor Analyse numérique*, 8(R2) (1974) 119–127.

[3] R. W. Clough, J. L. Tocher. Finite element stiffness matrices for analysis of plates in bending, *Proc. Conference on Matrix Methods in Structural Mechanics, Wright-Paterson A. F. B., Ohio*, 515–545, 1985.

[4] M. Powell, M. Sabin. Piecewise quadratic approximations on triangles, *ACM Trans Math Softw* 3 (1977) 316–325.

[5] D. Sbibih, A. Serghini, A. Tijini. C^1 quadratic and C^2 quartic macro-elements on a modified Morgan-Scott triangulation, *Mediterr J Math*, 10 (2013) 1273–1292.

[6] D. Barrera, S. Eddargani, M. J. Ibáñez, A. Lamnii, A geometric characterization of Powell-Sabin triangulations allowing the construction of C^2 quartic splines,*Computers & Mathematics with Applications* 100 (2021) 30–40.

[7] J. Grošelj, M. Krajnc. Quartic splines on Powell-Sabin triangulations, *Comput Aided Geom Design*, 49 (2016) 1–16.

Influence of Monte-Carlo sampling on the convergence rates of greedy algorithms for reduced-basis methods

Virginie Ehrlacher
Ecole Nationale des Ponts et Chaussées & INRIA
virginie.ehrlacher@enpc.fr

In this talk will be presented recent results about the mathematical study of the algorithm proposed in [1] where the authors proposed a variance reduction technique for the computation of parameter-dependent expectations using a reduced basis paradigm. We study the effect of Monte-Carlo sampling on the theoretical properties of greedy algorithms which were established in the ideal case in [3]. In particular, using concentration inequalities for the empirical measure in Wasserstein distance proved in [2], we provide sufficient conditions on the number of samples used for the computation of empirical variances at each iteration of the greedy procedure to guarantee that the resulting method algorithm is a weak greedy algorithm with high probability. These theoretical results are not fully practical and we therefore propose a heuristic procedure to choose the number of Monte-Carlo samples at each iteration, inspired from this theoretical study, which provides satisfactory results on several numerical test cases

Joint work with: Mohammed-Raed Blel, Tony Lelièvre.

References

[1] S. Boyaval, T. Lelivre, et al. A variance reduction method for parametrized stochastic differential equations using the reduced basis paradigm. *Communications in Mathematical Sciences*, 8(3):735–762, 2010.

[2] N. Fournier and A. Guillin. On the rate of convergence in wasserstein distance of the empirical measure. *Probability Theory and Related Fields*, 162(3-4): 707–738, 2015.

[3] R. DeVore, G. Petrova and P. Wojtaszczyk. Greedy algorithms for reduced bases in Banach spaces. *Constructive Approximation*, 37(3): 455–466, 2013.

Empirical adaptive Galerkin FEM for parametric PDEs

Martin Eigel
WIAS
eigel@wias-berlin.de

Adaptive stochastic Galerkin FEM (ASGFEM) with residual based a posteriori error estimation have shown to exhibit optimal convergence in practice for some standard parametric PDEs. However, their implementation is rather involved and requires significant effort when different problems should be tackled.

Motivated by recent results with empirical low-rank tensor regression in the framework of statistical learning, we examine a non-intrusive reconstruction method that only uses samples of the solution and yields the Galerkin projection with high probability. This can be seen as an easy to apply generalization of deterministic ASGFEM. For the sum of error and estimator, the proposed adaptive algorithm can be shown to converge.

To realize the error estimator, a sufficiently accurate tensor representation of the coefficient is required, which easily becomes challenging for instance when it is defined as an exponential function. We consider this common case and recall that it corresponds to the solution of a differential equation. It hence can be computed by means of a Petrov-Galerkin method for which error estimators are presented.

Joint work with: Nando Farchmin (PTB), Philipp Trunscke (Centrale Nantes).

References

[1] M. Eigel, N. Farchmin, S. Heidenreich, P. Trunschke. Efficient approximation of high-dimensional exponentials by tensor networks. arXiv:2105.09064, 2021.

[2] M. Eigel, N. Farchmin, S. Heidenreich, P. Trunschke. Adaptive non-intrusive reconstruction of solutions to high-dimensional parametric PDEs. arXiv:2112.01285, 2021.

Maximum relative distance between real rank-two and rank-one tensors

Henrik Eisenmann
MPI MiS Leipzig
henrik.eisenmann@mis.mpg.de

We investigate the maximum distance of a rank-two tensor to rank-one tensors. An equivalent problem is given by the minimal ratio of spectral and Frobenius norm of a tensor. For matrices the distance of a rank k matrix to a rank r matrices is determined by its singular values, but since there is a lack of a fitting analog of the singular value decomposition for tensors, this question is more difficult in the regime of tensors. We extend the results in [1] and show that the distance of a rank-two tensor $\mathbf{A}$ of order d to the set of rank-one tensors is bounded by

$$\min_{\operatorname{rank}\mathbf{B}=1} \|\mathbf{A}-\mathbf{B}\|_{\mathsf{F}} < \sqrt{1-\left(1-\frac{1}{d}\right)^{d-1}}\,\|\mathbf{A}\|_{\mathsf{F}},$$

where $\|\cdot\|_{\mathsf{F}}$ is the Frobenius norm. It is in particular remarkable that the constant in the right-hand side is uniformly bounded by $\sqrt{1-\left(1-\frac{1}{d}\right)^{d-1}} < \sqrt{1-\frac{1}{e}}$ and is again sharp for $d \to \infty$. We therefore have a bound for the distance of a rank-two tensor of any order to the set of rank-one tensors.

Joint work with: André Uschmajew.

References

[1] H. Eisenmann and A. Uschmajew. Maximum relative distance between symmetric rank-two and rank-one tensors. *ArXiv:*2111.12611, 2021.

Intrinsic versus extrinsic dimensionality of ground truths

Dennis Elbrächter
ETH Zurich
delbraechter@mins.ee.ethz.ch

Neural networks tend to be particularly successful in scenarios where the data points are high-dimensional. The learned neural network then, by it's nature, represents a function defined for any input in a high-dimensional space. Thus it is natural to also think of the ground truth as a function on a high-dimensional domain when considering it's approximation by neural networks. However, looking at, e.g., image data we can be quite sure that most potential inputs will never actually appear in any relevant task (e.g. in the case of images, only a tiny subset of all possible configurations of pixel values will produce a humanly meaningful picture).
In particular one might argue that interesting ground truths need to be of significantly lower complexity, i.e. intrinsic dimensionality, than the dimensionality of their input allows (even under other assumptions on their simplicity as, e.g., some kind of smoothness). One could now be so bold to go further and conjecture that, in fact, this combination of low intrinsic and high extrinsic dimensionality is a key prior which allows for successful learning by neural networks.
I will present my considerations on a formal notion of intrinsic dimensionality, which is designed to be particularly suitable for the study of approximation by neural networks, and moreover, has an empirical proxy which can be efficiently computed for finite sets of data points.

Joint work with: Helmut Bölcskei, Pavol Harar

Graph Wedgelets: an Adaptive Tool for Data Compression on Graphs based on Binary Wedge Partitioning Trees

Wolfgang Erb
University of Padova
wolfgang.erb@unipd.it

In this talk, we'll introduce graph wedgelets [1] as an adaptive tool for data compression on graphs. Graph wedgelets approximate signals on graphs by piecewise constant functions on adaptively generated binary wedge partitionings. In particular, they are discrete variants of continuous wedgelets and binary space partitionings that are frequently used for the compression of 2D images. We prove that continuous results on best m-term approximation with geometric wavelets can be transferred to the discrete graph setting and show that the wedgelet representation of graph signals can be encoded and implemented in a simple way by a binary tree structure. We will also illustrate how this graph-based method can be applied for the compression and segmentation of images.

References

[1] W. Erb. Graph Wedgelets: Adaptive Data Compression on Graphs based on Binary Wedge Partitioning Trees and Geometric Wavelets. *arXiv:2110.08843* (2021).

Concentration of solutions of optimization problems

Paul Escande
CNRS, Institut de Mathématiques de Marseille
paul.escande@univ-amu.fr

Let $(\mathbb{X}, d, \mu)$ be a metric measure space with μ being a probability measure. Furthermore, let $(\mathscr{M}, \vartheta)$ be another metric space with distance ϑ. This work focuses on the following generic optimization problem

$$\phi_* \in \operatorname*{arg\,min}_{\phi \in \mathscr{M}} \mathscr{J}(\phi) = \int_{\mathbb{X}} l(\phi, x) d\mu(x) + \mathscr{R}(\phi) \tag{1}$$

where $\mathscr{J} : \mathscr{M} \to \mathbb{R}$ is the objective function to be minimized, $l : \mathscr{M} \times \mathbb{X} \to \mathbb{R}$ is the integrand defining the data-fidelity term and $\mathscr{R} : \mathscr{M} \to \mathbb{R} \cup \{+\infty\}$ is an optional regularization promoting the a priori structure of the solution.

In practice, the measure μ is rarely known but samples $(x_i)_{i=1}^n$ drawn i.i.d. form it are usually accessible. The empirical risk is therefore minimized in place of (1):

$$\widehat{\phi} \in \operatorname*{arg\,min}_{\phi \in \mathscr{M}} \widehat{\mathscr{J}}(\phi) = \frac{1}{n} \sum_{i=1}^{n} l(\phi, x_i) + \mathscr{R}(\phi). \tag{2}$$

This abstract framework encompasses many estimation problems such as estimation of barycenters, penalized barycenters in the Wasserstein space, eigenspaces of covariance matrices, penalized linear regression (LASSO) and neural networks to name a few. Studying the generalization error $\mathscr{J}(\widehat{\phi}) - \inf \mathscr{J}$ is an important question started in the 70's with [3] and pursued in many works [4, 6, 5]. This is still an active research field [1, 2].

Little is however known regarding the convergence of the minimizers in the sense $\vartheta(\widehat{\phi}, \operatorname{arg\,min} \mathscr{J})$ and some work recently addressed this question [7, 8]. Yet, they do not provide optimal results. In this work, I am providing an alternative view point of this problem that allows to settle the assumptions from which optimal convergence rates can be proven. Based on a fine characterization of the behavior of $\mathscr{J}$ around its minimizers, those results leverage tools from geometry, optimization and probability theory.

References

[1] Klochkov, Yegor and Zhivotovskiy, Nikita Stability and Deviation Optimal Risk Bounds with Convergence Rate $O(1/n)$ *Advances in Neural Information Processing Systems*, 2021.

[2] Zhang, Chiyuan and Bengio, Samy and Hardt, Moritz and Recht, Benjamin and Vinyals, Oriol Understanding deep learning (still) requires rethinking generalization *Communications of the ACM*, 2021.

[3] Vapnik, Vladimir. On the uniform convergence of relative frequencies of events to their probabilities. *Doklady Akademii Nauk USSR*, 181(4):781–787, 1968.

[4] Vapnik, Vladimir. Principles of risk minimization for learning theory. *Advances in neural information processing systems*,1991.

[5] Devroye, Luc and Györfi, László and Lugosi, Gábor *A probabilistic theory of pattern recognition, 1996.*

[6] Bousquet, Olivier and Elisseeff, André Stability and generalization, The Journal of Machine Learning Research,2002.

[7] Bousquet, Olivier and Elisseeff, André Convergence rates for the generalized Fréchet mean via the quadruple inequality *Electronic Journal of Statistics*, 2019.

[8] Ahidar-Coutrix, Adil and Le Gouic, Thibaut and Paris, Quentin Convergence rates for empirical barycenters in metric spaces: curvature, convexity and extendable geodesics *Probability theory and related fields.* 2020.

A use of the generalized Hopf fibration in minimal energy problems

Ujué Etayo
Universidad de Cantabria
etayomu@unican.es

During this talk we will explain how to make use of the internal geometric structure of the spheres of odd dimension to fairy distribute points in them.

Getting into the details: we will say that a set of points $\omega_N = \{x_1, \dots, x_N\} \subset \mathbb{S}^d$ is well distributed if its associated discrete logarithmic or Riesz s-energy defined by

$$\mathcal{E}_{\log}(\omega_N) = -\sum_{i=1}^{N} \log ||x_i - x_j||, \qquad \mathcal{E}_s(\omega_N) = \sum_{i=1}^{N} \frac{1}{||x_i - x_j||^s} \tag{1}$$

is small. We will use well distributed points in $\mathbb{S}^2$ and $\mathbb{PC}^d$ and the generalized Hopf fibration $\mathbb{S}^1 \hookrightarrow \mathbb{S}^{2d+1} \to \mathbb{PC}^d$ to fairy distribute points in $\mathbb{S}^{2d+1}$. We use this technique with random point processes (determinantal point processes), see [1], for odd dimensional spheres and with a deterministic family of points: the so called Diamond ensemble, see [2].

Joint work with: Carlos Beltrán, Pablo García-Arce.

References

[1] Carlos Beltrán and Ujué Etayo. The Projective Ensemble and Distribution of Points in Odd-Dimensional Spheres. *Constructive Approximation*, 48(1):163–182, 2018.

[2] Carlos Beltrán and Ujué Etayo. The Diamond ensemble: A constructive set of spherical points with small logarithmic energy. *Journal of Complexity*, 59, 2020.

Singular cases of planar and spatial C^1 Hermite interpolation problems based on quintic Pythagorean-hodograph curves

Kai Hormann
Università della Svizzera italiana
kai.hormann@usi.ch

A well-known feature of the Pythagorean-hodograph (PH) curves is the multiplicity of solutions arising from their construction through the interpolation of Hermite data. In general, there are four distinct planar quintic PH curves that match first-order Hermite data [1], and a two-parameter family of spatial quintic PH curves compatible with such data [2]. Under certain special circumstances, however, the number of distinct solutions is reduced [3]. Specifically, in the planar case it turns out that there may be only three (but not less) distinct Hermite interpolants, of which one is a "double" solution (see Fig. 1). In the spatial case, a constant difference between the two free parameters reduces the dimension of the solution set from two to one, resulting in a family of quintic PH space curves of different shape but identical arc lengths. The values of the free parameters that result in formal specialization of the (quaternion) spatial problem to the (complex) planar problem are also identified, demonstrating that the planar PH quintics, including their degenerate cases, are subsumed as a proper subset of the spatial PH quintics.

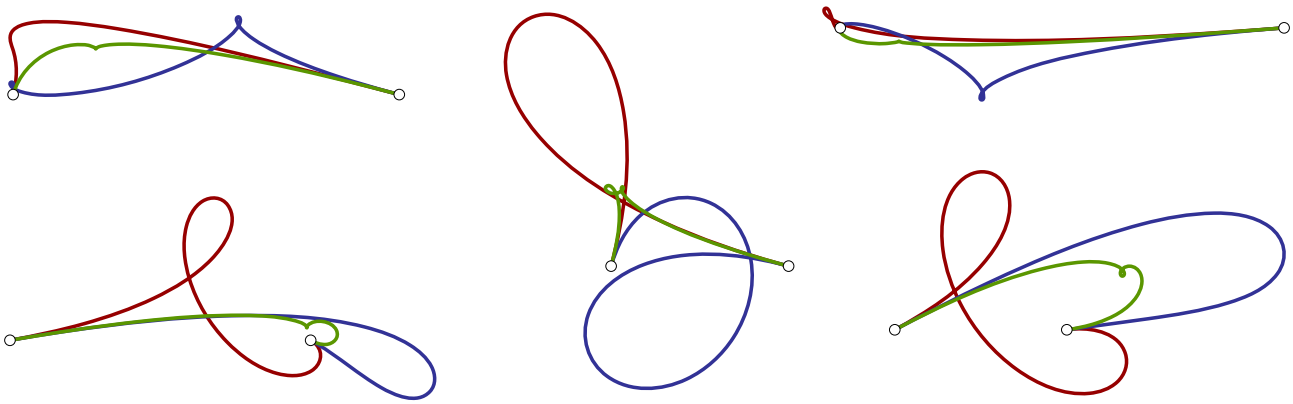

Figure 1: Examples of planar cases with only three distinct PH quintic Hermite interpolants. In each case, the green curve corresponds to the "double" solution.

Joint work with: Rida Farouki, Federico Nudo

References

[1] R. T. Farouki and C. A. Neff. Hermite interpolation by Pythagorean-hodograph quintics. *Mathematics of Computation*, 64(212):1589–1609, Oct. 1995.

[2] R. T. Farouki, M. al-Kandari, and T. Sakkalis. Hermite interpolation by rotation-invariant spatial Pythagorean-hodograph curves. *Advances in Computational Mathematics*, 17(4):369–383, Nov. 2002.

[3] R. T. Farouki, K. Hormann, and F. Nudo. Singular cases of planar and spatial C^1 Hermite interpolation problems based on quintic Pythagorean-hodograph curves. *Computer Aided Geometric Design*, 82:Article 101930, 13 pages, Oct. 2020.

Convergence of adaptive stochastic collocation with finite elements

Michael Feischl
Institute of Analysis and Scientific Computing, TU Wien, Austria
michael.feischl@tuwien.ac.at

We consider an elliptic partial differential equation with a random diffusion parameter discretized by a stochastic collocation method in the parameter domain and a finite element method in the spatial domain. We prove for the first time convergence of a stochastic collocation algorithm which adaptively enriches the parameter space as well as refines the finite element meshes.

Joint work with: Andrea Scaglioni

References

[1] M. Feischl, A. Scaglioni. Convergence of adaptive stochastic collocation with finite elements. *Computers & Mathematics with Applications*, 98: 139-156, 2021.

Computational optimal transport: mature tools and open problems

Jean Feydy
INRIA Paris, HeKA team
jean.feydy@inria.fr

Optimal transport is a fundamental tool to deal with discrete and continuous distributions of points [1, 2]. We can understand it either as a generalization of **sorting** to spaces of dimension D > 1, or as a **nearest neighbor projection** under a mass preservation constraint. Over the last decade, a sustained research effort on numerical foundations has led to a $\times 1,000$ speed-up for most transport-related computations. This has opened up a wide range of research directions in geometric data analysis, machine learning and computer graphics.

This talk will discuss the consequences of these game-changing numerical advances from a **user's perspective**. We will focus on:

1. Mature libraries and **software tools** that can be used as of 2022 [3, 4, 5, 6, 7, 8], with a clear picture of the current state-of-the-art [9].
2. New ranges of applications in **3D shape analysis**, with a focus on population analysis [10] and point cloud registration [11].
3. **Open problems** that remain to be solved by experts in the field.

Joint work with: Minh-Hieu Do, Olga Mula-Hernandez, Marc Niethammer, Gabriel Peyré, Bernhard Schmitzer, Thibault Séjourné, Zhengyang Shen, Anna Song, Alain Trouvé, François-Xavier Vialard.

References

[1] G. Peyré and M. Cuturi. Computational optimal transport. https://optimaltransport.github.io/book/

[2] J. Feydy. Geometric data analysis, beyond convolutions. https://www.jeanfeydy.com/geometric_data_analysis.pdf

[3] R. Flamary et al. Python Optimal Transport. https://pythonot.github.io/

[4] M. Cuturi et al. Optimal Transport Tools. https://ott-jax.readthedocs.io/

[5] Alice INRIA team. Geogram software. http://alice.loria.fr/software/geogram

[6] B. Schmitzer. MultiScale-OT toolbox. https://bernhard-schmitzer.github.io/MultiScaleOT

[7] Q. Mérigot et al. PyMongeAmpere. https://github.com/mrgt/PyMongeAmpere

[8] J. Feydy. GeomLoss. https://www.kernel-operations.io/geomloss/

[9] J. Feydy et al. Optimal Transport benchmarks. https://optimal-transport-benchmarks.com/

[10] A. Song. Generation of tubular and membranous shape textures with curvature functionals. SIAM Journal of Mathematical Imaging and Vision (2022).

[11] Z. Shen et al. Accurate point cloud registration with robust optimal transport. NeurIPS 2021.

On the monotonicity of generalized barycentric coordinates on convex polygons

Michael S. Floater
University of Oslo
michaelf@math.uio.no

Generalized barycentric coordinates (GBCs) have several applications, including triangular mesh parameterization, and morphing and image deformation, as well as to allow more flexibility in designing shape functions for the finite element method. So it seems worthwile to derive some basis properties of GBCs. A property that is shared by many well known kinds of GBCs on a convex polygon is a monotonicity property: the coordinate function associated with each vertex is monotonically increasing in the direction towards the vertex. I will discuss how to derive this property for various GBCs and also explore the question of whether some GBCs are also convex in these same directions.

References

[1] M. S. Floater. Generalized barycentric coordinates and applications. *Acta Numerica*, 24:227–229, 2015.

[2] M. S. Floater, On the monotonicity of generalized barycentric coordinates on convex polygons. *Comp. Aided Geom. Design*, 42:34–39, 2016.

On LASSO-type Regularizations and Sparsity of their Minimizers

Simon Foucart
Texas A&M University
foucart@tamu.edu

This talk showcases that the sparsity of the LASSO minimizer is comparable to the sparsity of the original vector being measured when the measurement matrix satisfies the restricted isometry property. This result holds even in the noisy setting provided that the regularization parameter is not too small. Accompanying two-sided bounds on the recovery error will also be given. The result will then be extended to variations of the standard LASSO, including squared LASSO. We will highlight connections of the latter with nonnegative least-squares and with orthogonal matching pursuit.

On the numerical stability of barycentric rational interpolation

Chiara Fuda
Università della Svizzera italiana
chiara.fuda@usi.ch

The barycentric forms of polynomial and rational interpolation have recently gained popularity, because they can be computed with simple, efficient, and numerically stable algorithms [1, 2, 3]. In this talk, we show more generally that the evaluation of any function that can be expressed as $r(x) = \sum_{i=0}^{n} a_i(x) f_i / \sum_{j=0}^{m} b_j(x)$ in terms of data values f_i and some functions a_i and b_j for $i = 0, \ldots, n$ and $j = 0, \ldots, m$ with a simple algorithm that first sums up the terms in the numerator and the denominator, followed by a final division, is forward and backward stable under certain assumptions. This result includes the two barycentric forms of rational interpolation as special cases. Our analysis further reveals that the stability of the second barycentric form depends on the Lebesgue constant associated with the interpolation nodes, which typically grows with n, whereas the stability of the first barycentric form depends on a similar, but different quantity, that can be bounded in terms of the mesh ratio, regardless of n. We support our theoretical results with numerical experiments, which indicate that the first barycentric form is stable even in situations where the second barycentric form is completely unstable, as shown in Figure 1.

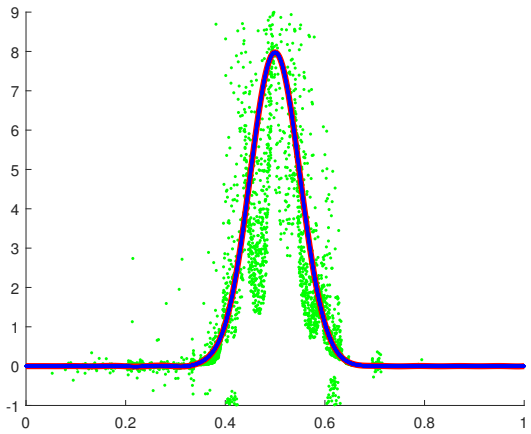

Figure 1: Multiple-precision implementation of a rational barycentric interpolant $r(x)$ for $x \in [0, 1]$ (red) and numerical approximation $\hat{r}(x)$ in double precision for $10,000$ equidistant evaluation points in $[10^3\varepsilon, 1 - 10^3\varepsilon]$, where ε is the machine epsilon, using the standard implementations of the first (blue dots) and the second (green dots) barycentric form.

Joint work with: Kai Hormann, Rosanna Campagna.

References

[1] A.P. de Camargo. On the numerical stability of Floater–Hormann's rational interpolant. *Numerical Algorithms*, 72(1), 131–152, 2016.

[2] N.J. Higham. The numerical stability of barycentric Lagrange interpolation. *IMA Journal of Numerical Analysis*, 24, 547–556, 2004.

[3] W. Mascarenhas, A. Camargo. The backward stability of the second barycentric formula for interpolation. *Dolomites Research Notes on Approximation*, 7, 1–12, 2014.

Provable Phase retrieval via Mirror descent

Jean-Jacques GODEME
Normandie Univ, ENSICAEN, CNRS, GREYC, France
jean-jacques.godeme@unicaen.fr

We consider the problem of phase retrieval, recovering an $n-$dimensional real vector from the magnitude of its $m-$ linear measurements. This paper presents a new approach [1] allowing to lift the classical global Lipschitz continuity requirement through the use of a non-euclidean Bregman divergence, to solve the nonconvex formulation of the phase retrieval problem [2]. We show that when the measurements are sufficiently large, with high probability we can recover the desired vector up to a global sign change. Our set-up uses careful initialization via a spectral method and refines it using the mirror descent with a backtracking procedure to find the optimal solution. We show local linear convergence with a rate and step-size independent of the dimension. Our results are stated for two types of measurements: those drawn independently from the standard Gaussian, and those obtained by Coded Diffraction Patterns (CDP) for Randomized Fourier Transform.

Problem Formulation: Our goal is to recover a vector $x \in \mathbb{R}^n$ from $y_r = |a_r^* x|^2, r \in \{0, 1, .., m\}$, where $a_r \in \mathbb{C}^n$ are the sensing vectors. We cast this as solving the following non-convex optimization problem: $\min_{x\in\mathbb{R}^n} f(x) = \frac{1}{4m}\sum_{r=1}^{m}\left(y_r - |a_r^* x|^2\right)^2$. Our recovery procedure starts at some vector x^0 via a spectral method, and then for $k = 1, 2, \ldots$, implements the iteration

$$x^k = (\nabla\psi)^{-1}\left(\nabla\psi(x^{k-1}) - \gamma_k \nabla f(x^{k-1})\right) \qquad \text{(Mirror Descent)}$$

where $\psi(x) = \frac{1}{4}\|x\|^4 + \frac{1}{2}\|x\|^2$ is a kernel generating distance proposed in [3] and γ_k is the stepsize sequence either fixed in $]0, 1/(3+\delta)]$, $\delta > 0$, or adjusted via backtracking. ψ enjoys many desirable properties making the (Mirror Descent) scheme very efficient. Our main result is the following.

Theorem 0.1 *Let $\delta > 0$ sufficiently small. Suppose that the number of measurements m is large enough i.e $m \geq C(\delta)n\log(n)$ in the gaussian case (respectively $m \geq C(\delta)n\log(n)^3$ in the CDP case). If* (Mirror Descent) *is initialized with a spectral method, then with probability at least $1 - 10e^{-cn} - \frac{8}{n^2}$ ($c > 0$ is a fixed numerical constant) for the gaussian (respectively $1 - \frac{1}{n^3}$ for the CDP model) , we have*

$$\operatorname{dist}^2(x^k, x) = \mathcal{O}\left(\left(1 - \frac{1}{3(3+\delta)}\right)^k\right) \qquad (1)$$

where $\forall z \in \mathbb{R}^n$, $\operatorname{dist}(z, x) = \min\{\|z - x\|, \|z + x\|\}$.

Joint work with: Jalal Fadili, Xavier Buet, Myriam Zerrad, Claude Amra and Michel Lequime.

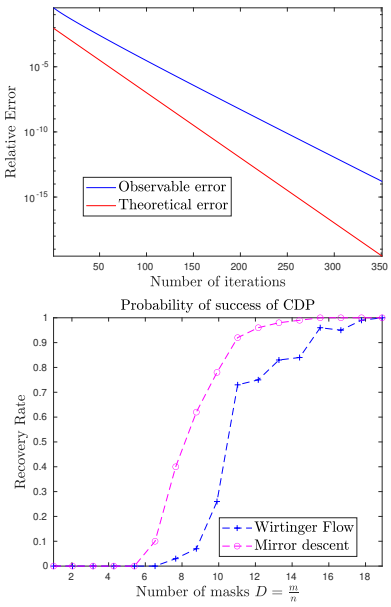

Figure 1: Example of relative error and phase transition

References

[1] Jean-Jacques Godeme, Jalal Fadili, Xavier Buet, Michel Lequime, Claude Amra, "Provable Phase Retrieval via Mirror descent", 2021, (to be submitted).

[2] Emmanuel Candès, Xiaodong Li, and Mahdi Soltanolkotabi, "Phase Retrieval via Wirtinger Flow: Theory and Algorithms," IEEE Transactions on Information Theory, vol. 61, no. 4, pp. 1985-2007, 2015.

[3] Jérôme Bolte, Shoham Sabach, Marc Teboulle, and Yakov Vaisbourd, "First Order Methods beyond Convexity and Lipschitz Gradient Continuity with Applications to Quadratic Inverse Problems", SIAM Journal on Optimization, vol. 28, no. 3, pp. 2131?2151, 2018.

Comparison of 2 PDE models for anisotropic non local interactions in 2D

André GALLIGO
Université Côte d'Azur, LJAD and INRIA Aromath, Nice, France.
andre.galligo@univ-cotedazur.fr

We compare model 1, developed by B. During et al. [1], aimed at studying fingerprint formation, and model 2 aimed at studying the dynamics of complex root sets of random polynomials under differentiation. [2]. The illustrations below show at left the ridges of a "stabilised" fingerprint formation. At right, the "trajectories" of the root set of a random polynomial P_n (represented by black solid boxes) and the root sets of several iterated derivatives of P_n.

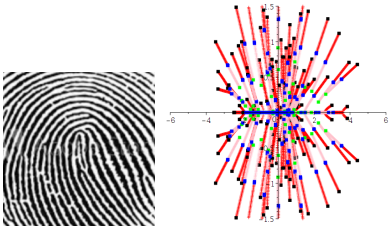

Both phenomena are produced by anisotropic non local interactions in a bounded domain in 2D.
In both cases,

- When the number n of particles tends to infinity the sets of particles are represented by density functions, and asymptotic behaviors, are considered. They are created by balanced repulsion/attraction forces acting on initial configurations.
- The velocity of a particle, hence the motion of the set, is estimated from a mean field approximation.
- The anisotropy is represented by a local property, expressed by either a 2-tensor $T(x_j)$ or by an infinitesimal moving rectangle centered at x_j, (which can also be represented by a 2-tensor) in order to capture the stress created by the motion.

However,

- Model 1 was primarily designed for computing the stationary solutions of the PDE, whereas model 2 aims at understanding the begining of the motion, say for times t between 0 and 0.5, t is associated to $round(tn)$ derivations of P_n for $n >> 1$.
- The symbolic representations of the forces are different. Model 1 relies on explicit ensatz, which coefficients are quadratic combinations of exponentials of the distance between two roots. Model 2 relies on an electrostatic interpretation of the logarithmic derivative of P_n. The repulsion force is then computed by an intricate geometric construction.
- In model 1, a parameter χ must be chosen in advance for the definition of the tensor. In model 2 the variable c, which plays a similar role, is a function of the density, hence is time dependant.

And there are more differences ...

References

[1] B. During, C. Gottschlich, S. Huckemann, L. M. Kreusser, and C.-B. Schonlieb. *An Anisotropic Interaction Model for Simulating Fingerprints.* Journal of Mathematical Biology, 78 (2019), pp. 2171–2206.

[2] A. Galligo. *Modeling Complex Root Motion of Real Random Polynomials Under Differentiation.* hal 03577445 v1 (2022).

Dual subdivision and interpolation

Lucia Romani
Dept. of Mathematics, Alma Mater Studiorum Università di Bologna, Italy
lucia.romani@unibo.it

Subdivision schemes are well-established tools for the construction of curves and surfaces. Given an initial set of points attached to an initial grid, a subdivision scheme recursively refines the current grid and computes new data to be attached to it, in order to obtain a smooth limit. This talk concerns dual subdivision schemes working on one-dimensional grids and investigates their capability of generating limit curves that interpolate the initial data. Recalling the results in [2], we first show that, differently from primal schemes, their dual counterparts do not satisfy the step-wise interpolation property and are not defined via refinement rules that at each stage of the iteration leave the previous set of points unchanged. Then, after reviewing the work completed in [3], we prove that a whole family of dual interpolating schemes of arity larger than 2 can indeed be constructed and, as recently discussed in [1], its construction can be conveniently reduced to the solution of a certain Bézout-like polynomial equation. Moreover, under some suitable assumptions, it is also possible to study a priori the existence of a dual interpolating scheme of a certain arity, that fulfills specific requests about polynomial reproduction, support size and regularity.

Joint work with: Luca Gemignani (Università di Pisa), Alberto Viscardi (Università di Torino).

References

[1] L. Gemignani, L. Romani, A. Viscardi. Bézout-like polynomial equations associated with dual univariate interpolating subdivision schemes. *Adv. Comput. Math.*, 48(1), 4 2022.

[2] L. Romani. Interpolating m-refinable functions with compact support: the second generation class. *Appl. Math. Comput.*, 361:735–746, 2019.

[3] L. Romani, A. Viscardi. Dual univariate interpolatory subdivision of every arity: algebraic characterization and construction. *J. Math. Anal. Appl.*, 484(1), 123713, 2020.

Approximation speed of quantized *vs.* unquantized ReLU neural networks and beyond.

Antoine Gonon
Univ Lyon, EnsL, UCBL, CNRS, Inria, LIP, F-69342, LYON Cedex 07, France.
antoine.gonon@ens-lyon.fr

Neural networks are used to approximate functions with success in many applications. In line with the works [1, 2, 3], we are interested in understanding their approximation power in practice and in theory. Regarding practical applications, a key question is to be able to compare approximation properties of quantized versus unquantized neural networks. Another important question is to better understand non-trivial situations where neural networks can be expected (or not) to have better approximation properties than the best known approximation methods, quantized or not.

We are concerned with quantitatively characterizing the optimal polynomial speed $\gamma^{*\text{approx}}(\mathcal{C}|\Sigma)$ at which all functions of a set $\mathcal{C}$, subset of a pseudo-metric space $\mathcal{F}$, can be approximated by a sequence $\Sigma = (\Sigma_M)_{M\in\mathbb{N}}$ of sets Σ_M of "simpler" functions, such as ones that can be represented by polynomials of degree M, or ReLU neural networks with M non-zero parameters. We introduce a new property of the sequence Σ, called ∞-encodability, which forbids degenerate cases, where for example $\Sigma_1 = \mathcal{C}$ is already so rich that it yields unreasonable approximation rates. We show that:

(i) if Σ is ∞-encodable, then the Kolmogorov-Donoho complexity $\gamma^{*\text{encod}}(\mathcal{C})$, which measures the best polynomial asymptotic speed at which $\mathcal{C}$ can be *encoded* as binary sequences, and which is known for many classical functions sets such as balls of Sobolev spaces, bounds from above $\gamma^{*\text{approx}}(\mathcal{C}|\Sigma)$;

(ii) many sequences $\Sigma = (\Sigma_M)_{M\in\mathbb{N}}$ are ∞-encodable: when Σ_M contains M-terms linear combination of a dictionary, with boundedness conditions on the coefficients, or when Σ_M is Lipschitz-parameterized by some bounded set in finite dimension, the latter includes the case of ReLU neural networks for which we identify "simple" sufficient conditions on the considered architectures for this to hold;

(iii) when ∞-encodability is inherited from Lipschitz-parameterization, a simple quantization scheme turns Σ into a quantized sequence whose elements can be represented in a computer, attaining the same polynomial approximation speed as Σ on *every set* $\mathcal{C}$.

In light of point (ii), point (i) unifies and generalizes [2, Theorem VI.4][3, Theorem 5.24][4, Proposition 11].

Our framework applied to ReLU neural networks guarantees that uniformly quantized sparse ReLU networks with standard growth assumption on sparsity, depth and weight magnitudes, approximate every set of functions $\mathcal{C}$ with the same polynomial rate as their unquantized version. It also shows that approximation methods based on an ∞-encodable sequence defined with ReLU neural networks share a common upper-bound on approximation rates with other classical approximation methods also based on ∞-encodable sequences. As a consequence, given $\mathcal{C}$, if an ∞-encodable sequence is known such that $\gamma^{*\text{approx}}(\mathcal{C}|\Sigma) = \gamma^{*\text{encod}}(\mathcal{C})$, then no improved approximation rate can be hoped for using ReLU networks.

Joint work with: Nicolas Brisebarre, Rémi Gribonval, Elisa Riccietti.

References

[1] Ronald DeVore, Boris Hanin, and Guergana Petrova. Neural network approximation. *Acta Numer.*, 30:327–444, 2021.

[2] Dennis Elbrächter, Dmytro Perekrestenko, Philipp Grohs, and Helmut Bölcskei. Deep neural network approximation theory. *IEEE Trans. Inf. Theory*, 67(5):2581–2623, 2021.

[3] Philipp Grohs. Optimally sparse data representations. In *Harmonic and applied analysis*, Appl. Numer. Harmon. Anal., pages 199–248. Birkhäuser/Springer, Cham, 2015.

[4] Gérard Kerkyacharian and Dominique Picard. Entropy, universal coding, approximation, and bases properties. *Constr. Approx.*, 20(1):1–37, 2004.

Spurious minimizers in non uniform Fourier sampling optimization

Alban Gossard
Institut de Mathématiques de Toulouse
alban.paul.gossard@gmail.com

A recent research trend is the optimization of Fourier sampling schemes for specific datasets of signals such as the Fast-MRI database. Many works consider subset selection methods, which restrict the samples locations on a grid, while a few recent papers begin exploring the optimization of off-the-grid sampling schemes using continuous approaches with applications to Magnetic Resonance Imaging [6, 7]. Despite promising results in terms of image reconstruction improvements, the optimization routines seem to suffer from a strong dependency to the initialization.

In a recent work [4], we explain why choosing optimal non Cartesian Fourier sampling patterns is a difficult nonconvex problem by bringing to light two optimization issues. The first one is the existence of a combinatorial number of spurious minimizers for a generic class of signals. The spectral theory applied to Vandermonde matrices [1, 3, 2, 5] allows to show that the cost function is highly oscillating. This results in a number of minimizers larger than $\binom{M}{K} \cdot M!$, where M is the number of measurements and K scales as the number of maximizers of the Fourier transform modulus of the signal. The second issue is a vanishing gradient effect for the high frequencies. In practice, this results in optimization routines being very slow, or trapped in local minimizers: the final sampling schemes are close to the initialization.

We show how using large datasets can mitigate the first effect and we illustrate experimentally the benefits of using stochastic gradient algorithms with a variable metric. We also suggest globalization approaches to attack this challenging problem.

Joint work with: Frédéric de Gournay and Pierre Weiss.

References

[1] Céline Aubel and Helmut Bölcskei. Vandermonde matrices with nodes in the unit disk and the large sieve. *Applied and Computational Harmonic Analysis*, 47(1):53–86, 2019.

[2] Dmitry Batenkov, Laurent Demanet, Gil Goldman, and Yosef Yomdin. Conditioning of partial nonuniform fourier matrices with clustered nodes. *SIAM Journal on Matrix Analysis and Applications*, 41(1):199–220, 2020.

[3] Enrico Bombieri. On the large sieve. In *Goldbach Conjecture*, pages 227–252. World Scientific, 1984.

[4] A. Gossard, P. Weiss, and F. de Gournay. Spurious minimizers in non uniform fourier sampling optimization. 2021.

[5] Ankur Moitra. Super-resolution, extremal functions and the condition number of vandermonde matrices. In *Proceedings of the forty-seventh annual ACM symposium on Theory of computing*, pages 821–830, 2015.

[6] G. Wang, T. Luo, J.-F. Nielsen, D. C. Noll, and J. A. Fessler. B-spline parameterized joint optimization of reconstruction and k-space trajectories (bjork) for accelerated 2d mri. *IEEE Transactions on Medical Imaging*, 2021.

[7] T. Weiss, O. Senouf, S. Vedula, O. Michailovich, M. Zibulevsky, and A. Bronstein. Pilot: Physics-informed learned optimal trajectories for accelerated mri. *arXiv preprint arXiv:1909.05773*, 2019.

Deep Network Multi-Spline Approximation Method

Sefti Rania
University Mohammed I, FSO, LANO Laboratory, Oujda, Morocco,
University of Orleans, IDP Laboratory,UMR CNRS 7013, Orleans, France.
sefti.rania@ump.ac.ma

This paper introduces a new approximation method called Deep Multi Spline (DM-Spline) which is based on a deep learning model and various types of spline functions (B-Spline, UAT-Spline, hyperbolic-Spline, ...). The main idea is to combine different spline functions into a learning model that controls their contribution to the accurate approximation of the function to be built. We introduce a new bridge between Deep Neural Networks (DNNs) and spline approximation methods by developing a detailed theory in each layer and presenting some results on this subject. To test the robustness of the proposed approach, a comparison to state-of-the-art is achieved and shows the efficiency of our model. An application in the medical field is also provided.

Joint work with: Sbibih Driss, Jennane Rachid.

References

[1] R. Balestriero. A Spline Theory of Deep Networks. *In International Conference on Machine Learning*, PMLR. (pp. 374-383), 2018.

Point cloud registration for algebraic varieties using Riemannian optimization

Florentin Goyens
Université Paris Dauphine
goyensflorentin@gmail.com

We consider the registration of point clouds, that is, task of finding a transformation such that two point clouds overlap. We assume that the target and source point clouds belong to the same algebraic variety (up to a change in coordinates). Our method does not assume that a point correspondence is given.

Consider two algebraic varieties $V_1, V_2 \subset \mathbb{R}^n$ of the same degree d. We assume that there exists $Q \in \mathrm{SO}(n)$ and $a \in \mathbb{R}^n$ which define a rigid transformation $\mathcal{T}\colon \mathbb{R}^n \to \mathbb{R}^n$ such that the varieties V_1 and V_2 overlap, that is, for all $x_1 \in V_1$, we have $\mathcal{T}(x_1) := Qx_1 + a \in V_2$. Let $M_1 \in \mathbb{R}^{n\times s_1}$ and $M_2 \in \mathbb{R}^{n\times s_2}$ be composed of respectively s_1 samples in V_1 and s_2 samples in V_2. Given M_1 and M_2, our task is to estimate $Q \in \mathrm{SO}(n)$ and $a \in \mathbb{R}^n$ which define the transformation $\mathcal{T}$.

Our approach uses the monomial map, which is known to be rank deficient for matrices whose columns belong to an algebraic variety [2]. We use a rank-minimization procedure inspired from [2] using the Grassmann manifold. This allows us to write the registration as a smooth optimization problem defined on Riemannian manifolds, which we solve using off-the-shelf algorithms from the Manopt toolbox [1].

We also propose a framework that is robust to noise in the initial data. That is, given two point clouds $\hat{M}_1$ and $\hat{M}_2$, which are noisy versions of M_1 and M_2 we aim to find a rigid transformation $\mathcal{T}$ such that $\mathcal{T}(M_1)$ and M_2 overlap. To achieve this, we first attempt to recover M_1 and M_2 from $\hat{M}_1$ and $\hat{M}_2$, by solving a denoising problem, which is also formulated as a smooth Riemannian optimization problem in the manner of [2]. For the noisy and noiseless case, we show numerical results on synthetic examples which illustrate the efficiency and accuracy of our approach, see Figure 1.

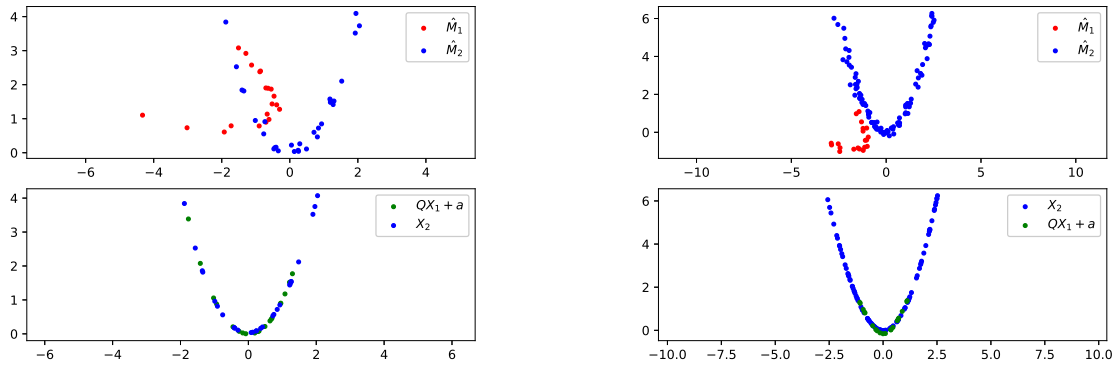

Figure 1: Noisy rigid registration of quadratic curves for overlapping and partially overlapping data sets. Input in the top image and output in the bottom image.

Joint work with: Coralia Cartis, Stéphane Chrétien.

References

[1] Boumal, N. and Mishra, B. and Absil, P.-A. and Sepulchre, R. Manopt, a Matlab Toolbox for Optimization on Manifolds, Journal of Machine Learning Research, 2014, http://www.manopt.org.

[2] Goyens, Florentin and Cartis, Coralia and Eftekhari, Armin. arXiv preprint arXiv:2109.06095, Nonlinear matrix recovery using optimization on the Grassmann manifold, 2021

Exploring refinement strategies for locally linear independent LR B-splines

Lisa Groiss
Johannes Kepler University, Linz/Austria
lisa.groiss@jku.at

Locally refined B-splines, which were introduced by Dokken et al. [2], provide a generalization of tensor-product B-splines to the case of locally refined meshes. While refinement strategies that ensure linear independence have been studied recently [4, 3], the construction of LR B-splines may potentially generate basis functions that possess the even stronger property of *local* linear independence (LLI). More precisely, LLI ensures that exactly $(p+1)^d$ basis functions take non-zero values on any cell of the mesh and entails optimal sparsity properties of the matrices that arise, e.g., in applications to numerical simulation. Motivated by the notion of semi-regular tensor-product B-splines, which was introduced by Weller and Hagen [1], we investigate related refinement strategies for locally linear independent LR B-splines in the bivariate case.

Joint work with: Bert Jüttler, Maodong Pan.

References

[1] F. Weller and H. Hagen. Tensor-product spline spaces with knot segments. In: *Mathematical Methods for Curves and Surfaces* (M. Dæhlen et al., eds), pages 563–572, Vanderbilt University Press, Nashville 1995.

[2] T. Dokken, T. Lyche and K.F. Pettersen. Polynomial splines over locally refined box-partitions. In: *Computer Aided Geometric Design* 30, pages 331–356, 2013.

[3] F. Patrizi, C. Manni, F. Pelosi and H. Speleers. Adaptive refinement with locally linearly independent LR B-splines: Theory and applications. In: *Computer Methods in Applied Mechanics and Engineering* 369, 2020.

[4] A. Bressan and B. Jüttler. A hierarchical construction of LR meshes in 2D. In: *Computer Aided Geometric Design* 37, pages 9–24, 2015.

Deformable Voxel Grids

Raphaël Groscot — Laurent D. Cohen
Université Paris-Dauphine
groscot@ceremade.dauphine.fr — cohen@ceremade.dauphine.fr

We introduce Deformable Voxel Grids (DVGs), an adaptation of Active Volumes for semi-automatic shape preprocessing. Intuitively, they deform the embedding space to a given shape in order to facilitate further shape processing and analysis, by means of shape-DVG registration. A DVG is parameterized like a Topological Active Volume [3], which is a volumetric extension of active contours [1, 2]. It is a lattice V on the unit cube, evolving with an energy designed to smoothly embrace shape S: $\mathcal{E}(V) = \lambda_e \mathcal{E}_{elastic}(V) + \lambda_b \mathcal{E}_{bending}(V) + \lambda_s \mathcal{E}_{S \subset V}(V)$. The last term, $\mathcal{E}_{S \subset V}$, penalizing the non-inclusion of S in V, acts as a stopping barrier against the contraction induced by $\mathcal{E}_{elastic}$. To compute it, we approximate V with a dense ball covering, because each cell is hexahedral.

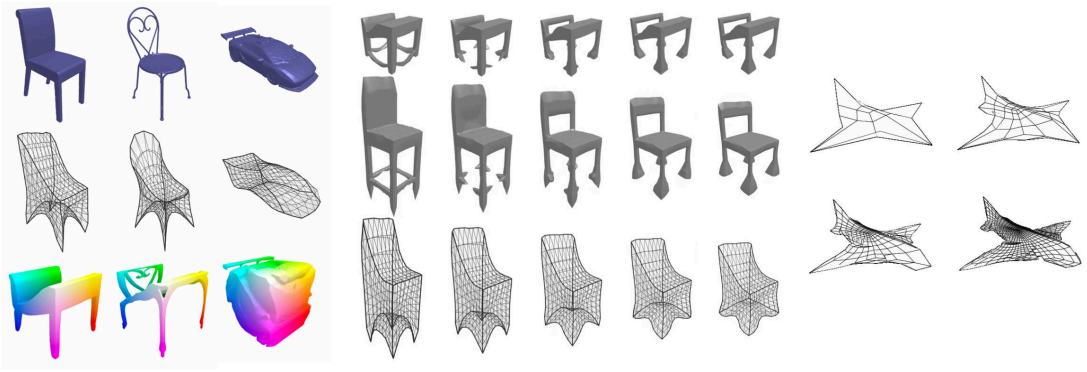

Once optimized, two things follow: (1) expressing S in coordinates $(u, v, w) \in [0, 1]^3$ taken from the same parameterization than $V(u, v, w)$; (2) attributing scalar values to the cells of V, corresponding to the volume occupancy of S within them. We call these operations *registration* and *cubification*. Indeed, (1) allows to deform S by moving the control points of V, while (2) gives a "cubic" representation of the topology of S (see accompanying image). DVGs provide a proxy for various applications, some of which are illustrated above:

Similarity search: Relying solely on V, which approximates the outer surface of S, gives a topological-invariant shape descriptor which can be used to retrieve models similar to a given query model.

Semantical editing: Learning deformation modes of V (e.g. with a PCA) on a dataset, to induce a similar deformation on DVG-registered shapes.

Topology transfer: Projecting a registered shape into the DVG of a different shape.

Basic correspondences: Cubified shapes tend to have similar parts in similar locations (color-coded above), which suggests a potential for estimating shape correspondences, using a naive closest-point matching.

Morphing: For a pair of registered shapes, interpolating separately on the V lattice and the cubified shapes (separating "form" and "content"). See above the three rows of interpolations (result in the center).

Progressive approximation with quadrilaterals: Surfaces given as triangle meshes can be approximated by quadrilateral meshes, by voxelizing the cubified shapes and reprojecting to the DVG.

References

[1] M. Kass et al. Snakes: Active contour models. *International Journal of Computer Vision*, 1(4):321-331, 1988.

[2] Laurent D. Cohen. On active contour models and balloons. *CVGIP: Image Understanding*, 53(2):211-218, 1991.

[3] N. Barreira et al. Topological Active Volumes. *Computer Analysis of Images and Patterns*, 337-344, 2003.

PR-DAD: Phase Retrieval Using Deep Auto-Decoders

Leon Gugel
D-ID and School of mathematical sciences, Tel-Aviv university
leon.gugel@gmail.com

Phase retrieval is a well known ill-posed inverse problem where one tries to recover images given only the magnitude values of their Fourier transform as input. In recent years, new algorithms based on deep learning have been proposed, providing breakthrough results that surpass the results of the classical methods. In this work we provide a novel deep learning architecture PR-DAD (Phase Retrieval Using Deep Auto-Decoders), whose components are carefully designed based on mathematical modeling of the phase retrieval problem. The architecture provides experimental results that surpass all current results.

Joint work with: Shai Dekel, School of mathematical sciences, Tel-Aviv university

Parallel transport for cardiac motion modeling: exploration of relative volume-preserving strategies

Nicolas Guigui
Université Côte d'Azur, Inria, Epione
nicolas.guigui@inria.fr

In this talk, I will apply the tools developed in Lorenzi et al. 2014; Guigui et al. 2021 to the study of the motion of the cardiac right ventricle under pressure or volume overload. The difficulty of this task lies in the interactions between shape and deformation. The central idea of this work is to filter out these interactions using the parallel transport of deformations to a reference shape, where deformations are considered in the Large Deformations Diffeomorphic Metric Mapping (LDDMM) framework. It appears that parallel transport alone is not sufficient to normalize deformations when large volume differences occur. We thus propose a normalization procedure for the amplitude of the deformation, and compare it with volume-preserving metrics. After normalization, we use a geodesic regression to represent the full cardiac contraction. The statistical analysis of the parameters of the model reveal insights into the dynamics of each disease. The method is applied to 3D meshes of the right ventricle extracted from echocardiographic sequences of 314 patients divided into three disease categories and a control group (Moceri et al. 2018).

Joint work with: Xavier Pennec, Pamela Moceri, Nicolas Duchateau.

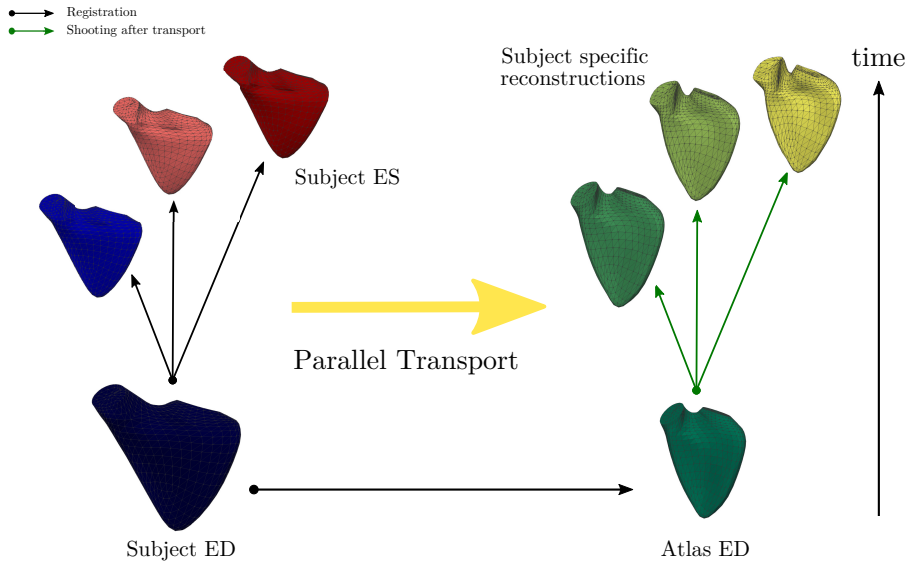

Figure 1: Our framework to normalize cardiac deformations: we rely on registration to estimate deformations, and parallel transport to normalize them.

References

Guigui, Nicolas and Xavier Pennec (June 2021). "Numerical Accuracy of Ladder Schemes for Parallel Transport on Manifolds". In: *Foundations of Computational Mathematics*. ISSN: 1615-3383. DOI: 10.1007/s10208-021-09515-x.

Lorenzi, Marco and Xavier Pennec (Sept. 2014). "Efficient Parallel Transport of Deformations in Time Series of Images: From Schild to Pole Ladder". In: *Journal of Mathematical Imaging and Vision* 50.1, pp. 5–17. ISSN: 1573-7683. DOI: 10.1007/s10851-013-0470-3.

Moceri, Pamela, Nicolas Duchateau, Delphine Baudouy, Elie-Dan Schouver, Sylvie Leroy, et al. (Apr. 2018). "Three-Dimensional Right-Ventricular Regional Deformation and Survival in Pulmonary Hypertension". In: *European Heart Journal - Cardiovascular Imaging* 19.4, pp. 450–458. ISSN: 2047-2404. DOI: 10.1093/ehjci/jex163.

Advances in patient-specific IGA-based cardiovascular simulation

David Joseph Gunderman
Purdue University, Stanford University
dgunderm@purdue.edu

Patient-specific simulations are an important, growing tool for biomedical research. In order to customize models for specific patients, anatomical structures are extracted from medical images, creating a geometric model that serves as the computational domain for simulation of physics phenomena. A common application is the numerical modelling of blood flow, tissue mechanics, or blood-tissue interaction in the cardiovascular system. These models can then be used to assess patient-specific disease condition, risk of complications, and test surgical interventions *in silico*.

Segmentation of medical image data for model geometry specification typically results in a discrete, flat-faced, triangulated boundary representation (surface mesh) of the segmented structure [3]. This geometry representation is suitable for low-order, classical finite element simulations of the physics. However, it has been shown that isogeometric analysis (IGA)-based modelling of cardiovascular geometries yields more accurate, robust, and efficient results in comparison to traditional low-order, FEM-based simulations [2]. Moreover, curved surface representations of the model facilitate systematic manipulation and optimization of the geometry. For example, the model can be unioned with a medical device, the geometry can be virtually altered to virtually plan a surgery, and the high-order mesh nodes can be used as degrees of freedom to optimize artificial vasculature design. Recently, higher medical image quality, streamlined image-to-model pipelines, and faster computational algorithms have eased the difficulties associated with simulating cardiovascular phenomena on patient-specific cardiovascular geometries [3]. However, these methods typically do not support high-order, curved surface geometry specifications.

The SimVascular team has shown that curved, analysis-suitable geometries can be extracted from labelled, low-order, patient-specific cardiovascular datasets [1]. In this presentation, I will discuss the state-of-the-field in applications of IGA to the cardiovascular system, present preliminary work demonstrating the steps in an image-to-analysis pipeline for IGA-based numerical simulations of cardiovascular dynamics on a open-source dataset of labeled patient-specific models, and pose future directions and challenges associated with IGA simulation of multiphysics problems associated with image-based cardiovascular fluid-structure interaction problems.

Joint work with: Alison L. Marsden, Hector Gomez, Craig J. Goergen.

References

[1] A. Updegrove, S. C. Shadden and N. M. Wilson. Construction of analysis-suitable vascular models using axis-aligned polycubes. *Journal of Biomechanical Engineering*, American Society of Mechanical Engineers, 141:6:060906, 2019.

[2] Y. Zhang, Y. Bazilevs, S. Goswami, C.L. Bajaj, T.J.R. Hughes. Patient-specific vascular NURBS modeling for isogeometric analysis of blood flow. *Computer methods in applied mechanics and engineering.* 196:29-30, pages 2943–2959, 2007.

[3] A. Updegrove, N.M. Wilson, J. Merkow, H. Lan, A.L. Marsden, and S.C. Shadden. SimVascular: an open source pipeline for cardiovascular simulation. *Annals of biomedical engineering*, 45:3:, pages 525-541, 2017.

Projective equivalences of rational algebraic space curves using differential invariants

Uğur Gözütok
Department of Mathematics,
Karadeniz Technical University,
Trabzon,Turkey
ugurgozutok@ktu.edu.tr

We present an alternative method to existing algorithms [1, 2] for computing the projective equivalences between two rational space curves. The method is inspired in [3], where torsion and curvature, two classical and well-known differential invariants of space curves, are used to compute the similarities between two given space rational curves. In our case, we produce two projective curvature-like invariants κ_1 and κ_2, that can be used to characterize the existence of projective equivalences. In more detail, given two rational curves C_1 and C_2 properly parametrized by p, q, we prove that C_1, C_2 are projectively equivalent if and only if

$$\kappa_1(p) = \kappa_1(q)(\varphi), \quad \kappa_2(p) = \kappa_2(q)(\varphi),$$

where φ is a Möbius transformation. Then we can detect projective equivalence by checking whether or not the gcd of the polynomials involved in the above equation has a Möbius-like factor. In the affirmative case φ is obtained, and from here the projective equivalence itself can be easily computed. After finding the gcd, we can also use polynomial system solving; but in that case the system is substantially smaller compared to other approaches, which leads to better timings. The method has been implemented in Maple. A full description of the algorithm and the ideas behind it can be found in [4].

Joint work with: Hüsnü Anıl Çoban, Yasemin Sağıroğlu

References

[1] M. Hauer and B. Jüttler. Projective and affine symmetries and equivalences of rational curves in arbitrary dimension. *Journal of Symbolic Computation*, 87:68–86, 2018.

[2] M. Bizzarri, M. Lávička, Jan Vršek. Computing projective equivalences of special algebraic varieties. *Journal of Computational and Applied Mathematics*, 367:112438, 2020.

[3] J.G. Alcázar, C. Hermoso and G. Muntingh. Symmetry detection of rational space curves from their curvature and torsion. *Computer Aided Geometric Design*, 33:51–65, 2015.

[4] U. Gözütok, H.A. Coşban, Y. Sağıroğlu. A differential approach to detecting projective equivalences and symmetries of rational $3D$ curves. *arXiv:2110.05436v2.*

Equivariant Subgraph Aggregation Networks

Haggai Maron
Nvidia Research
hmaron@nvidia.com

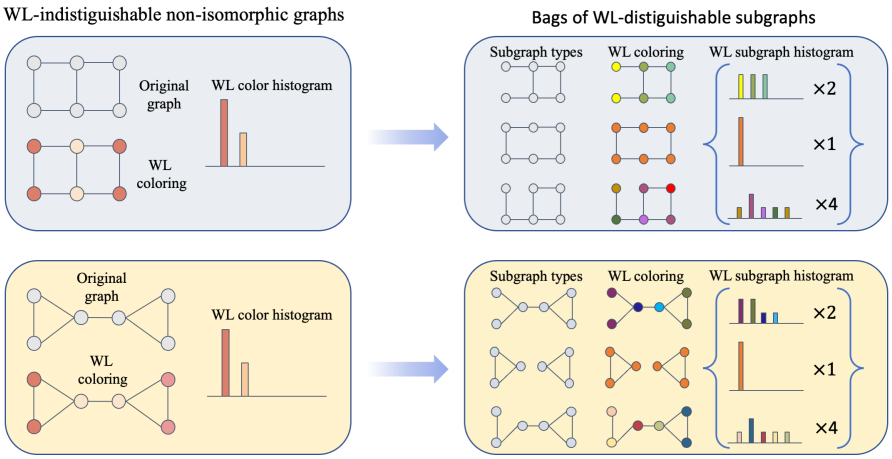

Figure 1: We present a provably expressive graph learning framework based on representing graphs as bags of subgraphs and processing them with an equivariant architecture, composed of GNNs and set networks. **Left panel:** A pair of graphs not distinguishable by the WL test. **Right panel:** The corresponding bags (multisets) of all edge-deleted subgraphs, which can be distinguished by our framework.

Message-passing neural networks (MPNNs) are the leading architecture for deep learning on graph-structured data, in large part due to their simplicity and scalability. Unfortunately, it was shown that these architectures are limited in their expressive power [2].

This work proposes a novel framework called Equivariant Subgraph Aggregation Networks (ESAN) to address this issue. Our main observation is that while two graphs may not be distinguishable by an MPNN, they often contain distinguishable subgraphs. Thus, we propose to represent each graph as a bag (multiset) of subgraphs derived by some predefined policy, and to process it using a suitable equivariant architecture. To deal with the increased computational cost, we propose a subgraph sampling scheme, which can be viewed as a stochastic version of our framework.

We develop novel variants of the 1-dimensional Weisfeiler-Leman (1-WL) [1] test for graph isomorphism, and prove lower bounds on the expressiveness of ESAN in terms of these new WL variants. We further prove that our approach increases the expressive power of both MPNNs and more expressive architectures. Moreover, we provide theoretical results that describe how design choices such as the subgraph selection policy and equivariant neural architecture affect our architecture's expressive power.

A comprehensive set of experiments on real and synthetic datasets demonstrates that our framework improves the expressive power and overall performance of popular GNN architectures.

Joint work with: Beatrice Bevilacqua, Fabrizio Frasca, Derek Lim, Balasubramaniam Srinivasan, Chen Cai, Gopinath Balamurugan, Michael M. Bronstein.

References

[1] B. Weisfeiler and A. Leman. The reduction of a graph to canonical form and the algebra which appears therein. *NTI, Series*, 2(9):12–16, 1968.

[2] K. Xu, W. Hu, J. Leskovec, and S. Jegelka. How powerful are graph neural networks? In *International Conference on Learning Representations*, 2019.

Learning Deformation Patterns of Surface Meshes of Different Sizes

Sara Hahner
Fraunhofer Center for Machine Learning and SCAI
University of Bonn
sara.hahner@scai.fraunhofer.de

We analyze the deformation of three-dimensional shapes that are represented by surface meshes. To detect underlying dynamics in the deformation behavior, we represent the data in a low-dimensional space using non-linear dimensionality reduction methods.

The area of geometry processing offers different ways to obtain these low-dimensional representations. The surface meshes can be projected onto Laplacian eigenvectors describing functions on the meshes. Autoencoders are a type of neural network for unsupervised representation learning that project the data to a learned low-dimensional space. These networks have successfully been applied to surface meshes combining graph convolutional filters and pooling operators, that reduce the mesh density.

The state-of-the-art methods generally depend on the adjacency matrix of the surface mesh. Therefore, knowledge and patterns, which have been learned and detected on the training data, cannot be transferred to surface data with a different mesh representation. In addition, note that a method that can handle meshes of different sizes and shapes has more training data available and can in particular be applied in scenarios where there are too few examples to train a separate network.

Based on this observation, we developed a novel approach to handle meshes of different shapes and sizes: *Mesh Convolutional Autoencoder for Semi-Regular Meshes of Different Sizes* [2]. We calculate an alternative discrete approximation of the surface data based on semi-regular meshes. Semi-regular meshes have regular regional patches, which means that every vertex inside the patch has exactly six neighbors. The local regularities in the meshes allow us to reutilize learned convolutional filters and define a pooling based on the local mesh regularity that is the same for all meshes of this type. Since the convolutional neural networks learn local features, we feed the regular regional patches, which all have the same meshing, separately to the network. The global context is not lost but fed to the network via padding. In this way, we use one network to analyze the deformation of shapes that have different mesh representations.

We apply the same mesh autoencoder to diverse classes of datasets, including moving humans and animals as well as deforming car components. Our reconstruction error is more than 50% lower than the error from state-of-the-art models [1, 3], which have to be trained for every mesh separately. Additionally, we visualize the underlying dynamics of unseen mesh sequences with an autoencoder trained on different classes of meshes (see Figure 1).

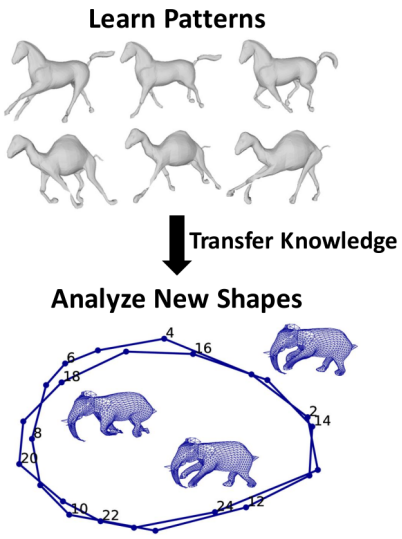

Figure 1: Analyze the deformation pattern of an elephant, which has not been presented to the network during training.

Joint work with: Jochen Garcke.

References

[1] G. Bouritsas, S. Bokhnyak et al. Neural 3D morphable models: Spiral convolutional networks for 3D shape representation learning and generation. *IEEE International Conference on Computer Vision*, 2019.

[2] S. Hahner and J. Garcke. Mesh Convolutional Autoencoder for Semi-Regular Meshes of Different Sizes. *IEEE Winter Conference on Applications of Computer Vision*, 2022.

[3] A. Ranjan, T. Bolkart et al. Generating 3D Faces Using Convolutional Mesh Autoencoders. *IEEE European Conference on Computer Vision*, 2018.

NL-Ridge: a novel statistical patch-based approach for image denoising

Sébastien Herbreteau and Charles Kervrann

SERPICO Project-Team Inria Centre Rennes - Bretagne Atlantique
UMR144 CNRS Institut Curie, PSL Research University, Sorbonne Université
sebastien.herbreteau@inria.fr and charles.kervrann@inria.fr

We present a novel statistical patch-based approach for image denoising [1]. The state-of-the-art unsupervised methods that only use a single noisy image are two-step algorithms [2] [3]. Leveraging the Stein's unbiased risk estimate (SURE) [4] for the first step and the "internal adaptation", a concept borrowed from deep learning theory [5], for the second one, we show that our NL-Ridge approach enables to reconcile several previous patch-based methods for image denoising. In the second step, our closed-form aggregation weights are computed through multivariate Ridge regressions. Experiments on artificially noisy images demonstrate that NL-Ridge may outperform state-of-the-art unsupervised denoisers such as BM3D [2] and NL-Bayes [3], and recent unsupervised deep learning methods such as Noise2Self [6], Self2Self [7], and Deep Image Prior [8] as well as supervised techniques such as DnCNN [9], while being much more simple conceptually.

Noisy / 22.09 dB | BM3D[2] / 31.72 dB | Self2Self[7] / 31.62 dB | DnCNN[9] / 31.06 dB | **NL-Ridge**[1] / **32.06 dB**

Figure 1: Denoising results (in PSNR) for *Barbara* corrupted with additive white Gaussian noise ($\sigma = 20$).

References

[1] S. Herbreteau and C. Kervrann. A unified view of unsupervised non-local methods for image denoising: the NL-Ridge approach *(in preparation)*.

[2] K. Dabov, A. Foi, V. Katkovnik, and K. Egiazarian. Image denoising by sparse 3D transform-domain collaborative filtering. *IEEE Transactions on Image Processing*, 16(8):2080–2095, 2007.

[3] M. Lebrun, A. Buades, and J.-M. Morel A Non-local Bayesian image denoising algorithm. *SIAM Journal on Imaging Science*, 6(3):1665–1688, 2013.

[4] C. Stein. Estimation of the mean of a multivariate normal distribution. *Annals of Statistics*, 9(6):1135–1151, 1981.

[5] G. Vaksman, M. Elad, and P. Milanfar. LIDIA: Lightweight Learned Image Denoising With Instance Adaptation. *Proc. of IEEE/CVF Conf. on Computer Vision and Pattern Recognition Workshops*, 2020.

[6] J. Batson and L. Royer. Noise2Self: Blind denoising by self-supervision. *Proc. of In. Conf. on Machine Learning*, pages 524-533, 2019.

[7] Y. Quan, M. Chen, T. Pang, and H. Ji. Self2Self with dropout: Learning self-supervised denoising from single image. *Proc. of IEEE/CVF Conf. on Computer Vision and Pattern Recognition*, pages 1890-1898, 2020.

[8] D. Ulyanov, A. Vedaldi, and V. Lempitsky. Deep image prior. *Proc. of IEEE Conf. on Computer Vision and Pattern Recognition*, pages 9446–9454, 2018.

[9] K. Zhang, W. Zuo, Y. Chen, D. Meng, and L. Zhang. Beyond a gaussian denoiser: residual learning of Deep CNN for image denoising. *IEEE Transactions on Image Processing*, 26(7):3142–3155, 2017.

Fast and memory-efficient independent component analysis using Lie group techniques

Matthias Hermann
HTWG Konstanz
mhermann@htwg-konstanz.de

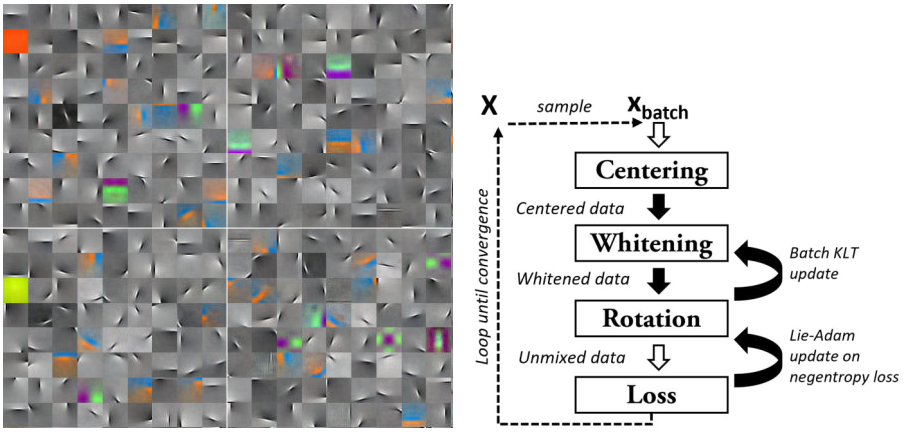

Figure 1: Examples of the first 484 independent components estimated from the ImageNet dataset ($1.2 \cdot 10^6$ examples and $d = 150528$) (left). In Lie-ADAM, we used a learning rate of 0.01 and a batch size of 484. The model was trained with three runs through the dataset which took $3h$ on standard hardware with a single GPU. A schematic overview of the algorithm is shown on the right.

We were interested in computing a mini-batch-capable end-to-end algorithm to identify statistically independent components (ICA) [1] in large scale and high-dimensional datasets. Current algorithms typically rely on pre-whitened data and do not integrate the two procedures of whitening and ICA estimation. Our online approach estimates a whitening and a rotation matrix with stochastic gradient descent on centered or uncentered data. We show that this can be done efficiently by combining Batch Karhunen-Löwe-Transformation [2] with Lie group techniques [3]. By using b-sized mini-batches the space complexity of the entire pipeline for d-dimensional inputs and k components is limited to $\mathrm{O}(d(k+b))$. Our algorithm is recursion-free and can be organized as feed-forward neural network which makes the use of GPU acceleration straight-forward. Because of the very fast convergence of Batch KLT, the gradient descent in the Lie group of orthogonal matrices stabilizes quickly. The optimization is further enhanced by integrating ADAM, an improved stochastic gradient descent (SGD) technique from the field of deep learning. We test the scaling capabilities by computing the independent components of the well-known ImageNet challenge (144 GB). Due to its robustness with respect to batch and step size, our approach can be used as a drop-in replacement for standard ICA algorithms where memory is a limiting factor.

Joint work with: Georg Umlauf, Matthias O. Franz

References

[1] P. Comon, "Independent component analysis, a new concept?" *Signal processing*, vol. 36, no. 3, pp. 287–314, 1994.

[2] A. Levy and M. Lindenbaum, "Sequential karhunen-loeve basis extraction and its application to images," in *Proceedings 1998 International Conference on Image Processing. ICIP98*, IEEE, vol. 2, 1998, pp. 456–460.

[3] M. D. Plumbley, "Geometry and manifolds for independent component analysis," in *2007 IEEE International Conference on Acoustics, Speech and Signal Processing-ICASSP'07*, IEEE, vol. 4, 2007, IV–1397.

Detecting projective equivalences of planar curves birational to elliptic and hyperelliptic curves

Carlos Hermoso
Universidad de Alcalá
carlos.hermoso@uah.es

Recognizing projective equivalence, i.e. detecting whether two objects are related by a projectivity, is important in applied fields like Pattern Recognition and Computer Vision. For rational curves the problem is well-understood, and efficient algorithms for detecting projective equivalence are available [3]. However, for other curves the problem is still open. Here we will consider curves birationally equivalent to elliptic and hyperelliptic planar curves, which are not rational, although they can be parametrized by rational functions and square-roots of rational functions. These curves are well-known in Mathematics, both for their rich mathematical properties and for their applications in Cryptography, and appear naturally in several constructions in Computer Aided Geometric Design [2], like offsets of rational curves, bisectors of certain curves or contour curves of rational canal surfaces. Four our purposes, the most useful property of these curves is that elliptic and hyperelliptic curves have a birational model in the plane defined by Weierstrass equations (Weierstrass normal forms), so that plane curves birationally equivalent to elliptic and hyperelliptic curves also inherit a Weierstrass model by composition of the birational mappings. Thus, from an algorithmic point of view, the key idea is to find a corresponding transformation between the Weierstrass forms of the curves, which in the case of elliptic curves can be completely characterized. The results presented in this talk can be found in [1].

Joint work with: Juan Gerardo Alcázar.

References

[1] J. G. Alcázar and C. Hermoso. Computing projective equivalences of planar curves birationally equivalent to elliptic and hyperelliptic curves, *Comput. Aided Geom. Des.* 91 (2021) 102048.

[2] M. Bizzarri, M. Lávička and J. Vršek, J., Piecewise rational approximation of square-root parameterizable curves using the Weierstrass form. *Comput. Aided Geom. Des.* 56 (2017), pp. 52–66.

[3] M. Hauer, M and B. Jüttler. Projective and affine symmetries and equivalences of rational curves in arbitrary dimension. *J. Symbolic Comput.* 87 (2018), pp. 68–86.

Results for the Weak Chebyshev Greedy Algorithm in Banach spaces

Eugenio Hernández
Universidad Autónoma de Madrid
eugenio.hernandez@uam.es

We present some results concerning Lebesgue-type inequalities for the Weak Chebyshev Greedy Algorithm (WCGA), which is a generalization to Banach spaces of the Orthogonal Matching Pursue (OMP) algorithm for Hilbert spaces. The results are proved in the context of uniformly smooth Banach spaces.

We shall present a result that improves earlier bounds in V.N. Temlyakov (*Sparse approximation and recovery for greedy algorithms in Banach spaces*, Forum Math. Sigma 2 (12) (2014)). We apply this result to derive optimal bounds for the Multivariate Haar system in L^p with $1 < p \leq 2$, under the Littlewood-Paley norm, and also for the canonical basis in the mixed norm sequence spaces $\ell^p(\ell^q)$ (for all $1 < p, q < \infty$). Several open questions will also be stated.

This is joint work with S. Dilworth, G. Garrigós, D. Kutzarova, and V.N. Temlyakov that was started during the program *Approximation, Sampling and Compression in Data Science* held at the Isaac Newton Institute for Mathematical Sciences, Cambridge (UK), during the first semester of 2019.

An algorithm for the unrefinement of domain parameterizations in isogeometric analysis

Teymur Heydarov
JKU Linz, Austria
teymur.heydarov@jku.at

This talk is devoted to unrefinement of representations of computational domains (parameterizations) in isogeometric analysis [1]. Unrefinement allows to perform faster simulations while maintaining a reasonable level of the precision in the specified area. We present an algorithm that creates a coarser parameterization $\tilde{\mathbf{p}}(u, v)$ (i.e. with the less degrees of freedom) from a given parameterization $\mathbf{p}(u, v)$. Both parameterizations are assumed to be represented via THB-splines [2]. Moreover, the coarser parameterization possesses the following properties:

- The dimension of the space spanned by the THB-splines basis functions, which are used to represent a $\tilde{\mathbf{p}}(u, v)$, is lower.
- The coarser parameterization $\tilde{\mathbf{p}}(u, v)$ is regular. In particular, no self-intersections are allowed to be present.
- The created parameterization $\tilde{\mathbf{p}}(u, v)$ approximates the initial parameterization $\mathbf{p}(u, v)$ globally with a given precision.
- On a part of a domain boundary ("feature") the coarser parameterization $\tilde{\mathbf{p}}(u, v)$ approximates $\mathbf{p}(u, v)$ globally with a given lower precision.

The algorithm uses local projectors [3] and different local optimization techniques [4] to ensure the approximation and regularity properties.

Joint work with: Annalisa Buffa, Bert Jüttler.

References

[1] T.J.R. Hughes, J.A. Cottrell, and Y. Bazilevs. Isogeometric analysis: CAD, finite elements, NURBS, exact geometry and mesh refinement. *Computer Methods in Applied Mechanics and Engineering*, 194, (39-41):4135–4195, 2005.

[2] C. Giannelli and B. Jüttler and H. Speleers. THB-splines: The truncated basis for hierarchical splines. *Computer Aided Geometric Design*, 29, 7:485–498, 2012.

[3] A. Giust and B. Jüttler and A. Mantzaflaris. Local (T) HB-spline projectors via restricted hierarchical spline fitting *Computer Aided Geometric Design*, 80 , 2020.

[4] A. Falini and J.Špeh and B. Jüttler. Planar domain parameterization with THB-splines. *Computer Aided Geometric Design*, 35, pages 95–108, 2015.

An RBF-FD Method for Solving Partial Differential Equations on Evolving Curves and Surfaces

Caleb Jacobs
University of Colorado Boulder
Caleb.Jacobs@colorado.edu

Many applications in the natural and applied sciences involve the solution of partial differential equations (PDEs) on surfaces. Application areas for PDEs on static surfaces include image processing, biology, and computer graphics. Applications for PDEs on moving surfaces also occur frequently. Notable examples arise in biology, material science, fluid dynamics, and computer graphics.

Radial Basis Function-generated Finite Difference (RBF-FD) methods have the properties of being meshfree (giving it flexibility to represent complex geometries in any spatial dimension), of providing a high order of accuracy, as well as having a low computational complexity. Although RBFs have been used for solving PDEs on static manifolds for a few years (e.g. [1, 2]), its application to solving PDEs on moving curves and surfaces is in its infancy. In this presentation, we introduce a procedure to solve PDEs on evolving surfaces. Our method is based on the RBF-FD method to discretize curve (or surface)-constrained differential operators, to accurately and efficiently evolve solutions, manifolds, and the computational grid. We will show that the proposed method is stable, has a high order of accuracy, and is computationally cheap compared to its various counterparts (e.g. [3]). We will present a number of examples to illustrate the numerical convergence properties of our proposed method.

Joint work with: C. Piret, J. Blazejewski.

References

[1] C. Piret. The Orthogonal Gradients Method: a radial basis functions method for solving partial differential equations on arbitrary surfaces. *J. Comput. Phys.*, 231, 2012, pp. 4662–4675.

[2] C. Piret, J. Dunn. Fast RBF OGr for solving PDEs on arbitrary surfaces. *AIP Conference Proceedings*, 1776(1), 070005.

[3] A.Petras, L.Ling, C. Piret, S. Ruuth. A least-squares implicit RBF-FD closest point method and applications to PDEs on moving surfaces. *J. Comput. Phys.*, 381, 2019, pp. 146–161.

On the optimal constants in the two-sided Stechkin inequalities

Thomas Jahn
TU Chemnitz
thomas.jahn@mathematik.tu-chemnitz.de

The ℓ_1-norm of a monotonically decreasing sequence of nonnegative numbers can be sandwiched by a sum involving the best n-term approximation errors measured in the ℓ_q-norm, suitably scaled by positive constants. But what are the optimal constants? In this talk, you will get in touch with the contributions of Copson, Stechkin, Pietsch, Temlyakov, and Bennett, the geometry behind the problem, and variants of the inequality, where the ℓ_1-norm is replaced by its weak counterpart or where sums are replaced by integrals.

Joint work with: Tino Ullrich.

References

[1] T. Jahn, T. Ullrich. On the optimal constants in the two-sided Stechkin inequalities. *J. Approx. Theory*, 269:105607, 2021.

Uniqueness of phase retrieval from three measurements

Philippe Jaming
IMB-Université de Bordeaux
philippe.jaming@math.u-bordeaux.fr

The phase retrieval in diffraction theory mainly consists in recovering a signal $f \in L^2(\mathbb{R}^d)$ from the modulus of its Fourier transform $|\widehat{f}|$. It is well known that this problem is severelly ill posed. One of the reasons for this is that the solution set $\{g \in L^2(\mathbb{R}^d) : |\widehat{g}| = |\widehat{f}|\}$ may be very large.

One may thus try to reduce the solution set by adding more measurements. For instance, one may add a mask which amounts to replacing the measurement $|\widehat{f}|$ by $|\widehat{mf}|$ where m is a masking function. A good description of this idea and actual experiments which are done this way can be found in [1] where the data $|\widehat{mf}|$ has been called a *coded diffraction patern*. The experiments may be summarized in the following picture taken from [1].

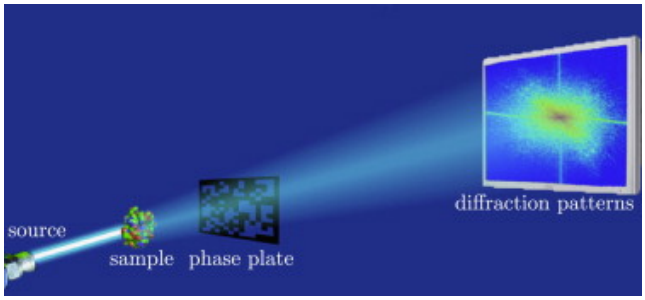

So far this problem has mainly been studied in the discrete setting, that is, with $L^2(\mathbb{R}^d)$ replaced by $L^2\big((\mathbb{Z}/N\mathbb{Z})^d\big)$, the Fourier transform being then the discrete Fourier transform. It is then known that 3 well chosen masks can determine almost all signals (but not all) while a small number of randomly chosen masks allow to determine all signals.

The aim of this talk is to show that the situation is better in the continuous setting:

Main result. *Let* $\gamma_1(t) = e^{-\pi t^2}$, $\gamma_2(t) = te^{-t^2/2}$ $\gamma_2(t) := 2\pi t\gamma(t)$, $\gamma_3(t) := (1-2\pi t)\gamma(t)$. *Let* $f, g \in L^2(\mathbb{R})$ *be such that* $|\widehat{f\gamma_j}| = |\widehat{g\gamma_j}|$ *then there exists* $c \in \mathbb{C}$ *with* $|c| = 1$ *such that* $f = cg$.

The proof uses complex analysis and the original idea comes from a paper by McDonald [2]. A stronger argument allows to construct more families of masks that lead to the same result. We will also explain that the direct analogues of these masks in the discrete setting don't work and that this is mainly an issue about under-sampling.

Joint work with: Martin Rathmair (Bordeaux)

References

[1] E.J. Candes, Y.C. Eldar, T. Strohmer, V. Voroninski Phase retrieval via matrix completion *SIAM J. Imaging Sci.*, 6(1):199–225, 2013.

[2] J. Mc Donald Phase retrieval and magnitude retrieval of entire functions *J. Fourier Anal. Appl.*, 10:259–267, 2004.

Optimization of a mutual shape based on the Fréchet-Nikodym metric for 3D shapes fusion

S. Jehan-Besson[1], P. Clarysse[1], R. Clouard[2], F. Frouin[3],

[1] Univ. Lyon, CNRS, Inserm, INSA Lyon, UCBL, CREATIS, UMR5220, U1294, 69621, Villeurbanne, France,

[2] Normandie Univ, UNICAEN, ENSICAEN, CNRS, GREYC, Caen, France,

[3] Institut Curie, Univ. PSL, Inserm U1288, Laboratoire LITO, 91400 Orsay, France

stephanie.jehan-besson@creatis.insa-lyon.fr

In the field of delineation of 2D or 3D regions of interest (ROI) in medical imaging, and especially due to the development of multimodal and multiparametric image acquisition devices, the combination of segmentations of anatomical structures from different sources is of interest. It is also essential to accurately evaluate the variability between experts delineation or algorithms with different parameters. In this work, we propose to estimate a mutual shape defined as the optimum of a statistical criterion based on information theory. Compared to our previous works [2, 3], we propose to interpret the mutual shape as a sum of distances of the Fréchet family and we extend our approach to 3D shapes fusion.

Let us consider $\{\Omega_1, ..., \Omega_n\}$, a set of n shapes corresponding to different segmentations of the same object. Shapes may include partial information or erroneous parts. Our goal is to compute a reference shape Ω_{ref} to estimate the considered object by combining the information given by all the regions Ω_i. In the literature, mean shapes are usually defined by minimizing the following functional: $J_1(\mu) = \sum_{i=1}^{n} d_1(\Omega_i, \Omega_{ref})$. The choice of the distance d is crucial and can lead to different results. For example, mean shapes can be computed by minimizing the sum of symmetric differences using $d_1(\Omega_i, \Omega_{ref}) = |\Omega_i \triangle \Omega_{ref}|$ where $\Omega_i \triangle \Omega_{ref} = (\Omega_i \cup \Omega_{ref}) \setminus (\Omega_i \cap \Omega_{ref})$.

Given a measure space (X, A, mes), a mutual shape can be defined more generally by minimizing the following functional: $J_2(\mu) = \sum_{i=1}^{n} d_2(\Omega_i, \Omega_{ref})$ where $d_2(\Omega_i, \Omega_{ref}) = mes(\Omega_i \triangle \Omega_{ref})$ is a finite signed measure of the symmetric difference not necessarily defined by the cardinality measure as in d_1. Under certain properties, such a distance is a shape metric known as the Fréchet-Nikodym distance [1]. This seems of interest because of the relevance of Fréchet distances in medical image analysis [4]. Such a distance can be considered under the umbrella of information theory. Indeed information theory quantities can be considered in terms of measure over sets. The joint entropy can be expressed using $H(D_i, T) = \text{mes}(\tilde{D}_i \cup \tilde{T})$ and the mutual information using $I(D_i, T) = \text{mes}(\tilde{D}_i \cap \tilde{T})$ where $\tilde{D}_i$ and $\tilde{T}$ are the abstract sets associated to Ω_i and Ω_{ref} (D_i and T define the random variables associated to the each characteristic functions). The mutual shape T is then defined by minimizing $E_2(T) = \sum_{i=1}^{n} (H(D_i, T) - I(D_i, T))$ expressed in a continuous framework and computed using shape optimization tools [2].

An example showing the interest of the combination of segmentation methods computed separately on four MRI modalities is given in [3]. In this current work, we extend our framework to 3D shapes fusion and we provide below a synthetic example to demonstrate the difference between the mutual shape (criterion J_2), the mean shape (criterion J_1) and the union of shapes. The algorithm is robust to the outlier Ω_6.

Ω_1 Ω_2 Ω_3 Ω_4 Ω_5 Ω_6 (a) Union (b) Mutual shape (c) Mean shape

Figure 1: (Ω_1 to Ω_6) : 2D Front views of 3D entries, (a) : Union of Ω_i (3D), (b) : Mutual Shape (3D), (c) : Mean shape (3D).

References

[1] M.M. Deza and E. Deza. *Encyclopedia of Distances*. Springer Berlin Heidelberg, 2016.

[2] S. Jehan-Besson, R. Clouard, and C. Tilmant et al. A mutual reference shape for segmentation fusion and evaluation. *arXiv:2102.08939*, 2021.

[3] S. Jehan-Besson, R. Clouard, and N. Boddaert et al. Optimization of a shape metric based on information theory applied to segmentation fusion and evaluation in multimodal MRI for DIPG tumor analysis. In *GSI*, Paris, July 2021.

[4] X. Pennec, S. Sommer, and T. Fletcher (Eds). *Riemannian Geometric Statistics in Medical Image Analysis*. Academic Press, 2020.

Virtual Assembly Using Haptic Force-Feedback Rendering

Jernej Barbič
University of Southern California
jnb@usc.edu

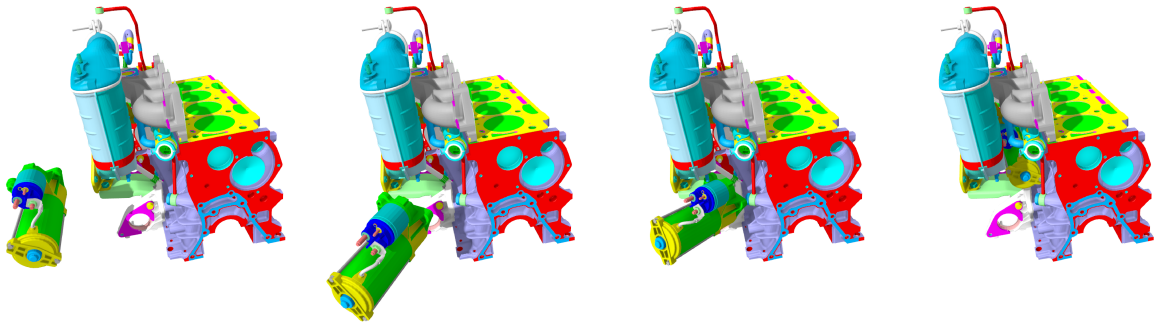

Figure 1: Virtual assembly of complex geometry: insertion of a car starter motor into the engine.

Six-DoF haptic rendering is useful for interactive applications in virtual assembly and maintenance of complex machinery, such as, for example, car engines and landing gears. Because mechanical components are often geometrically complex, such applications require efficient interactive simulation, involving collision detection and rigid and deformable object simulation. In simulations involving complex distributed contact, there are typically many simultaneous individual contacts, posing stability issues due to accumulated stiffness. In order for simulations to be useful, they must eliminate (or at least minimize) false-positives, i.e., paths that violate contact due to errors in the contact resolution algorithm. Friction is non-trivial, due to the large number of contacts and stringent time requirements. Similarly, preparing the signed distance fields and point clouds can take an unreasonably amount of time with models of realistic complexity. Even if the haptic rendering problem were to be completely solved, this alone is not sufficient for efficient training of virtual assembly, because users still need to be trained how to perform complex assembly paths.

In my talk, I will give recent advances on these problems in my group at the University of Southern California. I will discuss signed distance field generation, continuous collision detection, adaptive stiffness and friction. I will also discuss how to augment 6-DoF haptic rendering of contact to maximize virtual assembly training efficiency, by employing carefully selected visual and haptic guidance strategies.

Joint work with: Hongyi Xu, Danyong Zhao, Yijing Li, Mianlun Zheng.

References

[1] H. Xu and J. Barbič. Adaptive 6-DoF Haptic Contact Stiffness Using the Gauss Map. *IEEE Transactions on Haptics*, 9(3):323-332, 2016.

[2] H. Xu and J. Barbič. 6-DoF Haptic Rendering using Continuous Collision Detection Between Points and Signed Distance Fields. *IEEE Transactions on Haptics*, 10(2):151-161, 2017.

[3] D. Zhao and Y. Li and J. Barbič. 6-DoF Haptic Rendering of Static Coulomb Friction Using Linear Programming. *IEEE Transactions on Haptics*, 11(3):325-337, 2018

[4] M. Zheng and D. Zhao and J. Barbič. Evaluating the Efficiency of Six-DoF Haptic Rendering-Based Virtual Assembly Training. *IEEE Transactions on Haptics*, 14(1):212-224, 2021.

q-Bernstein bases over triangular domains

Jorge Delgado
Escuela de Ingeniería y Arquitectura
Universidad de Zaragoza
jorgedel@unizar.es

The q-Bernstein, $0 < q \leq 1$, basis of univariate polynomials has played an important role in several fields, such as Computer Aided Geometric Design (CAGD), Approximation Theory or Quantum Calculus. They have received much attention in recent research (cf. [3, 4, 5, 1, 2] and references in there). For the particular case $q = 1$, it coincides with the basis of Bernstein polynomials.

In this talk, q-Bernstein basis functions over a triangular domain will be presented and analyzed. Recurrence relations and properties such us partition of unity and degree elevation will be shown for them. Evaluation algorithms will be presented.

Joint work with: Héctor Orera, Juan Manuel Peña.

References

[1] R. Goldman, P. Simeonov. Two essential properties of (q,h)-Bernstein-Bézier curves. *Appl. Numer. Math.* 96:82–93, 2015.

[2] R. Goldman, P. Simeonov, Y. Simsek. Generating functions for the q-Bernstein bases. *SIAM J. Discrete Math.* 28:1009–1025, 2014.

[3] H. Oruç, G. M. Phillips. q-Bernstein polynomials and Bézier curves. *J. Comput. and Appl. Math.* 151:1–12, 2003.

[4] G. M. Phillips. A de Casteljau algorithm for generalized Bernstein polynomials. *BIT Numer. Math.* 36:232–236, 1996.

[5] G. M. Phillips. Bernstein polynomials based on the q-integers. *Ann. Numer. Math.* 4:511–518, 1997.

THB-spline projectors based on restricted hierarchical spline fitting and their application to weighted isogeometric collocation

Bert Jüttler
Johannes Kepler University, Linz/Austria
bert.juettler@jku.at

We describe a construction of locally supported spline projectors for truncated hierarchical (TH) B-splines. These operators, which are based on restricted hierarchical spline fitting, can be used to generate approximations of functions in adaptively refined spline spaces [1]. We discuss the computational efficiency of the resulting algorithms. In addition, we show that these projectors can be employed successfully for the discretization of partial differential equations via isogeometric collocation. More precisely, we combine the framework of weighted isogeometric collocation [2] with the THB-spline projectors and discuss the computational efficiency of the algorithms and the convergence properties of the resulting discretization scheme [3].

Joint work with: Alessandro Giust

References

[1] A. Giust, B. Jüttler and A. Mantzaflaris. Local (T)HB-spline projectors via restricted hierarchical spline fitting, *Computer Aided Geometric Design*, 80, article no. 101865, 2020.

[2] D. Schillinger, J. Evans, A. Reali, M. Scott and T. Hughes. Isogeometric collocation: Cost comparison with Galerkin methods and extension to adaptive hierarchical NURBS discretizations. *Computer Methods in Applied Mechanics and Engineering*, 267, pages 170–232, 2013.

[3] A. Giust and B. Jüttler. Weighted isogeometric collocation based on spline projectors, *Computer Methods in Applied Mechanics and Engineering*, 391, article no. 114554, 2022.

Dismantling varifold metrics for partial matchings

Irène Kaltenmark
MAP5, Université de Paris

Shape registration is a central problem in computational anatomy. The well-studied case where shapes are homologous is yet not always adapted. The reason can be the inter-individual variability, the study of pathological anomalies or some acquisition methods that provide cropped data.

In this talk, I will present an asymmetric data attachment term characterizing the inclusion of one shape in another. This term is based on the metrics of varifold spaces. Varifolds are representations of geometric objects, including curves and surfaces. Their specificity is to take into account the tangent spaces of these objects and to be robust to the choice of parametrization.

This new data attachment term widens the field of application of the pre-existing methods of matching by large diffeomorphic deformations (LDDMM). The partial registration is indeed induced by a diffeomorphic deformation of the source shape. The anatomical (topological) characteristics of this shape are thus preserved.

Joint work with: Pierre-Louis Antonsanti and Joan Glaunès.

References

[1] P-L. Antonsanti, J. Glaunès, T. Benseghir, V. Jugnon, I. Kaltenmark. Partial Matching in the Space of Varifolds. IPMI 2021.

[2] H-W. Hsieh, and N. Charon. Diffeomorphic Registration with Density Changes for the Analysis of Imbalanced Shapes. IPMI 2021.

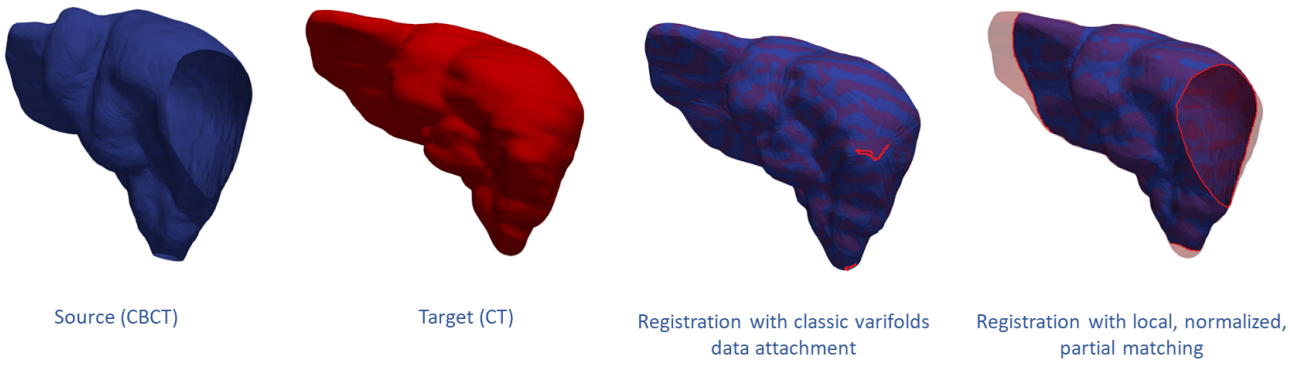

Curve-guided 5-axis CNC flank milling of free-form surfaces using custom-shaped tools

Kanika Rajain
(BCAM) Basque Center for Applied Mathematics,
kanika@bcamath.org

Abstract

A new method for 5-axis flank milling of free-form surfaces is proposed. Existing flank milling path-planning methods typically use on-market milling tools whose shape is cylindrical or conical, and is therefore not well-suited for meeting fine tolerances for manufacturing of benchmark free-form surfaces like turbine blades, gears, or blisks. In contrast, our optimization-based framework incorporates the shape of the tool into the optimization cycle and looks not only for the milling paths, but also for the shape of the tool itself. Given a free-form reference surface and a guiding path that roughly indicates the motion of the milling tool, tangential movability of quadruplets of spheres centered along a straight line is analyzed to indicate possible shapes and their motions. This results in G^1 Hermite data in the space of rigid body motions that are interpolated and further optimized, both in terms of the motion and the shape of the milling tool itself. We demonstrate our algorithm on synthetic free-form surfaces and industrial benchmark datasets, showing that the use of custom-shaped tools is capable of meeting fine industrial tolerances and outperforms the use of classical, on-market tools.

Joint work with: Oleksii Sliusarenko, Michal Bizzarri, and Michael Bartoň.

Supervised learning of sheared distributions using linearized optimal transport

Varun Khurana
University of California, San Diego
vkhurana@ucsd.edu

Detecting differences and building classifiers between distributions, given only finite samples, are important tasks in a number of scientific fields. Optimal transport (OT) has evolved as the most natural concept to measure the distance between distributions and has gained significant importance in machine learning in recent years. However, OT often fails to exploit reduced complexity in case the family of distributions is generated by simple group actions. In this talk, we discuss how optimal transport embeddings can be used to deal with this issue, both on a theoretical and a computational level. In particular, we embed the space of distributions into an L^2-space by mapping a distribution to its OT map with respect to a fixed reference distribution. We further give an exact characterization of distributions for which this embedding is an isometry. In the embedding space, we use regular machine learning techniques to achieve linear separability when the classes of distributions are generated by a family of shearings (which directly extends the work of [2]), describing conditions under which two classes of sheared distributions can be linearly separated. We also give necessary bounds on these shearing transformations to achieve a pre-specified separation level. Furthermore, embedding into multiple L^2 spaces allows for not only larger families of transformations but also a greater level of linear separation. Finally, our theoretical results are verified empirically on image classification tasks.

Joint work with: Harish Kannan, Alex Cloninger, Caroline Moosmüller.

References

[1] Varun Khurana, Harish Kannan, Alexander Cloninger, and Caroline Moosmüller. Supervised Learning of Sheared Distributions Using Linearized Optimal Transport. 2022. https://arxiv.org/abs/2201.10590

[2] Caroline Moosmüller and Alexander Cloninger. Linear Optimal Transport Embedding: Provable Wasserstein classification for certain rigid transformations and perturbations. 2020. https://arxiv.org/abs/2008.09165

A shape-preserving C^2 stationary subdivision schemes with the fourth-order accuracy

Jinyoung Kim
Department of Mathematics, Ewha Womans University, Seoul 03760, South Korea
jenypurum@naver.com

We present a shape-preserving subdivision scheme with a tension parameter that generalizes the four-point Deslauriers-Dubuc scheme and the cubic B-spline. Whereas many shape-preserving schemes are non-linear and non-uniform, the proposed scheme is linear and stationary. The refinement rule has the same support length as the four-point scheme and provides fourth-order accuracy. The scheme is nearly interpolant such that by sacrificing the interpolating property, it attains an improved smoothness, that is C^2, while the interpolatory four-point scheme is C^1. In addition, we show that the proposed scheme preserves monotonicity and convexity under some mild conditions. Some numerical examples are presented to illustrate the performance of the proposed scheme.

Joint work with: Hyoseon Yang and Jungho Yoon

References

[1] G. Deslauriers, S. Dubuc. Symmetric iterative interpolation. *Constr. Approx*, 5: 49–68, 1989.

[2] N. Dyn. Subdivision Schemes in Computer-Aided Geometric Design. *Advances in Numerical Analysis Vol. II: Wavelets, Subdivision Algorithms and Radial Basis Functions* (W.A. Light ed.), Oxford University Press, 36–104, 1992.

Direct inversion methods for the multivariate nonequispaced fast Fourier transform

Melanie Kircheis
Faculty of Mathematics
Chemnitz University of Technology
melanie.kircheis@math.tu-chemnitz.de

The well-known discrete Fourier transform (DFT) can easily be generalized to arbitrary nodes in the spatial domain. For $M \in 2\mathbb{N}$ we define the multi-index set

$$\mathcal{I}_{\boldsymbol{M}} \coloneqq \mathbb{Z}^d \cap \left[-\tfrac{M}{2}, \tfrac{M}{2}\right)^d = \left\{\boldsymbol{k} \coloneqq (k_t)_{t=1}^d \in \mathbb{Z}^d \colon\ -\tfrac{M}{2} \leq k_t < \tfrac{M}{2},\ t = 1, \ldots, d\right\}$$

with cardinality $|\mathcal{I}_{\boldsymbol{M}}| = M^d$. For given coefficients $\hat{f}_{\boldsymbol{k}} \in \mathbb{C}$, $\boldsymbol{k} \in \mathcal{I}_{\boldsymbol{M}}$, as well as arbitrary nodes $\boldsymbol{x}_j \in \left[-\frac{1}{2}, \frac{1}{2}\right)^d$, $j = 1, \ldots, N$, in the space domain, we are interested in the fast evaluation of the N values

$$f(\boldsymbol{x}_j) = \sum_{\boldsymbol{k} \in \mathcal{I}_{\boldsymbol{M}}} \hat{f}_{\boldsymbol{k}}\, \mathrm{e}^{-2\pi \mathrm{i} \boldsymbol{k} \boldsymbol{x}_j}\,, \quad j = 1, \ldots, N\,.$$

The fast procedure for this generalization is referred to as nonequispaced fast Fourier transform (NFFT) and has complexity $\mathcal{O}(|\mathcal{I}_{\boldsymbol{M}}| \log(|\mathcal{I}_{\boldsymbol{M}}|) + N)$.

Various applications such as MRI, solution of PDEs, etc. are interested in the inverse problem, i. e., computing Fourier coefficients $\hat{f}_{\boldsymbol{k}} \in \mathbb{C}$, $\boldsymbol{k} \in \mathcal{I}_{\boldsymbol{M}}$, from given nonequispaced data $f_j = f(\boldsymbol{x}_j) \in \mathbb{C}$, $j = 1, \ldots, N$. In contrast to iterative solvers we study direct methods for this inversion, when we are in the overdetermined setting. For this purpose, we use the matrix representation of the NFFT. Besides the study of the approach of so-called density compensation factors, we introduce a new method using optimization. Modifying one of the matrix factors of the NFFT leads to an optimization problem, which can simply be solved in a precomputational step using normal equations. Thereby, we are able to compute an inverse NFFT up to a certain accuracy by means of a modified adjoint NFFT, which preserves the arithmetic complexity of $\mathcal{O}(|\mathcal{I}_{\boldsymbol{M}}| \log(|\mathcal{I}_{\boldsymbol{M}}|) + N)$.

Joint work with: Daniel Potts.

References

[1] M. Kircheis and D. Potts. Efficient multivariate inversion of the nonequispaced fast Fourier transform. PAMM, 20(1):e202000120, 2021.

Physics-Based Character Animation in Real-Time

Martin Komaritzan
Computer Graphics & Geometry Processing Group, Dortmund University
martin.komaritzan@tu-dortmund.de

Virtual characters are ubiquitous in a wide range of graphics applications from real-time computer games to (offline) special effects in movies. Enabled by recent advances in 3D-scanning and character generation, realistic virtual avatars are also increasingly used in virtual reality applications, where they allow the user to act in and interact with the virtual environment. In particular in this rapidly growing field of research, the steadily improving fidelity of character appearance increases the demand for more realistic character animation - while retaining interactive frame rates. Existing approaches either suffer from artifacts, have high computational costs or require a lot of input data like multiple surface scans of the character in different poses or manually defined per-vertex skinning weights.

Our Fast Projective Skinning approach (FPS) [1, 2] introduces a two-layered model consisting of rigid bones and an elastic soft tissue layer that is efficiently constructed from a surface mesh of the character and its underlying skeleton. While maintaining real-time performance our method overcomes the well-known artifacts of commonly used geometric skinning approaches. It further enables dynamic effects and resolves local and global self-collisions. In particular, our method neither requires skinning weights, which are often expensive to compute or tedious to hand-tune, nor a complex volumetric tessellation, which fails for many real-world input meshes due to self-intersections. By developing a custom-tailored GPU implementation and a high-quality upsampling method, our approach is the first skinning method capable of detecting and handling arbitrary global collisions in real-time.

In the second part of our talk, we would like to briefly introduce our second model, which focuses on *human* virtual characters [3]. This restriction to human characters allows us to build an anatomically plausible three-layered representation of a person from a single surface scan. It is composed of three surfaces for bones, muscles and skin enclosing the volumetric skeleton, muscles and fat tissues. Our approach is able to compute this model for a specific person in just a few seconds. It includes a data-driven method for estimating the amount of muscle mass and fat mass from a surface scan, which provides more accurate fits to the variety of human body shapes compared to previous approaches. Our second model provides more realistic character animation than the former two-layered model and can further be used for physical simulation, statistical analysis and anatomical visualization in computer animation or in medical applications, which we demonstrate on several examples.

References

[1] M. Komaritzan and M. Botsch. Projective Skinning. *Proceedings of the ACM on Computer Graphics and Interactive Techniques*, 1, 2018.

[2] M. Komaritzan and M. Botsch. Fast Projective Skinning. *Proceedings of ACM Motion, Interaction and Games*, 22:1–22:10. 2019.

[3] M. Komaritzan, S. Wenninger and M. Botsch. Inside Humans: Creating a Simple Layered Anatomical Model from Human Surface Scans. *Frontiers in Virtual Reality*, 2. 2021.

Numerical Quadrature for Quadrilateral Gregory Patches

Jiří Kosinka
Bernoulli Institute, University of Groningen
j.kosinka@rug.nl

We investigate quadrature rules for quadrilateral Gregory patches [1], in short Gregory quads. We provide numerical and where possible symbolic quadrature rules for the space of twenty polynomial/rational functions associated with Gregory quads, as well as their derivatives, products, and products of derivatives, i.e., the derived (isogeometric) spaces. This opens up the possibility of incorporating Gregory quads in numerical simulations [2] without having to resort to imprecise quadratures.

Joint work with: Jun Zhou, Pieter Barendrecht, Michael Bartoň

References

[1] A. Gregory, Smooth interpolation without twist constraints, Computer aided geometric design, Elsevier, 1974, pp. 71–87.

[2] J.A. Cottrell, T.J. Hughes, Y. Bazilevs, Isogeometric analysis: toward integration of CAD and FEA, John Wiley & Sons, 2009.

Error estimates for harmonic and biharmonic interpolation splines with annular blocks

Ognyan Kounchev
Institute of Mathematics and Informatics, Bulgarian Academy of Sciences
kounchev@abv.bg

The main result in this paper is an error estimate for interpolation biharmonic polysplines defined in an annulus $A(r_1, r_N)$, with respect to a partition by concentric annular domains $A(r_1, r_2)$, ..., $A(r_{N-1}, r_N)$, for radii $0 < r_1 < .... < r_N$. By definition these are C^2 functions which are piecewise biharmonic, and interpolating a sufficiently smooth data function on the spheres $|x| = r_j$ for $j = 1, ..., N$, see [1]. We consider polysplines which satisfy so-called natural boundary conditions on the external boundaries, i.e. for $|x| = r_1$ and $|x| = r_N$. By analogy with a technique in one-dimensional spline theory established by C. de Boor, we base our proofs on error estimates for harmonic interpolation splines with respect to the partition by the annuli $A(r_{j-1}, r_j)$. Details are available in [2].

Joint work with: Hermann Rener, Tsvetomir Tsachev.

References

[1] O. Kounchev. Multivariate Polsyplines. Applications to Numerical and Wavelet Analysis *Academic Press / Elsevier*, London-San Diego, 2001.

[2] O. Kounchev, H. Render, Ts. Tsachev Error estimates for harmonic and biharmonic interpolation splines with annular geometry *https://arxiv.org/abs/2201.05521*, submitted to a journal, 2022.

Properties and applications of polygonal blending splines

Tatiana Kravetc

Department of Computer Science and Computational Engineering,
Faculty of Engineering Science and Technology,
UiT – The Arctic University of Norway
tatiana.kravetc@uit.no

In this talk we consider the evaluation of blending type splines on a polygon grid. One promising application of the blending spline surfaces is for isogeometric analysis. Polygon grids provide great flexibility for constructing a wide range of computational domain geometries. The blending spline basis functions possess the following properties: strict locality, C^d-smoothness over the polygon grid, and linear independence. The combined expo-rational functions that form the basis for blending splines are evaluated as a combination of the underlying basis functions defined on each polygonal element and multivariate Bernstein polynomials.

We present the main steps of the isogeometric analysis approach in terms of polygonal blending splines: polygon mesh generation, evaluation of the combined expo-rational basis on the parametric domain, approximation of the curvilinear computational domain, constructing and solving the linear matrix equation that represents a model problem. The talk mainly focuses on the isogeometric concept of the proposed method, i.e. the use of the special type of basis functions both in the domain construction and in the analysis. In addition, we discuss the properties of the combined expo-rational basis functions over the polygon grid and provide a numerical comparison of several refinement schemes.

The power of random information for function approximation on manifolds

Mathias Sonnleitner
Institute of Mathematics and Scientific Computing
University of Graz
Heinrichstrasse 36, 8010 Graz, Austria
mathias.sonnleitner@uni-graz.at

Suppose a function is sampled at a point set in order to reconstruct from the function values an approximant to the original function with the error being measured in an L_q-norm. For this task, point sets with good covering properties are often used. We show that on a compact Riemannian manifold one may as well use uniform random points, provided that suitable conditions on the Sobolev space containing the function hold. For this purpose we present a criterion of (asymptotic) optimality of point sets for this problem. We also discuss the related approximation of the integral using uniform random points.

Joint work with: David Krieg

References

[1] D. Krieg and M. Sonnleitner. Random points are optimal for the approximation of Sobolev functions. *arXiv e-prints*, arXiv:2009.11275 [math.NA], https://arxiv.org/abs/2009.11275, 2020.

[2] D. Krieg and M. Sonnleitner. Function recovery on manifolds using scattered data. *arXiv e-prints*, arXiv:2109.04106 [math.NA], https://arxiv.org/abs/2109.04106, 2021.

Sampling recovery in L_2

David Krieg
RICAM Linz
david.krieg@jku.at

We consider the problem of recovering a function $f\colon \Omega \to \mathbf{C}$ belonging to some class F based on a finite number of samples. The class F reflects our a priori knowledge about the function. Here, Ω is any compact domain or manifold and F is any compact subset of $C(\Omega)$. The error is measured in a worst case scenario (over the function class) and with respect to the L_2-distance. The following general result was recently obtained by the authors:

If the Kolmogorov widths of F show a polynomial decay of order $s > 1/2$,
then there is a weighted least squares estimator that achieves the same rate of convergence.

We discuss this result and address the following questions: What does the algorithm look like? What can be said in the case $s \leq 1/2$? What results do we obtain for the tractability of the problem in high dimensional settings? We also relate to recent results of Nagel/Schäfer/Ullrich, Temlyakov and Cohen/Dolbeault.

Joint work with: Aicke Hinrichs, Erich Novak, Mario Ullrich, Jan Vybíral, Henryk Woźniakowski.

References

[1] D. Krieg, M. Ullrich. Function values are enough for L_2-approximation. *Foundations of Computational Mathematics*, 66:101569, 2021.

[2] D. Krieg, M. Ullrich. Function values are enough for L_2-approximation: Part II. *Journal of Complexity*, 21:1141–1151, 2021.

[3] A. Hinrichs, D. Krieg, E. Novak, J. Vybíral. Lower bounds for integration and recovery in L_2. preprint, arXiv:2108.11853, 2021.

How much randomness is needed for high-confidence Monte Carlo integration?

Robert J. Kunsch
RWTH Aachen University
kunsch@mathc.rwth-aachen.de

We study Monte Carlo methods for integrating smooth functions based on n function evaluations.

The classical way of assessing the precision ε of a randomized integration method is based on the *root mean squared error* (RMSE) or the *mean error*. Optimal Monte Carlo error rates in terms of the mean error are well known for classical Sobolev spaces $W_p^r\left([0,1]^d\right)$ and can be achieved with methods like control variates, in some cases also via stratified sampling. For spaces $\mathbf{W}_p^{r,\mathrm{mix}}\left([0,1]^d\right)$ of dominating mixed smoothness, optimal integration methods based on a randomly shifted and dilated Frolov rule have been found in [1, 2]. If, however, the error is measured in terms of small error ε with high probability $1-\delta$, the so-called *probabilistic* error criterion, see [3], some of the aforementioned methods turn out to be suboptimal with the error $\varepsilon = e(n,\delta)$ depending polynomially on δ^{-1} instead of the polynomial dependence on $\log \delta^{-1}$ we hope for. Optimality in classical Sobolev spaces can be restored for control variates employing the median-of-means, for stratified sampling concentration phenomena (Hoeffding's inequality) can lead to optimality; in any event, the amount of random numbers in such optimal methods is proportional to n. The randomized Frolov rule which uses only $2d$ random parameters independently of n, however, turns out to be suboptimal with respect to the probabilistic error criterion.

This raises the question: How small can the probabilistic error be if we limit the amount of randomness? *Restricted* Monte Carlo methods that only use a small amount of random bits have been studied in [4] for the RMSE criterion. A similar study for the probabilistic error criterion of restricted Monte Carlo methods will be presented.

Joint work with: Daniel Rudolf.

References

[1] D. Krieg, E. Novak. A universal algorithm for univariate integration. *Found. Comput. Math.*, 17:895916, 2017.

[2] M. Ullrich. A Monte Carlo method for integration of multivariate smooth functions. *SIAM J. Numer. Anal.*, 55(3):1188–1200, 2017.

[3] R.J. Kunsch, D. Rudolf. Optimal confidence for Monte Carlo integration of smooth functions. *Adv. Comput. Math.*, 45:3095–3122, 2019.

[4] S. Heinrich, E. Novak, and H. Pfeiffer. How many random bits do we need for Monte Carlo integration? In: *Monte Carlo and Quasi-Monte Carlo Methods 2002* (H. Niederreiter, ed.), pages 27–49, 2004.

Infinite-dimensional STFT phase retrieval from lattice samples: uniqueness and stability

Lukas Liehr
University of Vienna
lukas.liehr@univie.ac.at

The STFT phase retrieval problem arises as the result of trying to invert the mapping that sends a square-integrable function $f \in L^2(\mathbb{R})$ to spectrogram samples of the form

$$|V_g f(\mathcal{L})| \coloneqq \{|V_g f(\ell)| : \ell \in \mathcal{L}\},$$

where $V_g f(x,\omega) = \int_{\mathbb{R}} f(t)\overline{g(t-x)}e^{-2\pi i\omega t}\,dt$ denotes the short-time Fourier transform of f with respect to a window function $g \in L^2(\mathbb{R})$ and $\mathcal{L} \subseteq \mathbb{R}^2$ is a sampling set in the time-frequency plane. An inversion of f from $|V_g f(\mathcal{L})|$ is only possible up to the ambiguity of a global phase factor. We say that f and h agree up to a global phase if there exists a constant $c \in \mathbb{C}, |c| = 1$, such that $f = ch$.

Regarded as a non-linear inverse problem, the investigation of uniqueness and stability of the STFT phase retrieval problem is of major importance. It is folklore in the phase retrieval community that under suitable assumptions on the window function g, every $f \in L^2(\mathbb{R})$ is determined up to a global phase from $|V_g f(\mathcal{L})|$ provided that $\mathcal{L}$ is a continuous domain such as an open set or the entire time-frequency plane. We are interested in the case where $\mathcal{L}$ is a separated set, most notably a lattice, i.e. $\mathcal{L} = L\mathbb{Z}^2$ for some $L \in \mathrm{GL}_2(\mathbb{R})$. First, we present a result which reveals a fundamental difference between the continuous and discrete case: there exists no window function $g \in L^2(\mathbb{R})$ and no lattice $\mathcal{L} \subset \mathbb{R}^2$ such that every $f \in L^2(\mathbb{R})$ is determined up to a global phase by $|V_g f(\mathcal{L})|$ [2, Theorem 1.2]. If the window function g is a Gaussian then the STFT phase retrieval problem is known as the Gabor phase retrieval problem. In this setting, uniqueness from lattice samples can be achieved by imposing a support condition: every $f \in L^4[-\frac{c}{2}, \frac{c}{2}]$ is determined up to a global phase by $|V_g f(\mathcal{L})|$ if g is a Gaussian and $\mathcal{L}$ is a rectangular lattice of the form $\mathcal{L} = \mathbb{Z} \times \frac{1}{2c}\mathbb{Z}$ [1, Theorem 3.1]. Finally, we consider shift-invariant spaces $\mathcal{V}^p_\beta(h) = \{\sum_{k\in\mathbb{Z}} c_k h(\cdot - \beta k) : \{c_k\} \in \ell^p(\mathbb{Z})\}$ where $h \in L^p(\mathbb{R})$ is a generating function and $\beta > 0$ is a step-size. We will demonstrate that Gabor phase retrieval in Gaussian shift-invariant spaces from lattice samples is possible under a suitable assumption on the step-size β which allows the application of the ergodic theorem [1, Theorem 3.6]. In addition, we highlight that the shift-invariant setting allows the design of a reconstruction algorithm which recovers functions in a provably and stably manner [3].

Joint work with: Philipp Grohs.

References

[1] P. Grohs and L. Liehr. Injectivity of Gabor phase retrieval from lattice measurements. *arXiv:2008.07238*, 2020.

[2] P. Grohs and L. Liehr. On foundational discretization barriers in STFT phase retrieval. *arXiv:2111.02227*, 2021.

[3] P. Grohs and L. Liehr. Stable Gabor phase retrieval in Gaussian shift-invariant spaces via biorthogonality. *arXiv:2109.02494*, 2021.

Spline based techniques to make any parametric curve/surface editable

Arne Lakså
UiT The Arctic University of Norway
arne.laksa@uit.no

Any parametric curve or surface where the formula is based on polynomials, rational functions, trigonometric functions, exponential functions, logarithmic functions, etc. can be made editable by adding some simple structures. That is, we can easily change the shape of any curve or surface by adding a set of interpolation "points" with associated structures, which can then be moved, rotated and scaled.

The method is a special case of blending splines, [1, 2], where we add knot vectors that generate 1^{st}-degree B-splines, but where the B-spline basic functions are smoothed with blending functions, [1, 3]. We then add some special coefficients, each of which is connected to knot values. These coefficients are homogeneous matrices. Each of these represents a point, i.e. a position, and a set of associated local coordinate axes that form a local coordinate system.

The construction and implementation will be explained in more detail and many examples will be given.

References

[1] L. T. Dechevsky, A. Lakså, and B. Bang. Expo-Rational B-splines. *International Journal of Pure and Applied Mathematics*, 27(3):319–369, 2006.

[2] A. Lakså, B. Bang, and L. T. Dechevsky. Exploring expo-rational B-splines for curves and surfaces. *In Mathematical methods for curves and surfaces: Tromsø 2004, Mod. Methods Math.*, pages 253–262. Nashboro Press, Brentwood, TN, 2005.

[3] H. Olofsen. Blending functions based on trigonometric and polynomial approximations of the fabius function. *In Open Journal Systems, Norsk Informatikk Konferanse*, 2019.

Modified Bernstein operator and new generalizations of Bézier curves

Paola Lamberti
Department of Mathematics, University of Torino
paola.lamberti@unito.it

Bernstein polynomials and Bézier curves play an important role in Computer Aided Geometric Design. Several generalizations of Bézier curves have been introduced in recent years. Aside from the natural generalizations represented by rational Bézier and B-spline curves, further generalizations have been investigated: among these, Polya polynomials [1, 2], q-Bézier curves [4], Bézier curves based on umbral calculus [5].

In this work we propose further results about generalized Bernstein operator which guarantees the second-order approximation property [3]. Specifically, a wider class of second-order operators is introduced, depending on a real parameter h.

Moreover we define and study a novel generalization of Bézier curves, based on such a new approach, showing numerical and graphical results.

Joint work with: Beatrice Azzarone, Department of Mathematics, University of Torino.

References

[1] P. J. Barry, R. N. Goldman. What is the Natural Generalization of a Bézier Curve?. *Academic Press*, 71–85, 1989.

[2] R. N. Goldman. Polya's Urn Model and Computer Aided Geometric Design. *SIAM Journal on Algebraic and Discrete Methods*, 6:1–28, 1985.

[3] H. Khosravian, M. Dehghan, Mehdi, M. Eslahchi. A new approach to improve the order of approximation of the Bernstein operators: theory and applications. *Numerical Algorithms*, 111–150, 2017.

[4] H. Oruç, G. M. Phillips. q-Bernstein polynomials and Bézier curves. *Journal of Computational and Applied Mathematics*, 151(1):1–12, 2003.

[5] R. Winkel. Generalized Bernstein Polynomials and Bézier Curves: An Application of Umbral Calculus to Computer Aided Geometric Design. *Advances in Applied Mathematics*, 27:51–81, 2001.

Image classification: A (new) statistical viewpoint

Sophie Langer
University of Twente
s.langer@utwente.nl

In this talk we consider supervised binary image classification. We introduce a (idealized) statistical model based on grayscale images where each image is subject to some random scaling and random dilation. We discuss different approaches to solve our classification problem. Interestingly, all classifiers improve with increasing dimension d and are able to perfectly separate classes. Our new perspective on an image classification problem helps us not to be affected by the curse of dimensionality.

Joint work with: Johannes Schmidt-Hieber

Topologically Unrestricted Isogeometric Splines on Multi-Patch Domains with Extraordinary Vertices

Philipp Langgruber
Johannes Kepler University, Linz/Austria
philipp.langgruber@jku.at

Isogeometric splines on multipatch domains (cf. [1]) are needed for the discretization of partial differential equations on general domains. However, achieving smoothness at extraordinary vertices (EVs) – while maintaining the approximation power – is a challenging problem. Several approaches for solving this problem have been explored in the rich literature on this topic. These may be classified into methods that (a) use the classical notion of geometric continuity between surface patches (e.g., [3]), (b) employ singularly parameterized surfaces (e.g., [2, 4]), (c) rely on subdivision surfaces (e.g., [5]) and (d) are based on the concept of manifolds from differential geometry (e.g. [6]). Our work aims at applications in isogeometric analysis, where it is essential to use discretization spaces spanned by relatively simple basis functions (suitable for efficient matrix assembly via numerical integration), which also possess good approximation power, ideally guaranteed by theoretical results. We focus on a construction of Prautzsch [7], which is based on composing polynomial mappings with spline parameterizations. We show how to generate suitable basis functions in the vicinity of EVs and discuss the approximation power of the resulting spline space.

Joint work with: Bert Jüttler

References

[1] F. Buchegger, B. Jüttler and A. Mantzaflaris. Adaptively refined multi-patch B-splines with enhanced smoothness. *Applied Mathematics and Computation*, 272, pages 159–172, 2015.

[2] U. Reif. TURBS - Topologically unrestricted rational B-splines. *Constructive Approximation*, 14 (1), pages 57-77, 1998.

[3] T. Nguyen, K. Karčiauskas and J. Peters. C1 finite elements on non-tensor-product 2d and 3d manifolds. *Applied Mathematics and Computation*, 272, pages 148-158, 2016.

[4] D. Toshniwal, H. Speleers and T.J.R. Hughes. Smooth cubic spline spaces on unstructured quadrilateral meshes with particular emphasis on extraordinary points: Geometric design and isogeometric analysis considerations. *Computer Methods in Applied Mechanics and Engineering*, 327, pages 411-458, 2017

[5] Q. Pan, G. Xu, G. Xu and Y. Zhang. Isogeometric analysis based on extended Catmull-Clark subdivision. *Computers and Mathematics with Applications*, 71, pages 105-119, 2016.

[6] M. Majeed, F. Cirak. Isogeometric analysis using manifold-based smooth basis functions *Computer Methods in Applied Mechanics and Engineering*, 316, pages 547-567, 2017.

[7] H. Prautzsch. Freeform splines. *Computer Aided Geometric Design*, 14, pages 201-206, 1997.

Algorithm for the modelling of the lung/bronchial tree coupling customised

Thomas Laporte
Université Côte d'Azur, CNRS, LJAD, Centre VADER, Nice, France
and Inria Sophia Antipolis - Méditerranée, Université Côte d'Azur, Sophia Antipolis, France
thomas.laporte@unice.fr

An accurate description of the morphometry of the lung and airways is essential to enable numerical simulations, related to the respiratory system, that are in line with the morphometric observations. The structure of the lung is governed both by its respiratory functions and by the inherent hierarchy of the bronchial tree, making it the complex organ that it is. The airways, defined by an asymmetric dichotomous tree, allow the transport of air to the blood exchange zones and thus the supply of oxygen.

In this paper, we present a scalable algorithm for generating individual-specific 3D models of the bronchial tree, based on morphological structures of the lung lobes and the first three generations of airways. These structures are the result of further work to extract them from a person's CT-Scan, using a Deep Learning method of multi-class segmentation.

The algorithm we present is based on mesh preprocessing, calculating the centre of the largest ball inscribed in a volume by an octree method, and applying physiological constraints.The statistical study of our model, correlated with the different morphometric data, allows us to validate the accuracy and fidelity aspects. The result is a 3D mesh of the lung surface and the bronchial tree that is suitable for numerical simulations.

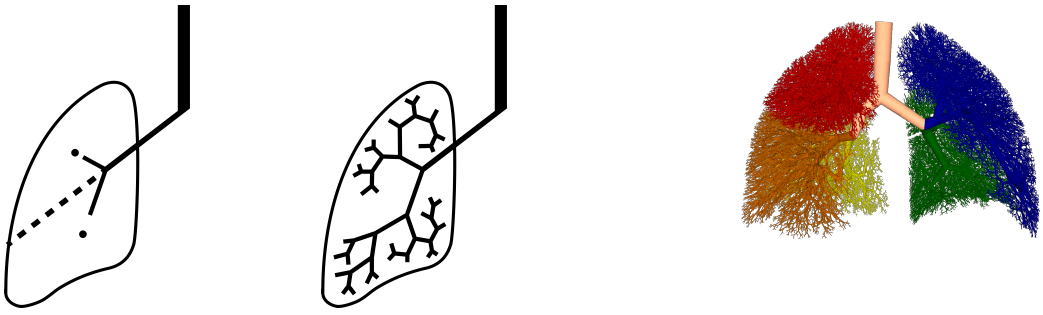

(a) (b) (c)

Figure 1: Bronchial tree generation in 2D, with our model. (a) Subdivision of the closed area mesh with the cutting plane, calculation of the barycentre and centroid and generation of daughter branches. (b) Repetition of the steps, (c) 3D mesh of the bronchial tree.

Joint work with: André Galligo, Angelos Mantzaflaris, Benjamin Mauroy, Bernard Mourrain.

References

[1] M. Tawhai and H. Burrowes. Developing integrative computational models of pulmonary structure. *The Anatomical Record Part B: The New Anatomist*, 275B.1:207-218, 2003.

[2] H. Kitaoka, R. Takaki and B. Suki. A three-dimensional model of the human airway tree. *Journal of Applied Physiology*, 87.6:2207-2217, 1999.

[3] T. Laporte, A. Galligo, A. Mantzaflaris, B. Mauroy and B. Mourrain. Algorithm for the modelling of the lung/bronchial tree coupling customised.

Segmentation of pulmonary lobe from CT-Scan with medial/skeleton geometric data structure

Thomas Laporte and André Galligo
Université Côte d'Azur, CNRS, LJAD, Centre VADER, Nice, France
and Inria Sophia Antipolis - Méditerranée, Université Côte d'Azur, Sophia Antipolis, France
thomas.laporte@unice.fr,andre.galligo@univ-cotedazur.fr

For medical purposes, it is important to obtain an accurate geometry of the human lungs and more precisely of the lung lobes, which are subdivisions of the lungs by the fissures. Deep Learning methods already exist, generally using 3D segmentation algorithms, which are very demanding in terms of computing resources. It is, moreover, a rather complex task, as two lung lobes are very similar when looking at their signal emitted on CT-Scans, see the left figure below.

The lungs, as a whole, being easier to obtain, we based our work on this morphological structure which we combined with a medial/skeleton structure process. We then started by extracting the lung structures from the images, using a U-Net architecture method, which requires less computational resources. We have exploited this architecture on the 3 CT-Scan planes (axial, coronal and sagittal), to create a 2.5D segmentation algorithm.

The next step is to generate a lung skeleton database from these morphological structures, using a package from the CGAL library, and then train a classification algorithm to separate the lung skeleton into lobar skeletons.

From these lobar skeletons and the lung geometry, we can then reconstruct the morphological structures associated with the lobes.

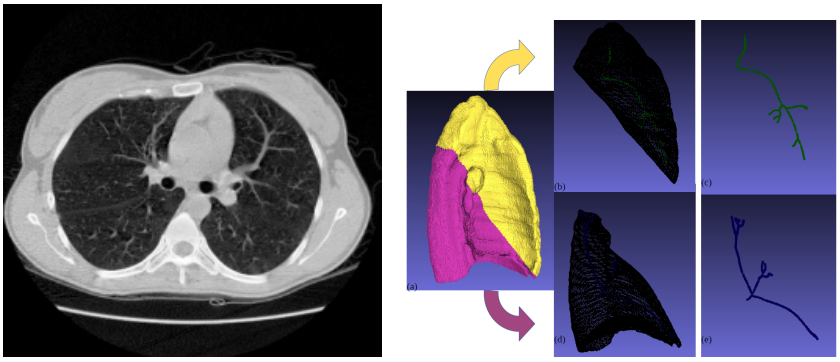

Figure 1: Left to Right : Axial slice of a CT-Scan, Method to extract skeleton from lobar meshes

References

[1] J. Damon. *Determining the boundaries of objects from medial data.* International Journal of Computer Vision, 63,2005, 45–64.

[2] Hao Tang and Chupeng Zhang and Xiaohui Xie *Automatic Pulmonary Lobe Segmentation Using Deep Learning.*, arXiv:1903.09879 (2019).

[3] Andrea Tagliasacchi, Ibraheem Alhashim, Matt Olson, and Hao Zhang *Mean curvature skeletons.* Computer Graphics Forum (Proceedings of the Symposium on Geometry Processing), 31(5):1735– 1744, 2012.

Effect of Periodic Arrays of Defects on Lattice Energy Minimizers

Laurent Bétermin
Institut Camille Jordan, Université Claude Bernard Lyon 1
betermin@math.univ-lyon1.fr

In this talk, I will consider interaction energies $E_f[L]$ between a point $O \in \mathbb{R}^d$, $d \geq 2$, and a lattice L containing O, where the interaction potential f is assumed to be radially symmetric and decaying sufficiently fast at infinity. The idea is to investigate the conservation of optimality results for E_f when integer sublattices kL are removed (periodic arrays of vacancies) or substituted (periodic arrays of substitutional defects). In particular, I will consider separately the non-shifted ($O \in kL$) and shifted ($O \notin kL$) cases and I will present several general conditions ensuring the (non-)optimality of a universal optimizer among lattices for the new energy including defects. Furthermore, in the case of inverse power laws and Lennard-Jones type potentials, I will present necessary and sufficient conditions on non-shifted periodic vacancies or substitutional defects for the conservation of minimality results at fixed density. Different examples of applications will be presented, including optimality results for the Kagome lattice and energy comparisons of certain ionic-like structures. This work can be read more in details in [1].

References

[1] L. Bétermin. Effect of periodic arrays of defects on lattice energy minimizers. *Annales Henri Poincaré*, 22:2995-3023, 2021.

Inferring cell dynamics by learning curves valued in the Wasserstein space

Hugo Lavenant
Bocconi University
hugo.lavenant@unibocconi.it

We tackle the "trajectory inference" which problem arises when one tries to study biological processes with new experimental technologies like single cell RNA sequencing and is interested in the evolution of cell states over time. Indeed these technologies provide high dimensional measurements of cell states, but they are destructive thus cannot track the trajectories of the cells over time.

We rephrase this problem as learning a curve valued in the space of probability distributions (a.k.a. Wasserstein space) and we explain how optimal transport, a mathematical theory which enables to compare probability distributions and compute couplings between random variables, can be used to solve this problem and reconstruct the temporal couplings as well as the trajectories and the fates of the cells. This method was tested on synthetic and real data, in particular to study differentiation of cells in developmental biology. We will also mention some of the theoretical challenges linked to this problem.

Joint work with: Stephen Zhang, Young-Heon Kim and Geoff Schiebinger.

References

[1] Geoffrey Schiebinger, Jian Shu, Marcin Tabaka, Brian Cleary, et. al. Optimal-transport analysis of single-cell gene expression identifies developmental trajectories in reprogramming. *Cell*, 176(4), 928-943, 2019.

[2] Hugo Lavenant, Stephen Zhang, Young-Heon Kim and Geoffrey Schiebinger. Towards a mathematical theory of trajectory inference. *Arxiv preprint 2102.09204*, 2021.

Surfaces with polynomial area element and related topics

Miroslav Lávička
Department of Mathematics & NTIS – New Technologies for the Information Society,
Faculty of Applied Sciences, University of West Bohemia,
Univerzitní 8, 301 00 Plzeň, Czech Republic
lavicka@kma.zcu.cz

Surfaces possessing Pythagorean normal vector fields (PN surfaces) were introduced in [8] as surface counterparts to the Pythagorean hodograph (PH) curves defined in [4]. PN surfaces have rational offsets and thus provide an elegant solution to many offset-based problems occurring in various practical applications. When we use as the defining property of these 2-surfaces in the Euclidean space $\mathbb{R}^3$ that they possess a polynomial/rational area element we may extend the study to higher dimensions and consider also non-Euclidean metrics. For instance in the Minkowski space $\mathbb{R}^{3,1}$ we obtain the so called MOS surfaces, see [5]. In addition, this approach better captures the analogy with the PH curves which have a polynomial/rational length element, cf. [3].

It is interesting to study these objects both from a theoretical point of view and from the point of view of applications (for instance with emphasis on interpolation and approximation techniques). It is also a challenge to find which well known surfaces fall into the distinguished classes with Pythagorean property. We present some examples of these shapes, some construction algorithms, their application in geometric modelling, categorize recent results into a number of broad themes, and we also mention some open question in this area.

Joint work with: Michal Bizzarri, Jiří Kosinka, Zbyněk Šír & Jan Vršek.

References

[1] M. Bizzarri, M. Lávička, and J. Kosinka. Skinning and blending with rational envelope surfaces. *Computer-Aided Design*, 87:41–51, 2017.

[2] M. Bizzarri, M. Lávička, J. Vršek, and J. Kosinka. A direct and local method for computing polynomial Pythagorean-normal patches with global G^1 continuity. *Computer-Aided Design*, 102:44–51, 2018.

[3] R. Farouki. *Pythagorean-Hodograph Curves: Algebra and Geometry Inseparable*. Springer, 2008.

[4] R. Farouki and T. Sakkalis. Pythagorean hodographs. *IBM Journal of Research and Development*, 34(5):736–752, 1990.

[5] J. Kosinka and B. Jüttler. MOS surfaces: Medial surface transforms with rational domain boundaries. In *The Mathematics of Surfaces XII*, volume 4647 of *Lecture Notes in Computer Science*, 245–262. Springer, 2007.

[6] M. Lávička, Z. Šír, and J. Vršek. Smooth surface interpolation using patches with rational offsets. *Computer Aided Geometric Design*, 48:75–85, 2016.

[7] M. Lávička and J. Vršek. On a special class of polynomial surfaces with Pythagorean normal vector fields. In *Lecture Notes in Computer Science (including subseries Lecture Notes in Artificial Intelligence and Lecture Notes in Bioinformatics)*, volume 6920, 431–444, 2012.

[8] H. Pottmann. Rational curves and surfaces with rational offsets. *Computer Aided Geometric Design*, 12(2):175–192, 1995.

[9] J. Vršek and M. Lávička. Translation surfaces and isotropic transport nets on rational minimal surfaces. In *Lecture Notes in Computer Science (including subseries Lecture Notes in Artificial Intelligence and Lecture Notes in Bioinformatics)*, volume 10521, 186–201, 2017.

[10] J. Vršek and M. Lávička. Surfaces with Pythagorean normals along rational curves. *Computer Aided Geometric Design*, 31:451–463, 2014.

A tour of algorithms for curves on surfaces

Francis Lazarus
CNRS, G-SCOP, Grenoble
francis.lazarus@grenoble-inp.fr

In this talk I will consider closed curves drawn on a surface and look at topological or geometric questions such as: Can this curve be deformed continuously to this other curve? What if we additionally require that the length of the curves do not exceed some fixed length during the deformation? Among all continuous deformations of a curve, what is the minimal number of self-intersections, or how long is the shortest curve?

I will survey recent techniques to answer these questions efficiently in a discrete setting where the curves and the surface are described in a combinatorial way, say by closed walks on a triangulation.

Fisher information geometry of beta and Dirichlet distributions

Alice Le Brigant
SAMM - University Paris 1
alice.le-brigant@univ-paris1.fr

Abstract: The Fisher information metric provides a Riemannian framework to compare probability distributions inside a parametric family. The most well-known example is the univariate Gaussian case, where the Fisher information geometry amounts to hyperbolic geometry. In this talk we will investigate the Fisher information geometry of Dirichlet distributions, and beta distributions as a particular case. We show that it is negatively curved and geodesically complete [1]. This guarantees the uniqueness of the notion of mean and makes it a suitable geometry to apply the K-means algorithm, e.g. to compare and classify histograms [2].

Joint work with: Stephen Preston, Stéphane Puechmorel, Nicolas Guigui, Sana Rebbah.

References

[1] A. Le Brigant, S. C. .Preston and S. Puechmorel. Fisher-Rao geometry of Dirichlet distributions. *Differential Geometry and its Applications*, 74, 101702, 2021.

[2] A. Le Brigant, N. Guigui, S. Rebbah and S. Puechmorel. Classifying histograms of medical data using information geometry of beta distributions. *IFAC-PapersOnLine*, 54(9):514–520, 2021.

Symbolically separable low-dimensional nonlinear least squares

Wen-shin Lee
University of Stirling
Scotland, UK
wen-shin.lee@stir.ac.uk

Sparse interpolation, also called Prony's method or exponential analysis [1], consists in fitting a model of the form

$$\sum_{j=1}^{n} \alpha_j \exp(\phi_j t)$$

or

$$\sum_{j=1}^{n} \alpha_j t^{\phi_j}$$

to data y_k collected at sample points t_k for $k = 0, \ldots, N$ with $N \geq 2n - 1$.

A drawback of the method is the fact that the interpolation data need to be collected equidistantly.

Variable projection [2] applies to so-called separable problems, in which data are fitted by a linear combination of simple functions characterised by some nonlinear parameters, such as the above models. The nonlinear parameters are computed separately through optimisation and the linear coefficients are the solution of a least squares problem.

A drawback is that the method, when applied to higher-dimensional problems, easily gets stuck in a local minimum, unless one can supply a quite accurate starting point for the optimisation.

We consider some low-dimensional separable least squares problems of a Prony-like type, which offer the advantage that the objective function can be written down analytically, following ideas from [3].

Joint work with: Costanza Conti (University of Florence, Italy) and Annie Cuyt (University of Antwerp, Belgium).

References

[1] R. de Prony. Essai expérimental et analytique sur les lois de la dilatabilité des fluides élastiques et sur celles de la force expansive de la vapeur de l'eau et de la vapeur de l'alkool, à différentes températures. *J. Ec. Poly.*, 1(22):24–76, 1795.

[2] Gene Golub and Victor Pereyra. Separable nonlinear least squares: the variable projection method and its applications. *Inverse Problems*, 19(2):R1–R26, 2003.

[3] Yongliang Zhang, Annie Cuyt, Wen-shin Lee, Giovanni Lo Bianco, Gang Wu, Yu Chen, and David Day-Uei Li. Towards unsupervised fluorescence lifetime imaging using low dimensional variable projection. *Opt. Express*, 24(23):26777–26791, 2016.

High-dimensional hyperbolic wavelet regression using low-dimensional structures

Laura Lippert
Chemnitz University of Technology
laura.lippert@math.tu-chemnitz.de

We propose a tool for high-dimensional approximation based on hyperbolic wavelet regression, where we only allow low-dimensional dimension interactions. We adapt wavelets on the real axes to construct finite-dimensional periodic wavelet spaces. For functions in Sobolev or Besov-Nikolskij spaces we give a characterization in terms of the wavelet coefficients. This gives us certain decay of the wavelet coefficients. We study the problem of scattered-data approximation, where we evaluate the basis functions at the given sample points, create a matrix and solve the matrix equation with an LSQR-algorithm to get an approximation. In our case this matrix is sparse, since we deal with compactly supported wavelets. If we choose the number of parameters such that we have logarithmic oversampling, we can give a lower bound for the norm of the Moore-Penrose inverse, so that the LSQR-algorithm gives useful results.
If we are concerned with i.i.d. samples, we show that the approximation error decays with the same rate as the error of the projection onto the finite dimensional function space with high probability. We can even bound the worst-case error for the whole class of functions in a Sobolev or Besov-Nikolskij space.
If the function has low effective dimension, we additionally determine the ANOVA decomposition of the approximated function, which allows us to omit ANOVA-terms with low variance in a second step in order to increase the accuracy.

Joint work with: Daniel Potts, Tino Ullrich.

References

[1] L. Lippert, D. Potts, T. Ullrich. Fast Hyperbolic Wavelet Regression meets ANOVA. *ArXiv: 2108.13197*, 2021.

Generalizable Surface Reconstruction with Neural Fields

Or Litany
NVIDIA
or.litany@gmail.com

Neural fields [4] have proven a useful representation for surfaces. However, when coupled with a standard pointclouds network and directly trained for surface reconstruction the resulting model often fails to generalize beyond the training distribution of category and pose. I will discuss three recent works to tackle this issue.

1. Vector Neurons [1]: a framework for constructing rotation-equivariant 3D pointcloud networks that allows shape reconstruction from arbitrary poses.
2. Learnable Kernel Fields [3]: a neural fields representation based on kernels that can generalize to out-of-category shapes (see figure).
3. Lipschitz regularization [2] which promotes smooth latent space interpolation of neural fields.

Joint work with: co-author name 1, co-author name 2.

References

[1] Congyue Deng, Or Litany, Yueqi Duan, Adrien Poulenard, Andrea Tagliasacchi, and Leonidas Guibas. Vector neurons: A general framework for so(3)-equivariant networks, 2021.

[2] Hsueh-Ti Derek Liu, Francis Williams, Alec Jacobson, Sanja Fidler, and Or Litany. Learning smooth neural functions via lipschitz regularization, 2022.

[3] Francis Williams, Zan Gojcic, Sameh Khamis, Denis Zorin, Joan Bruna, Sanja Fidler, and Or Litany. Neural fields as learnable kernels for 3d reconstruction, 2021.

[4] Yiheng Xie, Towaki Takikawa, Shunsuke Saito, Or Litany, Shiqin Yan, Numair Khan, Federico Tombari, James Tompkin, Vincent Sitzmann, and Srinath Sridhar. Neural fields in visual computing and beyond. 2021.

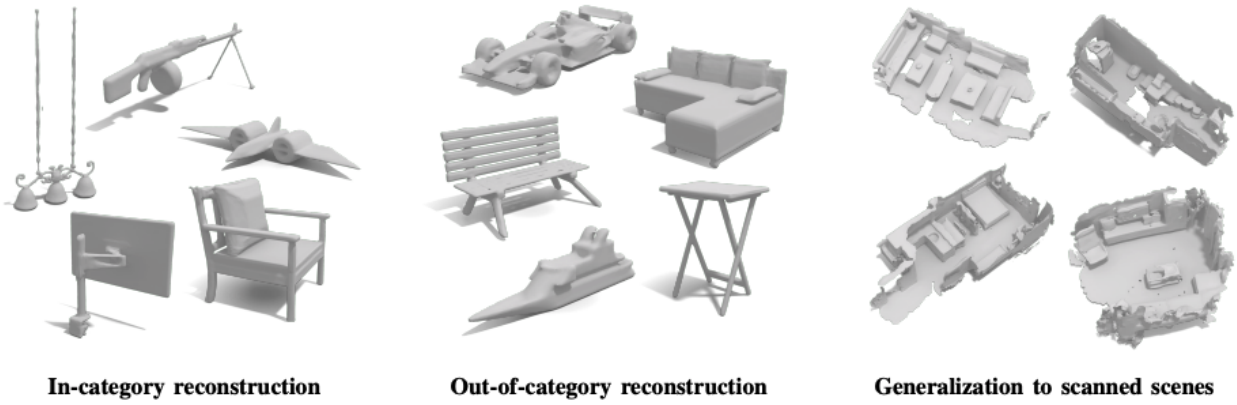

Figure 1: Example results from LKF[3]

Convexification of branched transport

Julius Lohmann
University of Münster, Germany
juliuslohmann@uni-muenster.de

The *branched transport problem* is a non-convex and non-smooth variational problem on Radon measures. In this one tries to find an optimal mass flux $\mathcal{F}$ (in the Eulerian formulation a vector-valued measure) between two given probability measures μ_+ and μ_-, which may for example describe the initial and final distribution of some material. The optimality here is with respect to a subadditive *transportation cost* describing the effort $\tau(m)$ to move an amount of material m per unit distance. The subadditivity of the transportation cost leads to a branched structure of the network on which the transport described by $\mathcal{F}$ takes place. We study a convexification of this problem to a *multimaterial transport problem* [1], which is also of its own interest. The cost function h appearing in this relaxed problem is nonnegative homogeneous and describes the effort to move combinations of certain artificially generated materials. With regard to the branched transport problem, for some cases one can design the function h such that the relaxation is tight.

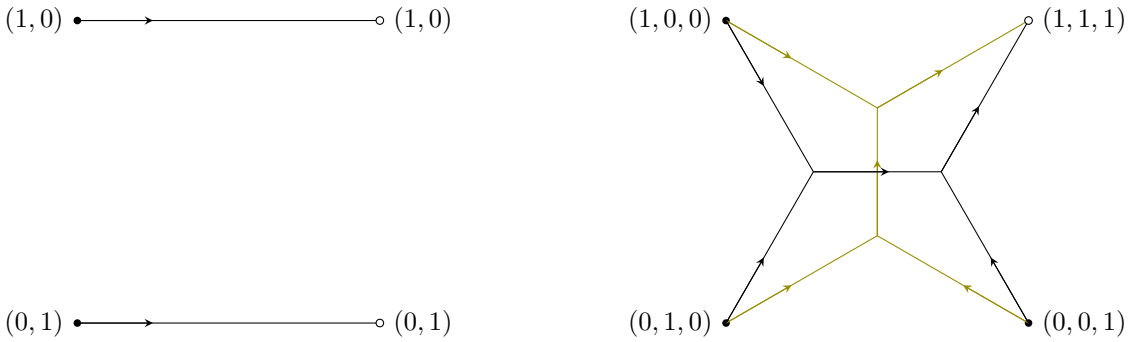

One can for example use the multimaterial problem to model the Steiner problem of finding the network with minimal total length connecting four nodes positioned at the corners of a square. In branched transport one would use $\tau = 1_{(0,\infty)}$. Using the approach with two materials in the left picture, one does not obtain the right solution to the Steiner problem (the network is not connected). The multimaterial distributions are indicated through the vectors and marks at the nodes, $\vec{\mu}_+ = (\delta_{(-\ell,\ell)}, \delta_{(-\ell,-\ell)})$ and $\vec{\mu}_- = (\delta_{(\ell,\ell)}, \delta_{(\ell,-\ell)})$. The approach with three materials in the right picture is the better choice: marking one point as the sink yields all possible solutions. Alternatively, one can swap the entries of $\vec{\mu}_-$ in the left figure.
Using Fenchel's duality theorem in combination with a result on the conjugation of integral functionals [2], we view the multimaterial transport problem as the dual problem to a variant of the Kantorovich–Rubinstein formula for the Wasserstein distance (which in its classical form is used to solve the transportation problem with $\tau(m) = m$). The primal-dual optimality conditions then naturally lead to our definition of a calibration, a certificate for optimality of a minimizing candidate of the (dual) multimaterial transport problem. Further, we relax the function space of the primal problem to ensure existence of solutions and simultaneously derive the notion of a weak calibration. We give conditions under which a weak calibration can be represented by a (strong) calibration and provide a procedure of how to construct a calibration from a weak calibration. Further, we give examples of calibrations and will use them to prove properties of branched transport networks.

Joint work with: Bernhard Schmitzer, Benedikt Wirth.

References

[1] A. Marchese, A. Massaccesi, R. Tione. A multi-material transport problem and its convex relaxation via rectifiable G-currents. *SIAM Journal on Mathematical Analysis*, 51(3):1965–1998, 2019.

[2] M. Valadier. Convex integrands on Suslin locally convex spaces. *Pacific Journal of Mathematics*, 20(3):267–276, 1975.

A continuous-time perspective for modeling acceleration in Riemannian optimization

Aurelien Lucchi
University of Basel
aurelien.lucchi@unibas.ch

We propose a novel second-order ODE as the continuous-time limit of a Riemannian accelerated gradient-based method on a manifold with curvature bounded from below. This ODE can be seen as a generalization of the ODE derived for Euclidean spaces, and can also serve as an analysis tool. We analyze the convergence behavior of this ODE for different types of functions, such as geodesically convex, strongly-convex and weakly-quasi-convex. We demonstrate how such an ODE can be discretized using a semi-implicit and Nesterov-inspired numerical integrator, that empirically yields stable algorithms which are faithful to the continuous-time analysis and exhibit accelerated convergence.

Joint work with: Foivos Alimisis, Antonio Orvieto, Gary Bécigneul.

Distributing points on the real projective plane

Pedro López-Gómez
Universidad de Cantabria, Spain
lopezpr@unican.es

In the last decades, the problem of distributing points on spheres and other spaces has attracted the attention of the mathematical community for both its theoretical interest and its numerous practical applications, constituting nowadays a very active field of research (see [2], a monograph containing the most relevant results to date). One of the main open problems in the area is Smale's 7th Problem ([4]), posed by Shub and Smale in [3], which asks for an algorithm for finding a collection of points in the sphere $\mathbb{S}^2$ whose logarithmic energy is quasioptimal.

While for the sphere $\mathbb{S}^2$ we have constructive procedures to generate collections of points with low logarithmic energy (see [1]), that is not the case in general for other spaces. In particular, one of the simplest spaces for which there are no such constructive procedures is the real projective plane. In this poster we tackle the problem of distributing points in this last space.

Joint work with: Carlos Beltrán, Ujué Etayo.

References

[1] C. Beltrán and U. Etayo (2020). *The Diamond Ensemble: A constructive set of points with small logarithmic energy.* Journal of Complexity, 59, 101471.

[2] S. V. Borodachov, D. P. Hardin and E. B. Saff (2019). *Discrete Energy on Rectifiable Sets.* Springer Monographs in Mathematics. Springer, New York.

[3] M. Shub and S. Smale (1987). *Complexity of Bezout's Theorem: III. Condition Number and Packing.* Journal of Complexity, 9, 4–14.

[4] S. Smale (1998). *Mathematical Problems for the Next Century.* The Mathematical Intelligencer, 20, nº 2, 7–15.

Non-oscillatory surfaces generation using subdivision schemes

Sergio López-Ureña
Facultat de Ciències Matemàtiques. Universitat de València
sergio.lopez-urena@uv.es

The computational generation of curves and surfaces can be efficiently done by subdivision schemes. A well-known linear interpolatory scheme for the generation of $\mathcal{C}^1$ surfaces is the butterfly subdivision scheme [1], which is capable of exactly reproducing third degree bivariate polynomials (when the initial data is of this kind). However, as most of the linear interpolatory schemes, it produces oscillations when the initial data has large gradients. This is a usual situation when dealing with data coming from piecewise smooth function with discontinuities.

In the univariate case, the authors in [2] explain how to transform a linear oscillatory scheme into a non-linear non-oscillatory one. The key idea is to express the given scheme as a convex combination of other schemes based on smaller stencil and, then, replace the linear averages appearing in the convex combination by non-linear analogues.

Here, we extend the ideas of [2] to the bivariate case, in particular to triangular grids, and we design a non-linear non-oscillatory version of the butterfly subdivision scheme.

This work may have applications in data compression and in the numerical solution of PDEs such as conservation laws.

Joint work with: Costanza Conti

References

[1] N. Dyn, D. Levine, J. Gregory. A butterfly subdivision scheme for surface interpolation with tension control. *ACM transactions on Graphics (TOG), 9(2)*, 160-169. 1990.

[2] R. Donat, S. López-Ureña, M. Santágueda. A family of non-oscillatory 6-point interpolatory subdivision schemes. *Advances in Computational Mathematics, 43(4)*, 849-883. 2017.

C^1 Simplex–Splines on Simplices in $\mathbb{R}^s$.

Jean-Louis Merrien
Univ Rennes, INSA Rennes, France,
jmerrien@insa-rennes.fr

Piecewise polynomials over triangles and tetrahedrons have applications in several branches ranging from finite element analysis, surfaces in computer aided design... The smoothness on tetrahedrons is obtained either by high degrees of polynomials or using smaller degrees when splitting the tetraehedron into smaller pieces.

Here we consider the Alfeld split [1] which generalizes the Clough–Tocher split [2] of a triangle. To describe it, let $\mathcal{T}_s := \langle\{\boldsymbol{p}_1, \boldsymbol{p}_1, \ldots, \boldsymbol{p}_{s+1}\}\rangle$ be a simplex in $\mathbb{R}^s$. Using the barycenter $\boldsymbol{p}_{\mathcal{T}_s} := \sum_{j=1}^{s+1} \boldsymbol{p}_j/(s+1)$, we can split $\mathcal{T}_s$ into $s+1$ **subsimplices** $\mathcal{T}_{s,j} := \langle\{\boldsymbol{p}_1, \ldots, \boldsymbol{p}_{s+1}, \boldsymbol{p}_{\mathcal{T}} \setminus \{\boldsymbol{p}_j\}\rangle$, $j = 1 \ldots, s+1$. On $\mathcal{T}_s$ we consider the linear space of C^1 piecewise polynomials of degree $d \in \mathbb{N}_0$

$$\mathbb{S}^1_{d,s} := \{f \in C^1(\mathcal{T}_s) : f_{|\mathcal{T}_{s,j}} \in \mathbb{P}_d(\mathbb{R}^s),\ j = 1 \ldots, s+1\}.$$

We denote by $\triangleq[\boldsymbol{i}; \ell] : \mathbb{R}^s \to \mathbb{R}$ the simplex spline with multiple knots $\{\boldsymbol{p}_1^{[i_1]}, \ldots, \boldsymbol{p}_{s+1}^{[i_{s+1}]}, \boldsymbol{p}_{\mathcal{T}}^{[\ell]}\}$, where the multiplicity vector $\boldsymbol{i} = (i_1, \ldots, i_{s+1})$ has nonnegative integer components. Generalizing [3], we consider degrees $d = 2s-1$ and construct a basis for $\mathbb{S}^1_{2s-1,s}$ consisting of simplex-splines $\triangleq[\boldsymbol{i}; \ell]$ for suitable $\boldsymbol{i}$ and ℓ.

The first argument about the dimension was shown in [4], i.e. for $d \in \mathbb{N}_0$

$$\dim\left(\mathbb{S}^1_{d,s}\right) = \binom{d+s}{s} + s\binom{d-1}{s}.$$

Secondly, we focus on two types of elements of $\mathbb{S}^1_{2s-1,s}$.

- Type (0): the elements corresponding to Bernstein polynomials $\triangleq(\boldsymbol{i}; \ell) = B^{2s-1}_{\boldsymbol{i-1}}$ with $\ell = 0$ and at least one i_j is equal to one ,
- Type (1): the elements $\triangleq(\boldsymbol{i}; \ell)$ with $\ell > 0$, exactly one of the $i_j = 1$ and the others $i_k \geq 2$.

Theorem: The set of elements of type (0) and (1) is a basis of $\mathbb{S}^1_{2s-1,s}$
The theorem is completed by propositions on Marsden Identities and Domain Points.

Joint work with: Tom Lyche, Dept. of Mathematics, Univ. of Oslo, Norway, tom@math.uio.no.

References

[1] P. Alfeld, *A trivariate Clough-Tocher scheme for tetrahedral data*, Comput. Aided Geom. Design, **1**(1984),

[2] R. W. Clough and J. L. Tocher, *Finite element stiffness matrices for analysis of plate bending*, in Proceedings of the conference on Matrix Methods in Structural Mechanics, Wright-Patterson A.F.B., Ohio, 1965.

[3] T. Lyche and JL. Merrien, *Simplex-splines on the Clough Tocher element*, Comput. Aided Geom. Design, **65** (2018),76–92.

[4] A. Kolesnikov and T. Sorokina, *Multivariate C^1-continuous splines on the Alfeld split of a simplex*, Approx. Th. XIV, San Antonio, 2013, 283–294.

Looking for invariance in Locally Linear Embedding

Elodie Maignant
Epione, Inria Sophia-Antipolis, France – Centre Borelli, ENS Paris-Saclay, France
elodie.maignant@inria.fr

Locally Linear Embedding [1] is a method for learning intrinsically low-dimensional data embedded in a high-dimensional space, for example points sampled from an underlying surface. It constructs a neighbourhood-preserving embedding and recovers the global nonlinear structure of the data from locally linear fits.

In the method, neighbourhoods are described using affine barycentric coordinates. This construction makes them invariant to rotations, translations and rescaling and thus should characterise the intrinsic local geometric properties of the data. Therefore, it is expected that the final embedding reflects the intrinsic structure of the data. However, some experiences have shown that these coordinates may not be rigid enough and could allow for unwanted reconstruction patterns [2].

In this work, we try to characterise under which assumptions, especially on the neighbourhood graph, the reconstruction is unique up to affine transformations. At the same time, we look for new invariants of local barycentric coordinates in order to predict the properties of the embeddings constructed by Locally Linear Embedding. Ultimately, we hope to understand better which part of the global structure of the data is recovered by the method and which is not.

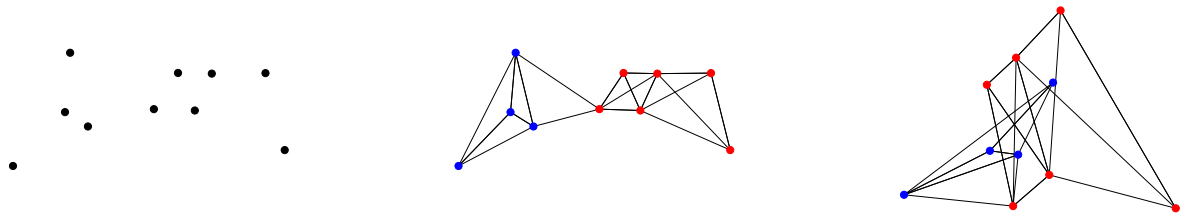

(a) Data points. (b) Neighbourhood graph. (c) Embedded points.

Figure 1: Some effect of the neighbourhood graph's connectivity in Locally Linear Embedding.

Joint work with: Xavier Pennec and Alain Trouvé.

References

[1] Sam T Roweis and Lawrence K Saul. Nonlinear dimensionality reduction by locally linear embedding. *Science*, 290(5500):2323–2326, 2000.

[2] Lin, Liren. Avoiding unwanted results in locally linear embedding: A new understanding of regularization. *arXiv preprint*, arXiv:2108.12680, 2021.

G^1-smooth Biquintic Approximation of Catmull-Clark Subdivision Surfaces

Michelangelo Marsala
Université Côte d'Azur, INRIA Sophia Antipolis-Méditerranée, France
michelangelo.marsala@inria.fr

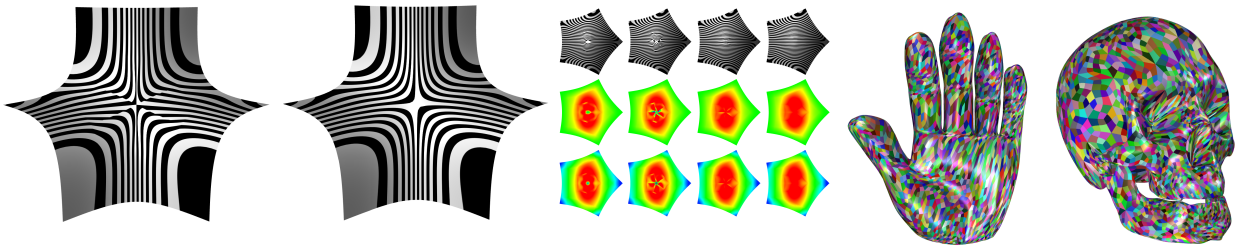

(a) (b) (c) (d) (e)

Figure 1: (a): isophotes on ACC_3 surface. (b): isophotes on our G^1 surface. (c): isophotes and curvature analysis for each of the four solving strategies. (d)-(e): surfaces from complex meshes with many of EVs.

In this work a new construction of a globally G^1 smooth family of Bézier surfaces, defined by smoothing masks approximating the well-known Catmull-Clark (CC) subdivision surface, is presented. The resulting surface is a collection of Bézier (quad) patches, which are bicubic C^2 around regular vertices and biquintic G^1 around Extraordinary Vertices (EVs) i.e., in our case, vertices with valence $N \neq 4$. Starting from the work of Loop and Shaefer [1], which provides a bicubic approximation of the CC limit surface with only C^0 regularity around EVs, we improve this construction to reach a surface with global G^1 smoothness. From the bicubic case, applying twice the classical degree elevation algorithm for Bézier surfaces, we achieve enough degree of freedom to impose G^1 conditions between adjacent patches: those conditions are assigned making use of quadratic gluing data functions [2] around EVs which depends just on their valence. This construction leads to a linear system of seven equations per interior edge to be solved: each equation involves smoothing masks of symmetric control points with respect to the edge. In the case of inner EVs, i.e. not lying on a boundary, some equations lead to (degenerate) circulant system to be solved and some return direct constrains: in all cases, we are able to solve in an explicit way these relations. We present explicit formulas for G^1 smoothing masks; moreover, these solutions possess degrees of freedom which can be fixed arbitrary. The entire system presents more than a way to be solved, and this yields a family of G^1 solutions; between all the possible solving strategies, we identify four of them and we analyze each to determine the best solving strategies returning the smoothest surface. In order to assert the quality of the resulting surfaces and identify the ones that lead to the best result, both visually and numerically, we conduct curvature analysis on an extensive benchmark of meshes with different features. We also treat the case of EVs on boundaries; in this setting, we keep unaltered the boundary masks for the ACC_3 surface presented in [1] and we force the inner edges to satisfy the G^1 relations. Similarly to the inner case, this construction leads to explicit formulas for G^1 smoothing masks.

The resulting construction is described by explicit masks applied to the input control mesh, providing efficient computation and fast rendering of smooth piecewise polynomial surfaces of low degree and arbitrary topology.

Joint work with: Angelos Mantzaflaris, Bernard Mourrain.

References

[1] C. Loop, S. Shaefer. Approximating Catmull-Clark subdivision surfaces with bicubic patches. *ACM Transactions on Graphics*, 10.1145/1330511.1330519, 2008.

[2] A. Blidia, B. Mourrain, N. Villamizar. G1-smooth splines on quad meshes with 4-split macro-patch elements. *Computer Aided Geometric Design*, 10.1016/j.cagd.2017.03.003, 2017.

Wasserstein distance, the Witten Laplacian, and Applications

Nicholas F. Marshall
Princeton University
nicholas.marshall@princeton.edu

This talk considers the problem of computing a linear approximation of quadratic Wasserstein distance W_2. In particular, we compute an approximation of the negative homogeneous weighted Sobolev norm whose connection to Wasserstein distance follows from a classic linearization of a general Monge-Ampére equation. We reduce the computational problem to solving an elliptic boundary value problem involving the Witten Laplacian, which is a Schrödinger operator of the form

$$H = -\Delta + V,$$

where V is a potential that depends on f, see Figure 1. We show that this connection provides a method of computation whose computational cost can be controlled by the amount of regularization used when defining the potential. For the case of probability distributions on the unit square $[0,1]^2$ represented by $n \times n$ arrays we present a fast code and several numerical examples demonstrating this approach.

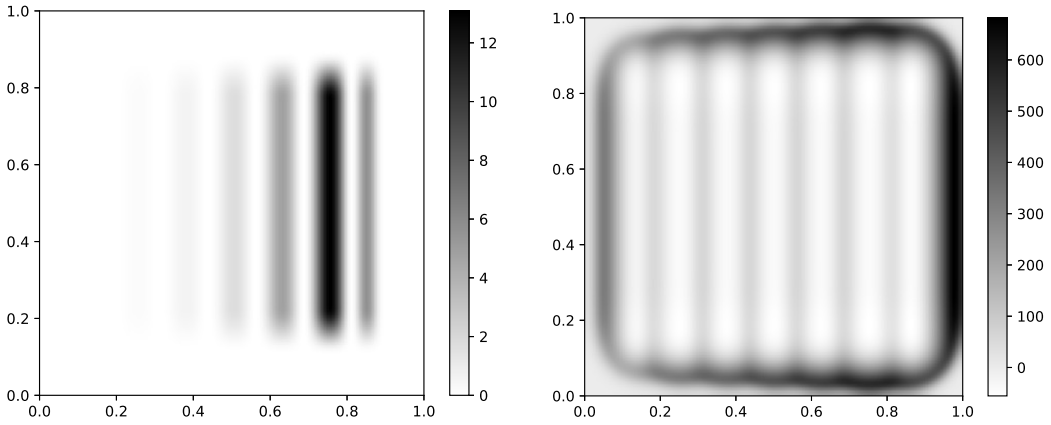

Figure 1: An example of a function f (left) and its regularized potential V (right).

The connection between the weighted negative homogeneous Soboelv norm and the Witten Laplacian has a number of interesting applications; in particular, we discuss applications to defining an embedding and smoothing. First, given probability density functions f, g, h we define an embedding $g \mapsto \Phi_f(g)$ such that

$$\|\Phi_f(g) - \Phi_f(h)\|_{L^2} \approx W_2(g,h),$$

whenever g and h are close to f (in a precise sense). Second, we consider the problem of smoothing g with respect to a diffusion defined by f. In particular, we define the diffusion operator

$$g \mapsto e^{-\tau H} g,$$

where H is the Witten Laplacian whose potential depends on f, and $\tau > 0$ is the diffusion time parameter that controls the amount of smoothing. Further applications and connections to other methods will also be discussed.

Joint work with: Philip Greengard, Jeremy G. Hoskins, Amit Singer

References

[1] Philip Greengard, Jeremy G. Hoskins, Nicholas F. Marshall, and Amit Singer, *On a linearization of quadratic wasserstein distance*, arXiv e-print (2022).

On gradient-based methods for ptychography

Oleh Melnyk
Helmholtz Center Munich, TU Munich
oleh.melnyk@helmholtz-muenchen.de

Ptychography is a lenseless imaging technique which became popular among the practitioners in last two decades. It considers a series of illuminations of the object of interest, where at a time a small region of the specimen is illuminated and the resulting diffraction pattern is captured by the detector in the far-field. As the regions overlap, this provides a surplus information and allows for a recovery from the collection of the observed diffraction patterns.

The rising popularity of ptychography sparked the rapid development of reconstruction algorithms [1, 2, 3]. Furthermore, many of the well-known and established methods for phase retrieval [4, 5, 6, 7] were adapted for ptychography since it can be viewed as a special case of the phase retrieval problem. With the large number of algorithms present, it is inevitable that some of the techniques share similarities and the analysis for one approach can be used to study another.

In this talk we consider three of the methods present in the literature. The first is the gradient descend technique for amplitude-based squared loss known as Amplitude Flow [7]. The second is the Error Reduction algorithm [4, 6], which is the alternating projections approach. The last is the Ptychographic Iterative Engine (PIE) [1, 2], a computationally fast method utilizing a single diffraction pattern at the time.

We show that the later two algorithms can also be viewed as the gradient methods for the same amplitude-based squared loss function. More precisely, we show that Error Reduction performs the scaled gradient descent and PIE is nothing else but the stochastic gradient descent. Based on the convergence theory for Amplitude Flow, we further establish the guaranteed convergence of both algorithms and show that the convergence speed is sublinear. We also discuss the implications of the algorithms being the gradient methods for the amplitude-based squared loss in terms of critical points.

Lastly, we compare their performance numerically. That is, the robustness of reconstruction under noise and the computation times are reported for synthetic data and the resulting reconstructed objects are presented.

References

[1] J.M. Rodenburg, H.M.L. Faulkner, A phase retrieval algorithm for shifting illumination. *Applied Physics Letters*, 85(20):4795–4797, 2009.

[2] A.M. Maiden, X. J.M. Rodenburg, An improved ptychographical phase retrieval algorithm for diffractive imaging. *Ultramicroscopy*, 109(10):1256–1262, 2009.

[3] A. Forstner, F. Krahmer, O. Melnyk, N. Sissouno, Well-conditioned ptychographic imaging via lost subspace completion. *Inverse Problems*, 36(10):105009, 2020.

[4] R.W. Gerchberg, W. O. Saxton, A practical algorithm for the determination of phase from image and diffraction plane pictures. *Optik*, 35:237, 1972.

[5] E. Candes, X. Li, M. Soltanolkotabi, PhaseLift: Exact and Stable Signal Recovery from Magnitude Measurements via Convex Programming. *Communications on Pure and Applied Mathematics*, 66(8):1241–1274, 2013.

[6] S. Marchesini, Y.-C. Tu, H.-T. Wu, Alternating projection, ptychographic imaging and phase synchronization. *Applied and Computational Harmonic Analysis*, 41(3):815–851, 2016.

[7] R. Xu, M. Soltanolkotabi, J.P. Haldar, W. Unglaub, J. Zusman, A.F.J. Levi, R.M. Leahy, Accelerated Wirtinger Flow: A fast algorithm for ptychography *https://arxiv.org/pdf/1806.05546*, 64(2):773–794, 2018.

Dupin cyclide spline surfaces of arbitrary topology

Jean Michel Menjanahary
Vilnius University, Lithuania
jean.menjanahary@mif.vu.lt

Regular circular quad-meshes with certain tangent data were used for smoothly blending principal Dupin cyclide patches [1]. Later this approach was extended in [2, 3] by allowing any $2n$-sided faces by filling them with virtually infinite rings composed of principal patches, when $n > 2$. Now we improve this approach: if all corner vertices of $2n$-sided hole are on a circle then this hole can be smoothly filled with the ring of $4n$ principal patches and one planar/spherical $2n$-sided patch in the middle. The method is demonstrated in the case of 3-beam corner in the left-side figure below.

Smooth blending of triangular patches of Dupin cyclides along principal diagonal curves is investigated and expected to have more flexibility in modeling surfaces with arbitrary topology. In the case of cubic cyclides, the spline construction dual to Powell–Sabin elements [4] was extended by introducing foldings and branchings of the Gaussian map. In particular, this approach allows us to blend patches with different signs of curvature as well as to model monkey saddles (see middle and right figures below).

In order to track singularities Möbius classification of principal patches and principal diagonal curves was investigated. Furthermore, some topological restrictions on cyclide splines were derived when they are not containing planar or spherical patches:

- if the surface is closed (without boundary) then it is of torus topology;
- if the surface is simply connected and its boundary is composed of principal circles then the sum of its angles is the same as for a polygon with the same number of corners on a plane.

This proves that planar/spherical patches cannot be avoided in the hole-filling solution described above.

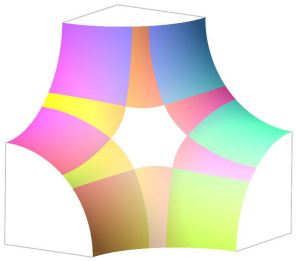

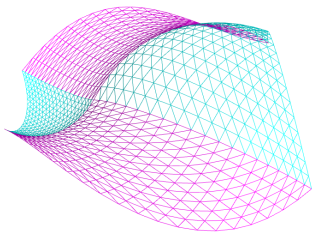

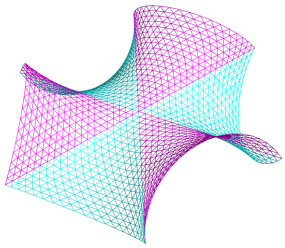

Joint work with: Rimvydas Krasauskas.

References

[1] Y.L. Srinivas, V. Kumar, D. Dutta, Surface design using cyclide patches, *Computer-aided Design*, 28: 263–276, 1996.

[2] R. Krasauskas, Circular meshes, cyclide splines and geometric algebra. In: *Algebraic geometry in the sciences*, Oslo, Slides of the talk, 2011, http://folk.uio.no/ranestad/krasauskas.pdf

[3] R. Mesnil, C. Douthe, O. Bavarel, B. Leger, Generalised Cyclidic Nets for Shape Modelling in Architecture, *International Journal of Architectural Computing* (2017), DOI:10.1177/1478077117714917.

[4] M. Peternel, H. Pottmann, Design of rational surfaces with rational offsets, in: *Advanced Topics in Multivariate Approximation*, F. Fontanella, K. Jetter and P.-J. Laurent (eds.), 275–286, 1996.

Fast Formation of Matrices for Least-Squares Fitting by Tensor-Product Spline Surfaces

Sandra Merchel
MTU Aero Engines AG
sandra.merchel@mtu.de

The task of creating mathematical representations of free-form surfaces from scattered data is an important and therefore well-studied problem [1], which is particularly challenging and useful in industrial applications [2, 3]. Least-square fitting by tensor-product spline surfaces is a well-established method for approximating unstructured data, and is widely used in industry.

However, assembling the system of equations via the straightforward approach can be quite time–consuming. We propose to accelerate this process by employing the technique of sum factorization, which is frequently used in the context of isogeometric analysis, [4, 5].

Our approach consists of two steps. First, we introduce a regular grid onto which the parameters of the unstructured data are projected. Consequently, the expressions of the matrix entries can be rewritten in the structure of nested sums using the tensor-product and grid structure. This form admits the use of sum factorization, which is then employed in the second step. This novel approach has the potential of significantly reducing the computational effort of the matrix assembly, which is a substantial part of the overall computation time.

In this presentation, we provide estimates on the complexity of both the matrix assembly via the straightforward approach and via our approach. Furthermore, we quantify the expected relative assembly cost of the new method with respect to the standard method. We give several examples, including an example involving industrial data, to demonstrate how the choice of the grid influences speed, precision, and quality of the results, and confirm the expected time savings of the proposed method.

Joint work with: Bert Jüttler, Dominik Mokriš, Maodong Pan.

References

[1] G. Greiner and K. Hormann. Interpolating and approximating scattered 3D-data with hierarchical tensor product B-splines. *Surface Fitting and Multiresolution Methods*, pages 163–172, 1997.

[2] C. Bracco, C. Giannelli, D. Großmann, S. Imperatore, D. Mokriš and A. Sestini. THB-spline approximations for turbine blade design with local B-spline approximations. Accepted to *SEMA-SIMAI granted to MACMAS 2019*, Springer.

[3] G. Kiss, C. Giannelli, U. Zore, B. Jüttler, D. Großmann and J. Barner. Adaptive CAD model (re-) construction with THB-splines. *Graphical models*, 76(5):273–288, 2014.

[4] P. Antolin, A. Buffa, F. Calabrò, M. Martinelli and G. Sangalli. Efficient matrix computation for tensor-product isogeometric analysis: The use of sum factorization. *Computer Methods in Applied Mechanics and Engineering*, 285:817–828, 2015.

[5] M. Pan, B. Jüttler and F. Scholz. Efficient matrix computation for isogeometric discretizations with hierarchical B-splines in any dimension. *Computer Methods in Applied Mechanics and Engineering*, 388:114210, 2022.

Wavelets on intervals derived from arbitrary compactly supported biorthogonal multiwavelets

Michelle Michelle
University of Alberta
mmichell@ualberta.ca

The construction of multiwavelets on a bounded interval, which can preserve most of their original properties on the real line, is fundamental in theory and applications (e.g., images and numerical PDEs). Except for a few concrete examples, no systematic construction method for multiwavelets on a bounded interval is available. Hence, given any compactly supported biorthogonal multiwavelet on the real line, we present a direct approach, to construct all possible locally supported biorthogonal multiwavelets on [0,1] satisfying prescribed vanishing moments, polynomial reproduction, and homogeneous boundary conditions. It neither explicitly involves dual refinable functions nor dual multiwavelets. For the sake of illustration, some examples of orthogonal and biorthogonal multiwavelets constructed on [0,1] will be given.

Joint work with: Bin Han.

References

[1] B. Han and M. Michelle, Wavelets on intervals derived from arbitrary compactly supported biorthogonal multiwavelets. *Appl. Comp. Harmon. Anal.* **53** (2021), 270-331.

Minimal Surface Generating Flow

Jiří Minarčík
Department of Mathematics, FNSPE, Czech Technical University in Prague
jiri.minarcik@fjfi.cvut.cz

This work introduces new geometric flow for space curves with positive curvature and torsion. Curves evolving according to this motion law trace out a zero mean curvature surface. We present properties of the motion law, discuss its limitations and outline future work directions.

Joint work with: Michal Beneš

References

[1] J. Minarčík, M. Beneš. Minimal surface generating flow for space curves of non-vanishing torsion. *Discrete & Continuous Dynamical Systems - B*, to appear, 2022.

[2] J. Minarčík, M. Beneš. Nondegenerate Homotopy and Geometric Flows. *Homology, Homotopy and Applications*, to appear, 2022.

Sobolev approximation on the ball

Misael E. Marriaga
Universidad Rey Juan Carlos, Spain
misael.marriaga@urjc.es

For $\mu > 0$, let

$$(f, g)_\mu = f(0)\, g(0) + \lambda \int_{B^2} \nabla f(x) \cdot \nabla g(x)\, (1 - ||x||^2)^\mu dx, \quad \lambda > 0,$$

be a Sobolev inner product defined on the linear space of polynomials of d variables. Here ∇f is the gradient of f, B^d is the unit ball of $\mathbb{R}^d$ and $||x||$ is the usual Euclidean norm of $x \in \mathbb{R}^d$. In this work, we determine an explicit orthogonal polynomial basis associated with $(\cdot, \cdot)_\mu$ and study approximation properties of Fourier expansions in terms of this basis. In particular, we deduce relations between the partial Fourier sums in terms of the Sobolev polynomials and the partial Fourier sums in terms of the classical ball polynomials. We give an estimate of the approximation error by polynomials of degree at most n in the corresponding Sobolev space. We also give upper bounds for the reproducing kernels for the Sobolev projection operators on the space of polynomials of degree at most n.

Joint work with: Marlon J. Recarte, Teresa E. Pérez, Miguel A. Piñar.

References

[1] Dai F., Xu Y., *Approximation theory and harmonic analysis on spheres and balls*, Springer Monographs in Mathematics, Springer, New York, 2013.

[2] Dunkl C.F., Xu Y., *Orthogonal polynomials of several variables*, Encyclopedia of Mathematics and its Applications, Vol. 155, 2nd ed., Cambridge University Press, Cambridge, 2014.

[3] Piñar M. A., Xu Y., *Best polynomial approximation on the unit ball*, IMA Journal of Numerical Analysis, Vol. 38, Issue 3 (2018), 1209-1228.

[4] Xu Y., *Asymptotics for orthogonal polynomials and Christoffel functions on a ball*, Methods Appl. Anal. **3** (1996), 257–272.

Riemannian optimization tools for optimal transport

Bamdev Mishra
Microsoft India
bamdevm@microsoft.com

Optimal transport or OT [PC19] has become a relevant tool in various machine learning applications. The rising popularity of OT is because it gives a principled approach in exploiting the underlying metric geometry to develop different notions of distances between probability distributions to be used in downstream applications. Consequently, there have been many works on developing computationally efficient tools to solve OT problems.

In this presentation, we look at the Riemannian approach to solving OT related optimization problems. The Riemannian approach has also got popular for solving structured nonlinear optimization problems [Bou20]. To that end, we discuss some of the recent works on exploiting Riemannian manifold structures to develop optimization-related ingredients for tackling OT formulations [HMJG22, MSKJ21]. We also look at various challenges and opportunities that lay ahead in making Riemannian tools a viable alternative for OT practitioners.

Joint work with: Andi Han, Pratik Jawanpuria, and Junbin Gao.

References

[Bou20] Nicolas Boumal, *An introduction to optimization on smooth manifolds*, Available online, Aug 2020.

[HMJG22] Andi Han, Bamdev Mishra, Pratik Jawanpuria, and Junbin Gao, *Riemannian block spd coupling manifold and its application to optimal transport*, Tech. report, arXiv preprint arXiv:2201.12933, 2022.

[MSKJ21] Bamdev Mishra, NTV Satyadev, Hiroyuki Kasai, and Pratik Jawanpuria, *Manifold optimization for non-linear optimal transport problems*, Tech. report, arXiv preprint arXiv:2103.00902, 2021.

[PC19] Gabriel Peyré and Marco Cuturi, *Computational optimal transport: With applications to data science*, Foundations and Trends® in Machine Learning **11** (2019), no. 5-6, 355–607.

Low-rank approximation of least squares fitting with bivariate tensor-product splines

Dominik Mokriš
MTU Aero Engines AG
dominik.mokris@mtu.de

MTU Aero Engines is Germany's leading engine manufacturer and an established global player in the industry. We engage in the design, development, manufacture and maintenance of aircraft engines in all thrust and power categories as well as of stationary gas turbines. These activities are supported by a broad spectrum of CAE (Computer-Aided Engineering) tools and processes. In particular, underlying the aerodynamic simulations is the in-house geometry generation software.

The last years have seen growing precision and availability of 3D scanning tools. Hand-in-hand with it grows also the interest of our engineers to use the scanned data as an input of the geometry generator and to convert them into high-quality NURBS surfaces suitable for further use. While considerable effort has been spent on improving this process (see, e.g., [1, 2, 3, 4]), high expectations of our users mean that there is always room for further improvement.

In this talk, I will show an early-stage work from this area. Assuming that the input data are a two-dimensional grid of scalars, one can write them in a matrix form. Instead of approximating them directly with a bivariate tensor-product function, a low-rank approximation of this matrix can be constructed in the form

$$Z \approx \sum_{r=1}^{s} t_r \mathbf{u}_r \otimes \mathbf{v}_r \ .$$

For each $\mathbf{u}_r$ and $\mathbf{v}_r$ a *univariate* least-squares approximation can be computed, thus obtaining vectors $\mathbf{d}_r$ and $\mathbf{e}_r$, respectively, of control points. These control points can be re-assembled into a matrix form

$$C = \sum_{r=1}^{s} t_r \mathbf{d}_r \otimes \mathbf{e}_r \ .$$

Taking C as control points of a *bivariate* spline function yields a good approximation of the original data Z.

This method is a generalization of an existing approach presented in [5]. However, there are two new contributions. First, using least-squares approximation instead of interpolation leaves more freedom in the choice of the data parametrization and fitting basis. Second, we prove that when s is equal to the rank of the data matrix Z, then the elements of C are in fact the control points of the bivariate least-squares approximation of Z. Additionally, this approach is generalized to weighted least-squares with separable weights, which is of advantage, e.g., when approximating functions in L^2-sense using quadrature rules.

Joint work with: David Großmann and Bert Jüttler.

References

[1] G. Kiss, C. Giannelli, U. Zore, B. Jüttler, D. Großmann and J. Barner. Adaptive CAD model (re-) construction with THB-splines. *Graph. Models*, 76(5):273–288, 2014.

[2] L. Groiss, B. Jüttler and D. Mokriš. 27 variants of Tutte's theorem for plane near-triangulations and an application to periodic spline surface fitting. *Comput. Aided Geom. Design*, 85: 101975, 2021.

[3] C. Bracco, C. Giannelli, D. Großmann, S. Imperatore, D. Mokriš and A. Sestini. THB-spline approximations for turbine blade design with local B-spline approximations. Accepted to *SEMA-SIMAI granted to MACMAS 2019*. Springer.

[4] S. Merchel, B. Jüttler and D. Mokriš. Adaptive and local regularization for geometry reconstruction by tensor-product spline surfaces. *Submitted*.

[5] I. Georgieva and C. Hofreither. An algorithm for low-rank approximation of bivariate functions using splines. *J. Comput. Appl. Math.*, 310: 80–91, 2017.

Hodograph based shape control for polynomial curves

Hwan Pyo Moon
Department of Mathematics, Dongguk University–Seoul, Korea
hpmoon@dongguk.edu

Although Bézier control polygons are useful tools to express and control the shape of polynomial curves, they are not suitable to control Pythagorean hodograph (PH) curves, since any slight modification of a single Bézier control points make the curve lose the PH property. To remedy this problem, different types of control polygons such as the Gauss–Legendre polygon [1, 2] and the Gauss–Lobatto polygon [2] were introduced. In this work, we analyze the shape control functionality of these polygons from the viewpoint of hodographs. Edges of these polygons can be understood as points in the hodograph space, and the curve construct process corresponds to computing the hodograph that interpolates the velocity data followed by integrating it. This approach can be applied not only to PH curves but also to general polynomial curves.

References

[1] S.H. Kim, H.P. Moon. Rectifying control polygon for planar Pythagorean hodograph curves. *Computer Aided Geometric Design*, 54:1–14, 2017.

[2] S.H. Kim, H.P. Moon. Deformation of spatial septic Pythagorean hodograph curves using Gauss–Legendre polygon. *Computer Aided Geometric Desig*, 73:16–34, 2019.

[3] S.H. Kim, H.P. Moon. Gauss–Lobatto polygon of Pythagorean hodograph curves *Computer Aided Geometric Desig*, 74:101768, 1–20, 2019.

Gauss–Legendre polynomial for the shape control of parametric curves

Soo Hyun Kim
Applied Algebra and Optimization Research Center, Sungkyunkwan University, Korea
5hkim@skku.edu

The Gauss–Legendre polygon was developed [1, 2] as the rectifying control polygon of Pythagorean hodograph (PH) curves, whose length is the same as the arc length of the corresponding PH curve. We here focus on the polynomial basis for the Gauss–Legendre polygon. As a Bézier curve is expressed as the linear combination of the Bézier control points with the coefficients given by the Bernstein polynomials, a PH curve can be expressed as the linear combination of the Gauss-Legendre control points with the coefficients determined by some polynomials, which we call the Gauss–Legendre polynomials. We show that the Gauss–Legendre polynomials can be constructed from the Lagrange interpolator defined over the roots of the Legendre polynomials. We investigate various properties of the Gauss–Legendre polynomials including symmetry, partition of unity, critical points, derivatives, and integrals. We also analyze the pros and cons of this polynomial over other polynomials.

Joint work with: Hwan Pyo Moon, Song-Hwa Kwon.

References

[1] S.H. Kim, H.P. Moon. Rectifying control polygon for planar Pythagorean hodograph curves. *Computer Aided Geometric Design*, 54:1–14, 2017.

[2] S.H. Kim, H.P. Moon. Deformation of spatial septic Pythagorean hodograph curves using Gauss–Legendre polygon. *Computer Aided Geometric Desig*, 73:16–34, 2019.

A factorization framework for Hermite subdivision schemes reproducing polynomials of high degree

Caroline Moosmüller
University of California, San Diego
cmoosmueller@ucsd.edu

Hermite subdivision schemes are iterative refinement algorithms which produce a function and its derivatives in the limit. In this talk we are interested in Hermite subdivision schemes which reproduce polynomials of high degree. We show that this can be characterized by operator factorizations involving Taylor operators and difference factorizations of a rank one vector scheme. Explicit expressions for these operators are derived, which are based on an interplay between Stirling numbers and p-Cauchy numbers. Furthermore, we discuss how this framework can be used to prove high smoothness of the limit functions.

The talk is based on the papers [1, 2].

Joint work with: Costanza Conti, Svenja Hüning, Tomas Sauer.

References

[1] C. Moosmüller, S. Hüning, C. Conti. Stirling numbers and Gregory coefficients for the factorization of Hermite subdivision operators. *IMA Journal of Numerical Analysis*, 41(4):2936–2961, 2021.

[2] C. Moosmüller, T. Sauer. Factorization of Hermite subdivision operators from polynomial over-reproduction. *Journal of Approximation Theory*, 271: article number 105645, 2021.

SHINE: SHaring the INverse Estimate for bi-level optimization

Thomas Moreau
Université Paris-Saclay, Inria, CEA, Palaiseau, 91120, France
thomas.moreau@inria.fr

In recent years, bi-level optimization has raised much interest in the machine learning community, in particular for hyper-parameters optimization [4] and implicit deep learning [1]. Bilevel optimization aims at minimizing a function whose value depends on the result of another optimization problem, that is:

$$\begin{aligned} &\min_{x\in\mathbb{R}^d} h(x) = F(z^*(x), x) \ , \\ &\text{such that } z^*(x) \in \arg\min_{z\in\mathbb{R}^p} G(z, x) \ , \end{aligned} \tag{1}$$

where F and G are two real valued functions defined on $\mathbb{R}^p \times \mathbb{R}^d$. This type of problems is often tackled using first-order that requires the computation of the gradient of h, whose expression can be obtained using the implicit function theorem: $\nabla h(x) = \nabla_2 F(z^*(x), x) - \nabla^2_{2,1} G(z^*(x), x)\left[\nabla^2_{1,1} G(z^*(x), x)\right]^{-1} \nabla_1 F(z^*(x), x)$. The computation of this gradient requires the computation of matrix-vector products involving the inverse of a large matrix $\nabla^2_{1,1} G$, which is computationally demanding.

In our work [5], we propose a novel strategy coined SHINE to tackle this computational bottleneck when the inner problem G can be solved with a quasi-Newton algorithm. The main idea is to use the quasi-Newton matrices estimated from the resolution of the inner problem to efficiently approximate the inverse matrix in the direction needed for the gradient computation $\left[\nabla^2_{1,1} G(z^*(x), x)\right]^{-1} \nabla_1 F(z^*(x), x)$. We prove that under some restrictive conditions, this strategy gives a consistent estimate of the true gradient. In addition, by modifying the quasi-Newton updates, we provide theoretical guarantees that our method asymptotically estimates the true implicit gradient under weaker hypothesis.

Figure 1 shows on a classical hyperparameter optimization benchmark [4] that our method accelerate the resolution of the bi-level problem compare to HOAG [4] and the Jacobian-Free method that replace the inverse by the identity. Experiments for multi-scale Deep-Equilibrium networks (DEQ [2]) in [5] applied to CIFAR10 and ImageNet show that SHINE reduces the computational cost of the backward pass by up to two orders of magnitude, while retaining performances close to the original training methods. While these results are encouraging, our method still suffer from small performance drop on DEQ for ImageNet, leaving room for further improvement.

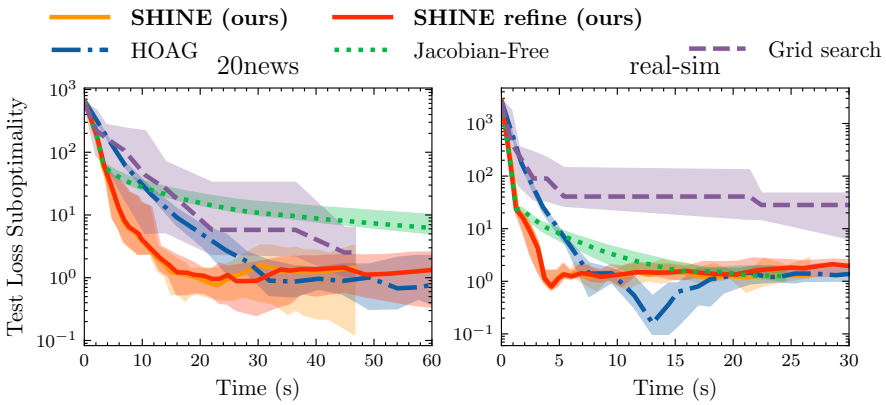

Figure 1: Convergence of test loss for different hyperparameter optimization methods on the ℓ_2-regularized logistic regression problem for the 2 datasets (20news and real-sim).

Joint work with: Z. Ramzi, S. Bai, F. Mannel, J.-L. Stark and P. Ciuciu.

References

[1] S. Bai, J. Kolter and V. Koltun. Deep Equilibrium Models. *NeurIPS*, 2019.

[2] S. Bai, V. Koltun and J. Kolter. Multiscale deep equilibrium models. *NeurIPS*, 2020.

[3] S. Fung, H. Heaton, Q. Li, D. Mckenzie, S. Osher, and W. Yin. Fixed Point Networks: Implicit Depth Models with Jacobian-Free Backprop. preprint ArXiv, 2021

[4] F. Pedregosa. Hyperparameter optimization with approximate gradient. *ICML*, 2016.

[5] Z. Ramzi, F. Mannel, S. Bai, J.-L. Starck, P. Ciuciu, T. Moreau. SHINE: SHaring the INverse Estimate from the forward pass for bi-level optimization and implicit models. *ICLR*, 2022.

Geometrically Smooth Splines for IGA

Bernard Mourrain
Inria, Université Côte d'Azur, France
bernard.mourrain@inria.fr

Geometrically smooth (G1) spline functions are piecewice polynomial functions defined on a mesh, that satisfy properties of differentiability across shared edges. They can be used to extend Isogeometric Analysis approaches on surfaces of arbitrary topology.

In this presentation, we consider G1 splines on quadrangular meshes with given quadratic glueing data along shared edges. We describe briefly their properties, analyse their spaces, and provide dimension formula.

Computing efficiently basis functions for these spaces is critical in the IGA approach. We investigate this problem and show how to construct efficiently such bases and how different choices of basis functions can influence output results in IGA methods. A few experimentation illustrate these developments.

Joint work with: Michelangelo Marsala, Angelos Mantzaflaris

References

[1] A. Blidia, B. Mourrain, N. Villamizar. G1-smooth splines on quad meshes with 4-split macro-patch elements. *Computer Aided Geometric Design*, 10.1016/j.cagd.2017.03.003, 2017.

[2] A. Blidia, B. Mourrain, Gang Xu. Geometrically smooth spline bases for data fitting and simulation, *Computer Aided Geometric Design*, 2020, 78, pp.101814. 10.1016/j.cagd.2020.101814

[3] M. Marsala, M.Mantzaflaris, B. Mourrain. *G^1 – smooth Biquintic Approximation of Catmull-Clark Subdivision Surfaces*. Preprint, 2022.

Robust Eigenvectors of Symmetric Tensors

Konstantin Usevich
CNRS, CRAN UMR 7039, Nancy
firstname.lastname@univ-lorraine.fr

With the rising demand for techniques to handle massive, high-dimensional datasets, many scientists have turned to finding adaptations of matrix algorithms to high-order arrays, known as tensors. In particular, the notions of eigenvalues and singular values can be generalized to the tensor case, which are particularly important due to their link to the rank-one approximation problem. The main obstacle, however, is that computing these quantities can be an NP-hard problem [1] for a general tensors. However, for a special case of orthogonal tensors, eigenvectors are well understood. In this talk, we report new results on eigenvectors of symmetric tensors and convergence of tensor power method for non-orthogonal case [4].

A real order d tensor $\mathcal{T} \in \mathbb{R}^{n\times\cdots\times n}$ is said to be *symmetric* if for all permutations of indices $\mathcal{T}_{i_1,\ldots,i_d} = \mathcal{T}_{i_{\sigma(1)},\ldots,i_{\sigma(d)}}$. A vector $\mathbf{v} \in \mathbb{R}^n$ is an *eigenvector* of $\mathcal{T}$ with *eigenvalue* $\mu \in \mathbb{R}$ if

$$\mathcal{T} \cdot \mathbf{v}^{d-1} = \mu \mathbf{v},$$

where $\mathcal{T} \cdot \mathbf{v}^{d-1}$ is a vector defined by *contracting* $\mathcal{T}$ by $\mathbf{v}$ along all of its modes except for one. The eigenvectors of $\mathcal{T}$ are the fixed points (up to sign) of an iterated method called the *tensor power method* given by

$$\mathbf{x}_{k+1} \mapsto \frac{\mathcal{T} \cdot \mathbf{x}_k^{d-1}}{\|\mathcal{T} \cdot \mathbf{x}_k^{d-1}\|}.$$

Yet another important characterization of the eigenvectors is that [2] they are the critical points of the symmetric best rank-one approximation problem $\min_{c,\mathbf{v}} \|\mathcal{T} - c\mathbf{v}^{\otimes d}\|_F^2$.

A non-symmetric version ot the tensor power method for non-symmetric tensors is known to be globally convergent [5]. For the symmetric case, fewer results are available on the convergence, examples are known when the method does not converge at all [2]. Our main result gives a sufficient condition on an eigenvector to be robust (i.e., to be an attracting fixed point of the power iteration).

Theorem 1. *let $\mathcal{T}_d$ be a symmetric $n \times \cdots \times n$ order-d tensor with symmetric decomposition*

$$\mathcal{T}_d = \sum_{i=1}^{r} \lambda_i \mathbf{v}_i^{\otimes d}, \tag{1}$$

with $\|\mathbf{v}_i\| = 1$ for all i. Then there exists a $D \in \mathbb{N}$ such that for all $d \geq D$, if $\mathbf{v}_j$ is an eigenvector of $\mathcal{T}_d$ with non-zero eigenvalue, then $\mathbf{v}_j$ is a robust eigenvector of $\mathcal{T}_d$.

Theorem 1 allows us to obtain find eigenvectors for some classes of non-orthogonal tensors, where the vectors $\mathbf{v}_j$ belong to an *equiangular set* or an *equiangular tight frame*, see [3] for more details.

Joint work with: Tommi Muller (University of Oxford), Elina Robeva (Univesity of British Columbia).

References

[1] C. Hillar and L.-H. Lim. Most tensor problems are NP-hard. *Journal of the ACM*, 60(6), 2013.

[2] E. Kofidis and P. A. Regalia. On the best rank-1 approximation of higher-order supersymmetric tensors. *SIAM Journal on Matrix Analysis and Applications*, 23(3):863–884, 2002.

[3] T. Muller, E. Robeva and K. Usevich. Robust Eigenvectors of Symmetric Tensors *arXiv:2111.06880*, 2021.

[4] E. Robeva. Orthogonal decomposition of symmetric tensors. *SIAM Journal on Matrix Analysis and Applications*, 37(1):86–102, 2016.

[5] A. Uschmajew. A new convergence proof for the higher-order power method and generalizations. *Pac. J. Optim.*, 11(2):309–321, 2015.

A new family of non-uniform subdivision scheme with two tension and one shape parameters.

Mohamed-Yassir Nour
Lorraine/Hassan First University
mohamedyassir.nour@gmail.com

Abstract

In this paper, we propose a new non-uniform subdivision scheme that includes a tension and shape parameters sequence. Each form parameter of the sequence is assigned at each edge of the initial control polygon. The proposed scheme can produce limiting curves that are more consistent with the original data points and the control polygon. It has also the advantage of generating a wide variety of shapes for the limiting curves. The convergence and smoothness of the proposed scheme are proven by using the asymptotic equivalence concept. Numerical results that illustrate the advantages of the proposed non-uniform scheme are given.

Joint work with: Abdellah Lamnii, Ahmed Zidna.

References

[1] C.V. Beccari, G. Casciola, L. Romani, Non-uniform non-tensor product local interpolatory subdivision surfaces. Comput. Aided Geom. Des. 30 (2013)357–373. Comput-Aided Des 1978;10(6):350–5.

[2] Conti C, Romani L. Affine combination of B-spline subdivision masks and its non-stationary counterparts. BIT 2010;50:269–99.

[3] C. Conti, N. Dyn, Convergence and smoothness of tensor-product of two non-uniform linear subdivision schemes. Comput. Aided Geom. Des. 66 (2018) 16-18.

[4] N. Dyn, D. Levin, Analysis of asymptotically equivalent binary subdivision schemes, J. Math. Anal. Appl. 193 (1995) 594-621.

[5] N. Dyn, D. Levin, J. Yoon, A new method for the analysis of univariate nonuniform subdivision schemes, Constr. Approx 40 (2014) 173–188

[6] Romani L. From approximating subdivision schemes for exponential splines to high-performance interpolating algorithms. J Comput Appl Math 2009;224.

[7] U. Reif, A unified approach to subdivision algorithms near extraordinary vertices. Comput Aided Geom Des 1995;12(2):153–74.

Approximation classes of tree tensor networks

Anthony Nouy
Nantes Université, Centrale Nantes
anthony.nouy@ec-nantes.fr

Tree Tensor networks (TTNs) are prominent model classes for the approximation of high-dimensional functions in computational and data science. After an introduction to approximation tools based on tensorization of functions and TTNs, we introduce their approximation classes and present some recent results on their properties. In particular, we show that classical smoothness (Besov) spaces are continuously embedded in TTNs approximation classes. For such spaces, TTNs achieve (near to) optimal rate that is usually achieved by classical approximation tools, but without requiring to adapt the tool to the regularity of the function. The use of deep networks is shown to be essential for obtaining this property. Also, it is shown that exploiting sparsity of tensors allows to obtain optimal rates achieved by classical nonlinear approximation tools, or to better exploit structured smoothness (anisotropic or mixed) for high-dimensional approximation. We also show that approximation classes of tensor networks are not contained in any Besov space, unless one restricts the depth of the tensor network. That reveals again the importance of depth and the potential of tensor networks to achieve approximation or learning tasks for functions beyond standard regularity classes. In particular, it is shown that some discontinuous or even nowhere differentiable functions can be approximated with exponential convergence rates, and that some classes of compositional functions can be approximated without the curse of dimensionality.

Joint work with Mazen Ali, Markus Bachmayr and Reinhold Schneider.

References

[1] M. Ali and A. Nouy. Approximation theory of tree tensor networks: Tensorized univariate functions - part i. *ArXiv*, abs/2007.00118, 2020.

[2] M. Ali and A. Nouy. Approximation theory of tree tensor networks: Tensorized univariate functions - part ii. *ArXiv*, abs/2007.00128, 2020.

[3] M. Ali and A. Nouy. Approximation theory of tree tensor networks: Tensorized multivariate functions. *arXiv preprint arXiv:2101.11932*, 2021.

[4] M. Bachmayr, A. Nouy, and R. Schneider. Approximation by tree tensor networks in high dimensions: Sobolev and compositional functions. *ArXiv e-prints*, 2020.

Minimum Height Drawings of Ordered Trees in Polynomial Time: Homotopy Height of Tree Duals

Tim Ophelders
Utrecht University, the Netherlands
TU Eindhoven, the Netherlands
t.a.e.ophelders@uu.nl

We consider minimum height drawings of graphs in the plane. We define the height of a drawing as the minimum value h such that any vertical line intersects the drawing in at most h points. Given a simple drawing of a planar graph, we are looking for a homeomorphism of the plane that minimizes the height of the resulting drawing. This problem is equivalent to the homotopy height problem in the plane, and the homotopic Fréchet distance problem. These problems were recently shown to lie in NP, but no polynomial-time algorithm or NP-hardness proof has been found since their formulation in 2009. We present the first polynomial-time algorithm for drawing trees with optimal height. This corresponds to computing the homotopy height of triangulations consisting of a single vertex incident to a set of loops.

Joint work with: Salman Parsa.

Subspaces for Simulation of Deformations and Contact

Miguel A. Otaduy
Universidad Rey Juan Carlos, Madrid, Spain
miguel.otaduy@urjc.es

As we approach a new world of interaction between the real and the virtual, one of the grand challenges is to create accurate, robust, and efficient digital models of humans and their interaction with their surroundings. Such digital models can serve to understand and digitalize the real world, to represent digital twins in the context of digital design, testing, and training, or also to create virtual worlds.

We propose to address the complexity of digitizing human biomechanics and the interaction of humans and surrounding objects by combining two fundamental methodologies of computational modeling: physics-based simulation and machine learning. The cornerstone of the approach lies in building subspace models of human biomechanics, object deformation, and human-object interaction that tightly connect physics-inspired and machine-learning representations. Such tight connection can lead to (1) effective simulation models with a superior cost-accuracy trade-off, and (2) robust model estimation algorithms with superior conditioning of the search space. Subspace models employ a parameterization of the deformation and interaction space that is decoupled from the discretization of object deformation, and hence allow more efficient simulations with comparable accuracy. However, finding suitable subspace representations is not easy.

In our research group, we have already gathered evidence of successful combinations of physics-based and machine-learning representations to build subspace simulation models, as summarized in the figure above. Santesteban et al. [2] augmented parametric human models with skeleton-driven dynamic deformations. Tapia et al. [4], on the other hand, endowed these augmented deformation dynamics with a physics-based model to support contact interactions. Santesteban et al. [3] designed a subspace of learning-based cloth animation that is inherently collision-free. And Romero et al. [1] developed a machine-learning model of contact-driven dynamic deformations. These recent works span subspace representations for skeleton-driven or physics-based deformations, with and without contact.

Joint work with: Igor Santesteban, Cristian Romero, Javier Tapia, Jesús Pérez, Dan Casas.

References

[1] Cristian Romero, Dan Casas, Jesús Pérez, and Miguel Otaduy. Learning contact corrections for handle-based subspace dynamics. *ACM Trans. Graph.*, 40(4), 2021.

[2] Igor Santesteban, Elena Garces, Miguel A. Otaduy, and Dan Casas. Softsmpl: Data-driven modeling of nonlinear soft-tissue dynamics for parametric humans. *Computer Graphics Forum*, 39(2):65–75, 2020.

[3] Igor Santesteban, Nils Thuerey, Miguel A Otaduy, and Dan Casas. Self-Supervised Collision Handling via Generative 3D Garment Models for Virtual Try-On. *IEEE/CVF Conference on Computer Vision and Pattern Recognition (CVPR)*, 2021.

[4] Javier Tapia, Cristian Romero, Jesús Pérez, and Miguel A. Otaduy. Parametric skeletons with reduced soft-tissue deformations. *Computer Graphics Forum*, 2021.

Efficient and robust learning on non-rigid surfaces

Maks Ovsjanikov
Ecole Polytechnique, IP Paris, France
maks@lix.polytechnique.fr

In this talk I will describe several approaches for learning on curved surfaces, represented as point clouds or triangle meshes, undergoing non-rigid deformations. I will first give a brief overview of geodesic convolutional neural networks (GCNNs) and their variants [1] and then present a recent approach based on diffusion. The key properties of this approach is that it avoids potentially error-prone and costly operations with robust and efficient building blocks that are based on learned diffusion and gradient computation [2]. I will then show several applications, ranging from RNA surface segmentation to non-rigid shape correspondence, while highlighting the invariance of this technique to sampling and triangle mesh structure.

Joint work with: Nick Sharp, Souhaib Attaiki, Keenan Crane

References

[1] J. Masci, D. Boscaini, M. Bronstein, P. Vandergheynst, Geodesic convolutional neural networks on Riemannian manifolds. *Proc. CVPRW*, 2015

[2] N. Sharp, S. Attaiki, K. Crane, M. Ovsjanikov Diffusionnet: Discretization agnostic learning on surfaces *Trans. on Graph.*, 2022

Computing with trivariate splines on irregular meshes

Jörg Peters
Univaristy of Florida
jorg.peters@gmail.com

Defining differentiable spline spaces over irregular hexahedral partitions has applications in modelling as well as solving differential equations. This talk gives an overview of possible approaches, and recent experiments to establish optimal convergence order for the weak formulation of second and fourth-order equations.

Joint work with: Jeremy Youngquist

References

[1] Jörg Peters Refinable tri-variate C^1 splines for box-complexes including irregular points and irregular edges *Computer Aided Geometric Design*, 80:1–21, 2020.

Isogeometric de Rham complex discretization in solid toroidal domains

Francesco Patrizi
Max Planck Institute for Plasma Physics (IPP)
Boltzmannstraße 2, 85748 Garching bei München, Germany
francesco.patrizi@ipp.mpg.de

We present an IGA discretization of the continuous de Rham complex by means of adequate spline spaces which assemble in a discrete complex sustaining the same cohomological structure, when the underlying physical domain is a toroidal solid. Discretizations preserving such homological invariant of the physical model are commonly exploited in electromagnetics to obtain numerical solutions satisfying important conservation laws at the discrete level. Thereby one avoids spurious behaviors and, on the contrary, improves accuracy and stability.

The toroidal geometries are of particular interest, for example, in the context of magnetically confined plasma simulations. The singularity of the parametrization of such physical domains demands the construction of suitable restricted spline spaces, called polar spline spaces, ensuring an acceptable smoothness to set up the discrete complex.

References

[1] D. N. Arnold, Finite Element Exterior Calculus, *SIAM*, 2018.

[2] A. Buffa, J. Rivas, G. Sangalli & R. Vázquez. Isogeometric discrete differential forms in three dimensions. *SIAM Journal on Numerical Analysis*, 49(2), 818-844, 2011.

[3] F. Patrizi. Isogeometric de Rham complex discretization in solid toroidal domains. arXiv preprint: https://arxiv.org/abs/2106.10470, 2021.

[4] D. Toshniwal & T. J.R. Hughes. Isogeometric discrete differential forms: Non-uniform degrees, Bézier extraction, polar splines and flows on surfaces. *Computer Methods in Applied Mechanics and Engineering*, 376, 113576, 2021.

Isogeometric Immersed Methods

Francesca Pelosi
Università di Roma "Tor Vergata"
pelosi@mat.uniroma2.it

In engineering applications, the description of the geometry and the mesh generation process are often bottlenecks in finite element approximations of elliptic boundary value problems. Some efforts have been made to develop meshless methods. However a central problem of such methods is to incorporate boundary conditions of Dirichlet type.

This motivates the interest in immersed boundary and interface methods, also known as fictitious domain or embedded domain methods. The traditional philosophy of immersed boundary methods is to embed the computational domain in a structured grid and employ simple, mesh-aligned numerical schemes. Clearly, immersed methods require a proper treatment of the cells that are cut by boundaries and/or interfaces with some special, and often ad hoc, technique to achieve acceptably accurate results.

Moreover, one of the current challenges both in CAD and IgA is dealing with trimmed geometries. Indeed, the most common description of CAD models is the B-rep, where an object is represented by its boundary surfaces, described by suitable geometry maps on the parametric domain. Often only certain regions of a surfaces are supposed to be part of the actual object and the unused areas are trimmed away. Trimming results in identifying complex geometries in the parametric domain which can be treated following an immersed approach.

In this talk we aim to present our ongoing results on immersed boundary Isogeometric analysis based on B-splines/NURBS defined in both rectangular and triangular regular meshes, for general, non-constant coefficients, elliptic problems.

Joint work with: Carla Manni, Hendrik Speleers.

Implicit Bias of SGD for Diagonal Linear Networks: a Provable Benefit of Stochasticity

Scott Pesme
EPFL
scott.pesme@epfl.ch

Understanding the implicit bias of training algorithms is of crucial importance in order to explain the success of overparametrised neural networks. We study the dynamics of stochastic gradient descent over diagonal linear networks through its continuous time version, namely stochastic gradient flow. We explicitly characterise the solution chosen by the stochastic flow and prove that it always enjoys better generalisation properties than that of gradient flow. Quite surprisingly, we show that the convergence speed of the training loss controls the magnitude of the biasing effect: the slower the convergence, the better the bias. To fully complete our analysis, we provide convergence guarantees for the dynamics. We also give experimental results which support our theoretical claims. Our findings highlight the fact that structured noise can induce better generalisation and they help explain the greater performances of stochastic gradient descent over gradient descent observed in practice.

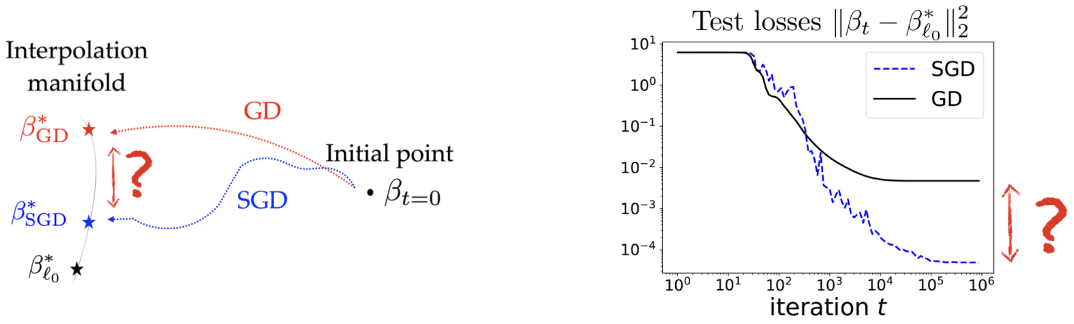

Figure 1: *Left (Drawing)*: For diagonal linear networks, the solutions recovered by SGD and GD differ. *Right*: Sparse regression with $n = 40$, $d = 100$, $\|\beta^*_{\ell_0}\|_0 = 5$, $x_i \sim \mathcal{N}(0, I)$, $y_i = x_i^\top \beta^*_{\ell_0}$. 2-layer diagonal linear network. SGD converges towards a solution which generalises better than GD, the sparsifying effect due to their implicit biases differ by more than an order of magnitude.

Joint work with: Loucas Pillaud-Vivien, Nicolas Flammarion

References

[1] S. Pesme, L. Pillaud-Vivien, N. Flammarion. Implicit Bias of SGD for Diagonal Linear Networks: a Provable Benefit of Stochasticity. *Advances in Neural Information Processing Systems 34 (2021).*

Smooth re-parametrizations for sparse regularization

Clarice Poon
University of Bath
cmhsp20@bath.ac.uk

Many low-complexity regularizers such as ℓ_1 or nuclear norm regularisation admit a quadratic variational form and this is the basis of the celebrated iteratively re-weighted least squares (IRLS) algorithms. In this work, we show how a simple re-parametrization of IRLS coupled with a bilevel formulation can lead to a smooth non-convex optimisation problem that can be handled with robust numerical procedures such as BFGS. Our formulation allows us to efficiently handle many popular optimisation settings, including the Lasso, total variation regularisation problems, sparsity problems with linear constraints, robust losses (such as the ℓ_1 loss), as well as non-convex ℓ_q minimisation. Our numerical benchmarking experiments demonstrate that this approach is highly versatile, leading to substantial performance advantages in a wide range of settings.

In additional to enabling the use of robust smooth optimisation tools, some of the reasons for the favourable behaviour of our proposed method are as follows. Although the resultant problem is non-convex, we show that there are no spurious minima since all saddle points are strict. Moreover, in the "fine-grids" setting where the columns of the matrix can be highly coherent with each other (this often occurs due to discretization in continuous problems), this re-parametrization leads to dimension free convergence rates – this is in stark contrast typical optimisation schemes based on the Euclidean distance such as Forward-Backward where convergence rates depend on the problem dimension.

Joint work with: Gabriel Peyré

Surfaces with a constant ratio of principal curvatures

Helmut Pottmann
Visual Computing Center, KAUST, Saudi Arabia
helmut.pottmann@kaust.edu.sa

Motivated by applications in architectural geometry [1], we study and compute surfaces with a constant ratio $a = \kappa_1/\kappa_2$ of principal curvatures (CRPC surfaces). While the special case of minimal surfaces ($a = -1$) is very well understood and has been studied in great detail, almost nothing is known about general CRPC surfaces.

Our computational approach is based on discrete differential geometry and numerical optimization [2, 3]. We discretize the so-called characteristic parameterizations of CRPC surfaces. For negative Gaussian curvature K, these parameterizations are asymptotic. For positive K they are conjugate and symmetric with respect to the principal curvature directions. CRPC surfaces are characterized by a constant angle between the parameter lines of the characteristic parameterization.

The developed computational methods also serve as an experimental basis for mathematical studies of the largely unexplored class of CRPC surfaces. Some phenomena suggested from computational results have already been verified by mathematical analysis. This concerns the classes of helical and spiral CRPC surfaces, for which we can provide explicit parameterizations and a study of the arising shapes.

Joint work with: Yang Liu, Olimjoni Pirahmad, Hui Wang.

References

[1] C. Jiang, C. Wang, E. Schling, H. Pottmann. Computational design and optimization of quad meshes based on diagonal meshes. *Advances in Architectural Geometry*, pages 38–60. Presses des Ponts, 2021.

[2] M. Jimenez, C. Müller, H. Pottmann. Discretizations of surfaces with constant ratio of principal curvatures. *Discrete Comp. Geometry*, 63:670–704, 2020.

[3] H. Wang, H. Pottmann. Characteristic parameterizations of surfaces with a constant ratio of principal curvatures. Preprint, 2021.

Identifying the non-trivial zeros of the Riemann zeta function for prime counting function approximation in the Loewner framework

Ion Victor Gosea
Max Planck Institute (MPI), Magdeburg, Germany.
gosea@mpi-magdeburg.mpg.de

Joint work with: Charles Poussot-Vassal (ONERA, Université de Toulouse, Toulouse, France), Pierre Vuillemin (ONERA, Université de Toulouse, Toulouse, France), and Athanasios C. Antoulas (Rice University, Houston, Max Planck Institute, Magdeburg, Germany and Baylor College of Medicine, Houston, USA).

The Loewner matrix pencil is an essential component of the realization and model reduction method for dynamical systems, originally proposed in [2] (known as the Loewner framework). This method was initially derived to construct reduced-order models (ROMs) of linear dynamical systems from data. More precisely, the transfer function of the ROM interpolates the original input-output data set corresponding to samples of a (rational) transfer function, or even of a complex irrational function (by enforcing rational approximation). Here, we are interested in the latter interpretation. We first describe a computationally and numerically simple procedure to estimate the "non-trivial" (harmonic) zeros of the famous Riemann ζ ("zeta") function (based on the Loewner framework); preliminary results are shown in Fig. 1. These approximated zeros are then used to recover the corrected Riemann prime counting function [1], approximating the prime number cardinality. We illustrate how efficient the Loewner framework is to recover this specific stair shape function.

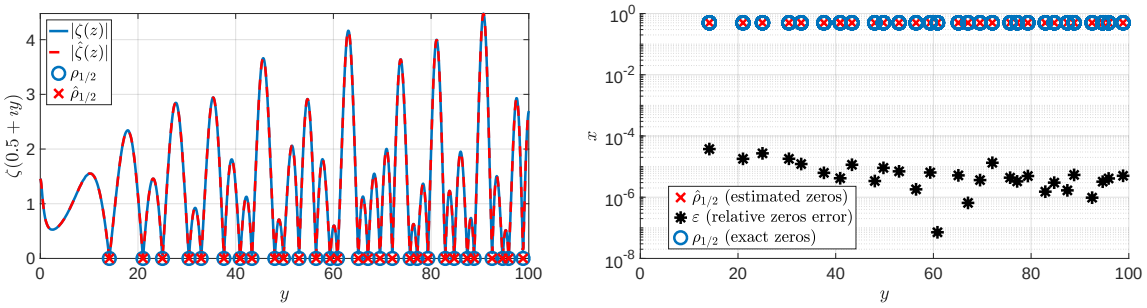

Figure 1: Left: comparison of the original and approximated functions for $y \in [0, 100]$. The zeros of each functions respectively are $\rho_{1/2}$ (blue circles) and $\hat{\rho}_{1/2}$ (red crosses). Right: exact (blue rounds) and estimated (red crosses) non-trivial complex zeros of the ζ function (x: real part, y: imaginary part). Relative point-wise mismatch error (black stars).

References

[1] B. Riemann. On the Number of Prime Numbers less than a Given Quantity (in German). *Monatsberichte der Berliner Akademie*, 1859.

[2] A. J. Mayo, A. C. Antoulas. A framework for the solution of the generalized realization problem. *Linear Algebra and its Applications*, vol.425, no. 2, pages 634–662, 2007.

Cutting convex polyhedra

Hartmut Prautzsch
Karlsruhe Institute of Technology
prautzsch@kit.edu

In Chaikin's algorithm, we iteratively smooth a polygonal line by cutting corners such that we arrive at a quadratic spline in the limit. For this and other edge preserving corner cutting schemes, we have de Boor's most general result that the limiting curve is differentiable if and only if the maximum angle flattens out eventually. In this talk, I will discuss face preserving cutting for convex polyhedra, explain why de Boor's result can not easily be generalized, go through counter examples and present results. Further, I introduce our 4-8 and 4-6-8 schemes, show outcomes of ongoing experiments, and may also briefly mention our honeycomb and $\sqrt{3}$ cutting schemes.

Joint work with: Yijun Xu.

On Bernstein-type operators preserving derivatives

Teresa E. Pérez
IMAG - Instituto de Matemáticas & Dpto. Matemática Aplicada
Universidad de Granada. Granada (Spain)
tperez@ugr.es

As it is well known, Bernstein polynomials were introduced by S. Bernstein in 1912 to provide a constructive proof of the Weierstrass approximation theorem, establishing that every continuous function defined on $[0,1]$ can be uniformly approximated by Bernstein polynomials.

In this work we study Bernstein-type operators that preserves the derivatives in the sense that the operator applied to the derivative of a function can be expressed as the derivative of the operator applied to the original function as was studied in [2], related to the operators defined in [1].

Joint work with: David Lara Velasco, Universidad de Granada (Spain).

References

[1] M. M. Derriennic. Sur l'approximation de fonctions intégrables sur $[0,1]$ par des polynômes de Bernstein modifiés. J. Approx. Theory 31(4):325–343, 1981.

[2] V. Gupta, A. J. López-Moreno, J. M. Latorre-Palacios. On simultaneous approximation of the Bernstein Durrmeyer operators. Appl. Math. Comput. 213(1):112–120, 2009.

[3] G. G. Lorentz. Bernstein Polynomials, second edition. Chelsea Publishing Co., New York, 1986.

Cut Pursuit and Geometric Applications

Hugo Raguet
LIFAT Univ Tours
hugo.raguet@insa-cvl.fr

We present an overview of the cut pursuit algorithm [1], together with different applications for image processing and 3D data analysis.

We consider the problem of minimizing functionals defined with respect to an undirected weighted graph $G = (V, E, w)$ with $w \in \mathbb{R}_+^E$ and with the following form:

$$F : \Omega^V \to \mathbb{R} : x \mapsto f(x) + \sum_{\{u,v\} \in E} w_{\{u,v\}} h(x_u, x_v) \ ,$$

where $f : \Omega^V \to \mathbb{R}$ is a function of interest depending on the context, and $h : \Omega^2 \to \mathbb{R}$ is a function that reaches its minimum only when $x_u = x_v$. More precisely, we are interested in functions h that encourage equality between x_u and x_v.

Such functionals, commonly encountered when handling spatial data, encourage their solutions to exhibit a particular kind of graph-structured sparsity. The motivation behind cut pursuit is to exploit this regularity to accelerate the minimization of F with a working-set iterative scheme.

Thanks to parsimonious computations and efficient parallelization [3], cut pursuit can be several orders of magnitude faster than other widely used optimization algorithms such as first-order proximal methods, or graph cut-based approaches. It can be used to minimize a large class of functionals and provides theoretical convergence guarantees in some settings without requiring convexity or differentiability of f [2].

Its principle can also be adapted to handle a variety of problems with a spatial structure, from inverse brain imaging to large-scale surface reconstruction [6]. Cut pursuit is also at the center of the SuperPoint Graph approach [4, 5], a state-of-the-art deep learning-based algorithm for the automated analysis of very large 3D point clouds.

Joint work with: Loïc Landrieu, IGN LaSTIG, Grand-Est University.

References

[1] Loïc Landrieu and Guillaume Obozinski. Cut pursuit: Fast algorithms to learn piecewise constant functions on general weighted graphs. *SIAM Journal on Imaging Sciences*, 10(4):1724–1766, 2017.

[2] Hugo Raguet and Loïc Landrieu. Cut-pursuit algorithm for regularizing nonsmooth functionals with graph total variation. *International Conference on Machine Learning*, 80:4244–4253, 2018.

[3] Hugo Raguet and Loïc Landrieu. Parallel Cut Pursuit For Minimization of the Graph Total Variation. *International Conference on Machine Learning*, Workshop on Learning and Reasoning with Graph-Structured Data, 2019.

[4] Loïc Landrieu and Martin Simonovsky. Large-scale Point Cloud Semantic Segmentation with Superpoint Graphs. *IEEE Conference on Computer Vision and Pattern Recognition*, 2018.

[5] Loïc Landrieu and Mohamed Boussaha. Point Cloud Oversegmentation with Graph-Structured Deep Metric Learning. *IEEE Conference on Computer Vision and Pattern Recognition*, 2019.

[6] Loïc Landrieu, Stéphane Guinard, Laurent Caraffa and Bruno Vallet. Piecewise-Planar Approximation of Large 3D Data as Graph-Structured Optimization. *ISPRS Annals of Photogrammetry, Remote Sensing and Spatial Information Sciences*, IV-2/W5:365–372, 2019.

Optimization of Curves Distributions Intersections for a Near to Eye Display Design

Fabian Rainouard[1,2,3], Christophe Martinez[1], Edouard Oudet[3] and Olivier Haeberlé[2]
1. CEA-LETI, Univ. Grenoble Alpes, F-38000 Grenoble, France
2. IRIMAS UR UHA 7499, Univ. Haute-Alsace Mulhouse, France
3. Laboratoire Jean Kuntzmann, Grenoble, France
fabian.rainouard@cea.fr

Our team works on an original concept of Near to Eye Display for Augmented Reality applications. This device requires mathematical research to optimize the diffraction phenomenon that forms the images onto the retina. Diffraction is an optical effect strongly related to periodicity and very well formulated by mathematics in particular through Fourier Optics. In order to break the periodicity of our display components we use improved mathematical models of curves. In this model, a first horizontal curve is described by a succession of segments with a unique absolute angle. The other curves are created by the translation of the first curve with a minimal gap equal to a value fixed by physicals constraints. We define vertical curves with the same principle. We use the B-Splines functions to approximate these successions of segments.

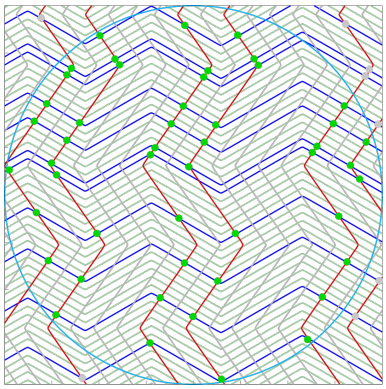

Figure 1: Mathematical model for waveguides and electrodes

In our concept, the horizontals curves represent light waveguides and verticals curves represent electrodes. Our design is based on the use of N_s laser sources and N_e electrical switches. Each source addresses a group of n_w random waveguides and each switch a group of n_e electrodes both drawn randomly without replacement in the curves set. When we turn on a laser source and a switch, the intersection between the corresponding n_w and n_e curves create an Emissive Points Ditribution (EPD). Our patented model of curves intend to define the best EPD surface density as close as possible from a pure random distribution. Our method improves by a factor 3.5 the number of EPD in comparison to an previous model. For our study, we use an iterative method adapted to B-Splines that allows for calculating the intersections between verticals and horizontals curves [1]. Figure 1 shows a graphical representation of the curves, red and blue curves representing activated electrodes and waveguides drawn form the set of periodic curves, respectively.

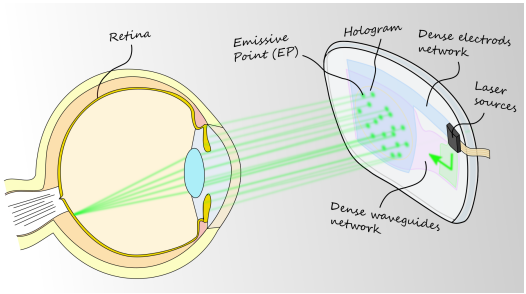

Figure 2: CEA-Leti concept of Near to Eye Display.

Figure 2 shows the concept of NED with a set of holograms, defined by an EPD, that sends light into the eye. The optical signal is diffracted through its propagation in the eye following what we call a self-focusing effect that creates a pixel on the retina [2]. To mathematically simulate the optical diffraction we calculate the Fourier Transform (FT) of the EPD. If the EPD is periodic, the result of the FT is periodic so that the pixel is repeated periodically on the retina without possibility to form an image. Conversely, a random EPD breaks the periodicity and allows isolating a single pixel on the retina. Depending on the surface density of this random EPD the contrast of this single pixel is improved. On the contrary, to form an image with a large number of pixels we need various EPD on the same surface. This leads to a compromise between randomness, surface density and surface diversity that represents one of our research target.

References

[1] K. Mørken et al. Computing intersections of planar spline curves using knot insertion. *Computer Aided Geometric Design*, 26(3):351–366, 2009.

[2] C. Martinez et al. See-through holographic retinal projection display concept. *Optica*, 5(10):1200, 2018.

New shape control tools for rational Bézier curve design

Andriamahenina Ramanantoanina
Università della Svizerra italiana
andriamahenina.ramanantoanina@usi.ch

Bézier curves are indispensable for geometric modeling and computer graphics. They have numerous favourable properties and provide the user with intuitive tools for editing the shape of a parametric polynomial curve, for example, by modifying the control points $P_0, \ldots, P_n$. Even more control and flexibility can be achieved by associating a shape parameter α_i with each control point P_i and considering rational Bézier curves, which comes with the additional advantage of being able to represent all conic sections exactly. In this talk, we explore the editing possibilities that arise from expressing a rational Bézier curve in barycentric form [1, 2], defined by a set of triplets (Q_i, β_i, t_i) of interpolation points Q_i, weights β_i, and nodes t_i. In particular, we show how to convert back and forth between the Bézier and the barycentric form, we discuss the effects of modifying the constituents (interpolation points, weights, nodes) of the barycentric form (see Fig. 1), and we study the connection between point insertion in the barycentric form with degree elevation of the Bézier form [3].

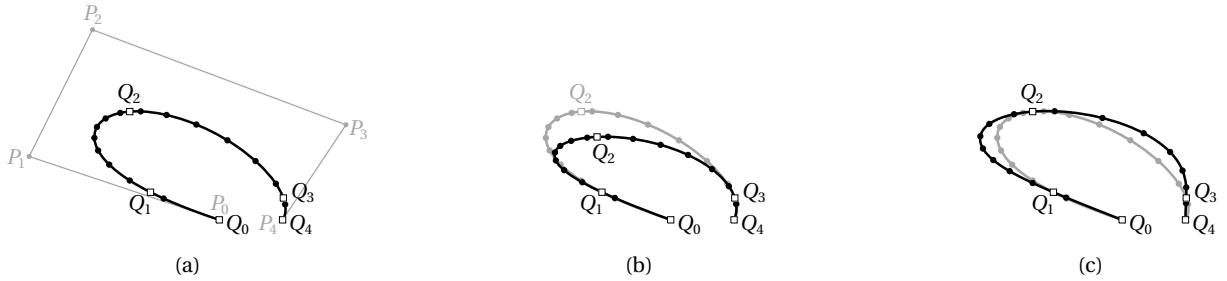

Figure 1: (a) converting a rational Bézier curve to the barycentric form; (b) the effect of moving the interpolation point Q_2; (c) the effect of decreasing the weight β_2 by 50%. The dots visualize the curve points $P(i/16)$ for $i = 0, \ldots, 16$.

Joint work with: Kai Hormann.

References

[1] Schneider, C. and Werner, W. Some new aspects of rational interpolation. *Mathematics of Computation* 47, 285–299. 1986.

[2] Berrut, J.P. and Mittelmann, H.D. Lebesgue constant minimizing linear rational interpolation of continuous functions over the interval. *Computers & Mathematics with Applications* 33, 77–86, 1997.

[3] Ramanantoanina A. and Hormann K. New shape control tools for rational Bézier curve design. *Computer Aided Geometric Design*, 88:102003, 2021.

Interactive Design with Developable Surfaces

Florian Rist
King Abdullah University of Science and Technology
florian.rist@kaust.edu.sa

Architects and designers share a long-standing interest in developable surfaces because of their aesthetic qualities and the advantages in fabrication they offer. This interest stems in part from the restrictions that the limitation to developable surfaces impose on the design. Digital design tools are required to handle these restrictions and allow the development of complex designs. While many CAD environments feature tools to create developable surfaces, existing tools are not adapted to the needs of designers, are inflexible and often even deliver erroneous or no results.

We address this problem by identifying categorically different design workflows and tasks and addressing each specifically in a unified design tool integrated into the commonly used CAD system Rhinoceros 3D. We co-developed interface metaphors and geometric representations best suitable for the specific tasks.

During an early stage of the design process, for example, a user might want to manipulate a surface freely in an intuitive way, willingly giving up some control over the shape, while later, during a phase of targeted design development, precise control over the shape in required. We demonstrate that this can be achieved by allowing the user to gradually add more constraints in the form of reference or guide geometry. Developing the design starting from a free-form surface by approximation is a very different problem, yet again.

We demonstrate novel solutions to these problems and their application in practice. Our efficient computational approach allows the optimization to run in the background and maintain a high degree of developability even while the user is interactively manipulating the surface – all integrated into Rhinoceros 3D.

Joint work with: Victor Ceballos Inza, Johannes Wallner, Helmut Pottmann.

References

[1] Glaeser, G. and Gruber, F. 2007. Developable surfaces in contemporary architecture. *Journal of Mathematics and the Arts*, 1, 1, 59-71. 10.1080/17513470701230004

[2] Jiang, C., Wang, C., Rist, F., Wallner, J. and Pottmann, H. 2020. Quad-mesh based isometric mappings and developable surfaces. *ACM Trans. Graph.*, 39 4, (July), 128:1-128:13. 10.1145/3386569.3392430

[3] Jiang, C., Mundilova, K., Rist, F., Wallner, J. and Pottmann, H. 2019. Curve-pleated structures. *ACM Trans. Graph.*, 38, 6, (November), 169:1-13. 10.1145/3355089.3356540

Recognition and approximation of space curves on 3D digital models

Chiara Romanengo
CNR-IMATI, Via de Marini 6, 16149 Genova, Italy
chiara.romanengo@ge.imati.cnr.it

Space curves play a fundamental role in conveying an object shape. Contours and curvilinear profiles are significant in manufacturing, art, design and medical applications. For instance, in reverse engineering, 3D scanning devices are used to digitize and validate a manually optimized physical prototype and it is extremely important that no details of the scanned object, e.g. sharp edges, corners and in general feature curves, are lost during the acquisition process. Indeed, when 3D models are acquired by scanning real objects, the resulting geometry does not explicitly encode these curves, especially when it is affected by noise or missing parts. This behavior is mainly due to measurement uncertainty, sampling resolution, or occlusion during the acquisition whereas, in applications like the digitisation of archaeological artefacts, these objects might be damaged, and then curves are partially missing.

The problem of recognising space curves and providing a mathematical representation of them can be addressed through the use of the Hough transform technique, which is well known for recognising curves in the plane and surfaces in space [1], but not yet sufficiently explored for space curves. Such a technique is robust to noise and outliers and does not suffer from missing parts. In this work, we will present and analyse the Hough transform (HT) to recognise and approximate space curves in 3D digital models (see [2]), a problem that is not currently addressed by the standard HT. In our approach, we take advantage of a recent HT formulation for algebraic curves to define both parametric and implicit curve representations. Specifically, we extend a first approach that applies directly the HT to the recognition of curves in space in parametric form, but it is limited to the case where the number of parameters is equal to the number of equations [3]. Regarding the implicit representation, we implement and follow the strategy defined in [4] that exploits the evaluation of the implicit functions and compares them with two theoretical bounds. To apply the HT to space curves, we assume that: *i*) the family of curves in which to search for the solution holds a regular parameterization for curves expressed in a parametric form; *ii*) the equations that define these curves are analytical for curves in implicit form.

The limited availability of templates for space curves has probably reduced the interest to the space curve fitting problem. To overcome this issue, we extend the existing dictionary of space curves by defining two types of families: we call *type I curves* the families of space curves equipped with an explicit representation, whereas we label *type II curves* the families obtained as the intersection of a quadric surface and a cylinder having a plane curve as its directrix, exploiting the large variety of plane curves available [5].

Joint work with: Silvia Biasotti, Bianca Falcidieno.

References

[1] M. C. Beltrametti, L. Robbiano. An algebraic approach to Hough transforms. *J. of Algebra*, 37 : 669–681, 2012.

[2] C. Romanengo, S. Biasotti, B. Falcidieno. Hough Transform for Detecting Space Curves in Digital 3D Models. *J. of Mathematical Imaging and Vision*, 2022.

[3] C. Romanengo, S. Biasotti, B. Falcidieno. HT-based identification of 3D feature curves and their insertion into 3D. *Computers & Graphics*, 89: 105–116, 2020.

[4] M. Torrente, M.C. Beltrametti, J.R. Sendra. r-norm bounds and metric properties for zero loci of real analytic functions. *J. of Computational and Applied Mathematics*, 336: 375 - 393, 2018.

[5] E. V. Shikin. Handbook and atlas of curves. CRC, 1995.

On the solution of a Riesz equilibrium problem and integral identities for special functions

Edward B. Saff
Vanderbilt University
edward.b.saff@vanderbilt.edu

ABSTRACT: We provide a full space quadratic external field extension of a classical result of Marcel Riesz for the equilibrium measure on a ball with respect to Riesz s-kernels. We address the case $s = d-3$ for arbitrary dimension d, in particular the logarithmic kernel in dimension 3. The equilibrium measure for this full space external field problem turns out to be a radial arcsine distribution supported on a ball with a special radius. As a corollary, we obtain new integral identities involving special functions such as elliptic integrals and more generally hypergeometric functions. It seems that these identities are not found in the existing tables for series and integrals, and are not recognized by advanced mathematical software. Among other ingredients, our proofs involve the Euler – Lagrange variational characterization, the Funk – Hecke formula, the Weyl regularity lemma, the maximum principle, and special properties of hypergeometric functions.

Joint work with Djalil Chafai, Robert Womersley.

Multi-sided surfaces interpolating arbitrary boundaries with intuitive interior control

Péter Salvi
Budapest University of Technology and Economics
salvi@iit.bme.hu

The representation of multi-sided (non-quadrilateral) surfaces is an interesting and difficult problem of computer-aided geometric design. The *de facto* standard solution in commercial systems is *trimming*, where the patch is defined by clipping the domain of a larger four-sided surface. This approach has several drawbacks. The larger surface is often underdetermined, and the connection to adjacent patches is generally not even exactly C^0-continuous. Another popular choice is to subdivide the multi-sided region into quadrilaterals, but determining the subdivision curves is a delicate matter, and this method may also harm internal continuity.

There is a line of research promoting the use of non-standard representations that ensure smooth connections to adjacent patches. This comes basically in two flavors:

- *Transfinite surface interpolation.* The surfaces are more-or-less completely defined by the boundary constraints, which are given in a very general form. Some types of interior control, such as snapping to auxiliary objects or a base surface, were attempted before (see e.g. [4, 1]), but these are not really suitable for an interactive design process.
- *Control-point–based approaches.* Representations such as the generalized Bézier patch [3], in addition to adhering to the boundary constraints, also offer a very intuitive control of the interior, but they are usually restricted to having (rational) polynomial boundaries. The recent generalized B-spline patch [2] is an exception, but it lacks the connected control network of its predecessor.

In this work I have attempted to combine these two worlds. The result—unlike [1]—is not CAD-exportable, and—unlike [2]—it cannot handle the multiply connected and/or concave, extreme configurations. What it does offer, on the other hand, is accurate interpolation of arbitrary boundaries *as well as* a natural control of the surface interior, suitable for interactive editing or approximation, while retaining the ability to smoothly connect to adjacent patches.

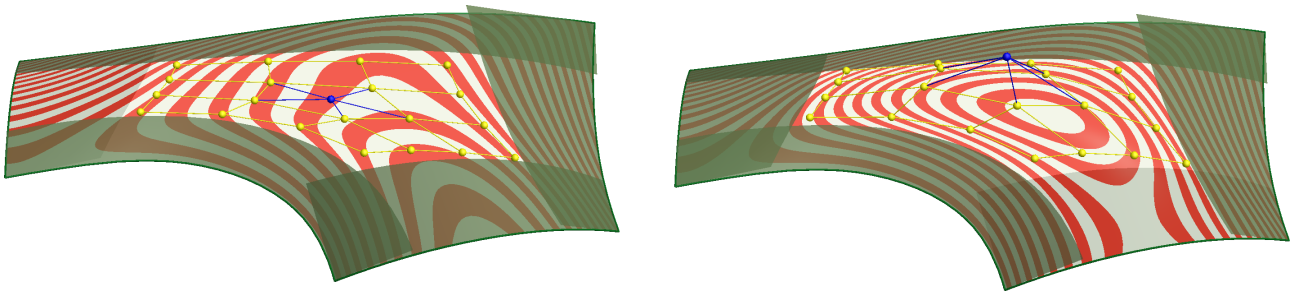

References

[1] F. Martin, U. Reif. Trimmed spline surfaces with accurate boundary control. *arXiv preprint*, 2009.02480v2, 2021.

[2] M. Vaitkus, T. Várady, P. Salvi, Á. Sipos. Multi-sided B-spline surfaces over curved, multi-connected domains. *Computer Aided Geometric Design*, 89:102019, 2021.

[3] T. Várady, P. Salvi, Gy. Karikó. A multi-sided Bézier patch with a simple control structure. *Computer Graphics Forum*, 35(2):307–317, 2016.

[4] T. Várady, P. Salvi, A. Rockwood. Transfinite surface interpolation with interior control. *Graphical Models*, 74(6):311–320, 2012.

Construction of G^2 Hermite interpolants with prescribed arc lengths

Maria Lucia Sampoli
Department of Information Engineering and Mathematics, University of Siena
marialucia.sampoli@unisi.it

Most methods to construct curves rely on the interpolation of discrete data, such as points, tangents or curvatures. If, in addition, we want to prescribe the total length of the resulting curve, in general we need to use iterative approximate methods. Pythagorean–hodograph (PH) curves are polynomial curves with the distinctive property of possessing arc lengths exactly determined by simple algebraic expressions in their coefficients. Hence the problem of constructing G^2 curves, that interpolate points, tangent directions and curvatures, and in addition have prescribed arc-length, can be exactly addressed. In this talk both the planar and the spatial problems are investigated considering PH curves of degree 7. For planar curves it is shown that in order to have a solution for any data, it is convenient to consider *biarcs*, keeping the degree to 7. In this case the solution of the G^2 continuity equations can be derived in a closed form, depending on four free parameters. By fixing two of them to zero, it is proven that the length constraint can be satisfied for any data. The proposed method is easy to implement and simple to use in practice, moreover, it can be directly applied to a (local) construction of G^2 continuous interpolating splines. Its extension to the spatial case is also possible and the main ideas behind this construction will be presented.

Joint work with: Marjeta Knez (University of Ljubljana) and Francesca Pelosi (University of Roma Tor Vergata).

Momentum Residual Neural Networks

Michael E. Sander
DMA, ENS and CNRS
michael.sander@ens.fr

Abstract: The training of deep residual neural networks (ResNets) with backpropagation has a memory cost that increases linearly with respect to the depth of the network. A way to circumvent this issue is to use reversible architectures. We propose to change the forward rule of a ResNet by adding a momentum term. The resulting networks, momentum residual neural networks (Momentum ResNets), are invertible. Unlike previous invertible architectures, they can be used as a drop-in replacement for any existing ResNet block. We show that Momentum ResNets can be interpreted in the infinitesimal step size regime as second-order ordinary differential equations (ODEs) and exactly characterize how adding momentum progressively increases the representation capabilities of Momentum ResNets. Our analysis reveals that Momentum ResNets can learn any linear mapping up to a multiplicative factor, while ResNets cannot. In a learning to optimize setting, where convergence to a fixed point is required, we show theoretically and empirically that our method succeeds while existing invertible architectures fail. We show on CIFAR and ImageNet that Momentum ResNets have the same accuracy as ResNets, while having a much smaller memory footprint, and show that pre-trained Momentum ResNets are promising for fine-tuning models.

Joint work with: Pierre Ablin, Mathieu Blondel and Gabriel Peyré [1].

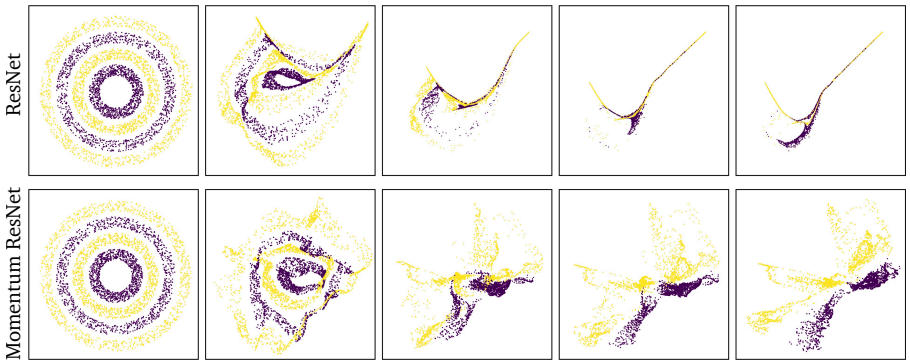

Figure 1: **Separation of four nested rings** using a ResNet (upper row) and a Momentum ResNet (lower row). From left to right, each figure represents the point clouds transformed at layer $3k$. The ResNet fails whereas the Momentum ResNet succeeds.

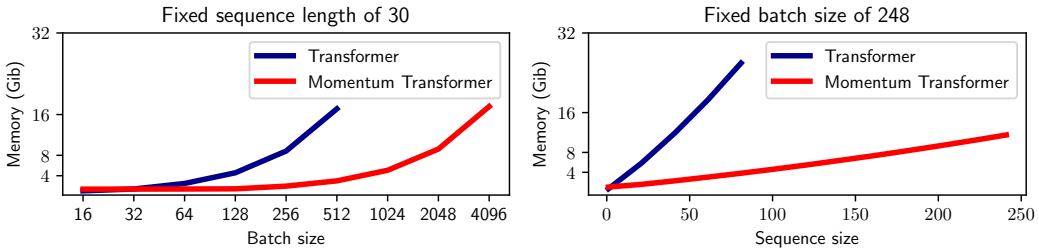

Figure 2: **Memory used** (using a profiler) for a Transformer and a Momentum Transformer on one training epoch, as a function of the batch size (left) and sequence size (right).

References

[1] Sander, M. E., Ablin, P., Blondel, M., and Peyré, G. Momentum residual neural networks. *In Proceedings of the 38th International Conference on Machine Learning, volume 139*, 9276–9287, 2021.

C^1 isogeometric spaces with optimal order of approximation

Giancarlo Sangalli
Dipartimento di Matematica "F. Casorati", Università di Pavia, Italy
giancarlo.sangalli@unipv.it

Abstract: In this talk I will present results (from papers in collaboration) about the construction of C^1 isogeometric quadrilateral elements that could be seen as extensions of the the classical Argyris triangular element. The structure is different (triangular and quadrilateral elements are structurally different) but the d.o.f.s and space contraints have some similarities. When the quadrilateral is a spline patch, the optimal order of approximation requires some constraints of the parametrization that needs to be "analysis-suitable G^1". An alternative is to enforce the C^1 interelement continuity in a weak sense, e.g. by the mortar method.

Joint work with: Mario Kapl, Gabriele Loli, Thomas Takacs

References

[1] Argyris, J. H., I. Fried, and D. W. Scharpf (1968). The TUBA family of plate elements for the matrix displacement method. The Aeronautical Journal 72(692), 701–709.

[2] Benvenuti, A. (2016). Isogeometric Analysis for C^1-continuous Mortar Method. Ph. D. thesis, University of Pavia.

[3] Brenner, S. C. and L.-Y. Sung (2005). C^0 interior penalty methods for fourth order elliptic boundary value problems on polygonal domains. Journal of Scientific Computing 22(1-3), 83–118.

[4] Collin, A., G. Sangalli, and T. Takacs (2016). Analysis-suitable G^1 multi-patch parametrizations for C^1 isogeometric spaces. Computer Aided Geometric Design 47, 93 – 113.

[5] Kapl, M., G. Sangalli, and T. Takacs (2021). A family of C^1 quadrilateral finite elements. Advances in Computational Mathematics 47 (6), 1–38.

A Phase-field Approach to Variational Hierarchical Surface Segmentation

Josua Sassen
University of Bonn
josua.sassen@uni-bonn.de

In this talk, we will discuss a phase-field model to partition a curved surface into path-connected segments with minimal boundary length as introduced in [1]. Phase-fields offer a powerful tool to represent diffuse interfaces with controlled width and to optimize them in a variational framework. We demonstrate how the multiplicative combination of phase-field functions can be used to effectively compute a hierarchical partition of unity. This induces an associated hierarchy of atlases, whose charts naturally overlap and thus are well-suited for applications such as texture mapping. To ensure connectedness of the charts, we employ a constraint introduced for phase-fields in [3]. Furthermore, we obtain distortion minimizing segmentations via a PDE-constrained optimization approach where the phase-field model allows direct use of Lagrangian calculus. Following [2], the Yamabe equation, which allows computing the distortion induced by segment flattening, is considered as the constraint. This way, we obtain end-to-end diffuse formulations of variational problems in surface segmentation that are straightforward to treat computationally. Various examples will illustrate the flexibility and robustness of this approach.

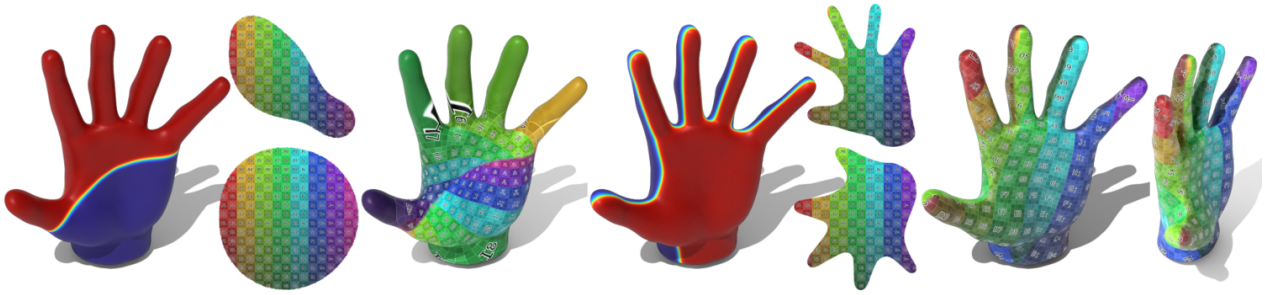

Figure 1: Our phase-field approach produces segments with diffuse interfaces, shown as red to blue colormap, by solving a variational problem. From this, we produce charts, shown are their images in the plane, and use them to map textures to the surface. However, the charts exhibit high distortion when only using the perimeter as objective (left). Thus, we minimize the distortion using the Yamabe equation as PDE-constraint (right).

Joint work with: Janos Meny (Bonn), and Martin Rumpf (Bonn)

References

[1] J. Meny, M. Rumpf, and J. Sassen. A Phase-field Approach to Variational Hierarchical Surface Segmentation. *Computer Aided Geometric Design*, 89, 2021.

[2] N. Sharp, and K. Crane. Variational Surface Cutting. *ACM Transactions on Graphics*, 37(4), 2018.

[3] P. Dondl, A. Lemenant, and S. Wojtowytsch. Phase Field Models for Thin Elastic Structures with Topological Constraint. *Archive for Rational Mechanics and Analysis*, 223, pages 693–736, 2017.

Image Processing for Large Volume Data in Sparse Representations

Tomas Sauer
University Passau & Fraunhofer IIS
Tomas.Sauer@uni-passau.de

Modern industrial computed tomography can generate volume data of the size of 1TB and larger and many of the scanned objects are unique, for example cars in reverse engineering or cultural heritage. To handle such "bigtures" on normal hardware, compression is unavoidable and methods have to be carefully designed that work on the sparse compressed data only. Once wavelet compression is the tool of choice, this means that we can only use the wavelet coefficients while access to the full decompressed image is out of question. This affects all stages of the process, from vizualization and standard image manipulations up to segmentation.

The talk presents some application examples and the mathematical background especially for efficient real time denoising based on an approximation of the TV norm from wavelet coefficients and a semi-automatic segmentation process based on feature learning.

Joint work with: Benedikt Diederichs, Thomas Lang, Andreas Michael Stock

Asymmetric compressive learning guarantees with applications to quantized sketches

Vincent Schellekens and Laurent Jacques
UCLouvain, Belgium
vschellekens95@gmail.com,laurent.jacques@uclouvain.be

The compressive learning framework reduces the computational cost of training on large-scale datasets. In a sketching phase, a dataset $\mathcal{X} = \{\boldsymbol{x}_i\}_{i=1}^n \subset \mathbb{R}^d$ with n samples is first compressed to a lightweight, m-dimensional sketch vector $\boldsymbol{z}_{\Psi,\mathcal{X}}$, obtained by mapping the data samples through a well-chosen feature map Ψ, and averaging those contributions (see Fig. 1). In a learning phase, the desired model parameters are then extracted from this sketch by solving an optimization problem, which also involves a feature map Φ. When the feature map is identical during the sketching and learning phases ($\Psi = \Phi$), formal statistical guarantees (excess risk bounds) have been proven [1, 2].

However, the desirable properties of the feature map are different during sketching and learning (such as quantized outputs, and differentiability, respectively). We thus study the relaxation where this map is allowed to be different for each phase ($\Psi \neq \Phi$). First, we prove that the existing guarantees carry over to this asymmetric scheme, up to a controlled error term, provided some Limited Projected Distortion (LPD) property holds. We then instantiate this framework to the setting of quantized sketches, by proving that the LPD indeed holds for binary sketch contributions. Finally, we further validate the approach with numerical simulations, including a large-scale application in audio event classification.

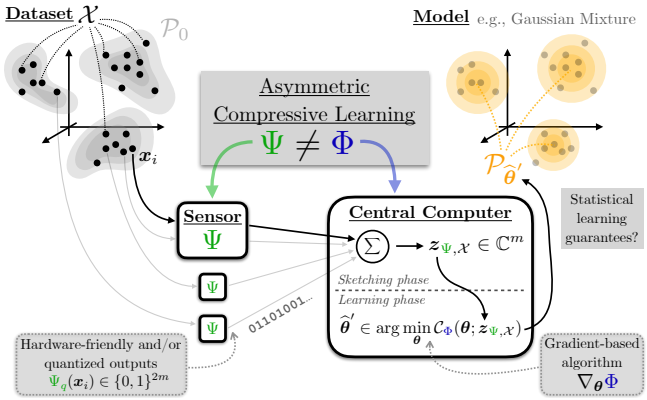

Figure 1: *Our Asymmetric Compressive Learning (ACL) scheme: a dataset $\mathcal{X}$ of n examples $\boldsymbol{x}_i$ (sampled i.i.d. from $\mathcal{P}_0$) is first compressed as a lightweight vector—the* sketch *—by averaging data features $\Psi(\boldsymbol{x}_i)$. This operation can be performed in parallel by a sensor network, which benefits greatly from hardware-friendliness and quantization. A model $\widehat{\boldsymbol{\theta}}'$ is then learned from the sketch $\boldsymbol{z}_{\Psi,\mathcal{X}}$ by solving a CL optimization procedure (minimizing a task-specific cost function $\mathcal{C}_\Phi$ between the sketch and the model) that uses a different, differentiable map $\Phi \neq \Psi$. Our goal is to prove statistical learning guarantees (w.r.t. $\mathcal{P}_0$) for the model $\widehat{\boldsymbol{\theta}}'$.*

References

[1] Rémi Gribonval, Gilles Blanchard, Nicolas Keriven, and Yann Traonmilin. Compressive statistical learning with random feature moments. *Mathematical Statistics and Learning*, 3(2):113–164, 2021.

[2] Rémi Gribonval, Antoine Chatalic, Nicolas Keriven, Vincent Schellekens, Laurent Jacques, and Philip Schniter. Sketching data sets for large-scale learning: Keeping only what you need. *IEEE Signal Processing Magazine*, 38(5):12–36, 2021.

The Kolmogorov-Arnold representation theorem revisited

Johannes Schmidt-Hieber
University of Twente
a.j.schmidt-hieber@utwente.nl

There is a longstanding debate whether the Kolmogorov-Arnold representation theorem can explain the use of more than one hidden layer in neural networks. The Kolmogorov-Arnold representation decomposes a multivariate function into an interior and an outer function and therefore has indeed a similar structure as a neural network with two hidden layers. But there are distinctive differences. One of the main obstacles is that the outer function depends on the represented function and can be wildly varying even if the represented function is smooth. We derive modifications of the Kolmogorov- Arnold representation that transfer smoothness properties of the represented function to the outer function and can be well approximated by ReLU networks. It appears that instead of two hidden layers, a more natural interpretation of the Kolmogorov-Arnold representation is that of a deep neural network where most of the layers are required to approximate the interior function.

On Gabor phase retrieval from samples

Rima Aliafari
ETH Zurich
rima.alaifari@sam.math.ethz.ch

We study the problem of recovering signals from magnitudes of their short-time Fourier transform. We ask whether it is possible to recover a signal uniquely from samples of its Gabor transform magnitude and analyze the connection of this problem to stability of Gabor phase retrieval from full (unsampled) measurements.

The Linearized Hellinger-Kantorovich Distance

Bernhard Schmitzer
Uni Goettingen
schmitzer@cs.uni-goettingen.de

Optimal transport provides a geometrically intuitive Lagrangian way of comparing distributions by mass rearrangement. The metric can be approximated by representing each sample as deformation of a reference distribution. Formally this corresponds to a local linearization of the underlying Riemannian structure. When combined with subsequent data analysis and machine learning methods this new embedding usually outperforms the standard Eulerian representation. We show how the framework can be extended to the unbalanced Hellinger–Kantorovich distance to improve robustness to noise and mass fluctuations.

Joint work with: Tianji Cai, Junyi Cheng, Matthew Thorpe

References

[1] T. Cai, J. Cheng, B. Schmitzer, and M. Thorpe. The linearized Hellinger–Kantorovich distance. SIAM Journal on Imaging Sciences 15(1), 45–83, 2022.

Repulsive Curves and Surfaces

Henrik Schumacher
Chemnitz University of Technology
henrik.schumacher@mathematik.tu-chemnitz.de

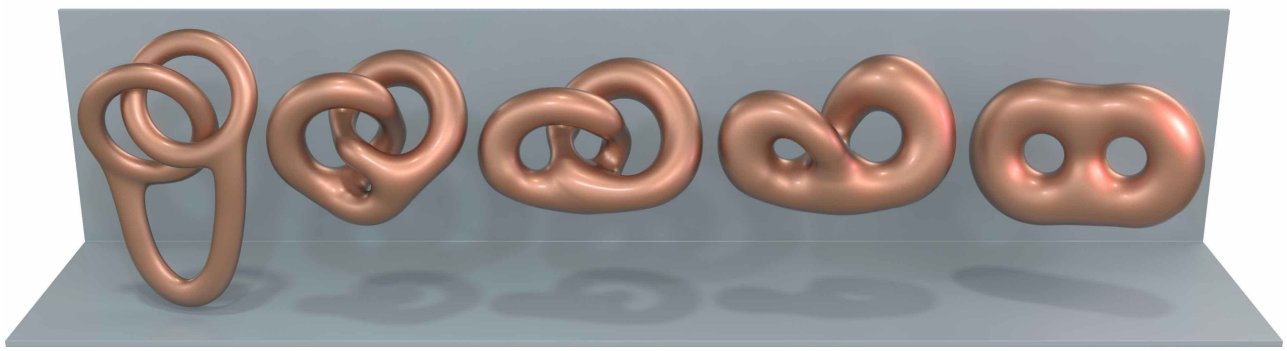

Functionals that penalize bending or stretching of a surface play a key role in geometric and scientific computing, but to date have ignored a very basic requirement: in many situations, surfaces must not pass through themselves or each other. This paper develops a numerical framework for optimization of surface geometry while avoiding (self-)collision. The starting point is the tangent-point energy, which effectively pushes apart pairs of points that are close in space but distant along the surface. We develop a discretization of this energy for triangle meshes, and introduce a novel acceleration scheme based on a fractional Sobolev inner product. In contrast to similar schemes developed for curves (cf. [2]), we avoid the complexity of building a multiresolution mesh hierarchy by decomposing our preconditioner into two ordinary Poisson equations, plus forward application of a fractional differential operator. We further accelerate this scheme via hierarchical approximation, and describe how to incorporate a variety of constraints (on area, volume, etc.). Finally, we explore how this machinery might be applied to problems in mathematical visualization, geometric modeling, and geometry processing.

Joint work with: Chris Yu, Caleb Brakensiek, Keenan Crane

References

[1] C. Yu, C. Brakensiek, H. Schumacher, and C. Keenan Repulsive Surfaces. *ACM Trans. Graph.*, 40(6):1–19, 2021.

[2] C. Yu, H. Schumacher, and C. Keenan Repulsive Curves. *ACM Trans. Graph.*, 40(2):1-21, 2021.

Deep Network Multi-Spline Approximation Method

Sefti Rania
University Mohammed I, FSO, LANO Laboratory, Oujda, Morocco,
University of Orleans, IDP Laboratory,UMR CNRS 7013, Orleans, France.
sefti.rania@ump.ac.ma

This paper introduces a new approximation method called Deep Multi Spline (DM-Spline) which is based on a deep learning model and various types of spline functions (B-Spline, UAT-Spline, hyperbolic-Spline, ...). The main idea is to combine different spline functions into a learning model that controls their contribution to the accurate approximation of the function to be built. We introduce a new bridge between Deep Neural Networks (DNNs) and spline approximation methods by developing a detailed theory in each layer and presenting some results on this subject. To test the robustness of the proposed approach, a comparison to state-of-the-art is achieved and shows the efficiency of our model. An application in the medical field is also provided.

Joint work with: Sbibih Driss, Jennane Rachid.

References

[1] R. Balestriero. A Spline Theory of Deep Networks. *In International Conference on Machine Learning*, PMLR. (pp. 374-383), 2018.

The Unbalanced Gromov-Wasserstein distance

Thibault Séjourné
DMA, ENS, PSL
thibault.sejourne@ens.fr

Optimal transport is an increasingly popular tool to compare distributions or compute assignments for machine learning and statistical inference. It takes advantage of the data's geometry, but suffers three limitations: (i) It is expensive to compute; (ii) it only compares probabilities; (iii) the distributions must be defined on the same space. Those restrictions are problematic to scale in applications, to discard geometric outliers, or to compare graphs with different structures. To alleviate each difficulty, it has been proposed to use entropic regularization [1], unbalanced optimal transport (UOT) [2] and the Gromov-Wasserstein distance (GW) [3]. The goal of this presentation is to combine the above three ideas to define a new formulation called unbalanced Gromov-Wasserstein (UGW) [4].

I first introduce the UOT formulation, and its entropically regularized version. I detail the Sinkhorn algorithm which solves the UOT problem on GPUs with a linear convergence. I then introduce the GW distance which is a non-convex quadratic assignment problem. It compares spaces equipped with a metric and a distribution, such as a graph with its geodesic distance and positive weights on nodes. I present two unbalanced extensions of this GW formulation. I show that the first one is a distance. The second one is computable on GPUs using entropic regularization by solving a sequence of regularized UOT problems. I end with ML experiments highlighting the applicability of UGW. If time permits, I will detail a new variant of Sinkhorn algorithm which accelerates the approximation of UOT and UGW [5].

Joint work with: François-Xavier Vialard, Gabriel Peyré.

GitHub Implementation: thibsej/unbalanced_gromov_wasserstein

Références:

[1] Cuturi, M. (2013). Sinkhorn distances: Lightspeed computation of optimal transport. Advances in neural information processing systems, 26, 2292-2300.

[2] Liero, M., Mielke, A., & Savaré, G. (2018). Optimal entropy-transport problems and a new Hellinger–Kantorovich distance between positive measures. Inventiones mathematicae, 211(3), 969-1117.

[3] Mémoli, F. (2011). Gromov–Wasserstein distances and the metric approach to object matching. Foundations of computational mathematics, 11(4), 417-487.

[4] Séjourné, T., Vialard, F. X., & Peyré, G. (2021). The unbalanced Gromov Wasserstein distance: Conic formulation and relaxation. Advances in Neural Information Processing Systems, 34.

[5] Séjourné, T., Vialard, F. X., & Peyré, G. (2022). Faster Unbalanced Optimal Transport: Translation invariant Sinkhorn and 1-D Frank-Wolfe. arXiv preprint arXiv:2201.00730.

Distance related problems in planar graphs and graphs on surfaces

Sergio Cabello
University of Ljubljana and Institute of Mathematics, Physics and Mechanics, Slovenia
myemail@myemail.com

Let G be graph and let $d_G(u, v)$ denote the distance between vertices u and v of G. Three key values associated to the graph are

- the *Wiener index*, defined by $\sum_{u,v \in V(G)} d_G(u, v)$ and closely related to the *average distance* of G;
- the *sum of inverse geodesic lengths*, defined as $\sum_{u \neq v \in V(G)} \frac{1}{d_G(u,v)}$ and closely related to the *total efficiency* of G;
- the *diameter*, defined by $\max\{d_G(u, v) \mid u, v \in V(G)\}$.

All these values can be computed trivially by explicitly computing all the pairwise distances in G. Can we compute these values faster, without computing all the pairwise distances? Lower bounds assuming the Strong Exponential Time Hypothesis (SETH) were shown by Roditty and Vassilevska Williams [3]. Most interestingly, if the graph has n vertices and $\Theta(n)$ edges, no algorithm can compute those values in $O(n^{1.99999})$, assuming SETH.

I will discuss how these values can be computed in subquadratic, namely $\tilde{O}(n^{9/5})$ time, for n-vertex planar graphs and graphs on surfaces of constant genus. The main ideas are from [1, 2], but I will explain an alternative point of view that represents all distances in the graph a compact way.

References

[1] S. Cabello. Subquadratic algorithms for the diameter and the sum of pairwise distances in planar graphs. *ACM Transactions on Algorithms*, 2018.

[2] S. Cabello. Computing the inverse geodesic length in planar graphs and graphs of bounded treewidth. *ACM Transactions on Algorithms*, accepted

[3] L. Roditty and V. Vassilevska Williams. Fast approximation algorithms for the diameter and radius of sparse graphs. *Proc. 45th ACM Symposium on Theory of Computing*, STOC 2013.

Interpolation of 3D data streams with C^2 PH quintic splines

Alessandra Sestini
University of Firenze, Italy
alessandra.sestini@@unifi.it

Algorithms for real–time interpolation of data streams are very useful for trajectory planning where, as a new target position (and possibly an associated direction of motion) becomes available, a suitable interpolating path has to be accordingly successively extended. In such context the flexibility of splines is clearly very useful, see [1] for their application to planar data stream interpolation. In this talk we will show how spatial PH quintic biarc splines can be effectively adopted in order to define a globally C^2 spatial path interpolating a stream of 3D Hermite data. The local interpolation scheme has three free parameters which can highly influence the shape of the local interpolating path, as usual with PH curves [2]. In order to facilitate the real-time usage of the method, such parameters are selected with analytic formulas which ensure fourth approximation order to the scheme [3]. The flexibility of the method is also extended adapting it also to the case where only streams of positions are given. Extensions of this research of interest for real-time rigid body motions are under development and will be possibly also briefly introduced.

Joint work with: Carlotta Giannelli, Lorenzo Sacco.

References

[1] R. Debski. Streaming Hermite interpolation using cubic splinelets. *CAGD*, 88(2):102011, 2021.

[2] R. T. Farouki, C. Giannelli, A. Sestini. New developments in Theory, Algorithms, and Applications for Pythagorean–Hodograph Curves. *Advanced Methods for Geometric Modeling and Numerical Simulation*, C. Giannelli and H. Speleers eds., Springer INdAM Series :123–172, 2019.

[3] C. Giannelli, L. Sacco, A. Sestini. Interpolation of 3D data streams with C^2 PH quintic splines, submitted, 2021.

Multiscaling manifold-valued data via approximation subdivision schemes

Nir Sharon
School of Mathematical Sciences, Faculty of Exact Sciences, Tel Aviv University, Israel
nsharon@tauex.tau.ac.il

The close connection between subdivision schemes and wavelets has been studied for decades. One milestone is Donoho's work from the nineties about the direct application of interpolatory subdivision operators as upscaling operators in a pyramid transform [1]. However, it has been established only recently how to use non-interpolatory operators similarly [2].

In this talk, I will briefly survey this hierarchical analysis and introduce the lifting of multiscale pyramid transform for analyzing manifold-valued functions. Then, we describe this construction in detail and present its analytical properties, including stability and coefficient decay. Finally, we numerically demonstrate the results and show the application of our method for denoising and abnormalities detection.

Joint work with: Wael Mattar.

References

[1] David L Donoho. Interpolating wavelet transforms. *Preprint, Department of Statistics, Stanford University*, 2(3):1–54, 1992.

[2] Nira Dyn and Xiaosheng Zhuang. Linear multiscale transforms based on even-reversible subdivision operators. In *Excursions in Harmonic Analysis, Volume 6*, pages 297–319. Springer, 2021.

Nonsmooth Implicit Differentation for Machine Learning

Antonio Silveti-Falls
Toulouse School of Economics
tonys.falls@gmail.com

Introduction Many problems in machine learning can be solved efficiently by taking advantage of implicit differentiation, from hyperparameter tuning [1] to training neural networks with implicitly defined layers [3, 2]. The key ingredient to applying implicit differentiation is the implicit function theorem which guarantees the existence of an implicit function and its differentiability, with a calculus for the implicit gradient. A bottleneck for extending such methods in practice is the lack of smoothness present in many machine learning problems. Although there is a rich literature on nonsmooth implicit function theorems already, the focus has primarily been on proving the existence and regularity of implicit functions rather than on developing a practical calculus.

Main Result We construct a theory of implicit differentiation for path differentiable functions [4] with a flexible calculus that allows one to compute implicit gradients using the analogous formulas from the smooth setting, in a way that is compatible with backpropagation and algorithmic differentiation. Path differentiable functions were studied in [4] as a subset of locally Lipschitz functions which admit a *conservative Jacobian*, denoted $\mathcal{J}_F$ for a function F. Our main contribution is the following theorem.

Theorem. Let $F : \mathbb{R}^n \times \mathbb{R}^m \to \mathbb{R}^m$ be path differentiable and $(\hat{x}, \hat{y}) \in \mathbb{R}^n \times \mathbb{R}^m$ be such that $F(\hat{x}, \hat{y}) = 0$. Assume $\mathcal{J}_F(\hat{x}, \hat{y})$ is convex and $\forall [A\ B] \in \mathcal{J}_F(\hat{x}, \hat{y})$, B is invertible. Then $\exists U \subset \mathbb{R}^n$ a neighborhood of $\hat{x}$ and a path differentiable function G such that

$$\forall x \in U \qquad F(x, G(x)) = 0.$$

A conservative Jacobian of G can be computed from the formula

$$\mathcal{J}_G(x) = \left\{ -B^{-1}A : [A\ B] \in D_F(x, G(x)) \right\}.$$

Applications With the previous theorem and the framework of conservative Jacobians, we are able to prove almost sure convergence guarantees for training neural networks with implicitly defined layers. These are networks with layer outputs defined as fixed points to an equation [2] or solutions to an optimization problem [3].

We also examine hyperparameter tuning for the LASSO. The problem of choosing the best weight λ for the LASSO problem can be formulated as a bilevel optimization problem:

$$\min_{\lambda \in \mathbb{R}} C(\hat{\beta}(\lambda)) \quad \text{such that} \quad \hat{\beta}(\lambda) \in \operatorname*{argmin}_{\beta \in \mathbb{R}^p} \frac{1}{2} \|X\beta - y\|_2^2 + \lambda \|\beta\|_1$$

where C is some measure of task performance, e.g. the cross validation loss, the holdout loss, the stein unbiased risk estimate, etc. By writing the optimality condition as a fixed point equation, we can apply our theorem to compute a conservative Jacobian for the solution $\hat{\beta}(\lambda)$.

Joint work with: Jérôme Bolte, Tam Le, and Edouard Pauwels.

References

[1] Pedregosa, Fabian Hyperparameter optimization with approximate gradient *International conference on machine learning* 2016

[2] Bai, Shaojie and Kolter, J Zico and Koltun, Vladlen. Deep equilibrium models *Advances in Neural Information Processing Systems* 2019

[3] Agrawal, Akshay and Amos, Brandon and Barratt, Shane and Boyd, Stephen and Diamond, Steven and Kolter, J Zico Differentiable convex optimization layers *Advances in neural information processing systems* 2019

[4] Bolte, Jérôme and Pauwels, Edouard Conservative set valued fields, automatic differentiation, stochastic gradient methods and deep learning *Mathematical Programming* 2021

Polynomiality vs. rationality of Pythagorean hodograph/normal curves and surfaces

Zbyněk Šír
Charles University in Prague
zbynek.sir@mff.cuni.cz

We will discuss the relation between the polynomial and rational curves with pythagorean hodograph in $\mathbb{R}^2$ and $\mathbb{R}^3$ as well as the rational and polynomial pythagorean normal surfaces in $\mathbb{R}^3$.

The planar cases are considered rather for the seek of completeness and as a motivation. Indeed the relation between the planar polynomial and rational PH curves was already fully analyzed in [3]. We will however compare these two families of curves using a different method based on solving a system of linear equations.

The situation is much more interesting in $\mathbb{R}^3$. Historically the polynomial PH curves [1] are much better studied then the rational ones, [4, 8]. On the other hand the rational PN surfaces were fully described already in [2] but only examples of polynomial PN surfaces are available, see e.g. [5, 6]

We propose a new method for studying these problems. It is based on determining the corresponding motion polynomial, [7, 9]. While the primal (rotation) component of the motion polynomial is arbitrary, the dual (translation) part is determined be a linear system of equations. This system is analysed and possible denominators of the resulting PH/PN curves and surfaces are discussed. Polynomial object in this approach appear as special cases of the polynomial ones. From a certain point of view however the polynomial objects appear to be the generic cases.

Joint work with: Hans-Peter Schröcker, Daniel Scharler, Bahar Kalkan.

References

[1] R. T. Farouki and T. Sakkalis, Pythagorean-hodograph space curves, *Adv. Comp. Math.*, **2**, 41–66, 1994.

[2] H. Pottmann, Rational curves and surfaces with rational offsets, *Comput. Aided Geom. Design* **12**, 177–192, 1995.

[3] R. T. Farouki and H. Pottmann, Polynomial and rational Pythagorean-hodograph curves reconciled, in *The Mathematics of Surfaces VI* (G. Mullineux, ed.), Oxford University Press, 355-378 (1996).

[4] R. T. Farouki and Z. Šír, Rational Pythagorean-hodograph space curves, *Comput. Aided Geom. Design* **28**, 75-88 (2011).

[5] J. Kozak, M. Krajnc, V. Vitrih, A quaternion approach to polynomial PN surfaces, *Comput. Aided Geom. Design* **47**, 172-188, 2016.

[6] M. Bizzarri, M. Lávička, Z. Šír and J. Vršek, Hermite interpolation by piecewise polynomial surfaces with polynomial area element, *Comput. Aided Geom. Design* **51**, In Computer Aided Geometric Design, 30-47, 2017.

[7] Z. Li, J. Schicho, and H.-P. Schröcker, Factorization of motion polynomials. *J. Symbolic Comput.*, **92**, 190-202, 2019.

[8] R. T. Farouki and Z. Šír, Mapping rational rotation-minimizing frames from polynomial curves on to rational curves, *Comput. Aided Geom. Design* **78**:101833, 2020.

[9] B. Kalkan and D. F. Scharler and H.-P. Schröcker and Zbyněk Šír, Rational Framing Motions and Spatial Rational Pythagorean Hodograph Curves, submitted to *Comput. Aided Geom. Design* , arXiv:2111.04600.

Optimal recovery of operator sequences

Dmytro Skorokhodov
DNU
dmitriy.skorokhodov@gmail.com

We consider two recovery problems based on information given with an error. First is the problem of optimal recovery of the class $W_q^T = \{(t_1h_1, t_2h_2, \ldots) \in \ell_q : \|h\|_q \leq 1\}$, where $1 \leq q < \infty$ and $t_1 \geq t_2 \geq \ldots \geq 0$, in the space ℓ_q when in the capacity of inexact information we know either the first $n \in N$ elements of a sequence with an error measured in the space of finite sequences ℓ_r^n, $0 < r \leq \infty$, or a sequence itself is known with an error measured in the space ℓ_r. The second is the problem of optimal recovery of scalar products acting on Cartesian product $W_{p,q}^{T,S}$ of classes W_p^T and W_q^S, where $1 < p, q < \infty$, $\frac{1}{p} + \frac{1}{q} = 1$ and $s_1 \geq s_2 \geq \ldots \geq 0$, when in the capacity of inexact information we know the first n coordinate-wise products $x_1y_1, x_2y_2, \ldots, x_ny_m$ of the element $x \times y \in W_{p,q}^{T,S}$ with an error measured in the space ℓ_r^n. We find exact solutions to above problems and construct optimal methods of recovery. As an application of our results we consider the problem of optimal recovery of classes in Hilbert spaces by Fourier coefficients known with an error measured in the space ℓ_p with $p > 2$, which is close to the ill-posed problems considered in [1].

Joint work with: Vladislav Babenko, Nataliia Parfinovych.

References

[1] P. Mathé, S. V. Pereverzev. Stable Summation of Orthogonal Series with Noisy Coefficients *J. Approx. Theory*, 118(1):66–80, 2002.

Direct (and inverse) modeling of inflatables and other wrinkled thin shells

Mélina Skouras
Université Grenoble Alpes, Inria, CNRS, Grenoble INP, LJK
melina.skouras@inria.fr

Inflatables are structures made of flat planar membranes that are sealed or sewn to each other and that assume complex curved shapes once pressurized. Wrinkles tend to form at the locations of the seams, which makes the numerical simulation and, a fortiori, the inverse design, of such structures very challenging: not only does one need to finely discretize the mesh in order to accurately reproduce the geometry of these wrinkles, but one also has to deal with the numerical instabilities that arise in the system.

In this presentation, I will show that relying on tension field theory to convexity the constitutive material law of the membrane material allows us to correctly predict the global shape of the structure, even when we use coarsely discretized meshes. We can then use this convexified model in an interactive design tool that automatically adjusts the shape of the panels of the inflatable so as to create a structure of a desired shape [1].

In addition, we will see that we can subsequently recover the geometry of the missing wrinkles by parametrizing them by an amplitude and phase field that we solve for over the coarse base mesh. This approach allows us to recover complex wrinkle patterns with wavelength much smaller than the resolution of the base mesh while requiring much fewer degrees of freedom than required by traditional shell solvers [2].

References

[1] M. Skouras, B. Thomaszewski, P. Kaufmann, A. Garg, B. Bickel, E. Grinspun, M. Gross. Designing Inflatable Structures. *ACM Transactions on Graphics*, 33(4), 2014.

[2] Z. Chen, H.-Y. Chen, D. Kaufman, M. Skouras, E. Vouga. Fine Wrinkling on Coarsely Meshed Thin Shells. *ACM Transactions on Graphics*, 40(5), 2021.

Learning spline parameterization for noisy data fitting

Sofia Imperatore
University of Florence
sofia.imperatore@unifi.it

In different application fields related to geometric modeling and data processing, it is common to deal with corrupted data, due to the nature of their generation or collection process. As concerns spline fitting schemes, a necessary preprocessing step, which highly affects the shape and accuracy of the (re-)constructed model, consists in computing the parametric values associated with each input data. We propose a data-driven learning method based on a neural network which takes in input the relative distances of a variable number of data points and returns a suitable parameterization of randomly measured points. Different spline fitting approximation schemes will be considered both for the network design and for the numerical experiments on synthetic and real data configurations.

Joint work with: Carlotta Giannelli, Angelos Mantzaflaris.

Edge adaptive methods and machine learning for high-resolution image reconstruction

Somacal Agustín
Laboratoire Jacques-Louis Lions, Sorbonne Université
agustin.somacal@sorbonne-universite.fr

Edge-adapted methods have been introduced in the context of image processing [1, 2] to reconstruct high-resolution images from coarser cell averages. In particular, when images consist of piece-wise smooth functions, the interfaces can be approximated by a pre-specified functional class (lines, circle arcs, etc) through optimization (LVIRA [2]) or specific preprocessing (ENO-EA [1]). In this work, we extend the ENO-EA approach to polynomials of degree higher than 1 and compare this algebraic approach to that introduced in [2] as well as to learning-based methods [3] in which an artificial neural network (NN) (or in principle any other non linear sufficiently rich function family) is used to attain the same goal.

Joint work with: Cohen Albert, Dolbeault Matthieu, Mula Olga.

References

[1] F. Arandiga, A. Cohen, R. Donat, N. Dyn, B. Matei. Approximation of piecewise smooth func-tions and images by edge-adapted (ENO-EA) nonlinear multiresolution techniques. Applied andComputational Harmonic Analysis, 24(2), 225250, 2008. doi :10.1016/j.acha.2007.06.009.

[2] J. E. Pilliod, E. G. Puckett Second-order accurate volume-of-fluid algorithms for tra-cking material interfaces. Journal of Computational Physics, 199(2), 465502, 2004. doi :10.1016/j.jcp.2003.12.023.

[3] B. Desprs, H. Jourdren Machine Learning design of Volume of Fluid schemes for compressibleflows. Journal of Computational Physics, 408, 2020. doi :10.1016/j.jcp.2020.109275.

Optimal spline subspaces for outlier-free isogeometric analysis

Hendrik Speleers
University of Rome Tor Vergata
speleers@mat.uniroma2.it

Spectral analysis can be used to study the error in each eigenvalue and eigenfunction of a numerical discretization of an eigenvalue problem. For a large class of boundary and initial-value problems the total discretization error on a given mesh can be recovered from its spectral error. This is of primary interest in engineering applications.

The isogeometric approach for eigenvalue problems has been widely investigated in the literature; see, e.g., [1, 3, 4]. Maximally smooth spline spaces on uniform grids are an excellent choice for addressing eigenvalue problems. Yet, they still present a flaw: a very small portion of the eigenvalues are poorly approximated and the corresponding computed values are much larger than the exact ones. These spurious values are usually referred to as outliers. The number of outliers increases with the degree p. However, for fixed p, it is independent of the degrees of freedom for univariate problems, while a "thin layer" of outliers is observed in the multivariate setting.

Outlier-free discretizations are appealing, not only for their superior description of the spectrum of the continuous operator, but also for their beneficial effects in various contexts, such as an efficient selection of time-steps in (explicit) dynamics and robust treatment of wave propagation. For a fixed degree, the challenge is to remove outliers without loss of accuracy in the approximation of all eigenfunctions.

In this talk we discuss isogeometric Galerkin discretizations of eigenvalue problems related to the Laplace operator subject to any standard type of homogeneous boundary conditions conditions in certain optimal spline subspaces [5]. Roughly speaking, these optimal subspaces are obtained from the full spline space defined on specific uniform knot sequences by imposing specific additional boundary conditions. The spline subspaces of interest have been introduced in the literature some years ago when proving their optimality with respect to Kolmogorov n-widths [2]. For a fixed number of degrees of freedom, all the eigenfunctions and the corresponding eigenvalues are well approximated, without loss of accuracy in the whole spectrum when compared to the full spline space. Moreover, there are no spurious values in the approximated spectrum. In other words, the considered subspaces provide accurate outlier-free discretizations in the univariate and in the multivariate tensor-product case. The role of such spaces as accurate discretization spaces for addressing general problems is discussed as well.

Joint work with: Carla Manni, Espen Sande.

References

[1] J.A. Cottrell, A. Reali, Y. Bazilevs, and T.J.R. Hughes. Isogeometric analysis of structural vibrations. *Computer Methods in Applied Mechanics and Engineering*, 195:5257–5296, 2006.

[2] M.S. Floater and E. Sande. Optimal spline spaces for L^2 n-width problems with boundary conditions. *Constructive Approximation*, 50:1–18, 2019.

[3] C. Garoni, H. Speleers, S-E. Ekström, A. Reali, S. Serra-Capizzano, and T.J.R. Hughes. Symbol-based analysis of finite element and isogeometric B-spline discretizations of eigenvalue problems: Exposition and review. *Archives of Computational Methods in Engineering*, 26:1639–1690, 2019.

[4] R.R. Hiemstra, T.J.R. Hughes, A. Reali, and D. Schillinger. Removal of spurious outlier frequencies and modes from isogeometric discretizations of second- and fourth-order problems in one, two, and three dimensions. *Computer Methods in Applied Mechanics and Engineering*, 387:114115, 2021.

[5] C. Manni, E. Sande, and H. Speleers. Application of optimal spline subspaces for the removal of spurious outliers in isogeometric discretizations. *Computer Methods in Applied Mechanics and Engineering*, 389:114260, 2022.

Continuous Time Frank-Wolfe Does Not Zig-Zag, But Multistep Methods Do Not Accelerate

Yifan Sun
Stony Brook University
yifan.sun@stonybrook.edu

The Frank-Wolfe algorithm has regained much interest in its use in structurally constrained machine learning applications. However, one major limitation of the Frank-Wolfe algorithm is the slow local convergence property due to the zig-zagging behavior. We observe that this zig-zagging phenomenon can be viewed as an artifact of discretization, as when the method is viewed as an Euler discretization of a continuous time flow, that flow does not zig-zag. For this reason, we propose multistep Frank-Wolfe variants based on discretizations of the same flow whose truncation errors decay as $O(\Delta^p)$, where p is the method's order. This strategy "stabilizes" the method, and allows tools like line search and momentum to have more benefit. However, in terms of a convergence rate, our result is ultimately negative, suggesting that no Runge-Kutta-type discretization scheme can achieve a better convergence rate than the vanilla Frank-Wolfe method. We believe that this analysis adds to the growing knowledge of flow analysis for optimization methods, and is a cautionary tale on the ultimate usefulness of multistep methods.

Joint work with: Zhaoyue Chen, Mokhwa Lee.

A streamlined NURBS-based workflow for precise Additive Manufacturing

Javier Sánchez-Reyes
IMACI, ETS Ingeniería Industrial Ciudad Real, Universidad de Castilla-La Mancha, Spain
Javier.SanchezReyes@uclm.es

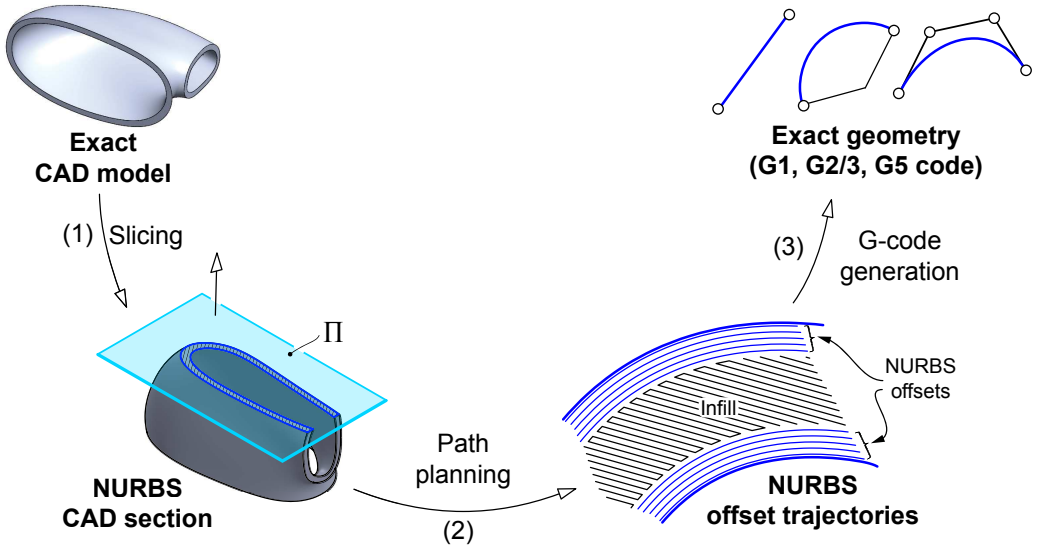

Figure 1: Our approach for generating accurate G-code for AM

We put forward a streamlined AM workflow, with a seamless transfer from the initial CAD description to the final G-code. Polygonal approximations and associated errors are avoided by adhering to the NURBS standard at all steps. Experimental results confirm a considerable improvement in quality over the traditional AM workflow, consisting of an initial polygonization of the object (e.g., via STL), slicing this approximation, offsetting the polygonal sections, and finally generating G-code made up of polyline trajectories (G1 commands). This traditional AM workflow does not meet the requirements for truly functional parts regarding quality and precision, especially in large-scale 3D printing, hence wasting the possibilities of existing AM hardware.

Our proposal (Fig. 1) bypasses the polygonal approximation and then proceeds as follows:

(1) Direct slicing of the CAD model in the NURBS environment provided by a NURBS-based CAD system.
(2) Path planning, including offset trajectories, in this NURBS environment.
(3) Accurate G-code generation of NURBS: circular arcs (G2/3 code), Bézier cubics (G5), and polylines (G1).

Slicing (1) and offsetting, the most complex geometry operation in path planning (2), are already available in any CAD system in a reliable way. Therefore, there is no need to develop ad-hoc procedures, as we can access these capabilities through a suitable programming environment. In particular, we employ a NURBS-based commercial CAD system (Rhino3D along with its programming environment Grasshopper) for direct slicing of the model, offset generation, and trimming.

Our main contribution is sticking to the NURBS standard at the last step (3) of AM, namely G-code generation, a possibility overlooked in both the literature and commercial applications. To this aim, we exploit the possibilities of exiting firmware controlling 3D printers, such as Marlin, incorporating G2/3 (circular arcs) and G5 (cubic Bézier curves) commands. Since trajectories resulting from offsetting in Rhino3D usually restrict to circles and polynomial (cubic or quadratic) splines, the exact conversion into G2/3 and G5 code is readily performed via standard NURBS geometry processing, such as knot-insertion and degree-elevation.

Research supported by grant PID2019-104586RB-I00, funded by MCIN/AEI/10.13039/501100011033.

Joint work with: Jesús M. Chacón, Javier Vallejo, Pedro J. Núñez.

Planar Polynomial PH Curves revisited

Salim Taleb
Ceramaths Lab
UPHF
59313 Valenciennes, France
salim.taleb@uphf.fr

A polynomial Pythagorean-hodograph (PH) curve has the property that its parametric speed — i.e., the derivative of the arc length with respect to the curve parameter — is a polynomial rather than the square root of a polynomial. Many computational advantages derive from this property and are useful in offsets, path planning, geometric design and similar applications.

In this talk, a geometric characterization for planar polynomial PH curves is presented. It is based on a variant of the dual representation of planar curves, where a curve may be regarded as the envelope of its tangent lines. The approach used here is illustrated with many examples.

A comparison is made with the state-of-art method : three–stage procedure that transforms any differentiable plane curve $r(t)$ into a PH curve $\hat{r}(t)$ through the use of the conformal map $z \to z^2$. In this framework, the Pythagorean structure of the hodograph $\hat{r}'(t)$ is achieved through the complex variable model. The *a priori* implementation is done through an algebraic model.

In the technique presented here, the Pythagorean property of the hodograph is achieved by a suitable geometric model. Notorious results for cubic PH curves and quintic PH curves are generalized. This geometric characterization provides an alternative three–stage procedure of generating plane polynomial PH curves. This work contributes to a different explanation of the theory and the applied algorithms for planar PH curves. It can be developed in various other related topics.

Almost-C^1 splines

Deepesh Toshniwal
Delft Institute of Applied Mathematics, Delft University of Technology
d.toshniwal@tudelft.nl

Isogeometric Analysis generalizes classical finite element analysis and intends to integrate it with the field of Computer-Aided Design. A central problem in achieving this objective is the reconstruction of analysis-suitable models from Computer-Aided Design models, which is in general a non-trivial and time-consuming task. This talk will present new spline constructions [1, 2] that enable model reconstruction, as well as simulation of high-order PDEs on the reconstructed models. The proposed *almost-C^1 splines* [2] are finite piecewise-biquadratic splines on fully unstructured quadrilateral meshes (i.e., without restrictions on placements or number of extraordinary vertices). This is the lowest-degree unstructured spline construction that can be used to solve fourth-order problems on surfaces of arbitrary topology.

The definition of almost-C^1 splines builds upon the one from [1], and leads to splines that are C^1 smooth almost everywhere – that is, at all vertices and across most edges, and in addition almost (i.e. approximately) C^1 smooth across all other edges. Moreover, the proposed refinement scheme yields a C^1 smooth limit surface. The spline basis described has no parametric singularities, has several B-spline-like properties (e.g., partition of unity, non-negativity, local support), and can be implemented using Bézier-extraction. Numerical tests suggest that the basis is well-conditioned and exhibits optimal approximation behaviour.

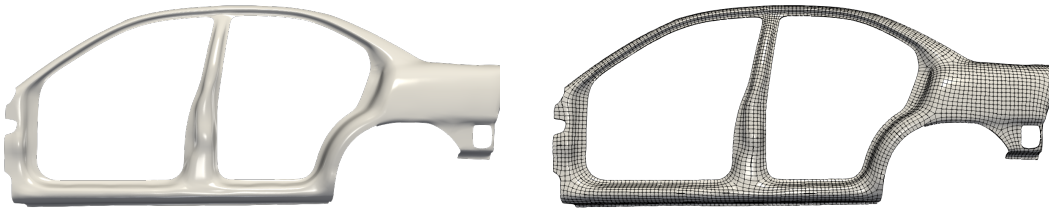

Figure 1: Example of an analysis-suitable model of a Dodge Neon reconstructed using almost-C^1 splines. The left figure shows the spline surface, the underlying Bézier mesh is shown on the right.

Joint work with: Thomas Takacs (Johann Radon Institute for Computational and Applied Mathematics)

References

[1] D. Toshniwal. Quadratic splines on quad-tri meshes: Construction and an application to simulations on watertight reconstructions of trimmed surfaces. *Computer Methods in Applied Mechanics and Engineering*, 388:114174, 2022.

[2] T. Takacs and D. Toshniwal. Almost-C^1 splines: Biquadratic splines on unstructured quadrilateral meshes and their application to fourth order problems. *arXiv preprint*, arXiv:2201.11491, 2022.

A new max-based compression algorithm for surrogate modelling. Application to the processing of neutronics data

Olivier TRUFFINET CEA Saclay - SERMA/LPEC laboratory
olivier.truffinet@cea.fr

Many research and industry codes tend to generate large amounts of intermediate data, for instance under the form of tabulated values of physical quantities. This data can be quite redundant (i.e of small effective dimension), justifying the use of lossy compression methods such as Singular Values Decomposition (SVD) for storing and accessing it more efficiently. But said redundancy could also be exploited in other ways, for instance by extrapolating it with some *surrogate model* to reduce unnecessary calculation on close configurations.

This is the lead we are following in this article, by introducing a new compression tool based on the Empirical Interpolation Method, an algorithm initially developed in the framework of partial differential equations [2]. Unlike SVD, this EIM-compression method is based on the infinite norm $\|\cdot\|_\infty$, and proceeds in a greedy way by iteratively trying to approximate the data and incorporating the chunks of information which cause the largest error. In the process, it provides a vector basis and a set of interpolation points, which can be used to approximate future data from very little information. The algorithm is competitive in terms of speed and accuracy, but also very suitable for parallelization and out-of-core computation (processing of data too large for the computer RAM).

We apply this algorithm to a neutronics problem: the computation of homogenized cross-sections. These quantities, which measure the interaction of neutrons with matter, are generated in large amounts (up to hundred of gigabytes) by nuclear reactor simulators, stored as tabulated multivariate functions, and have already been shown to be highly redundant [1]. The already mentionned EIM basis and interpolation points enable us to build an elementary surrogate model for these cross-sections: they make it possible to reconstruct a full grid of any of them using only its values at a small number of points. By training this model on a well-chosen subset of the data, we can greatly speed up the calculation by interpolating most of the sections instead of computing them explicitly. We assess the performance of this method on realistic nuclear data, and discuss the impact of several modeling choices - especially normalization, which is of great importance in the problem at hand.

Joint work with: Karim AMMAR, Bertrand BOURIQUET, Nicolas GERARD-CASTAING.

References

[1] M. Barrault & al. An empirical reduced-basis interpolation method: application to efficient discretization of partial differential equations. *C. R. Acad. Sci. Paris, Ser.I 339*, Numerical Analysis, 2004.

[2] D. Tomatis. A multivariate representation of compressed pin-by-pin cross sections. *EPJ Nuclear Sciences & Technologies*, 2021.

Approximate C^1-smoothness for isogeometric analysis over multi-patch domains

Thomas Takacs
Johann Radon Institute for Computational and Applied Mathematics, Linz, Austria
thomas.takacs@ricam.oeaw.ac.at

In this talk we study discretization spaces over multi-patch domains, which can be used for isogeometric analysis of fourth order partial differential equations (PDEs). While standard Galerkin discretization of fourth order PDE problems require C^1-smooth discretizations, we propose a method that uses approximate C^1-smoothness, cf. [2, 4].

A key property of IGA is that it is simple to achieve high order smoothness within a single tensor-product B-spline (or NURBS) patch. However, to increase the geometric flexibility, one has to construct spaces beyond such a tensor-product structure. This can be done using unstructured splines, e.g., as in [3], or using a multi-patch construction. While C^0-matching multi-patch domains are easy to construct, C^1-smoothness is harder to achieve. It was shown in [1], that C^1-smooth isogeometric discretizations over G^1-smooth multi-patch domains do in general not possess sufficient approximation power. This issue was circumvented in [1] by restricting to a smaller class of G^1-smooth multi-patch parametrizations, so called analysis-suitable G^1 multi-patch parametrizations, which yield C^1-smooth isogeometric spaces. However, to avoid this additional restriction, we relax the smoothness constraints and construct isogeometric spaces that yield optimal convergence rates in numerical experiments while being only approximately C^1.

Such constructions are of interest when solving numerically fourth-order problems, such as the biharmonic equation or Kirchhoff-Love plate and shell formulations. The approximate C^1 method is advantageous when compared to alternatives that rely on a weak imposition of smoothness, such as Nitsche's method. In contrast to weakly imposing coupling conditions, the approximate C^1 construction is explicit and no additional terms need to be introduced to penalize the jump of the derivative at the interface. Thus, the approximate C^1 method can be used more easily as no additional parameters need to be estimated.

Joint work with: Pascal Weinmüller.

References

[1] A. Collin, G. Sangalli, and T. Takacs. Analysis-suitable G^1 multi-patch parametrizations for C^1 isogeometric spaces. *Computer Aided Geometric Design*, 47:93–113, 2016.

[2] P. Weinmüller and T. Takacs. Construction of approximate C^1 bases for isogeometric analysis on two-patch domains. *Computer Methods in Applied Mechanics and Engineering*, 385:114017, 2021.

[3] T. Takacs and D. Toshniwal. Almost-C^1 splines: Biquadratic splines on unstructured quadrilateral meshes and their application to fourth order problems. *arXiv preprint arXiv:2201.11491*, 2022.

[4] P. Weinmüller and T. Takacs. An approximate C^1 multi-patch space for isogeometric analysis with a comparison to Nitsche's method. *arXiv preprint arXiv:2202.04516*, 2022.

The uniform sparse FFT with application to PDEs with random coefficients

Fabian Taubert
Chemnitz University of Technology, Faculty of Mathematics
fabian.taubert@math.tu-chemnitz.de

Parametric operator equations have gained significant attention in recent years. In particular, partial differential equations with random coefficients play an important role in the study of uncertainty quantification. Therefore, the numerical solution of these equations and how to compute them in an efficient and reliable way has become more and more important. The usual example is the following model problem, describing the diffusion characteristics of inhomogeneous materials and therefore being called diffusion equation:

Let the domains $D \subseteq \mathbb{R}^{d_{\boldsymbol{x}}}$, typically with $d_{\boldsymbol{x}} = 1, 2$ or 3, and $D_{\boldsymbol{y}} \subseteq \mathbb{R}^d$ as well as the random coefficient $a : D \times D_{\boldsymbol{y}} \to \mathbb{R}$ and the right-hand side $f : D \to \mathbb{R}$ be given. Then, find $u : D \times D_{\boldsymbol{y}} \to \mathbb{R}$, such that for all $\boldsymbol{y} \in D_{\boldsymbol{y}}$ there holds

$$\begin{aligned} -\nabla \cdot (a(\boldsymbol{x}, \boldsymbol{y}) \nabla u(\boldsymbol{x}, \boldsymbol{y})) &= f(\boldsymbol{x}) && \boldsymbol{x} \in D,\ \boldsymbol{y} \in D_{\boldsymbol{y}} \\ u(\boldsymbol{x}, \boldsymbol{y}) &= 0 && \boldsymbol{x} \in \partial D,\ \boldsymbol{y} \in D_{\boldsymbol{y}}. \end{aligned}$$

The differential operator ∇ is always used w.r.t. the spatial variable $\boldsymbol{x}$. The one-dimensional components of $\boldsymbol{y}$ are assumed to be i.i.d. with a prescribed distribution and the dimension d of the random vector $\boldsymbol{y}$ is typically very large.

We present an efficient, non-intrusive algorithm to solve such differential equations, our so-called *uniform sparse FFT* or short *usFFT*. The aim is the approximation of the solution u on a discretization $\{\boldsymbol{x}_g \in D, g = 1, \dots, G\}, G < \infty$, of the spatial domain D, e.g., a finite element mesh. We receive an approximation

$$u_{\boldsymbol{x}_g}(\cdot) \coloneqq u(\boldsymbol{x}_g, \cdot) \approx \sum_{\boldsymbol{k} \in \mathrm{I}} c_{\boldsymbol{k}}^{\mathtt{usFFT}}(u_{\boldsymbol{x}_g})\, \mathrm{e}^{2\pi \mathrm{i} \boldsymbol{k} \cdot}$$

for each node $\boldsymbol{x}_g$, where the frequency set I is a priori unknown. Our dimension-incremental approach realizes this by detecting a good frequency set I adaptively as well as computing approximations $c_{\boldsymbol{k}}^{\mathtt{usFFT}}(u_{\boldsymbol{x}_g}), \boldsymbol{k} \in \mathrm{I}$, of the corresponding Fourier coefficients for all nodes $\boldsymbol{x}_g$, $g = 1, \dots, G$, simultaneously. In particular, the usFFT does not need any a-priori information except for a suitable search domain $\Gamma \supset \mathrm{I}$, which can easily be chosen large enough without disturbing the algorithm. Further, the detected frequency set I is independent of g and therefore provides a good approximation basis for all $\boldsymbol{x}_g$, $g = 1, \cdots, G$, uniformly. Also, the usFFT only needs samples of the solution u at multiple points $\boldsymbol{y}$, which can be computed by any common PDE solver for each fixed $\boldsymbol{y}$. Hence, the method can be adapted to other types of differential equations, boundary conditions or domains easily by swaping this PDE solver with a suitable one for the new setting.

We test our algorithm on some examples with different diffusion coefficients $a(\boldsymbol{x}, \boldsymbol{y})$ and uniformly or standard normally distributed random variables $\boldsymbol{y}$ up to dimension $d = 20$. The results are analysed using common error norms. Further, the detected frequency set I as well as the approximated Fourier coefficients $c_{\boldsymbol{k}}^{\mathtt{usFFT}}(u_{\boldsymbol{x}_g}), \boldsymbol{k} \in \mathrm{I}$, provide detailed information on the influence and the interactions of the random variables $\boldsymbol{y}$.

Joint work with: Lutz Kämmerer, Daniel Potts.

References

[1] L. Kämmerer, D. Potts and F. Taubert. The uniform sparse FFT with application to PDEs with random coefficients. *ArXiv e-prints*, arXiv:2109.04131 [math.NA], 2021.

Alignment and convergence of kernels in deep learning

Matus Telgarsky
University of Illinois
myemail@myemail.com

Despite nonconvexity and even nonsmoothness of deep network training, both the gradient descent trajectory and corresponding sequence of kernels are convergent under minimal assumptions. This talk will explore the basic proof technique, namely an alignment property of gradient descent that appears more fundamental than previously discovered implicit bias phenomena, and discuss consequences on sample complexity and comparison to the standard initial kernel (what is typically called the neural tangent kernel).

Greedy algorithms in numerical integration

V.N. Temlyakov
University of South Carolina
temlyakovv@gmail.com

We consider numerical integration in classes, for which we do not impose any smoothness assumptions. We illustrate how nonlinear approximation, in particular greedy approximation, allows us to guarantee some rate of decay of errors of numerical integration even in such a general setting with no smoothness assumptions.

Variational Graph Methods for Efficient Point Cloud Sparsification

Daniel Tenbrinck
Friedrich-Alexander-Universität Erlangen-Nürnberg
daniel.tenbrinck@fau.de

In recent years new application areas have emerged in which one aims to capture the geometry of objects by means of three-dimensional point clouds, e.g., via LiDAR, stereo vision, or depth-by-motion techniques. Often the obtained data consist of a dense sampling of the object's surface, containing many redundant 3D points. These unnecessary data samples lead to high computational effort in subsequent processing steps. Thus, *point cloud sparsification* or *compression* is often applied as a preprocessing step. The two standard methods to compress dense 3D point clouds are random subsampling and approximation schemes based on hierarchical tree structures, e.g., octree representations. However, both approaches give little flexibility for adjusting point cloud compression based on a-priori knowledge on the geometry of the scanned object. Furthermore, these methods lead to suboptimal approximations if the 3D point cloud data is prone to noise.

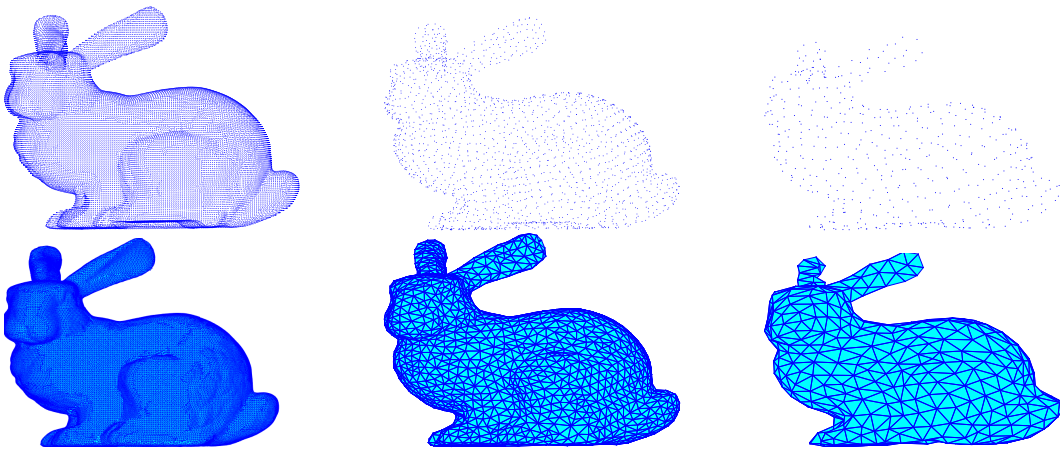

Figure 1: Point cloud sparsification of the 3D Stanford bunny model (top) and resulting triangulations (bottom).

This talk is based on our findings in [3], in which we propose a variational method defined on finite weighted graphs, which allows to sparsify a given 3D point cloud while giving the flexibility to control the appearance of the resulting approximation based on the chosen regularization functional. The main idea of our approach is a novel coarse-to-fine optimization scheme for point cloud sparsification, inspired by the efficiency of the *Cut Pursuit algorithm* for total variation denoising proposed in [1]. This strategy gives a substantial speed up in computing sparse point clouds compared to a direct application on all points as done in previous works, e.g., in the seminal work in [2], and renders variational methods now applicable for this task. We compare different settings for our point cloud sparsification method both on unperturbed as well as noisy 3D point cloud data.

Joint work with: Fjedor Gaede, Martin Burger

References

[1] L. Landrieu, G. Obozinski. Cut Pursuit: Fast Algorithms to Learn Piecewise Constant Functions on General Weighted Graphs. *SIAM Journal on Imaging Sciences 10(4)*, pages 1724–1766, 2017.

[2] F. Lozes, A. Elmoataz, O. Lezoray. Partial Difference Operators on Weighted Graphs for Image Processing on Surfaces and Point Clouds. *EEE Transactions on Image Processing 23(9)*, pages 3896–3909, 2014.

[3] D. Tenbrinck, F. Gaede, M. Burger. Variational Graph Methods for Efficient Point Cloud Sparsification. *arXiv preprint*, arXiv:1903.02858, 2019.

Conical surfaces

Jonas Tervooren
Technische Universität Wien
jtervooren@geometrie.tuwien.at.ac

The tangent planes along each parameter-line of a conjugate net, $f : \mathbb{R}^2 \supset U \to \mathbb{R}^3$, envelop a developable surface. We call a conjugate net *conical*, if the developable surfaces along one of the families of parameter-lines are cones or cylinders. Hence, one can easily approximate a given surface by tangential cone patches, if a conical parametrization is known. This has interesting applications for cladding of building facades, because conical strips are only curved in one direction and can be constructed by bending metal sheets or glass. The collection of cone patches, can be understood as a semi discrete surface itself, by considering the intersection curves of neighboring cones, which are a discrete family of smooth curves. We found a way to design semi-discrete conical surfaces by using NURBS curves.
Conical surfaces are not only of practical interest, but also exhibit a rich theory. Similar to isometric surfaces, which can be characterized by the existence of a transformation group (Darboux transformations), we proved that a conjugate net is conical if and only if there exist a special family of Combescure transformations, called *conical Combescure transformations* (CCT). Since every non zero function of one parameter defines a CCT, conical nets always appear as a families of parallel related nets. Further, conical nets are invariant under projective transformations of the ambient space. A special subclass of conical nets, containing the well known canal surfaces, is given by the orthogonal ones. We proved that an orthogonal net is conical if and only if every curve of one family of parameter-lines has constant geodesic curvature and consequently lies on a sphere. This observation enabled us to find an explicit construction for all orthogonal conical nets. Another interesting subclass are nets, that have tangential cones at both families of parameter-lines. We call them double conical nets and proved that a conical net is *double conical* if and only if it is a Koenigsnet. Applying a theorem of Darboux, gave us that every orthogonal double conical net is Möbius equivalent to a surface of revolution, cone or cylinder.
Finally, we found a discretization of conical nets as quadrilateral surfaces $f : \mathbb{Z}^2 \supset U \to \mathbb{R}^3$ and showed that most of the results for smooth conical nets stay true for their discrete counterparts. In the talk, we will give a general introduction to conical nets and then present the new results and constructions for both smooth and discrete conical surfaces.

Joint work with: Christian Müller, Martin Kilian.

A novel algorithm to compute the joint spectral radius – Feta flavoured Ipa

Thomas Mejstrik
NuHAG
Faculty of Mathematics
University of Vienna
thomas.mejstrik@gmx.at

The problem of computing the joint spectral radius (JSR) [1] of several matrices plays an exceptional role e.g. in the theory of refinable surfaces, subdivision schemes and wavelets. In particular, the JSR characterizes the smoothness of refinable curves and surfaces and the convergence of subdivision schemes. However, the problem of the JSR's computation is notoriously hard. Currently there exist only two algorithms which can compute the joint spectral radius exactly, the invariant polytope algorithm [2, 3, 4, 5] and the finite expressible tree algorithm [6]. The former tries to construct an invariant norm for all matrices, the latter constructs an infinite tree of matrices whose branches are all multiplicatively bounded.

In this talk we compare these two algorithms, show that they can handle different classes of examples and construct a new algorithm combining both ideas which converges in all cases when one of aforementioned algorithms does. The efficiency of the new algorithm is illustrated with various examples. In particular, we prove the finiteness conjecture [7, 8] for all pairs of binary 3×3 matrices, and are able to compute the joint spectral radius of random matrices of dimension 25 in reasonable time.

Joint work with: Ulrich Reif, Technical University Darmstadt, Germany; Vladimir Yu. Protasov, Lomonosov Moscow State University, Russia.

References

[1] G. C. Rota, G. Strang, *A note on the joint spectral radius*, Kon. Nederl. Acad. Wet. Proc. 63 (60), doi: 10.1016/S1385-7258(60)50046-1.

[2] N. Guglielmi, V. Yu. Protasov, *Exact computation of joint spectral characteristics of linear operators*, Found. Comput. Math., 13 (2013) 1, 37–39, doi: 10.1007/s10208-012-9121-0.

[3] N. Guglielmi, V. Yu. Protasov, *Invariant polytopes of sets of matrices with applications to regularity of wavelets and subdivisions*, SIAM J. Matr. Anal. Appl., 37 (2016) 1, 18–52, doi: 10.1137/15M1006945.

[4] T. Mejstrik, *Improved invariant polytope algorithm and applications*, ACM Trans. Math. Softw., 46 (2020) 3 (29), 1–26, doi: 10.1145/3408891.

[5] T. Mejstrik, V. Yu. Protasov, *Elliptic polytopes and Lyapunov norms of linear operators*, SIMAX, under review, arXiv: https://arxiv.org/abs/2107.02610.

[6] C. Möller, U. Reif, *A tree-based approach to joint spectral radius determination*, Linear Alg. Appl., 463 (2014), 154–170, doi: 10.1016/j.laa.2014.08.009.

[7] J. C. Lagarias, Y. Wang, *The finiteness conjecture for the generalized spectral radius of a set of matrices*, Lin. Alg. Appl., 214 (1995), 17–42. doi: 10.1016/0024-3795(93)00052-2.

[8] St. S. Capizzano, A. Cicone, N. Guglielmi, M. Zennaro, *Finiteness property of pairs of* 2×2 *sign-matrices via real extremal polytope norm*, Linear Algebra Appl., 432 (2010) 01, 796–816, doi: 10.1016/j.laa.2009.09.022.

A framework for optimal convex regularization for the recovery of low-dimensional models

Yann Traonmilin
Univ. Bordeaux, Bordeaux INP, CNRS, IMB, UMR 5251,F-33400 Talence
yann.traonmilin@math.u-bordeaux.fr

We consider the problem of recovering an element x_0 of a low-dimensional model $\Sigma \subset \mathbb{R}^n$ (e.g. Σ_k the set of k-sparse vectors) from under-determined linear measurements $y = Mx_0$ where M is a linear map. To perform recovery, we consider the minimization of a convex regularizer subject to a data-fit constraint

$$x^* = \arg \min_{Mx=y} R(x). \tag{1}$$

This minimization can be proven successful for sparse models and their generalizations (such as low rank models) with the right choice of measurement matrices M (e.g. random Gaussian matrices with enough measurements) [2, 4, 1, 3]. Given a model, we ask ourselves what is the "best" convex regularizer to perform its recovery. A framework to define the optimality of a convex regularizer for the recovery of a given low dimensional model was introduced in [6]. Based on explicit recovery guarantees of elements of Σ, it defines optimal regularizers as functions R^* that maximize a *compliance measure* $A_\Sigma(R)$ that quantifies the recovery capabilities of elements of Σ by using minimization (1) with R:

$$R^* \in \arg\max_{R \in \mathcal{C}} A_\Sigma(R). \tag{2}$$

where $\mathcal{C}$ is a set of convex functions. It was shown that the ℓ^1-norm was an optimal atomic norm for the recovery of sparse models in minimal cases ($k = 3$) for compliance measures based on exact recovery guarantees and an optimal atomic norm in the general case for compliance measures based on best known recovery guarantees using the restricted isometry property [6, 7].

In this work (available as a full paper [5]), we build on these ideas and give elementary properties of the maximization of compliance measures. We show the optimality of the ℓ^1-norm and the nuclear norm for the recovery of sparse and low rank models respectively in the set of coercive continuous *convex* functions for compliances based on the restricted isometry property. Finally, we *construct* near-optimal regularizers for sparsity in levels models within the set of ℓ^1-norms weighed by levels. This result is a first example of explicit construction of optimal regularizers beyond classical sparsity models.

Joint work with: Rémi Gribonval (Univ Lyon, ENS de Lyon, UCBL, CNRS, Inria, LIP, F-69342 Lyon, France), Samuel Vaiter (CNRS, Université Côte d'Azur, LJAD, Nice, France).

References

[1] E. J. Candes and Y. Plan. Matrix completion with noise. *Proceedings of the IEEE*, 98(6):925–936, 2010.

[2] E. J. Candès, J. Romberg, and T. Tao. Robust uncertainty principles: exact signal reconstruction from highly incomplete frequency information. *Information Theory, IEEE Transactions on*, 52(2):489–509, 2006.

[3] S. Foucart and H. Rauhut. *A mathematical introduction to compressive sensing*. Springer, 2013.

[4] B. Recht, M. Fazel, and P. Parrilo. Guaranteed Minimum-Rank Solutions of Linear Matrix Equations via Nuclear Norm Minimization. *SIAM Review*, 52(3):471–501, 2010.

[5] Y. Traonmilin, R. Gribonval, and S. Vaiter. A theory of optimal convex regularization for low-dimensional recovery. HAL preprint https://hal.archives-ouvertes.fr/hal-03467123, 2021.

[6] Y. Traonmilin and S. Vaiter. Optimality of 1-norm regularization among weighted 1-norms for sparse recovery: a case study on how to find optimal regularizations. *Journal of Physics: Conference Series*, 1131:012009, 2018.

[7] Y. Traonmilin, S. Vaiter, and R. Gribonval. Is the 1-norm the best convex sparse regularization? In *iTWIST'18 - international Traveling Workshop on Interactions between low-complexity data models and Sensing Techniques*, 2018.

The local sample complexity of non-linear least squares approximation

Philipp Trunschke
École Centrale de Nantes, Université de Nantes
philipp.trunschke@univ-nantes.fr

We consider the problem of approximating a function in general nonlinear subsets of L^2 when only a weighted Monte Carlo estimate of the L^2-norm can be computed. Standard concentration of measure arguments can be used to provide a worst-case bound for the probability that a certain error is achieved with a prescribed number of sample points. For model classes of tensor networks, however, this bound depends exponentially on the order of the networks and is independent of the regularity of the sought function. This behaviour is not observed in many practical applications but can indeed be demonstrated in numerical experiments. Restricting the model class to a neighborhood of the best approximation, we can derive a new bound that is able to utilize the regularity and thereby reduce the number of samples that are required to reach a prescribed accuracy.

Energy-Preserving Hamiltonian Neural Networks for Stock Price Forecasting

George Tzagkarakis
Institute of Computer Science, Foundation for Research and Technology-Hellas, Greece
and
Research Institute for the Management of Organizations, University of Bordeaux, France
geotzag@gmail.com

The stock market is known for being volatile, dynamic, and nonlinear. Accurate stock price prediction is extremely challenging because of multiple (macro and micro) factors, such as politics, global economic conditions, unexpected events, a company's financial performance, and so on. Despite the volatility, stock prices are not just randomly generated numbers. So, they can be analyzed as a sequence of discrete-time data, or, in other words, as time series observations taken at successive points in time, usually on a daily basis.

In a recent work [1], we were the first to elaborate on the interrelation between the concept of risk, as perceived by the financial experts, and the energy distribution of continuously compounded returns (defined as the logarithm of the ratio of consecutive stock prices). To this end, we borrowed the physical definition of kinetic energy, E_k, of an object, which is defined as the energy that the object possesses due to its motion, and depends on the object's mass, m, and its speed, v. Furthermore, the equation $E_k = q^2/(2m)$ relates the kinetic energy and the momentum, q, of an object, which is a vector quantity with both magnitude and direction, thus it can be used to predict the resulting direction and speed of motion of the object. Then, by relying on the analogue of mass for stock prices that can be thought of as the value of a stock, and the analogue of speed which is related precisely to the price variation per time unit, or, in other words, to the stock returns, we can express the energy and momentum of a stock in financial terms.

In Hamiltonian mechanics, Hamiltonian systems are physical models whose state is characterized by a set of coordinate vectors, $S = (\mathbf{p}, \mathbf{q}) \in \mathbb{R}^{2N}$, where $\mathbf{p} \in \mathbb{R}^N$ represents the position and $\mathbf{q} \in \mathbb{R}^N$ the momentum of the system in time. The behaviour of Hamiltonian systems can be completely described by a single function $H(\mathbf{p}, \mathbf{q})$. Solving the system of Hamilton's equations, $\{\dot{\mathbf{q}} = -\nabla_{\mathbf{p}} H(\mathbf{p}, \mathbf{q}),\ \dot{\mathbf{p}} = \nabla_{\mathbf{q}} H(\mathbf{p}, \mathbf{q})\}$, one can obtain the trajectories $S(t)$ in physical space. The main property of these trajectories is that their total energy represented by the Hamiltonian function $H(S(t))$ is constant over time.

In the framework of Machine Learning, a physics-informed neural network, the Hamiltonian Neural Network (HNN), was proposed in [2]. The HNN is capable of generating a single scalar value corresponding to the energy of the physical system, whilst predicting the state of the system (i.e., position and momentum) in time.

Motivated by the above concepts, in this work we propose a predictive model for stock prices, in the form of an HNN architecture. In particular, assuming an unleveraged investment strategy operating with the initial capital without using any borrowed money, we train an HNN by adding an additional constraint, namely, the total energy preservation of the Hamiltonian function of the physical system, or equivalently, in financial terms, of the overall capital invested on a given stock. The input of the HNN consists of the current stock's position (i.e., its price) and stock's momentum (i.e., its value multiplied by its current return), while the output is the predicted position and momentum in the next time instant (next day in our case). To the best of our knowledge, this is the first time to bridge the fields of Hamiltonian systems and financial stocks forecasting.

Experimental evaluation with real stocks reveals the promising performance of the proposed framework, when compared against well-established approaches, such as ARIMA-based models and benchmark neural network architectures, which are not capable of exploiting the energy preservation constraint.

Joint work with: Frantz Maurer, KEDGE Business School, France.

References

[1] G. Tzagkarakis and F. Maurer. An energy-based measure for long-run horizon risk quantification. *Annals of Operations Research*, 289(2):363–390, 2020.

[2] S. Greydanus *et al.,* Hamiltonian Neural Networks. *Advances in Neural Information Processing Systems*; Ed. by H.Wallach *et al.*, Vol. 32, 2019

Constructive sparsification of finite frames with application in optimal function recovery

Tino Ullrich
Chemnitz University of Technology
tino.ullrich@math.tu-chemnitz.de

We present a new constructive subsampling technique for finite frames to extract (almost) minimal plain (non-weighted) subsystems which preserve a good lower frame bound. The technique is based on a greedy type selection of frame elements to positively influence the spectrum of rank one updates of a matrix. It is a modification of the 2009 algorithm by Batson, Spielman, Srivastava and produces an optimal size subsystem (up to a prescribed oversampling factor) without additional weights. It moreover achieves this in polynomial time and avoids the Weaver subsampling (based on the Kadison-Singer theorem) which has been applied in earlier work, yielding rather bad oversampling constants. In the second part of the talk we give applications for multivariate function recovery. Here we consider the particular problem of L_2 and L_∞ recovery from sample values. In this context, the presented subsampling technique allows to determine optimal (in cardinality) node sets even suitable for plain least squares recovery. It can be applied, for instance, to reconstruct functions in dominating mixed-smoothness Sobolev spaces, where we are able to discretize trigonometric polynomials with frequencies from a hyperbolic cross with nodes coming from an implementable subsampling procedure. In addition we may apply this to subspaces coming from hyperbolic cross wavelet subspaces. Numerical experiments illustrate the theoretical findings.

Joint work with: Felix Bartel (Chemnitz), Martin Schäfer (Chemnitz)

Dynamical low-rank approximation for parabolic problems

André Uschmajew
Max Planck Institute for Mathematics in the Sciences, Leipzig, Germany
uschmajew@mis.mpg.de

Dynamical low-rank approximation is a framework for time integration of matrix valued ODEs on a fixed-rank manifold based on a time dependent variational principle. Several applications arise from PDEs on product domains, but setting up a corresponding well-posed problem in function space (before discretization) may not be straightforward. Here we present a weak formulation of dynamical low-rank approximation for parabolic PDEs in two spatial dimensions. The existence and uniqueness of weak solutions is shown using a variational time-stepping scheme on the low-rank manifold which is related to practical methods for low-rank integration.

Joint work with: Markus Bachmayr, Henrik Eisenmann, and Emil Kieri.

References

[1] M. Bachmayr, H. Eisenmann, E. Kieri, and A. Uschmajew. Existence of dynamical low-rank approximations to parabolic problems. *Mathematics of Computation*, 90(330):1799–1830, 2021.

Visual Haptic Feedback for Training of Robotic Suturing

Brice Valentin
InSimo
brice.valentin@insimo.fr

Current surgical robotic systems are teleoperated and do not have force feedback. Considerable practice is required to learn how to use visual input such as tissue deformation upon contact as a substitute for tactile sense. Thus, unnecessarily high forces are observed in novices, prior to specific robotic training, and visual force feedback studies demonstrated reduction of applied forces. Simulation exercises with realistic suturing tasks can provide training outside the operating room. This paper presents contributions to realistic interactive suture simulation for training of suturing and knot-tying tasks commonly used in robotically-assisted surgery. To improve the realism of the simulation, we developed a global coordinate wire model with a new constraint development for the elongation. We demonstrated that a continuous modeling of the contacts avoids instabilities during knot tightening. Visual cues are additionally provided, based on the computation of mechanical forces or constraints, to support learning how to dose the forces. The results are integrated into a powerful system-agnostic simulator, and the comparison with equivalent tasks performed with the da Vinci Xi system confirms its realism.

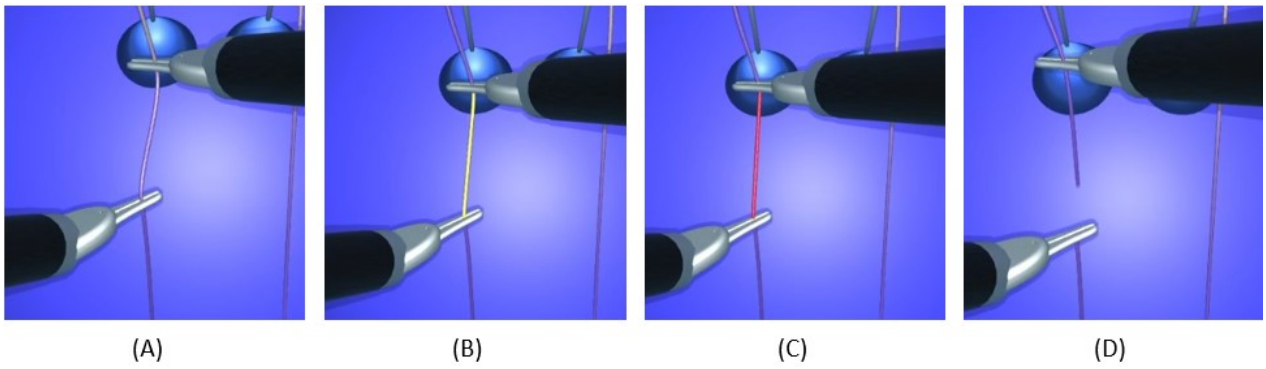

Figure 1: Visual stress on a thread from floppy (A) to tight (B, C) condition until suture breakage with tension release (D).

Joint work with: François Jourdes, Jérémie Allard, Christian Duriez and Barbara Seeliger.

References

[1] Tool-tissue forces in surgery: A systematic review *Golahmadi, Aida Kafai and Khan, Danyal Zaman and Mylonas, George P and Marcus, Hani J*,https://doi.org/10.1016/j.amsu.2021.102268

[2] Effects of visual force feedback on robot-assisted surgical task performance *Reiley, Carol E and Akinbiyi, Takintope and Burschka, Darius and Chang, David C and Okamura, Allison M and Yuh, David D*, 10.1016/j.jtcvs.2007.08.043

[3] Proposal and evaluation of visual haptics for manipulation of remote machine system *Haruna, Masaki and Ogino, Masaki and Koike-Akino, Toshiaki*, https://doi.org/10.3389/frobt.2020.529040

[4] Suturing simulation based on complementarity constraints *Guébert, Christophe and Duriez, Christian and Cotin, Stephane and Allard, Jérémie and Grisoni, Laurent* Symposium on Computer Animation, 2009

[5] SOFA: A Multi-Model Framework for Interactive Physical Simulation *Faure, François and Duriez, Christian and Delingette, Hervé and Allard, Jérémie and Gilles, Benjamin and Marchesseau, Stéphanie and Talbot, Hugo and Courtecuisse, Hadrien and Bousquet, Guillaume and Peterlik, Igor and Cotin, Stéphane* , https://hal.inria.fr/hal-00681539

Revisiting Riemannian optimization for the symmetric eigenvalue problem.

Bart Vandereycken
Department of Mathematics, University of Geneva
bart.vandereycken@unige.ch

Computing dominant eigenpairs of a symmetric matrix is one of the most prototypical problems for Riemannian optimization. In particular, it naturally leads to the maximization of a smooth objective function on the Stiefel manifold (of orthonormal matrices) or the Grassmann manifold (of subspaces). Several well-known algorithms in numerical linear algebra for the symmetric eigenvalue problem can be elegantly analyzed by exploiting this Riemannian point of view.

In this talk, we revisit this program and show how recent advances in non-convex optimization, like weak quasi convexity, can be generalized to the Grassmann manifold and the symmetric problem matrix. In particular, in contrast to existing results on local convexity, we are able to show that Riemannian steepest descent linearly converges to the dominant subspace if it is started from any initial point (excluding a measure zero set).

While steepest descent is not a competitive algorithm compared to Krylov methods or even subspace iteration, it has the benefit that it is very robust to perturbations in the matrix and that it can be accelerated with a momentum term. We will illustrate this empirically and compare to existing methods.

Joint work with: Foivos Alimisis (Geneva) and Yousef Saad (Minnesota).

Geometric Hermite interpolation in R^n

Hofit Ben Zion Vardi
Tel Aviv University
hofitbenzion@mail.tau.ac.il

The geometric Hermite data consists of point samples and their associated tangent vectors of unit length. Thus, the geometric Hermite interpolation problem is to interpolate such data. Extending the classical Hermite interpolation of functions, this geometric Hermite problem has become popular in recent years and has ignited a series of solutions in the 2D plane and 3D space such as in [1, 2, 4, 5, 6]. We propose a general approach for constructing a broad class of operators approximating high-dimensional curves, which are based on geometric Hermite data. In particular, we present a method for approximating curves that is valid in any dimension.

As the basic building block, we pose the notion of Hermite average. In my talk, I will present a formal definition of the latter, while addressing some of the fundamental challenges accompanying such an attempt. I will introduce the Bézier average which is an example of a Hermite average, and demonstrate how we use it to modify subdivision schemes which are based on repeated averages. The special case of interpolating Hermite data by repeatedly refining it with Hermite averages, is proved to converge. Furthermore, its limit inherits geometric properties of the average, such as circle preserving. We will address the latter and discuss the key arguments in the proof.

We will also consider some properties of approximation. While subdivision schemes commonly achieve their full approximation power under restricted assumptions about the sampling method as investigated in [3], our result is an interpolatory approximation which is robust to sampling, that is, it does not depend on a particular sampling policy. In fact, it is implied numerically that refining data by Bézier average yields a fourth order approximation. This, as well as other numerical examples, elucidate the advantages of our approach. Finally, we observe that such an approach naturally extends to a more general setting of approximating manifold valued curves by a suitable adjustment of the Hermite average.

The figure below presents the process of refining two given Hermite samples by inserting their Bézier average.

Joint work with: Nira Dyn, Nir Sharon.

References

[1] Pavel Chalmoviansk̀y and Bert Jüttler. A non-linear circle-preserving subdivision scheme. *Advances in Computational Mathematics*, 27(4):375–400, 2007.

[2] Costanza Conti, Lucia Romani, and Michael Unser. Ellipse-preserving Hermite interpolation and subdivision. *Journal of Mathematical Analysis and Applications*, 426(1):211–227, 2015.

[3] Michael S Floater and Tatiana Surazhsky. Parameterization for curve interpolation. In *Studies in Computational Mathematics*, volume 12, pages 39–54. Elsevier, 2006.

[4] Evgeny Lipovetsky. Subdivision of point-normal pairs with application to smoothing feasible robot path. *The Visual Computer*, pages 1–14, 2021.

[5] Evgeny Lipovetsky and Nira Dyn. A weighted binary average of point-normal pairs with application to subdivision schemes. *Computer Aided Geometric Design*, 48:36–48, 2016.

[6] Ulrich Reif and Andreas Weinmann. Clothoid fitting and geometric Hermite subdivision. *Advances in Computational Mathematics*, 47(4):1–22, 2021.

Learning Scale Invariant Signatures for Planar Curves

Roy Velich
Technion - Israel Institute of Tecnology
royve@campus.technion.ac.il

An important theorem by É. Cartan [2, p. 183, Thrm. 8.53] states that two curves are related by a group of transformation iff their signature curves w.r.t. the transformation group are identical. Signature curves are defined by differential invariants, such signatures of planar curves involve the evaluation of invariant differential measures. In practice, planar curves are digitally represented as a discrete set of points, which implies that the computation of differential invariant quantities, such as the group-curvature at a point, can only be numerically approximated using finite differences techniques. Since differential invariants often involve high-order derivatives, their approximations are prone to numerical instabilities due to sensitivity to sampling noise.

Here, we focus on the similarity group of transformations. Also known as *uniform scaling*, similarity transforms introduce numerical challenges for constructing reparametrization-invariant analysis procedures. E.g., similarity-invariant heat flow of planar curves, traditionally used to produce multi-scale representations, is an unstable operation in the uniform scaling case [1]. Motivated by the above challenges, we propose a novel deep-learning approach, to produce numerically-stable and reparametrization-invariant approximation models for the differential invariants of planar curves w.r.t. the similarity group. We qualitatively evaluate our results by plotting matching invariant signatures for equivalent curves w.r.t. the similarity group.

The following figure presents an example of similarity-invariant signature-curves estimated by our learning models. **Left**: Two equivalent curves w.r.t. the similarity group, both sampled non-uniformly. The black points define corresponding reference points. Curve traversal is done in clock-wise fashion. **Top-Right**: Our learned group-curvature at each point as a function of the point indices. The two plots do not align since the two curves were sampled differently. **Bottom-Right**: Our learned group-curvature at each point as a function of our learned group arc-length. When learning the group arc length, these new signature graphs do align.

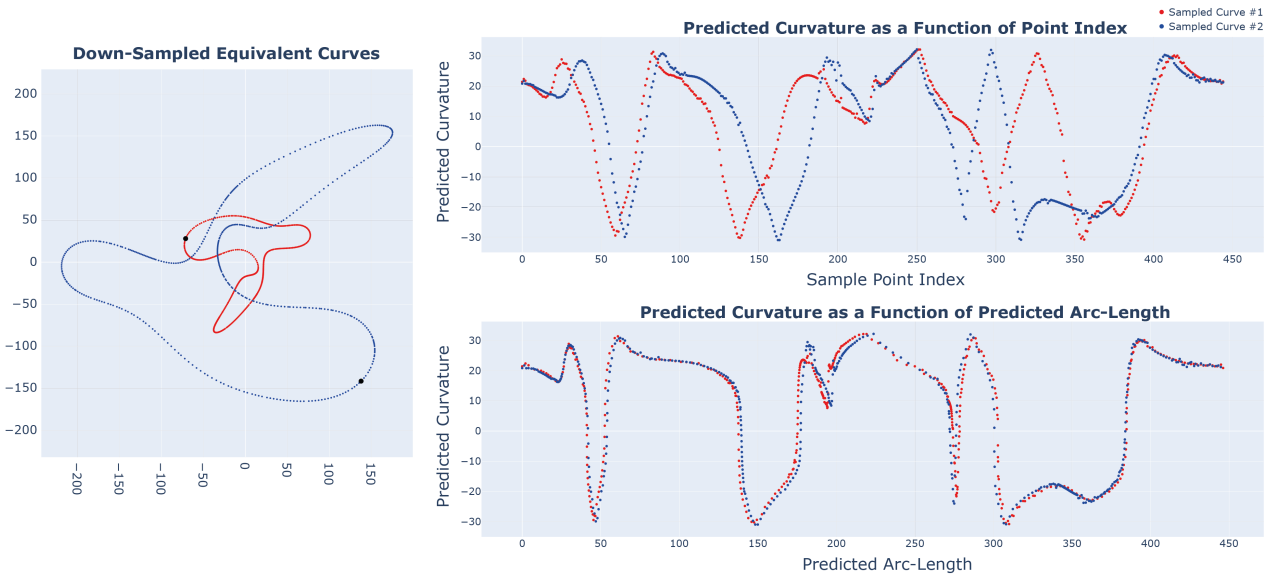

Joint work with: Ron Kimmel, Technion.

References

[1] Alfred Bruckstein and Doron Shaked. *On Projective Invariant Smoothing and Evolutions of Planar Curves and Polygons*. Vol. 7. June 1997, pp. 225–240. DOI: 10.1023/A:1008226427785.

[2] Peter J. Olver. *Classical Invariant Theory*. London Mathematical Society Student Texts. Cambridge University Press, 1999. DOI: 10.1017/CBO9780511623660.

Pythagorean-hodograph projections of spatial polynomial curves

Jan Vršek
Department of Mathematics & NTIS – New Technologies for the Information Society,
Faculty of Applied Sciences, University of West Bohemia,
Univerzitní 8, 301 00 Plzeň, Czech Republic
vrsekjan@kma.zcu.cz

Our goal is to study whether spatial polynomial curve can be projected to a planar PH curve. This problem is motivated by [1], where the PH curves possessing projection to PH curve were constructed. By considering the set of all tangent directions to a given spatial curve C as the subset of projective plane $\mathbb{P}^2$ we obtain a planar curve T_C whose points correspond to the tangent directions to the original spatial curve. Since PH property is intimately related to the tangent behaviour of the curve it is not surprising that the it is encoded in the geometry of T_C. Indeed, with some additional assumptions, we show that C is PH curve if and only if T_C intersects the so called absolute conic in smooth points with even multiplicity. Similar geometric characterization can be formulated for planar curves as well. This approach enables to study the problem with the tools of projective geometry of planar curves. For example it can be easily seen that generic spatial cubic possesses exactly two orthogonal projections on PH curve, whereas curves of higher degrees cannot be projected in general. This motivates us to study obligue projections as well. Thus we will close by showing how spatial quintics can be projected in order to obtain PH curves.

Joint work with: Miroslav Lávička.

References

[1] Rida T. Farouki and Marjeta Knez and Vito Vitrih and Emil Žagar. Planar projections of spatial Pythagorean-hodograph curves. Computer Aided Geometric Design, 91: 102049, 2021.

Designing asymptotic geodesic hybrid gridshells

Hui Wang
King Abdullah University of Science and Technology
hui.wang.1@kaust.edu.sa

Certain types of freeform shells can be fabricated by bending originally flat and straight slats into curved structural elements. In their final position, one obtains a grid of surface strips forming the basis of an architectural structure. We present recent work on structures which are formed by three or four families of strips, arranged in a web.

In their final curved position, the strips can be modeled as rectifying developable surfaces of their boundaries: Each tangent plane of a strip is orthogonal to the osculating plane at the corresponding boundary curve point. Thus, if a strip is placed orthogonal to an underlying reference surface S, it has to follow an asymptotic curve of S. If it is arranged tangentially to S, if follows a geodesic curve on S. Hence, these gridshells are designed from hybrid webs of *asymptotic* (A) and *geodesic* (G) curves on freeform surfaces.

Previous work focused mainly on a quadrilateral grid arrangement. If both families of strips are placed orthogonal to S, one obtains the asymptotic gridshells (AA) of Eike Schling [1]. Under the additional constraint of orthogonal node angles, the underlying surface is a minimal surface. The case (GG) of two tangential families of strips has recently been studied from the perpective of deployment from an arrangement of planar straight strips [2].

We present a computational workflow for the design of various types of hybrid asymptotic geodesic webs, using methods of discrete differential geometry, numerical optimization and a spline representation for the final strips. The following types are presented:

- *AGG* web: geodesic net (G-net) with one family of diagonal asymptotic curves (Fig.1-(a)).
- *AAG* web: asymptotic net (A-net) with one family of diagonal geodesic curves (Fig.1-(b)).
- *AAGG* web: A-net and G-net are diagonal to each other (Fig.1-(c)).

Physical models are made to verify the computational process and simulate the kinetic behavior during the erection process.

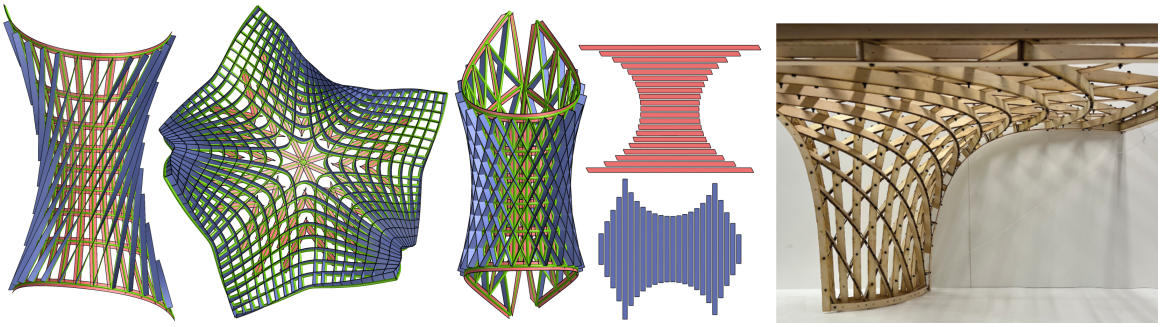

(a) AGG web (b) AAG web (c) AAGG web and unrolled strips (d) AAG timber model

Figure 1: Various types of hybrid asymptotic geodesic gridshells. Geodesic strips (red) are tangent to the underlying surface and asymptotic strips (blue) orthogonal to the surface. (c) one family of asymptotic and geodesic strips are also shown in their flat position. (d) A timber prototype of an AAG gridshell.

Joint work with: Helmut Pottmann, Eike Schling, Sebastian Hoyer.

References

[1] E. Schling, M. Kilian, H. Wang, D. Schikore, and H. Pottmann. Design and construction of curved support structures with repetitive parameters. *Advances in Architectural Geometry (AAG)*,140-165, 2018.

[2] S. Pillwein, and P. Musialski. Generalized deployable elastic geodesic grids. *ACM Transactions on Graphics (TOG)*, 40 (6), 2021.

Phase retrieval of entire functions

Matthias Wellershoff
Seminar for Applied Mathematics, ETH Zurich
matthias.wellershoff@math.ethz.ch

In this talk, we will discuss what information about an entire function may be recovered from measurements of its magnitude on different subsets of the complex plane. This *phase retrieval problem for entire functions* plays a decisive role in many contemporary works on the recovery of signals from magnitude-only measurements [1, 2, 4, 5]. We will present the theory for the phase retrieval of entire functions starting with some basic observations. We will then discuss Mc Donald's characterisation of entire functions whose magnitudes agree on a single line in the complex plane [6] and, finally, propose some extensions to situations in which magnitude information on two or more lines is available [7].

Our presentation will be based on well-known complex-analytic techniques: the Hadamard factorisation theorem, in particular, plays an important role in the characterisation of entire functions whose magnitudes agree on certain lines in the complex plane. The main new results which we will discuss are

1. a full characterisation of all (finite order) entire functions whose magnitudes agree on two arbitrary lines in the complex plane — this extends work by Jaming [4] — and
2. a full characterisation of all entire functions of exponential-type whose magnitudes agree on infinitely many equidistant parallel lines.

These new results have interesting applications to Gabor phase retrieval. Among other things, they allow for a full characterisation of all L^2-functions whose Gabor transform magnitudes agree on two arbitrary lines in the time-frequency plane. We also emphasise that our theory can be used to generate functions in L^2 which do not agree up to global phase but whose magnitudes agree on infinitely many equidistant parallel lines. We have recently used this insight to find counterexamples for sampled Gabor phase retrieval [1], i.e. functions in L^2 which do not agree up to global phase but whose Gabor transform magnitudes agree on fairly general lattices (this work has just been generalised in [3]).

Finally, a good understanding of the theory of functions allows for the construction of many more interesting examples. Personal favourites of ours are the "universal counterexamples" for sampled Gabor phase retrieval: those are functions $f \in L^2(\mathbb{R})$ and $(g_n)_{n\geq 1} \in L^2(\mathbb{R})$ such that for all $n \geq 1$, it holds that f and g_n do not agree up to global phase while their Gabor transform magnitudes agree on the semidiscrete set $\mathbb{R} \times \frac{1}{n}\mathbb{Z}$ [7].

Joint work with: Prof. Rima Alaifari, Seminar for Applied Mathematics, ETH Zurich

References

[1] Rima Alaifari and Matthias Wellershoff. Phase retrieval from sampled Gabor transform magnitudes: counterexamples. *Journal of Fourier Analysis and Applications*, 28(9):1–8, December 2021.

[2] Karlheinz Gröchenig. Phase retrieval in shift-invariant spaces with Gaussian generator. *Journal of Fourier Analysis and Applications*, 26(52):1–15, June 2020.

[3] Philipp Grohs and Lukas Liehr. On foundational discretisation barriers in STFT phase retrieval. arXiv:2111.02227 [math.FA], November 2021.

[4] Philippe Jaming. Uniqueness results in an extension of Pauli's phase retrieval problem. *Applied and Computational Harmonic Analysis*, 37(3):413–441, November 2014.

[5] Stéphane Mallat and Irène Waldspurger. Phase retrieval for the Cauchy wavelet transform. *Journal of Fourier Analysis and Applications*, 21:1251–1309, April 2015.

[6] John N. Mc Donald. Phase retrieval and magnitude retrieval of entire functions. *Journal of Fourier Analysis and Applications*, 10:259–267, January 2014.

[7] Matthias Wellershoff. Phase retrieval of entire functions and its implications for Gabor phase retrieval. arXiv:2202.03733 [math.CV], February 2022.

Adaptive meshfree solving of linear PDEs: Analysis of target-data dependent greedy kernel methods

Tizian Wenzel
Institute for Applied Analysis and Numerical Simulation,
University of Stuttgart, Germany
tizian.wenzel@mathematik.uni-stuttgart.de

We consider meshless solving of PDEs

$$Lu = f \quad \text{on } \Omega, \quad u = g \quad \text{on } \partial\Omega \tag{1}$$

via symmetric kernel collocation by using greedy kernel methods. In this way we avoid the need for a mesh generation, which can be challenging for non-standard domains Ω or manifolds. We introduce and discuss different kind of greedy selection criteria, such as the PDE-P-greedy and the PDE-f-greedy.
Subsequently we analyze the convergence rates of these algorithms and provide bounds on the approximation error in terms of the number of greedily selected points. Especially we prove that target-data dependent algorithms exhibit faster convergence rates.
The provided analysis is applicable to PDEs both on domains and manifolds. This and the advantages of target-data dependent algorithms is highlighted by numerical examples.

Joint work with: Daniel Winkle, Gabriele Santin, Bernard Haasdonk.

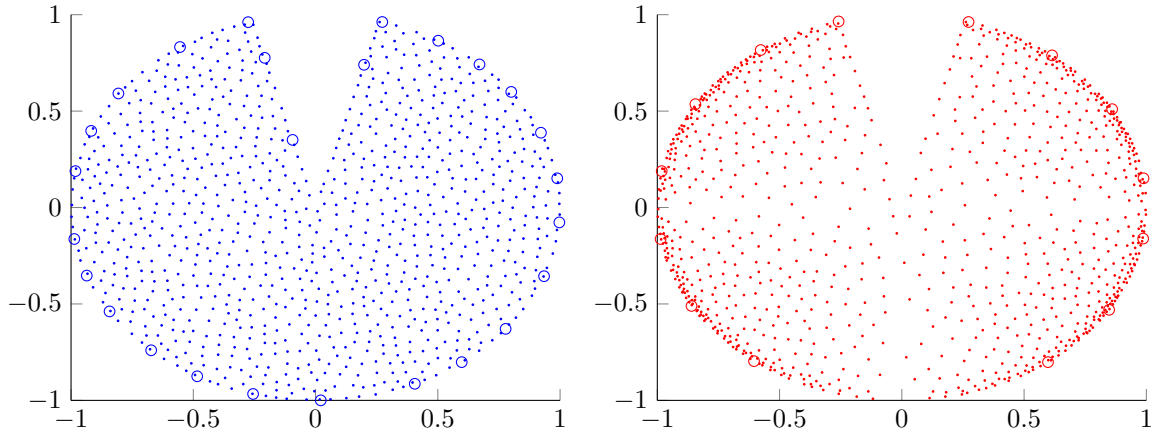

Figure 1: Visualization of the selected points for PDE-P-greedy (left) and PDE-f-greedy (right) for a Laplace equation with Dirichlet boundary conditions on a domain which is given by a circle without a cone. The circled points correspond to points on the boundary $\partial\Omega$. The PDE-f-greedy points (right) are better adapted to the given PDE and the domain and therefore give a better approximation of the solution.

References

[1] Tizian Wenzel, Daniel Winkle, Gabriele Santin, Bernard Haasdonk Adaptive meshfree solving of linear PDEs: Analysis of target-data dependent greedy kernel methods. *In preparation*, 2022.

[2] Tizian Wenzel, Gabriele Santin, Bernard Haasdonk Analysis of target data-dependent greedy kernel algorithms: Convergence rates for f-, $f \cdot P$- and f/P-greedy. *ArXiv*, (2105.07411), 2021. Submitted.

Analysis of Regularized Learning in Banach Spaces

Qi Ye
South China Normal University
yeqi@m.scnu.edu.cn

In this talk, we show a new way to study the theory of regularized learning for generalized data in Banach spaces including representer theorems and convergence theorems. The generalized data are composed of linear functionals and real scalars as the input and output elements to represent the discrete information of black-box and white-box local models. By the extension of the classical machine learning, the empirical risks are computed by the generalized data and the loss functions. According to the techniques of regularization, the exact solutions are approximated globally by minimizing the regularized empirical risks over the Banach spaces. The existence and convergence of the approximate solutions are guaranteed by the relative compactness of the generalized input data in the predual spaces of the Banach spaces. The work of the regularized learning provides another road to investigate the algorithms of machine learning including the interpretability in approximation theory, the nonconvexity and nonsmoothness in optimization theory, and the generalization and overfitting in probability theory. Based on the theorems of the regularized learning, we will construct the hybrid algorithms combining support vector machines, artificial neural networks, and decision trees for our current research projects of the big data analytics in education and medicine.

References

[1] Q. Ye. Analysis of Regularized Learning in Banach Spaces. *arXiv:2109.03159*, pages 1-32, 2021.

A shape preserving C^2 non-linear, non-uniform, subdivision scheme with fourth-order accuracy

Jungho Yoon
Department of Mathematics, Ewha Womans University, Seoul, 120-750, S. Korea
yoon@ewha.ac.kr

The objective of this study is to present a shape-preserving non-linear subdivision scheme generalizing the exponential B-spline of degree 3, which is a piecewise exponential polynomial with the same support as the cubic B-spline. The subdivision of the exponential B-spline has a crucial limitation in that it can reproduce at most two exponential polynomials, yielding the approximation order *two*. Also, finding a best-fitting shape parameter in the exponential B-spline is a challenging and important problem. In this regard, we present a method for selecting an optimal shape parameter and then formulate it in the construction of new refinement rules. As a result, the new scheme provides an improved approximation order *four* while maintaining the same C^2 smoothness as the (exponential) B-spline of degree 3. Moreover, we show that the proposed method preserves geometrically important characteristics such as monotonicity and convexity, under some suitable conditions. Some numerical examples are provided to demonstrate the ability of the new subdivision scheme.

Joint work with: Hyoseon Yang.

G^1 Hermite interpolation method for spatial PH curves over planar PH curves

Yoonae Song
Department of Mathematics, Dongguk University-Seoul, Korea
syoonae@dongguk.edu

A special type of spatial Pythagorean hodograph (PH) curves, whose planar projection also has the PH property, were introduced recently in [1]. In this work, we present a G^1 Hermite interpolation method for this type of curves. While the projection plane is fixed as the xy plane, these curves can be regarded as spatial PH curves over planar PH curves, which we call PH over PH (PHoPH) curves. Because of the additional constraint, PHoPH curves should have more complicated algebraic structure than usual spatial PH curves. We investigate this structure using the quaternion algebra to obtain a compact representation of PHoPH from quaternion generator polynomials. Based on this representation, we address the G^1 Hermite interpolation problem using quintic PHoPH curves. The problem is formulated as a system of nonlinear equations involving trigonometric functions, which can be solved by numerical methods. We analyze the feasibility of this problem and present some computed examples.

Joint work with: Soo Hyun Kim, Hwan Pyo Moon.

References

[1] Farouki, Rida T and Knez, Marjeta and Vitrih, Vito and Žagar, Emil. Planar projections of spatial Pythagorean-hodograph curves. *Computer Aided Geometric Design*, 91:102049, 2021.

Symmetry and Saddle Points in the Numerical Solutions of Geometric Variational Problems

Thomas Yu
Drexel University
yut@drexel.edu

In this talk, we report a number of curious cases in the numerical solutions of specific geometric variational problems [1, 2] in which (i) the solution surface of the continuous problem is invariant under a symmetry group G, (ii) that the space of finite-dimensional space of discrete solutions accomodates surfaces invariant under a finite subgroup H of G, (iii) but yet the optimal discrete solution does not possess the H-symmetry one would expect.

At the same time, many numerical optimization algorithms – gradient descent, accelerated gradient descent, BFGS etc. for unconstrained problems, and their variants for constraint problems – are invariant under orthogonal change of coordinates. In the aforementioned situations, or in situations when we solve a geometric optimization with an initial guess with the *wrong symmetry*, this innocent invariance in the optimization algorithm means that the numerical optimization method can get stuck at a suboptimal saddle point. In the latter case, the saddle point is likely far from being optimal or desirable. But in the former case, the symmetric but suboptimal saddle point, by an approximation result to be presented, can actually approximate the continuous solution better than the discrete minimizer.

Joint work with: Tom Duchamp and Isaiah Siegl, and my co-authors in the two articles below.

References

[1] J. Chen, T. Yu, P. Brogan, R. Kusner, Y. Yang and A. Zigerelli. Numerical Methods for Biomembranes: Conforming subdivision versus Non-conforming PL methods. *AMS Mathematics of Computation*, 90(328):471–516, 2021.

[2] P. Mohan, N.K. Yip and T. Yu. Minimal Energy Configurations of Bilayer Plates as a Polynomial Optimization Problem. *Submitted to Nonlinear Analysis, special issue on 'Variational Models for Discrete Systems'*, 2021.

Bear subdivision schemes for modeling smooth surfaces

Tatyana Zaitseva
Lomonosov Moscow State University
zaitsevatanja@gmail.com

We suggest a new class of stationary subdivision schemes based on matrix dilation for modeling smooth surfaces. In each iteration our scheme doubles the number of nodes, their new coordinates are weighted averages of old coordinates along one direction. This direction changes every iteration and never repeats. We propose a method for calculating the Holder regularity of limit surfaces based on the work [1] and program [2]. The results of these calculations are surprising and show that the regularity of such schemes in some cases exceeds the regularity of classical schemes of the same order.

Recall that one-dimensional schemes are defined by a finite set of the coefficients $\{c_k\}_{k\in\mathbb{Z}}$. A corresponding subdivision operator S maps a sequence $u \in \ell_\infty(\mathbb{Z})$ to the sequence $Su \in \ell_\infty(\mathbb{Z})$: $Su(k) = \sum_{j\in\mathbb{Z}} c_{k-2j} \cdot u(j)$. Let $f_0(\cdot) = u(\cdot)$ be an initial function ($\mathbb{Z} \to \mathbb{R}$) (control polygon). Then the next sequence f_1 is defined on $\mathbb{Z}/2$ as $f_1(\frac{1}{2}k) = Su(k)$. Repeating this process we get sequences f_i defined on $\mathbb{Z}/2^n$ which in case of the convergence tend to a limit curve (pointwise).

In the case of matrix dilation, the subdivision operator $S : \ell(\mathbb{Z}^2) \to \ell(\mathbb{Z}^2)$ is generalized as (see, for example, [3]) $Su\,(k) = \sum_{j\in\mathbb{Z}^2} c_{k-Mj} \cdot u\,(j)$, where M is an expanding matrix (i.e. all its eigenvalues $|\lambda_i| > 1$).

Our schemes exploit a Bear matrix $M_B = \begin{pmatrix} 1 & -2 \\ 1 & 0 \end{pmatrix}$. It is expanding with the property $m := |\det M| = 2$. It is known that there are three different (up to affine similarity) expanding integer matrices with $m := |\det M| = 2$, the Bear matrix is one of them.

The coefficients of our schemes are defined as follows

$$c(k_1, 0) = \frac{1}{2^{K-1}} \binom{K}{k_1}$$

for $k_1 = 0, 1, \ldots, K$, where K is a parameter. The scheme with $K = 4$ is illustrated on fig 1. All these schemes have a low complexity because of a small number of coefficients (all coefficients are from one line). Using the method based on the notion of joint spectral radius of transition matrices, we calculate the regularity of their limit surfaces for $K \le 5$. The most interesting result is that the scheme with $K = 3$ produces C^2 surfaces, the scheme with $K = 4$ produces C^3 surfaces, and the scheme with $K = 5$ produces C^4 surfaces which is better than for corresponding classical schemes with the same degree of th mask.

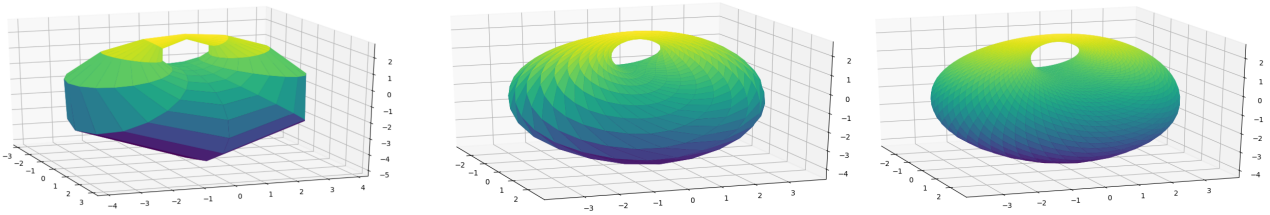

Figure 1: A Dupin cyclide generated by our scheme with $K = 4$: iterations 0, 2 and 4.

References

[1] M. Charina, V.Yu. Protasov. Regularity of anisotropic refinable functions. *Appl. Comput. Harmon. Anal.*, 47(3): 95–821, 2019.

[2] T. Mejstrik Algorithm 1011: Improved Invariant Polytope Algorithm and Applications *ACM Transactions on Mathematical Software (TOMS)*, 46(3): 1–26, 2020.

[3] A.S. Cavaretta, W. Dahmen, Ch.A. Micchelli. Stationary subdivision. *American Mathematical Soc.*, Vol. 453., 1991.

Analyticity and sparsity in uncertainty quantification for PDEs with Gaussian random field inputs

Jakob Zech
Universität Heidelberg
jakob.zech@uni-heidelberg.de

We establish summability results for coefficient sequences of Wiener-Hermite polynomial chaos expansions for countably-parametric solutions of linear elliptic and parabolic divergence-form partial differential equations with Gaussian random field inputs. The proof is based on analytic continuation of parametric solutions into the complex domain. This holomorphy-based argument yields a "differentiation-free" sparsity analysis in various scales of function spaces. It also applies to certain posterior densities in Bayesian inverse problems subject to Gaussian priors on uncertain inputs from function spaces. This allows us to prove dimension-independent convergence rates of various constructive high-dimensional deterministic numerical approximation schemes such as single-level and multi-level versions of anisotropic sparse-grid Hermite-Smolyak interpolation and quadrature in both forward and inverse computational uncertainty quantification. Finally we discuss some implications for neural network approximation.

Joint work with: Dinh Dũng, Van Kien Nguyen, Christoph Schwab

References

[1] Dinh Dũng, Van Kien Nguyen, Christoph Schwab and Jakob Zech. Analyticity and sparsity in uncertainty quantification for PDEs with Gaussian random field inputs. arXiv:2201.01912, 2022.

[2] Deep Learning in High Dimension: Neural Network Approximation of Analytic Functions in $L^2(\mathbb{R}^d, \gamma_d)$. Christoph Schwab and Jakob Zech. arXiv:2111.07080, 2021.

Convergence analysis of Hermite subdivision schemes of any arity

Zeze Zhang
University of Alberta, Northwestern Polytechnical University
zeze@ualberta.ca

Hermite subdivision schemes are particular vector subdivision schemes which produce function vectors consisting of consecutive derivatives of a certain function. The convergence and smoothness of Hermite subdivision schemes have been widely studied, while they are restricted in binary case. To fill this theoretical gap in the literature, we study the convergence of Hermite subdivision schemes covering every arity, which can be seen as a generalization of [7]. The convergence analysis is based on the connections among Hermite subdivision schemes, vector subdivision schemes and refinable function vectors. We provide a tool used to estimate the smoothness of Hermite subdivision schemes of every arity by exploiting a quantity defined by sum rules and can construct Hermite subdivision schemes of arbitrarily high smoothness from a convergent vector scheme of any arity.

Joint work with: Hongchan Zheng(Northwestern Polytechnical University), Jie Zhou(Xian Polytechnic University).

References

[1] B. Han. Vector cascade algorithms and refinable function vectors in sobolev spaces. *Journal of Approximation Theory*, 124(1): 44–88, 2003.

[2] S. Dubuc and J.-L. Merrien. Hermite subdivision schemes and taylor polynomials. *Constructive Approximation*, 29(2): 219–245, 2009.

[3] C. Conti, J.-L. Merrien, and L. Romani. Dual hermite subdivision schemes of de rham-type. *BIT Numerical Mathematics*, 54(4): 955–977, 2014.

[4] C. Conti, L. Romani, and M. Unser. Ellipse-preserving hermite interpolation and subdivision. *Journal of Mathematical Analysis and Applications*, 426(1): 211–227, 2015.

[5] J.-L. Merrien and T. Sauer. Generalized taylor operators and polynomial chains for Hermite subdivision schemes. *Numerische Mathematik*, 142(1): 167–203, 2019.

[6] M. Cotronei, C. Moosmüller, T. Sauer, and N. Sissouno. Level-dependent interpolatory hermite subdivision schemes and wavelets. *Constructive Approximation*, 50(2): 341–366, 2019.

[7] B. Han. Analysis and convergence of Hermite subdivision schemes. *Foundations of Computational Mathematics*, 1–54, 2021.

[8] C. Moosmüller and T. Sauer. Factorization of hermite subdivision operators from polynomial overreproduction. *Journal of Approximation Theory*, 271: 105645, 2021.

Short canonical decompositions of non-orientable surfaces

Arnaud de Mesmay
Univ Gustave Eiffel, CNRS, LIGM, F-77454 Marne - la- Vallée, France
arnaud.de-mesmay@univ-eiffel.fr

Suppose that S is a surface and $G \subset S$ is an embedded graph. In many applications, in algorithm design, geometry processing, or even just to represent the embedding, there is a basic task: to cut S into a single disk. When S is orientable, it has long been known how to compute a canonical cutting system that is also "short": each arc of the system runs along each edge of G at most a constant number of times.

In this talk we survey what is known about such cutting problems. We then explain how to obtain a short canonical system when S is non-orientable.

Joint work with: Niloufar Fuladi and Alfredo Hubard.

References

[1] N. Fuladi, A. Hubard and A. de Mesmay. Short topological decompositions of non-orientable surfaces. *38th International Symposium on Computational Geometry (SoCG 2022)*, to appear.

Super-resolution of generalized spikes and spectra of confluent Vandermonde matrices

Nuha Diab
Department of Applied Mathematics, Tel-Aviv University, Tel-Aviv, Israel.
nuhadiab@tauex.tau.ac.il

The problem of computional super-resolution (SR) is to recover the fine details of an unknown object from inaccurate measurements of inherently low resolution (see [1]). In recent years, there is much intrest in the problem of reconstructing a signal modeled by a linear combination of Dirac $\delta-$distributions with higher-order derivatives:

$$\mu(x) = \sum_{j=1}^{s} \sum_{l=0}^{n-1} a_{j,l} \delta^{(l)}(x - \xi_j), \ \xi_j \in [-\pi, \pi) \tag{1}$$

from noisy Fourier measurements:

$$y_k := \hat{\mu}(k) + \eta_k, \quad k = 0, 1, ..., M, \ |\eta_k| \leq \varepsilon, \tag{2}$$

where $\delta^{(l)}$ is the l-th distributional derivative of the Dirac measure. The stability of this generalized problem is of importance in several applications including modern sampling theory beyond the Nyquist rate, algebraic signal recovery, and multi-exponential analysis, to name a few (see [4] and references therein).

For $n = 1$, the measurment vector $\boldsymbol{y} = \{y_k\}_{k=0}^{M} \in \mathbf{C}^{M+1}$ can be expressed as $\boldsymbol{y} = V\boldsymbol{a} + \boldsymbol{\eta}$, where V is the $(M + 1) \times s$ Vandermonde matrix with the nodes on the unit circle:

$$V := [e^{ik\xi_j}]_{k=0,...,M}^{j=1,...,s}.$$

In order to describe the stability of this inverse problem, suppose that the nodes ξ_j belong to a grid of step size Δ, and define the super-resolution factor (SRF) as $\frac{1}{(M\Delta)}$. Suppose that at most $\ell \leq s$ nodes form a "cluster" of size $O(\Delta)$. In the "super-resolution regime" $SRF \gg 1$ [3, 2] showed that $\sigma_{min}(V)$ scales like $SRF^{\ell-1}$ and consequently the worst-case reconstruction error rate of μ as in (1) from noisy measurements (2) is of the order $SRF^{2\ell-1}\varepsilon$ and it is minimax, meaning that on one hand, it is attained by a certain algorithm for all signals of interest, and on the other hand, there exist worst case examples for which no algorithm can achieve an essentially smaller error.

In this work we extend the above methods and results to $n = 2$. In particular, the Vandermonde matrix V is replaced by the confluent Vandermonde matrix U, which is defined as:

$$U := [e^{ik\xi_j} \ ke^{i(k-1)\xi_j}]_{k=0,...,M}^{j=1,...,s}.$$

Under the partial clustering assumptions, we prove a sharp lower bound for the smallest singular value of U in the super-resolution regime, and show that it scales like $SRF^{2\ell-1}$. We also obtain sharp minimax bounds of order $SRF^{4\ell-1}\varepsilon$ for the problem of sparse superresolution on a grid.

Joint work with: Dmitry Batenkov.

References

[1] Donoho, D.L. Superresolution via Sparsity Constraints. *SIAM Journal on Mathematical Analysis*, 23(5):1309–1331, 1992.

[2] Weilin, Li and Wenjing, Liao. Stable super-resolution limit and smallest singular value of restricted Fourier matrices. *Applied and Computational Harmonic Analysis*, 51:118–156, 2020.

[3] D. Batenkov, L. Demanet, G. Goldman and Y. Yomdin. Conditioning of Partial Nonuniform Fourier Matrices with Clustered Nodes. *SIAM Journal on Matrix Analysis and Applications*, 44(1):199–220, 2020.

[4] D. Batenkov. Stability and super-resolution of generalized spike recovery. *Applied and Computational Harmonic Analysis*, 45(2):299–323, 2018.

Construction of polynomial minimal surfaces with Pythagorean normals

Emil Žagar
Faculty of mathematics and physics
University of Ljubljana
Institute of mathematics, physics and mechanics
Ljubljana, Slovenia
emil.zagar@fmf.uni-lj.si

A novel approach to the construction of polynomial minimal surfaces (surfaces of zero mean curvature) with isothermal parameterizations from Pythagorean triples of complex polynomials will be presented. The resulting surfaces turn out to be Pythagorean normal (PN), i.e., their unit normal vectors have a rational dependence on the surface parameters. This construction generalizes a prior approach based on Pythagorean triples of real polynomials, and yields more shape parameters for surfaces of a specified degree. Moreover, when one of the complex polynomials is just a constant, the minimal surfaces have the Pythagorean–hodograph (PH) preserving property (a planar PH curve in the parameter domain is mapped to a spatial PH curve on the surface). Cubic and quintic examples of these minimal PN surfaces will be presented, including examples of solutions to the Plateau problem, with boundaries generated by planar PH curve segments in the parameter domain. Finally, an application to the problem of interpolating three given points in the space as the corners of a triangular cubic minimal surface patch, such that the three patch sides have prescribed lengths, will be addressed.

Joint work with: Rida T. Farouki, Marjeta Knez and Vito Vitrih.

Author Index


SMAI'
SIGMA


FSMP
FONDATION SCIENCES
MATHÉMATIQUES DE PARIS


RÉGION
Nouvelle-
Aquitaine


GdR
MIA


erc


IUF


Institut de
Mathématiques de
Bordeaux


LABORATOIRE
JEAN KUNTZMANN